

Development of electrochemical immunosensors and immunoassays for breast cancer biomarker analysis

Maria Cristina Castro Freitas

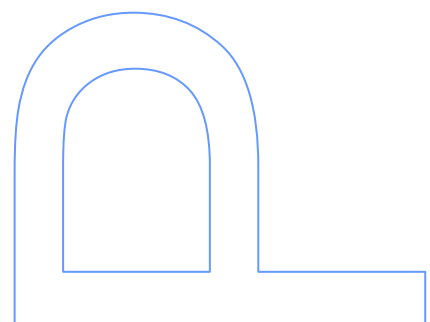
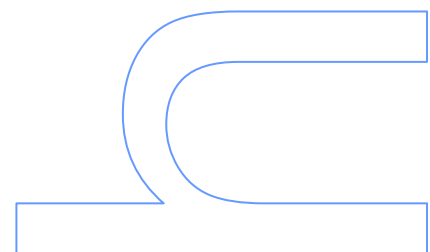
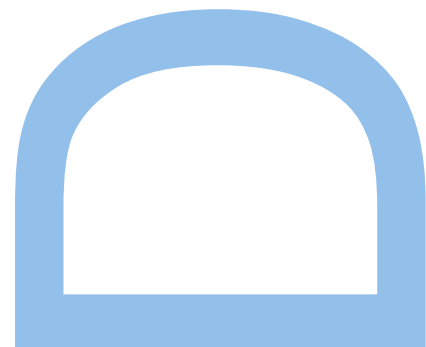
Doutoramento em Química Sustentável
Departamento de Química e Bioquímica
2020

Orientador

Cristina Maria Fernandes Delerue Alvim de Matos
Professora Coordenadora Principal
REQUIMTE/LAQV, Instituto Superior de Engenharia do Porto,
Instituto Politécnico do Porto

Coorientador

Hendrikus Petrus Antonius Nouws
Professor Adjunto
REQUIMTE/LAQV, Instituto Superior de Engenharia do Porto,
Instituto Politécnico do Porto



Development of electrochemical immunosensors and immunoassays for breast cancer biomarker analysis

Maria Cristina Castro Freitas

Thesis submitted to the Universidade do Porto, in fulfilment of the requirements
for the PhD degree in Sustainable Chemistry

Under the supervision of

Cristina Maria Fernandes Delerue Alvim de Matos

Hendrikus Petrus Antonius Nouws

Porto, 2020

© It is authorized the partial reproduction of this thesis (subject to previous authorization by the publishers where the scientific papers were published) only for the purpose of scientific research and with a written statement of the person involved.

Previous Note (Nota Prévia)

Bearing in mind that this thesis is written in English, the candidate presents a previous note written in Portuguese, related to the request for authorization under the General Regulation of the Third Cycles of Studies of the Universidade do Porto (Porto, Portugal), to use a coherent set of research work already published in journals with commissions of selection of recognized international merit and with scientific arbitration, which integrate some of the chapters of the thesis. In addition, the candidate would like to inform that this gathering and processing of information is intended solely to include it in a thesis at this University/Faculty. Permission is not required but is necessary to ensure that the candidate references the journal as the original source. In this context, authorizations to use the articles were requested. According to Copyright Clearance Center's RightsLink service that offers a variety of options for reusing the content, a permission was given following some requirements. This service provides permission for reuse only. As the author of the articles, the candidate retains the right to include it in a thesis or dissertation, provided it is not published commercially.

Nota Prévia

Na elaboração da presente tese, e ao abrigo do número 2 do Artigo 4º do Regulamento Geral dos Terceiros Ciclos de Estudos da Universidade do Porto e do Artigo 31º do D.L. 74/2006, de 24 de março, com a nova redação introduzida pelo D.L. 65/2018, de 16 de agosto, foi efetuado o aproveitamento de um conjunto coerente de trabalhos de investigação já objeto de publicação em revistas com comissões de seleção de reconhecido mérito internacional e com arbitragem científica, os quais integram alguns dos capítulos da tese. A identificação de cada um dos trabalhos de investigação, incluindo nome e volume da revista de publicação e eventuais coautores, é apresentada neste documento. Os trabalhos referidos tiveram o apoio e colaboração de outros coautores. A candidata esclarece que em todos os trabalhos participou ativamente no planeamento, execução, conceção, análise de dados, discussão de resultados, escrita dos manuscritos e atividades científicas de divulgação dos trabalhos desenvolvidos.

Acknowledgements

This work received financial support from "Fundação para a Ciência e a Tecnologia (FCT)/Ministério da Ciência, Tecnologia e Ensino Superior (MCTES)" through national funds (Portugal) (LAQV - UID/QUI/50006/2013 and UID/QUI/50006/2019, and CINTESIS, R&D - Unit - reference UID/IC/4255/2019).

I am grateful to FCT for the financial support through the doctoral research Grant SFRH/BD/111942/2015.

To the Board of Directors of the Doctoral Program in Sustainable Chemistry, together with Universidade de Aveiro, Universidade Nova de Lisboa and Universidade do Porto.

The studies presented in this thesis were performed in "Grupo de Reação e Análises Químicas – GRAQ" (member of the Associate Laboratory – REQUIMTE – Laboratório Associado para a Química Verde), at the "Instituto Superior de Engenharia do Porto – Instituto Politécnico do Porto (ISEP/PP)". In addition, part of the work was developed in collaboration with the Department of Biomedicine – Unit of Biochemistry, Faculty of Medicine, University of Porto. I am deeply grateful for ensuring the conditions required for this PhD project.

I would like to formally express a special acknowledgement and gratitude to my supervisors, Doctor Cristina Delerue-Matos and Doctor Hendrikus Nouws for all the scientific support and shared knowledge.

To Elisa Keating, Marta Neves and Virginia Cruz Fernandes who helped me to solve some challenging tasks that came across during the process of sensors development and validation. To my lab colleagues in GRAQ/REQUIMTE who daily helped with whatever was needed.

To my friends who have supported my choices over the years and for always being around on my journey. To my family for the unconditional love and support.



Abstract

The lack of non-invasive methodologies for accurate detection of carcinogenic biomarkers in the bloodstream is a real concern. Minimizing patient pain and reducing the time required to obtain the analysis result is of the utmost importance. Breast cancer, a malignant lesion commonly diagnosed in women, has become a serious health problem. In the era of new targeted therapies, challenges include diagnosis, definition of high-risk recurrence population, early diagnosis of recurrence and guidance through the different lines of treatment in the management of the disease. Despite the use of conventional methodologies for screening and early detection, namely mammography, the advance of non-invasive analytical techniques can lead to a remarkable evolution.

The development of biosensors alongside technological progress allows the improvement of portable and miniaturized diagnostic platforms. Biosensors, defined as small devices composed of a transducer (an electrode, in the case of electrochemical biosensors), a bioreceptor (an antibody, in the case of immunoassays) and signal amplifiers and processors, are alternative analytical tools for biomarker detection in diagnosis and follow-up.

Cancer biomarkers present on the cell surface and/or their Extracellular Domains (ECD) are important targets for a specific breast cancer detection. The ExtraCellular Domain of the Human Epidermal growth factor Receptor 2 (HER2-ECD) was selected as the target analyte for this thesis and high-performance electrochemical non-competitive (sandwich) immunoassays for its determination were developed. The assays were performed either directly (immunosensor) or indirectly (magnetic immunoassay) on the transducer surface (screen-printed carbon electrode, SPCE). Besides the determination of HER2-ECD in human serum, the developed assays were tested for the analysis of HER2-positive (SK-BR-3) and HER2-negative (MCF-7 and MDA-MB-231) cancer cells.

The electrochemical immunoassays were grouped according to the applied detection strategy: (i) assays based on metalloenzymatic detection and (ii) assays using Quantum Dot (QD) detection labels. In each of the strategies immunosensors and magnetic immunoassays were included. To improve the method's performance, nano- and micro materials were applied in the construction of the transducer and/or the detection label.

In the metalloenzymatic detection, the SPCE was modified with carboxylic acid-functionalized multiwalled carbon nanotubes and electrodeposited gold nanoparticles (MWCNT/AuNP). A magnetic immunoassay was also performed using carboxylic acid-functionalized magnetic beads (HOOC-MBs). After the capture antibody immobilization, a solution containing the antigen and a detection (biotinylated) antibody was added, followed by a streptavidin-alkaline phosphate (Strep-AP, signalling probe). 3-indoxyl phosphate (3-IP, enzymatic substrate) and silver nitrate were added to detect the immunological interaction through the voltammetric analysis, using linear sweep voltammetry (LSV), of enzymatically generated metallic silver.

In the detection strategy involving QDs, bare SPCEs were selected for the immunosensor's construction and HOOC-MBs were used for the magnetic immunoassay. After the capture antibody's immobilization and the addition of a solution containing the antigen and the biotinylated antibody, the affinity process was detected using core/shell strep-CdSe@ZnS QDs as electroactive label. The analytical signal was obtained after QD dissolution (Cd^{2+} ions were released through acidic dissolution of the QDs) through differential pulse anodic stripping voltammetry (DPASV).

The developed assays provided accurate and precise results, and excellent limits of detection, that were well below the cut-off value of the biomarker (15 ng/mL), in assays times of about 2 h. The hands-on times for each assay was about 20-30 min. Selectivity studies were carried out with other cancer biomarkers and possible serum interferents (cancer antigen 15-3 (CA 15-3), alpha-fetoprotein (AFP), Cystatin C (CysC) and human serum albumin (HSA)).

This thesis encompasses the development of several distinct voltammetric immunoassays for the complex task of detecting and quantifying a breast cancer biomarker using two main detection strategies. The accomplishment of such analytical challenges has been demonstrated in practical terms using human serum and live cancer cells, with nanomaterials and bead-based approaches. Overall, the developed assays have point-of-care (POC) detection possibilities and can be alternative tools to traditional methods in oncology for biomarker detection in biological fluids.

Keywords: Breast cancer, bead-based assay, biomarker, biosensor, electrochemistry, electrochemical biosensing, HER2-ECD, immunosensor, immunomagnetic assay, magnetic bead, nanomaterial, quantum dot, screen-printed electrode, tumour cell, voltammetry.

Resumo

A falta de metodologias não invasivas para deteção eficaz de biomarcadores cancerígenos na corrente sanguínea é uma preocupação real. Minimizar a dor do paciente e reduzir o tempo necessário para obter o resultado da análise são fatores de elevada importância. O cancro da mama, uma lesão maligna comumente diagnosticada em mulheres, tornou-se um sério problema de saúde. Na era das novas terapias direcionadas, os desafios incluem diagnóstico, definição de população de reincidência de alto risco, diagnóstico precoce de reincidência e orientação através das diferentes linhas de tratamento da doença. Apesar do uso de metodologias convencionais para rastreio e deteção precoce, nomeadamente a mamografia, o desenvolvimento de técnicas analíticas não invasivas pode levar a uma evolução notável. O desenvolvimento de biossensores, juntamente com o progresso tecnológico, permite o aprimoramento de plataformas de diagnóstico portáteis e miniaturizadas. Biossensores, definidos como pequenos dispositivos compostos por um transdutor (elétrodo, no caso de biossensores eletroquímicos), um bioreceptor (anticorpo, no caso de imunoensaios) e amplificadores/processadores de sinal, são ferramentas analíticas alternativas para deteção de biomarcadores no diagnóstico e acompanhamento da doença.

Os biomarcadores de cancro presentes na superfície celular e/ou os seus domínios extracelulares são alvos importantes para a deteção específica do cancro de mama. O Domínio ExtraCelular do Recetor 2 do Fator de Crescimento Epidérmico Humano (HER2-ECD) foi selecionado como analito alvo para a realização desta tese e foram desenvolvidos imunoensaios eletroquímicos não competitivos (do tipo sandwich) com elevado desempenho para sua determinação. Os ensaios foram realizados diretamente (imunossensor) ou indiretamente (imunoensaio magnético) na superfície do transdutor (elétrodo de carbono serigrafado, SPCE). Além da determinação de HER2-ECD no soro humano, os ensaios desenvolvidos foram testados para a análise de células cancerígenas HER2-positivas (SK-BR-3) e HER2-negativas (MCF-7 e MDA-MB-231).

Os imunoensaios eletroquímicos desenvolvidos foram agrupados de acordo com a estratégia de deteção aplicada: (i) deteção metaloenzimática e (ii) usando "Quantum Dot" (QD). Em cada uma das estratégias foram incluídos imunossensores e imunoensaios magnéticos. Para melhorar o desempenho do método, nano/micro-materiais foram aplicados na construção do transdutor e/ou no marcador de deteção.

Na detecção metaloenzimática, o SPCE foi modificado com nanotubos de carbono de paredes múltiplas funcionalizados com ácido carboxílico e com nanopartículas de ouro eletrodepositadas (HOOC-MWCNT/AuNP). Também foi realizado um imunoensaio magnético utilizando esferas magnéticas funcionalizadas com ácido carboxílico (HOOC-MBs). Após a imobilização do anticorpo de captura, foi adicionada uma solução contendo o antígeno e o anticorpo de detecção (biotinilado), seguindo-se a adição de estreptavidina-fosfatase alcalina (Strep-AP, marcador enzimático). Adicionou-se 3-indoxil fosfato (3-IP, substrato enzimático) e nitrato de prata para detetar a interação imunológica através da análise voltamétrica de varrimento linear (LSV) da prata metálica gerada enzimaticamente.

Na estratégia de detecção envolvendo QD, os SPCE não modificados foram selecionados para a construção do imunossensor e as HOOC-MBs foram usadas para o imunoensaio magnético. Após a imobilização do anticorpo de captura e a adição de uma solução contendo o antígeno e o anticorpo biotinilado, o processo de afinidade foi detetado usando QD CdSe@ZnS revestidos com estreptavidina como marcador eletroativo. O sinal analítico foi obtido após a dissolução de QD (os iões Cd²⁺ são libertados pela dissolução ácida dos QD) usando a voltametria de redissolução anódica de pulso diferencial (DPASV).

Os ensaios desenvolvidos permitiram obter resultados exatos e precisos, e excelentes limites de detecção, abaixo do valor limite estabelecido para o biomarcador (15 ng/mL), em tempos de ensaios de cerca de 2 h. O tempo de execução para cada ensaio variou entre 20 a 30 minutos. Foram realizados estudos de seletividade com outros biomarcadores de cancro e possíveis interferentes do soro (antígeno 15-3 (CA 15-3), alfa-fetoproteína (AFP), cistatina C (CysC) e albumina do soro humano (ASH)).

Esta tese abrange o desenvolvimento de vários imunoensaios voltamétricos para a complexa tarefa de detetar e quantificar um biomarcador de cancro da mama, usando duas estratégias principais de detecção. Os desafios analíticos propostos foram atingidos e demonstrados através de abordagens baseadas em nanomateriais e esferas magnéticas, utilizando soro humano e células cancerígenas. No geral, os ensaios desenvolvidos possibilitam a detecção rápida no local de atendimento e podem ser ferramentas alternativas aos métodos tradicionalmente usados em oncologia para a detecção de biomarcadores em fluidos biológicos.

Palavras-chave: cancro da mama, ensaio baseado em esferas, biomarcador, biossensor, eletroquímica, biodeteção eletroquímica, HER2-ECD, imunossensor, ensaio imunomagnético, esfera magnética, nanomaterial, quantum dot, eletrodo serigrafado, célula tumoral, voltametria.

List of Publications

Publications in International Peer-reviewed journals

(Included in chapters 2, 3 and 4 of the present thesis)

1. **Maria Freitas**, Henri P.A. Nouws, Cristina Delerue-Matos.
Electrochemical Biosensing in Cancer Diagnostics and Follow-up. *Electroanalysis* 30 (8) (2018) 1576-1595. doi.org/10.1002/elan.201800193
2. **Maria Freitas**, Henri P.A. Nouws, Cristina Delerue-Matos.
Electrochemical Sensing Platforms for HER2-ECD Breast Cancer Biomarker Detection. *Electroanalysis* 31 (1) (2019) 121-128. doi.org/10.1002/elan.201800537
3. **Maria Freitas**, Henri P.A. Nouws, Elisa Keating, Cristina Delerue-Matos.
High-performance electrochemical immunomagnetic assay for breast cancer analysis. *Sensors and Actuators: B. Chemical* 308 (2020) 120766. doi.org/10.1016/j.snb.2020.127667
4. **Maria Freitas**, Marta M. P. S. Neves, Henri P.A. Nouws, Cristina Delerue-Matos.
Quantum Dots as Nanolabels for Breast Cancer Biomarker HER2-ECD Analysis in human serum. *Talanta* 208 (2020) 120430. doi.org/10.1016/j.talanta.2019.120430
5. **Maria Freitas**, Henri P.A. Nouws, Elisa Keating, Virginia Cruz Fernandes, Cristina Delerue-Matos.
Immunomagnetic bead-based bioassay for the voltammetric analysis of the breast cancer biomarker HER2-ECD and tumour cells using quantum dots as detection labels. *Microchimica Acta* 187 (3) (2020) 184. doi.org/10.1007/s00604-020-4156-4

Publications in Scientific Meeting Proceedings (with peer revision)

1. **Maria Freitas**, Henri P.A. Nouws, Cristina Delerue-Matos
Nano- and Micro Material-Based Electrochemical Bioassays for the Non-Invasive Detection of HER2-ECD, a Breast Cancer Biomarker. *Proceedings* 15 (20) (2019) 1-4. doi:10.3390/proceedings2019015020

List of presentations in Scientific Meetings

Communications in National and International Scientific Meetings

Oral presentation

1. **Maria Freitas**, Henri P.A. Nouws, Cristina Delerue-Matos.
Non-invasive analysis of the Breast Cancer Biomarker HER2-ECD through Electrochemical Biosensing Strategies. *III Meeting of Medicinal Biotechnology / Iberian Congress on Medicinal Biotechnology*. Porto, Portugal. May 18, 2018.

Poster presentation

1. **Maria Freitas**, Henri P.A. Nouws, Cristina Delerue-Matos
Electrochemical immunosensor for detection of a Breast cancer biomarker based on distinct carbon- and gold- based nanomaterial-modified sensing platform. *2nd Workshop on Electrochemical Devices / 3rd Workshop ELECTROBIONET*. Oviedo, Spain. November 9–10, 2017.
2. **Maria Freitas**, Henri P.A. Nouws, Cristina Delerue-Matos
Electrochemical immunosensing platforms for breast cancer detection. *XXIII Meeting of the Portuguese Society of Electrochemistry*. Porto, Portugal. May 2–4, 2018.
3. **Maria Freitas**, Henri P.A. Nouws, Cristina Delerue-Matos
Nano- and Micro Material-Based Electrochemical Bioassays for the Non-Invasive Electrochemical Detection of HER2-ECD, a Breast Cancer Biomarker. *7th International Symposium on Sensor Science*. Napoli, Italy. May 9–11, 2019.
4. **Maria Freitas**, Henri P.A. Nouws, Cristina Delerue-Matos
Electrochemical detection of HER2-ECD breast cancer biomarker using quantum dots as nanolabels. *International Congress on Analytical Nanoscience and Nanotechnology - IX NyNA*. Zaragoza, Spain. July 2–4, 2019.

Table of Contents

Acknowledgements	vii
Abstract	ix
Resumo	xi
List of publications	xiii
List of presentations in Scientific Meetings	xiv
Table of contents	xv
List of figures	xvii
List of tables	xxiii
List of abbreviations	xxv
Relevance and motivation	xxvii
Thesis objectives	xxviii
Thesis outline	xxix
Chapter 1 General Introduction	1
1.1 (Breast) Cancer: challenges and impact in diagnosis and follow-up for personalized medicine	3
1.2 Breast cancer classification	4
1.3 Biomarkers for non-invasive analysis	5
1.4 HER2-positive breast cancer: biology and clinical relevance	6
1.5 Diagnostic tests in breast cancer: from prediction to follow-up	8
1.6 POC devices: the case of biosensors	8
1.7 Voltammetric transduction	10
1.8 Electrochemical immunosensors and magnetic immunoassays	15
1.8.1 Metalloenzymatic detection	17
1.8.2 Metallic nanoparticles as electrochemical detection labels	18

Chapter 2 Electrochemical biosensing in cancer – insights and challenges	23
Overview	25
2.1 Electrochemical Biosensing in Cancer Diagnostics and Follow-up.....	27
2.2 Electrochemical strategies for HER2 detection: an update	49
Chapter 3 Electrochemical immunoassays with metalloenzymatic detection	61
Overview	63
3.1 Electrochemical Sensing Platforms for HER2-ECD Breast Cancer Biomarker Detection	65
3.2 High-performance electrochemical immunomagnetic assay for breast cancer analysis	75
Chapter 4 Electrochemical immunoassays using Quantum Dots as detection labels	93
Overview	95
4.1 Quantum Dots as Nanolabels for Breast Cancer Biomarker HER2-ECD Analysis	97
4.2 Immunomagnetic bead-based bioassay for the voltammetric analysis of the breast cancer biomarker HER2-ECD and tumour cells using quantum dots as detection labels	111
Chapter 5 General conclusions and future perspectives	131
Conclusions	133
Future perspectives	135

List of Figures

Chapter 1 General Introduction

Figure 1. Tumour subtyping scheme	4
Figure 2. Breast cancer biomarkers classification.....	5
Figure 3. Simplified representation of normal cell and HER2(+) cancer cell	7
Figure 4. Biosensors classification	9
Figure 5. (a) Linear potential sweep and (b) resulting i-E curve (voltammogram) ...	10
Figure 6. SEM images of the SPCE surfaces (used throughout this work). (a) non-modified SPCE, (b) SPCE-AuNP, (c) SPCE-MWCNT, (d) SPCE-MWCNT/AuNP, (e) SPCE-Fe ₃ O ₄ @AuNP and (f) SPCE-MBs.....	12
Figure 7. (a) Excitation signals and (b) voltammogram for a DPV experiment	13
Figure 8. Scheme of an electrochemical immunosensor. Voltammetric signal is obtained for distinct analytes, which allows (1) simultaneous or (2) individual detection	16
Figure 9. Schematic representation of the metalloenzymatic detection strategy	17
Figure 10. Schematic representation of the detection strategy using quantum dots	18

Chapter 2 Electrochemical biosensing in cancer – insights and challenges

2.1 Electrochemical Biosensing in Cancer Diagnostics and Follow-up

Figure 1. Schematic Representation of an Electrochemical Immunosensor based on GO and Avidin modified sensing platform	42
Figure 2. Types of immunoassays (I – immobilized antibodies react with free antigens in competition with labelled antigens, II – immobilized antigens react with free and labelled antibodies	42
Figure 3. Schematic representation of a sandwich immunosensor for breast cancer protein biomarker detection	42
Figure 4. Electrochemical signal amplification strategy.....	43
Figure 5. Example of a label free assay, using [Fe(CN) ₆] ^{3-/4-} as redox probe	44

Figure 6. Schematic representation of Competitive electrochemical immunosensor for NSE detection	44
Figure 7. Strategies on immobilization of recognition element onto the surface of magnetic particles	45
Figure 8. Schematic representation of multiplexed detection of cancer biomarkers.	45

Chapter 3 Electrochemical immunoassays with metalloenzymatic detection

3.1 Electrochemical Sensing Platforms for HER2-ECD Breast Cancer Biomarker Detection

Scheme 1. Schematic representation of the electrochemical immunoassay	69
Figure 1. Schematic representation of the electrochemical immunoassay	70
Figure 2. Peak current intensities obtained using the tested sensing platforms	71
Figure 3. SEM images and respective histograms of (a) SPCE-AuNP and (b) SPCE-MWCNT/AuNP	72
Figure 4. (a) Examples of linear sweep voltammograms for the analysis of HER2-ECD: 0, 7.5, 15, 25, 35 and 50 ng/mL, (b) calibration plots in spiked human serum using SPCE-AuNP and SPCE-MWCNT/AuNP	72
Figure 5. Results obtained in the selectivity studies using the developed sensing strategies	73

3.2 High-performance electrochemical immunomagnetic assay for breast cancer analysis

Scheme 1. Representation of the immunoassay	79
Figure 1. SEM image of the SPCE covered with HOOC-MBs and the respective size distribution	80
Figure 2. Optimization of (A) the amount of Magnetic beads and (B) the Ab-C and Ab-D concentrations (HER2-ECD: 0 and 50 ng/mL)	81
Figure 3. Results of different assay strategies. (A) step-by-step assay, (B) pre-incubation of HER2 + Ab-D (60 min) and (C) pre-incubation of HER2 + Ab-D (120 min); (D) pre-incubation of Ab-D + S-AP (60 min); and (E) pre-incubation of HER2 + Ab-D + S-AP (60 min)	81
Figure 4. Analysis of HER2-ECD in undiluted Human serum (A) Calibration plots and (B) Representative linear sweep voltammograms ([HER2-ECD] (ng/mL): (1) 0, 5, 7.5, 15, 30 and 50; (2) 50, 75 and 100)	82
Figure 5. Selectivity studies using non-target proteins (the signal for HER2-ECD is included for comparison)	82

Figure 6. (A) Calibration plots for the analysis of SK-BR-3 and MDA-MB-231 breast cancer cell lines in human serum; (B) Calibration straight for the analysis of SK-BR-3 (HER2+ cancer cells): 1×10^2 , 1×10^3 , 1×10^4 and 1×10^5 cells/mL, Inset: Examples of linear sweep voltammograms 83

Figure S1. Optimization of the incubation time for the step-by-step assay: (1) HER2-ECD 30 min, Ab-D 30 min, S-AP 30 min; (2) HER2-ECD 30 min, Ab-D 60 min, S-AP 60 min; (3) HER2-ECD 60 min, Ab-D 60 min, S-AP 60 min; (4) HER2-ECD 30 min, Ab-D 60 min, S-AP 30 min. (Ab-C: 25 $\mu\text{g/mL}$, HER2-ECD: 0 and 50 ng/mL, Ab-D: 2 $\mu\text{g/mL}$) 88

Figure S2. Addition of BSA 0.5% (m/V) to (i) HER2-ECD, (ii) Ab-D or (iii) in both solutions (antigen and Ab-D). (Ab-C: 25 $\mu\text{g/mL}$, HER2-ECD: 0 and 50 ng/mL, Ab-D: 2 $\mu\text{g/mL}$) 89

Figure S3. (A) Effect of the addition of DEA 0.1 M or BSA 1% (m/V) to the S-AP solution and (B) Variation of S-AP concentration (including BSA 1% (m/V)). (Ab-C: 25 $\mu\text{g/mL}$, HER2-ECD: 0 and 50 ng/mL, Ab-D: 2 $\mu\text{g/mL}$) 89

Figure S4. Optimization of experimental parameters. (A) Temperature, and (B) Affinity of the MBs with the antigen, i.e. with and without capture antibody 90

Figure S5. Calibration plot in 0.1M Tris-HNO₃ buffer (pH 7.4) for the analysis of HER2-ECD: 7.5, 15, 30, 50, 75 and 100 ng/mL. Experimental conditions: Ab-C: 25 $\mu\text{g/mL}$, BSA: 2% (m/V), Ab-D: 2 $\mu\text{g/mL}$ 90

Figure S6. Obtained current intensities in the stability studies. (Ab-C: 25 $\mu\text{g/mL}$, HER2-ECD: 0 and 50 ng/mL, Ab-D: 2 $\mu\text{g/mL}$) 91

Chapter 4 Electrochemical immunoassays using Quantum Dots as detection labels

4.1 Quantum Dots as Nanolabels for Breast Cancer Biomarker HER2-ECD Analysis

Scheme 1. Representation of the immunosensor construction and detection strategy 101

Figure 1. Optimization of Ab-D concentration (1; 2 and 4 $\mu\text{g/mL}$). Experimental conditions: BSA (2%(m/V), Ab-C 25 $\mu\text{g/mL}$, HER2-ECD (0 and 50ng/mL), QD 5 nM101

Figure 2. (A) Optimization of QDs concentration (5; 10 and 20 nM) and (B) Current intensities obtained with QDs 5 nM in the absence and in the presence of BSA (0.5% (m/V)) in the solution. Experimental conditions: BSA (2% (m/V)), Ab-C (25 $\mu\text{g/mL}$), HER2-ECD (0 and 50 ng/mL), Ab-D (2 $\mu\text{g/mL}$) 102

Figure 3. Influence of the incubation time for step-by-step assay (A, B, C and D), and joining steps assay: HER2-ECD + Ab-D (E and F) and Ab-D + QDs (G). Experimental

conditions: BSA (2% (m/V), Ab-C (25 µg/mL), HER2-ECD (25 ng/mL), Ab-D (2 µg/mL), QDs (5 nM + BSA 0.5% (m/V)).....102

Figure 4. (A) Calibration plot using the developed immunosensor in the presence of growing concentrations of HER2-ECD in human serum and (B) examples of typical differential pulse voltammograms obtained within the established linear range (0, 10, 25, 50, 100 and 150 ng/mL), Experimental conditions: Ab-capture: 25 µg/mL, BSA: 2% (m/V), Ab-D: 2 µg/mL, QDs: 5 nM with addition of BSA 0.5% (m/V)).....103

Figure 5. Evaluation of the selectivity of the HER2-ECD sensor against other serum proteins. Experimental conditions: Ab-C: 25 µg/mL, BSA: 2% (m/V), Ab-D: 2 µg/mL, QDs: 5 nM with addition of BSA 0.5% (m/V)). Serum proteins concentration: HER2-ECD: 50 ng/mL, CA 15–3: 50 U/mL, Cystatin C: 550 ng/mL.....103

Figure S 1. S Study of non-specific adsorptions. Evaluation of the blocking agents (I) Casein 2% and (II) BSA 2% in the blocking surface step, and evaluation of BSA effect in different incubation steps: (III) BSA 0.5% (m/V) for both the antigen and the detection antibody solutions (Ab-D), and (IV) BSA 0.5% (m/V) to the antigen and 1% (m/V) to the Ab-D solutions. Experimental conditions: Ab-C (25 µg/mL), HER2-ECD (0 and 50 ng/mL), Ab-D (2 µg/mL), QDs (10 nM).....107

Figure S 2. Calibration plot in Tris buffer for the analysis of HER2-ECD: 0, 5, 10, 25, 50 and 100 ng/mL. Experimental conditions: Ab-C: 25 µg/mL, BSA: 2% (m/V), Ab-D: 2 µg/mL, QDs: 5 nM with addition of BSA 0.5% (m/V)).....108

Figure S 3. Obtained current intensities for stability studies. Experimental conditions: Ab-C: 25 µg/mL, BSA: 2% (m/V), Ab-D: 2 µg/mL, QDs: 5 nM with addition of BSA 0.5% (m/V))108

4.2 Immunomagnetic bead-based bioassay for the voltammetric analysis of the breast cancer biomarker HER2-ECD and tumour cells using quantum dots as detection labels

Scheme 1. Schematic representation of the magnetic immunoassay. **1** The MBs are first biomodified (i activation with EDC/NHS, ii addition of capture antibody, iii blocking with EA). **2** The magnetic assay is performed through the addition of iv a mixture containing the antigen (HER2-ECD or cancer cells) and the biotinylated antibody, followed by the addition of v a QD-strep solution. The magnetic beads are magnetically attracted to the working electrode. **3** Electrochemical determination of the released Cd²⁺ is performed. Voltammograms of increasing HER2-ECD concentrations are exemplified115

Figure 1. a Study of the electrochemical behaviour of cadmium (released from QDs 10 nM) with distinct nano- and micromaterials used on SPCEs. b Respective SEM images: (1 – bare SPCE; 2 – SPCE-MWCNT; 3 – SPCE-Fe ₃ O ₄ @Au nanoparticles; 4 – SPCE-MBs)	117
Figure 2. Calibration plot for the analysis of HER2-ECD in human serum (ip vs. HER2-ECD concentration) using the magnetic immunoassay. Inset: Differential pulse anodic stripping voltammograms of [HER2-ECD] (a-g): 0, 0.50, 1.0, 2.5, 5.0, 10, 25 and 50 ng·mL ⁻¹ . (Ab-C 25 µg·mL ⁻¹ ; Ab-D 2.0 µg·mL ⁻¹ ; QDs 5.0 nM. DPASV parameters: preconcentration +1.00 V for 60 s and -1.10 V for 300 s; potential scan -1.00 V to -0.70 V; pulse amplitude 0.05 V; step potential 0.01 V; modulation time 0.01 s; interval time 0.1 s).....	117
Figure 3. a Responses for HER2-ECD, buffer, serum and possible interferences (CA15-3 100 U·mL ⁻¹ ; AFP 1 µg·mL ⁻¹ and HSA 100 mg·mL ⁻¹). b Storage stability of the modified MBs, [HER2-ECD] 0 and 50 ng·mL ⁻¹	118
Figure 4. Results obtained for cancer cell analysis. a Selectivity study of the magnetic immunoassay in the presence of 1×10 ⁵ cells·mL ⁻¹ for SK-BR-3, MDA-MB-231 and MCF-7 cells. b Results obtained for distinct concentrations of HER2-positive cancer cells SK-BR-3 in human serum. Inset: Differential pulse anodic stripping voltammograms of [SK-BR-3] (a–e) 0, 1×10 ² , 5×10 ² , 1×10 ³ and 5×10 ³ cells·mL ⁻¹ . DPASV parameters: preconcentration +1.00 V for 60 s and -1.10 V for 300 s, potential scan -1.00 V to -0.70 V, pulse amplitude 0.05 V, step potential 0.01 V, modulation time 0.01 s, interval time 0.1 s	119
Figure S1. Calibration straight (A vs. HER2-ECD concentration) for the analysis of HER2-ECD in human serum using the ELISA kit	125
Figure S2. Electrochemical determination of the QDs through the addition of HCl and Bi(III) in distinct formats	126
Figure S3. Results of the optimizations. (a) Format assays (Format A: step-by-step assay, Format B: previously mixture step of antigen and Ab-detection, Format C: previously mixture step of Ab-detection and QDs), (b) QDs concentration (1.5, 5.0, 10 nM and 5.0 nM + BSA 0.5% (m/V)), (c) MBs amount (45, 30, 15 and 7.5 µg for each WE) and (d) concentration of Ab-C (10, 25 and 50 µg·mL ⁻¹) and Ab-D (1.0 and 2.0 µg·mL ⁻¹). (HER2-ECD (0 (blank) and 50 ng·mL ⁻¹)	129

List of Tables

Chapter 2 Electrochemical biosensing in cancer – insights and challenges

2.1 Electrochemical Biosensing in Cancer Diagnostics and Follow-up

Table 1. Some protein cancer biomarkers	30
Table 2. Lung cancer biomarker analysis with electrochemical immunosensors	32
Table 3. Breast cancer biomarker analysis with electrochemical immunosensors ..	33
Table 4. Colorectal and Stomach cancer biomarker analysis with electrochemical immunosensors	34
Table 5. Prostate cancer biomarker analysis with electrochemical immunosensors	35
Table 6. Liver cancer biomarker analysis with electrochemical immunosensors	37
Table 7. Stomach cancer biomarker analysis with electrochemical immunosensors	39

2.2 Electrochemical strategies for HER2 detection: an update

Table 1. Electrochemical immunosensors for analysis of HER2 breast cancer biomarker.....	52
Table 2. Electrochemical immunoassays for analysis of HER2 breast cancer biomarker.....	54
Table 3. Electrochemical bioassay-based analysis of HER2-expressing breast cancer cell lines	57

Chapter 3 Electrochemical immunoassays with metalloenzymatic detection

3.1 Electrochemical Sensing Platforms for HER2-ECD Breast Cancer Biomarker Detection

Table 1. Analytical characteristics of the developed electrochemical biosensors for the analysis of HER2-ECD in Human serum samples	72
Table 2. Characteristics of electrochemical immunosensors and immunoassays for HER2 analysis	73

3.2 High-performance electrochemical immunomagnetic assay for breast cancer analysis

Table 1. Figures of merit of the developed magnetic immunoassay for the analysis of HER2-ECD in Human serum	82
Table 2. Recovery values, relative standard deviations (RSD) and relative deviation obtained in the analysis of HER2-ECD using the developed immunoassay and a commercial ELISA kit	82
Table 3. A comparison of electrochemical immunoassays for breast cancer detection using magnetic beads (MBs)	84
Table S1. Optimization of the experimental parameters of the magnetic immunoassay	88

Chapter 4 Electrochemical immunoassays using Quantum Dots as detection labels

4.1 Quantum Dots as Nanolabels for Breast Cancer Biomarker HER2-ECD Analysis

Table 1. Figures of merit of the developed biosensor for the analysis of the cancer biomarker HER2-ECD in Human Serum samples	103
Table 2. Summary of experimental parameters of electrochemical immunoassay-based procedures for HER2 analysis.....	104
Table SI 1. Summary of experimental parameters of electrochemical immunoassay-based procedures for breast cancer biomarkers using Quantum Dots	109

4.2 Immunomagnetic bead-based bioassay for the voltammetric analysis of the breast cancer biomarker HER2-ECD and tumour cells using quantum dots as detection labels

Table 1. Recovery values (%), relative standard deviations (RSD, %) and relative deviations (%) for the electrochemical and ELISA analysis of HER2-ECD in human serum: 1.0, 2.5, 10, 20 and 50 ng·mL ⁻¹ . Comparison between the used labels, platforms, assay and hands-on times for the distinct methodologies	118
Table 2. Summary of experimental parameters of electrochemical bioassay-based procedures for HER2-expressing breast cancer cell lines.....	120
Table SI 1. Optimization of the experimental parameters of the immunomagnetic assay	128
Table SI 2. Figures of merit of the developed magnetic immunoassay for the analysis of HER2-ECD and the HER-positive breast cancer cell line SK-BR-3	130

List of Abbreviations

- 1-NP** – 1-naphthyl-phosphate
3-IP – 3-indoxyl phosphate
Ab – antibody
Ab-C – capture antibody
Ab-D – detection antibody
AE – auxiliary electrode
AFP – fetoprotein
AuE – gold electrode
AuNP – gold nanoparticle
AP – alkaline phosphatase
CA 15-3 – cancer antigen 15-3
CC – chronocoulometry
Cd²⁺ – cadmium ion
CEA – carcinoembryonic antigen
CTC – circulating tumour cell
CV – Cyclic voltammetry
CysC – cystatin C
DNA – deoxyribonucleic acid
DPV – differential pulse voltammetry
DPASV – differential pulse anodic stripping voltammetry
EC – electrochemical
EDS – energy dispersive X-ray spectroscopy
EGTM – European group on tumour markers
ELISA – enzyme-linked immunosorbent assay
E_p – peak potential
ER – estrogen receptor
FDA – food and drug administration
FISH – fluorescence in situ hybridisation
Fe₃O₄@AuNP – gold-coated iron magnetic nanoparticles
GCE – glassy carbon electrode
HER2 – human epidermal growth factor receptor 2
HER2 (+) – HER2 positive

HER2 (-) – HER2 negative

HOOC-MBs – carboxyl acid-functionalized magnetic beads

HSA – human serum albumin

IHC – immunohistochemistry

ISH – in situ hybridisation

i_p – peak current

IUPAC – international union of pure and applied chemistry

LSV – linear sweep voltammetry

MB – magnetic beads

MP – magnetic particles

MSep – magnetic separation

MWCNT – multiwalled carbon nanotube

NCDs – noncommunicable disease

POC – point-of-care

PR – progesterone receptor

QD – quantum dot

rGO – reduced graphene oxide

RNA – ribonucleic acid

RE – reference electrode

SEM – scanning electron microscopy

SPE – screen-printed electrode

SPCE – screen-printed carbon electrode

Strep-AP – streptavidin coated alkaline phosphatase

SWCNT – single-walled carbon nanotubes

SWV – square wave voltammetry

WE – working electrode

Relevance and motivation

Improved living standards and increased life expectancy lead to changes in the causes of death. Worldwide, the highest mortality rates are related to noncommunicable diseases (NCDs), corresponding to chronic long-term diseases such as cardiovascular and respiratory diseases, cancer and diabetes. Heart disease and stroke remain the leading causes of death in the last years [1], however, cancer is expected to far outweigh these in the 21st century [2]. Cancer mortality rates are growing rapidly due to complex reasons, distinct risk factors and socioeconomic development [3]. The highest percentage of cancer deaths occurred in high-income countries [4], however, to reduce mortality rates, screening programs are implemented at national levels [5]. Nevertheless, the lack of specific results in these traditional screening diagnoses can significantly lead to unfavourable clinical outcomes.

Breast cancer, the most frequent cancer among women, has increased steadily every year [3]. Mammography is routinely performed as a screening tool and is the most widely practiced and most cost-effective approach [6]. However, imaging results have limited sensitivity and do not allow to monitor tumour biomarker levels in a non-invasive way. Tumour biomarkers refer to substances (e.g. a molecule secreted by a tumour) or processes that are indicative of the presence of cancer in the body [7].

In this field, alternative methods are required to determine cancer biomarkers in biological fluids (serum, plasma) from screening to follow-up.

Biosensors with fast, accurate and point-of-care (POC) detection possibilities are a preeminent alternative to measure cancer biomarker levels in bodily fluids over the traditional methods [8]. The use of small size transducers, the reasonable short assay times and the low sample volumes are key features for the development of POC devices. In addition, electrochemical strategies based on the use of nanomaterials can improve the assays' performance [9].

Despite the continuous advances in science, there is still a lack of diagnostic platforms, with pocket-size dimensions, that enable simple medical tests to be performed with or nearby the patient in a fast or direct response time.

Thesis objectives

The overall goal of this thesis was the development of ultra-sensitive and highly selective voltammetric immunosensors and immunoassays for the detection of HER2-ECD, a breast cancer biomarker, in human serum. These assays could allow breast cancer screening and the establishment of biomarker levels. To achieve this overall goal several studies were carried out. The intermediate objectives were:

- Literature review on electrochemical immunosensors and cytosensors for cancer biomarkers;
- Optimization of distinct nano- and micro materials to be used as immobilization platforms for antibodies;
- Development and optimization of transducer surfaces and integration of biosensing strategies in miniaturized devices (SPCEs);
- Development of detection strategies for electrochemical immunoassays based on metalloenzymatic detection and/or Quantum Dots;
- Validation and evaluation of immunosensors and magnetic immunoassays for the determination of the breast cancer biomarker and cancer cells in human serum.

Thesis outline

The present thesis includes the work developed under the scope and objectives of the approved project. The structure of this thesis comprises 5 chapters.

The introduction – chapter 1 – highlights the fundamentals, main concepts and relevant topics related to the project, with emphasis on the cancer biomarker, electrode surface modification/functionalization, assay type, detection strategy and voltammetric techniques.

A general description of electrochemical immunosensors and immunoassays for protein biomarker detection related to the main cancer-types is presented in a comprehensive literature review – chapter 2. Particularly important, this chapter allowed to notice the relevant gaps in the field of electrochemical strategies, providing a pertinent contribution to the present thesis.

Chapters 3 and 4 describe the experimental work. In chapter 3, the developed electrochemical assays based on metalloenzymatic detection are described. For the immunosensor development, distinct nanomaterials on SPCEs were tested: (i) reduced graphene oxide (rGO), (ii) carboxylic acid-functionalized single-walled carbon nanotubes (SWCNT-COOH), (iii) carboxylic acid-functionalized multiwalled carbon nanotubes (MWCNT-COOH), and their conjugation with gold nanoparticles (AuNP): (iv) rGO/AuNP, (v) SWCNT/AuNP, (vi) MWCNT/AuNP. In addition, (vii) carboxylic acid-functionalized magnetic beads (HOOC-MBs) were used for the development of the magnetic immunoassay. Chapter 4 reports electrochemical assays using Quantum Dots as detection labels. Non-modified SPCEs were used as transducers and both an immunosensor and a magnetic immunoassay, using HOOC-MBs, were studied.

The literature review – chapter 2 and the experimental work – chapters 3 and 4 – were published during the period of the project.

The conclusions and future perspectives are described in chapter 5.

References

- [1] The Global Cancer Observatory (2019) Cancer fact sheet. World Heal Organ 876:2018–2019. <https://doi.org/L11\n10.1051/0004-6361/201016331>
- [2] F Bray, J Ferlay, I Soerjomataram, RL Siegel, LA Torre, A Jemal. Global cancer statistics 2018: GLOBOCAN estimates of incidence and mortality worldwide for 36 cancers in 185 countries. *CA: A Cancer Journal for Clinicians* **2018**, 68:394–424. <https://doi.org/10.3322/caac.21492>
- [3] J Ferlay, M Colombet, I Soerjomataram, T Dyba, G Randi, M Bettio, A Gavin, O Visser, F Bray. Cancer incidence and mortality patterns in Europe: Estimates for 40 countries and 25 major cancers in 2018. *European Journal of Cancer* **2018**, 103:356–387. <https://doi.org/10.1016/j.ejca.2018.07.005>
- [4] World Health Organization. World Health Statistics - Monitoring Health for the SDGs. *World Health Organ* **2016**, 1.121. <https://doi.org/10.1017/CBO9781107415324.004>
- [5] P Basu, A Ponti, A Anttila, G Ronco, C Senore, DB Vale, N Segnan, M Tomatis, I Soerjomataram, M Primic Žakelj, J Dillner, KM Elfström, S Lönnberg, R Sankaranarayanan. Status of implementation and organization of cancer screening in The European Union Member States—Summary results from the second European screening report. *International Journal of Cancer* **2018**, 142:44–56. <https://doi.org/10.1002/ijc.31043>
- [6] P Autier, M Boniol. Mammography screening: A major issue in medicine. *European Journal of Cancer* **2018**, 90:34–62. <https://doi.org/10.1016/j.ejca.2017.11.002>
- [7] S Mittal, H Kaur, N Gautam, AK Mantha. Biosensors for breast cancer diagnosis: A review of bioreceptors, biotransducers and signal amplification strategies. *Biosensors and Bioelectronics* **2017**, 88, 217–231. <https://doi.org/10.1016/j.bios.2016.08.028>
- [8] S Campuzano, P Yáñez-Sedeño, JM Pingarrón. Current trends and challenges in bioelectrochemistry for non-invasive and early diagnosis. *Current Opinion in Electrochemistry* **2018**, 12:81–91. <https://doi.org/10.1016/j.coelec.2018.04.015>
- [9] M Freitas, HPA Nouws, C Delerue-Matos. Electrochemical biosensing in cancer diagnostics and follow-up. *Electroanalysis* **2018**, 30, 1576-1595. <https://doi.org/10.1002/elan.201800193>

CHAPTER 1



GENERAL INTRODUCTION

1

Introduction

This thesis focuses on electrochemical immunosensors and magnetic immunoassays, for which nano- and micro materials, based on gold, carbon and magnetic materials and sustainable chemistry fields were employed. The methods are centered on voltammetric (sandwich-type) immunoassays for the determination of a breast cancer biomarker. Thus, this chapter presents a general introduction that aims to report a specific type of cancer – breast cancer – focusing on the biomarker under study – HER2-ECD – and its importance for early diagnosis and follow-up.

1.1 (Breast) Cancer: challenges and impact in diagnosis and follow-up for personalized medicine

The uncontrolled proliferation of cells, in certain tissues or organs, can lead to a group of diseases (neoplasms or malignant tumours), designed as cancer. Tumours are constituted by multiple and complex cell types. Benign tumours do not spread or invade other tissues (or other parts of the body). However, when cells spread from the original site of the body to another, a process known as metastasis occurs, which can be denoted as a malignant tumour [1].

The incidence of cancer has increased considerably. Cancer screening allows effective detection and appropriate treatments. Screening programs and clinical exams are applied at a national level to reduce mortality rates [2]. However, global cancer mortality rates are increasing due to complex reasons such as the aging population and changes

in the prevalence and distribution of major risk factors associated with socioeconomic development [3].

Breast cancer is the second most common cancer in the world and, by far, the most frequent among women, with an estimated 2.1 million cases in 2018 [4]. The more favorable survival in (high-incidence) developed regions is largely attributable to mammographic screening programs and advances in therapy [5]. However, there is still a long way to go in understanding tumour biology and the best suitable treatment [6].

1.2 Breast cancer classification

The purpose of breast cancer classification is to select the most adequate patient treatment. It can be divided into distinct categories, such as the stage of the tumour, the histopathological type, the protein and gene expression. Classifications are updated with the improvement of the knowledge related to advances in cancer cell biology.

Based on the status of important receptors (estrogen receptor (ER); progesterone receptor (PR); human epidermal growth factor receptor 2 (HER2)) breast cancer can be subdivided in four main classes: (i) Luminal A or (ii) Luminal B (hormone receptor positive – estrogen or progesterone), (iii) hormone receptor and HER2-positive and (iv) hormone receptor and HER2-negative (triple negative) [7]. A schematic representation of tumour subtyping is presented in Figure 1.

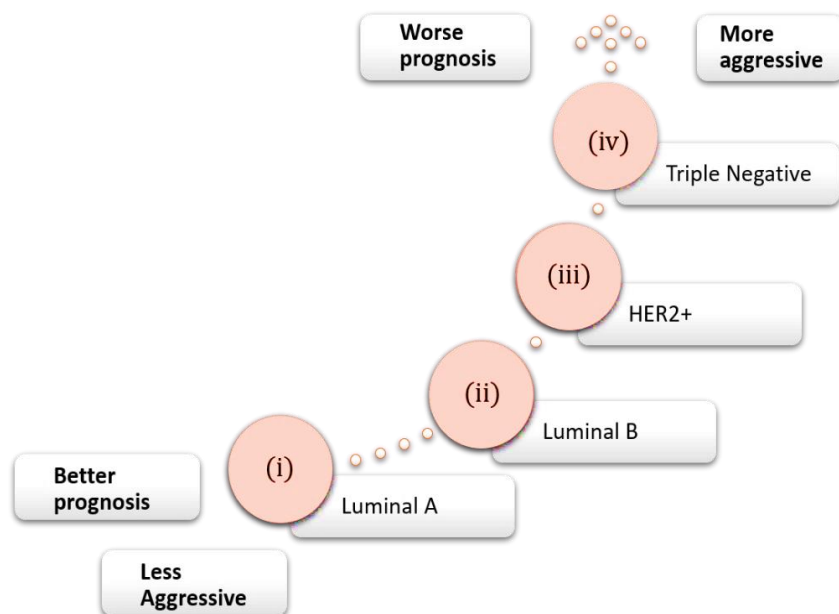


Figure 1. Tumour subtyping scheme. Adapted from [7].

1.3 Biomarkers for non-invasive analysis

Important research has been conducted to identify tumour biomarkers, which has led to advances in detection and treatments. The majority of biomarker assays are performed using cancer tissue. However, a simple blood test (liquid biopsy) that could detect cancer in its earliest stage could prevent millions of deaths, reduce the suffering of patients and the cost to society.

Tumour biomarkers are specific cancer related biomolecules (DNA, micro RNA, glycoproteins, hormone receptors, etc.) used in clinical settings for cancer detection and play a key role in the management of patients. Although there are many newly suggested breast cancer biomarkers (categorized in Figure 2), very few have been adopted into the clinic [8].

The commonly reported breast cancer biomarkers are: (i) the tissue markers – ERs, PRs, HER2; (ii) circulating markers – cancer antigen 15-3 (CA 15-3) and carcinoembryonic antigen (CEA). HER2 status characterization is now mandatory in all breast cancers and although it's an important prognostic biomarker, it's also a target for specific immunotherapies [9]. Detection of HER2's Extracellular Domain (HER2-ECD) in serum is not routine practice but is possible [10] and results may not only be important for diagnostic but also for prognosis, with even better results than tissue biopsy analysis [11]. So far, CA 15-3 has been adopted as a predictor of treatment failure in the metastatic setting. Indeed, with respect to CA 15-3 and CEA, a report has indicated that their combined detection may be more useful [9,11].

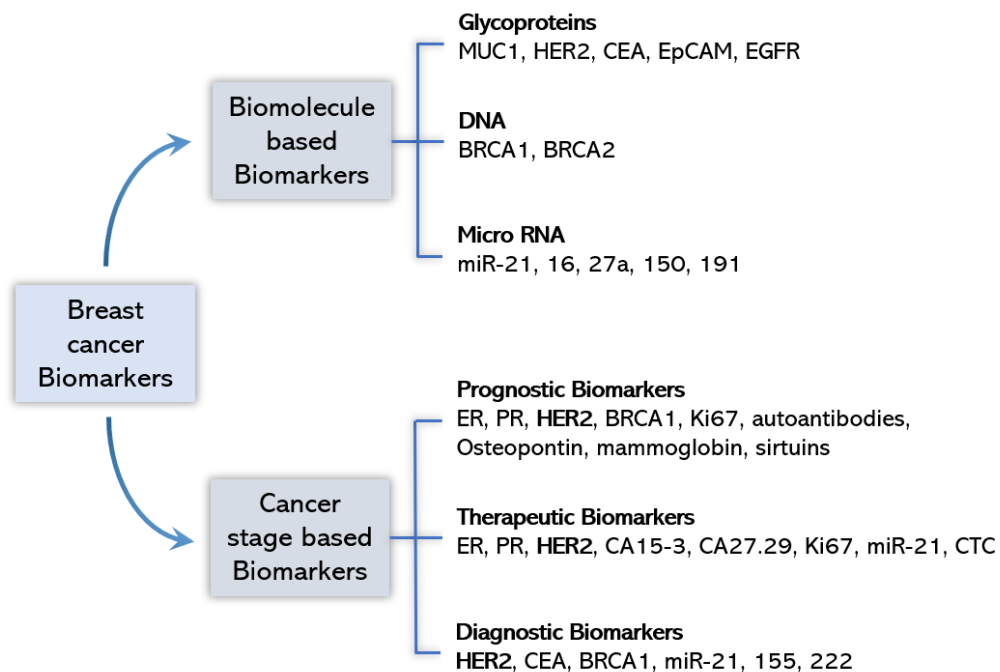


Figure 2. Breast cancer biomarkers classification. Adapted from [8].

Recent techniques for protein biomarker detection are based on enzyme-linked immunosorbent assays (ELISA) that are carried out in hospital laboratories. However, ELISAs are not sensitive enough to detect low biomarker concentrations present in the early stages of the disease [12]. Nonetheless, in diagnosed invasive breast cancer cases, estrogen and progesterone receptors must be measured [13].

The hot topic in cancer management at the moment is the enumeration and characterization of circulating tumour cells (CTCs). The ability of cell invasion and metastization is one of the cancer hallmarks and metastasis is the main responsible for deaths in breast cancer [14]. The enumeration of CTCs could be an important investigation area. However, the Food and Drug Administration (FDA)-approved method for CTC analysis (CellSearch®, Veridex, Raritan) is very expensive and its availability would be very limited if CTCs become a standard in clinical practice [15].

Regarding the analysis of the biomarkers in selected individuals, the necessary blood volume depends on the biomarker. For CA 15-3 and HER2 only a small amount (0.1-0.5 mL) is needed because their concentrations in positive samples are sufficiently high to be measured directly. For the determination of CTCs on the other hand a large volume (5-10 mL) is necessary because of the extremely low concentration of these cells in peripheral blood.

1.4 HER2-positive breast cancer: biology and clinical relevance

The human epidermal growth factor receptor family consists of four members: EGFR/ErbB1, HER2/ErbB2, HER3/ErbB3, HER4/ErbB4. The HER2 (HER2/neu, ErbB2 or CD340) is a 185 kDa glycoprotein, involved in normal cell growth. However, the increased expression levels of HER2 (protein overexpression) is usually associated with aggressive types of breast cancer and has also been described in other cancers (e.g. ovarian, stomach, pancreatic, lung, gastric, prostate) [16]. In this context, this protein is regarded as a key prognostic marker, or an effective therapeutic treatment target.

HER2 is considered an important biomarker in breast cancer detection. It is established as a diagnostic biomarker and is recommended for testing since it's overexpressed in approximately 20% of primary invasive breast cancers and is related with the most aggressive phenotypes [17].

Clinical treatment for HER2-positive breast cancer using biological drugs (anti-HER2 therapy) – e.g. trastuzumab, pertuzumab, lapatinib – was approved in metastatic breast cancer, being effective for eligible patients (with an excess of receptor levels), thus requiring appropriate screening tests [18].

The HER2 protein has three domains: (i) an extracellular region, (ii) a transmembrane hydrophobic section and (iii) an intracellular zone. The extracellular domain (ECD) of HER2 can be cleaved by matrix metalloproteases and therefore its levels can be measured in biological fluids [19]. HER2 is involved in cellular signaling pathways that can lead to cell proliferation, growth, apoptosis and differentiation. These processes have an important role on a cellular level, since loss of control of the signaling pathways is associated with disease [20]. Furthermore, research studies related to the analysis of live breast cancer cells, namely HER2-positive (HER2(+)) and HER2-negative (HER2(-)) cancer cell lines are of utmost importance to distinguish the different HER2 expression levels. Figure 3 outlines a normal cell and a HER2-positive cancer cell.

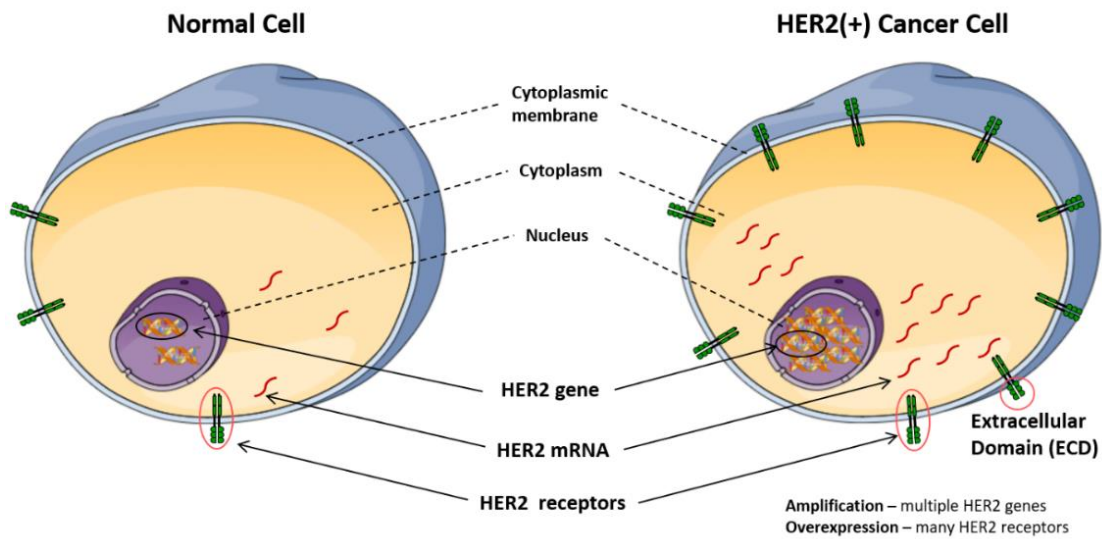


Figure 3. Simplified representation of normal cell and HER2(+) cancer cell.

1.5 Diagnostic tests in breast cancer: from prediction to follow-up

Breast self-examination is a screening method commonly recommended by healthcare professionals as a primary detection procedure. The examination is performed by palpation and the diagnosis is based on one's own opinion which may lead to a false positive or false negative result. To complement and avoid misdiagnosis, mammography is routinely performed for breast cancer screening. Although useful in an initial diagnosis, mammography's main shortcoming is that it's an imaging technique. This means that in the case of a positive result a biopsy is required to obtain a tissue sample [21].

Apart from these procedures, other methodologies/techniques are used for the diagnosis of breast cancer, namely magnetic resonance imaging (MRI), molecular breast imaging, thermography etc [8]. Moreover, different techniques have emerged and are performed for the analysis of protein biomarkers.

The FDA and the European Group on Tumour Markers (EGTM) reported that the main tests available to measure gene amplification and/or protein overexpression are immunohistochemistry (IHC), in situ hybridisation (ISH), fluorescence ISH (FISH) and ELISA [13,22]. However, for these tests often invasive procedures are required; a biopsy or the extraction of tissue samples, leading to patients suffering, and time-consuming and labour-intensive analysis. To overcome these problems, non-invasive analysis has emerged as a prominent alternative. Indeed, biomarker analysis allows early diagnosis, which is extremely useful in case of metastasis or even when the breast lumps are not visible due to their small size. Thus, new analytical methodologies that promote a sustainable alternative to the routine clinical methods have been reported.

1.6 POC devices: the case of biosensors

Point-of-care (POC) sensing strategies are widely demanded for the disease's detection in an early stage and during its management and follow-up. Biosensors with fast, accurate and POC detection possibilities are a preeminent alternative to measure cancer biomarker levels in bodily fluids over the traditional methods [23].

POC diagnostic platforms enable simple medical tests to be performed with or nearby the patient and allow results to be obtained in a fast or direct response time. The development and enhancement of lab-on-a-chip and biosensor technologies are in fact providing extraordinary tools for POC analysis [24].

The International Union of Pure and Applied Chemistry (IUPAC) has established the definition of Biosensor as “an integrated receptor-transducer device, which is capable of

providing selective quantitative or semi-quantitative analytical information using a biological recognition element” [25].

Biosensors can be classified according to the transducer and the bioreceptor. Usually, biosensors are composed of three components: the (physicochemical) transducer element, the biological recognition element and a signal processor. According to the bioreceptor, biosensors can be classified as enzymatic biosensors, genosensors, immunosensors, aptasensors, cytosensors, among others. Biosensors can also be divided into several categories based on the transduction process, such as electrochemical, optical, and mass-based biosensors [26], as can be observed in Figure 4.

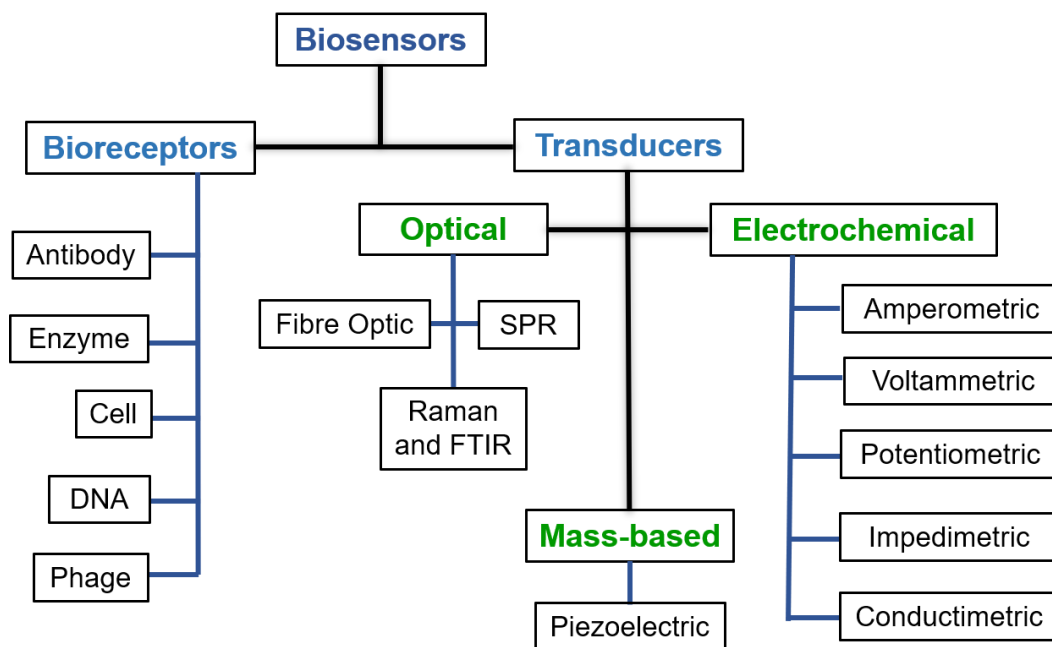


Figure 4. Biosensors classification. Adapted from [26].

The instrumentation needed to perform the analysis using biosensors has been reduced to (low-cost) pocket-size dimensions, which make them ideal for the inclusion in POC devices. In addition, the reasonable short assay times and the low sample volumes are also key features for a huge development of these devices [27]. Thus, the portability, miniaturization, low cost and rapid reliable response time of biosensors are some characteristics that could bridge the gap for in-field devices to be used for personalized medicine. In particular, research efforts towards the development of electrochemical biosensors to address important health issues have been growing in the last decades [28].



1.7 Voltammetric transduction

The basic principle of voltammetric transduction is the flow of electrons between electroactive species (i.e. a species that can be oxidised or reduced) and the electrode (transducer) surface when an adequate potential is applied. The resulting current can be measured by different voltammetric techniques that are widely used for fundamental studies of oxidation and reduction processes or electron transfer mechanisms.

The obtained signal is a characteristic current response called voltammogram (Figure 5). The potential of the oxidation/reduction peak (E_p) can be used for qualitative analysis and the peak current intensity (i_p) can be used for quantitative purposes [29,30].

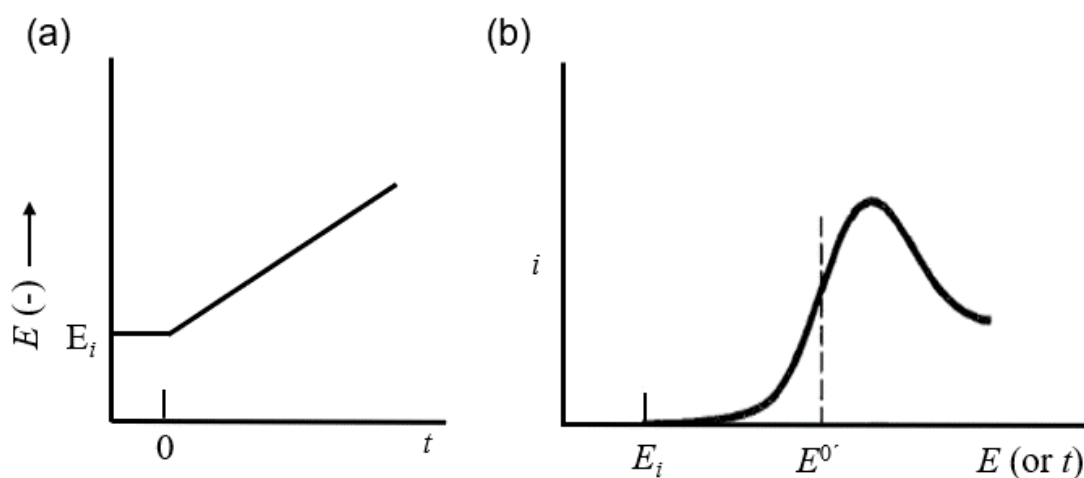


Figure 5. (a) Linear potential sweep and (b) resulting i - E curve (voltammogram). Adapted from [30].

Voltammetric cells generally incorporate a three-electrode configuration: reference-, auxiliary- and working electrodes (RE, AE and WE, respectively) that are placed in contact with the sample. The potential of the working electrode (WE), at which the analytical process of interest takes place, can be varied within a predefined potential range.

Despite excellent conventional electrodes, the development of screen-printed electrodes (SPE) allowed an improvement in the miniaturization process of the voltammetric cell and the measuring device. The SPE's configuration, where the three electrodes are located close to each other on a single platform, allows analysis to be performed with a reduced sample volume. Carbon, gold, graphite or platinum are commonly employed in the WE construction. Furthermore, the use of nanomaterials on the WE's surface can improve the assays' performance (e.g. sensitivity and selectivity), enabling advances in tracking (extremely) low levels of circulating biomarkers.

Gold and carbon-based nanomaterials, nanoparticles and magnetic materials are some of the most frequently applied in biosensor development. In this case, the nano- and micro-structured materials can improve the immobilization of the biomolecule of interest; enhance the sensor's sensitivity; increment the sensor's performance, among others [27].

Although several methods are reported for the synthesis of gold nanomaterials, a sustainable process consists of their electrodeposition using $[\text{AuCl}_4]^-$ [31].

Carbon-based nanomaterials allow efficient transducer modification that can be performed using graphene (reduced or oxidized) or single and multiwalled nanotubes. The combination of these materials is a prominent alternative for the construction and development of reliable biosensors [32].

On the other hand, superparamagnetic particles and/or beads (MP or MB) constitute a versatile tool for magnetic assays. The use of MPs or MBs in the practice of bioassays confers several advantages and alternatives, namely: the enhancement of sensitivity; the improvement of the assay performance; the reduction of the analysis time, allowing better biomolecule interactions and thus minimizing the matrix effect [33].

The use of modified/functionalized WEs in bioassay-based procedures with voltammetric detection can be adequate alternatives for biomarker analysis because of the high selectivity of the assay, the high sensitivity of voltammetry, which allows early detection of many diseases, and the speed of the analysis. Although research on the development of these assays for breast cancer markers has been increasing in the last years, the number of studies is still reduced when compared to other screening tools [34].

Examples of scanning electron microscopy (SEM) images of screen-printed carbon electrodes (SPCEs) modified with nano- and micro materials are presented in Figure 6: (a) non-modified SPCE, and SPCEs modified with (b) gold nanoparticles (AuNP), (c) multi-walled carbon nanotubes (MWCNT), (d) multi-walled carbon nanotubes and gold nanoparticles (MWCNT/AuNP), (e) gold-coated iron magnetic nanoparticles ($\text{Fe}_3\text{O}_4@$ AuNP) and (f) magnetic beads (MBs).

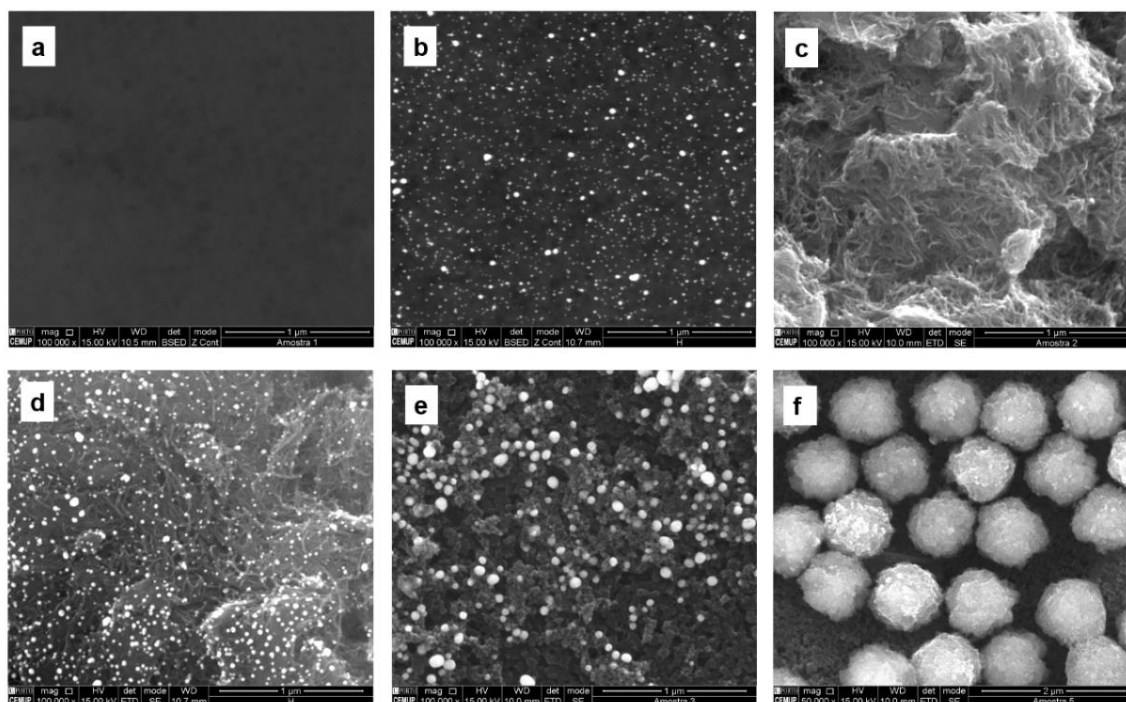


Figure 6. SEM images of the SPCE surfaces (used throughout this work). (a) non-modified SPCE, (b) SPCE-AuNP, (c) SPCE-MWCNT, (d) SPCE-MWCNT/AuNP, (e) SPCE-Fe₃O₄@AuNP and (f) SPCE-MBs.

In the electrochemical sensors developed using materials at nano- and micro scale, after the sensor construction the biological interaction can be transduced in a useful signal with an appropriate voltammetric technique [35].

The interest in voltammetric transduction resides in its excellent sensitivity, the accurate and precise results, high speed and experimental simplicity, allowing specific detection at low concentrations with reduced costs. For example, cyclic voltammetry (CV), linear sweep voltammetry (LSV), square wave voltammetry (SWV), and differential pulse voltammetry (DPV) are commonly employed.

Cyclic voltammetry (CV) is a powerful and versatile technique in the study of mechanisms of redox systems, allowing the characterization of oxidation/reduction potentials, the reversibility of the system, electron transfer kinetics, coupled chemical reactions, adsorption phenomena, etc. In CV the potential is swept between an initial potential (E₁) and a second potential (E₂) at a fixed rate v (V/s). When E₂ is reached, the direction of the potential sweep is reversed back to E₁ (various cycles can be performed).

LSV is a voltammetric technique in which the current at the WE is measured while the potential between the WE and RE is linearly swept over time [29].

Both CV and LSV present some limitations since the total measured current intensity includes both the faradaic current (resulting from the oxidation/reduction of the electroactive species) and the non-faradaic current (resulting from external currents; e.g. capacitive current and adsorption). A considerable instrumental improvement in the discrimination of the faradaic current from the capacitive current was possible due to the development of pulse techniques. Like this, the sensitivity is increased by increasing the ratio between the faradaic current and the capacitive/background currents [29,30].

DPV is a voltammetric technique where the potential perturbation, that consists of small pulses, is superimposed upon a staircase waveform. In this case the instrumentation has been developed in such a way that current measurements and potential pulses are performed at very short time intervals. More specifically, the current is sampled twice (before and after the pulse application) and the first current is subtracted from the second. The current difference is plotted versus the applied potential (Figure 7). DPV has become a widely used voltammetric technique and is useful to determine trace concentrations [36].

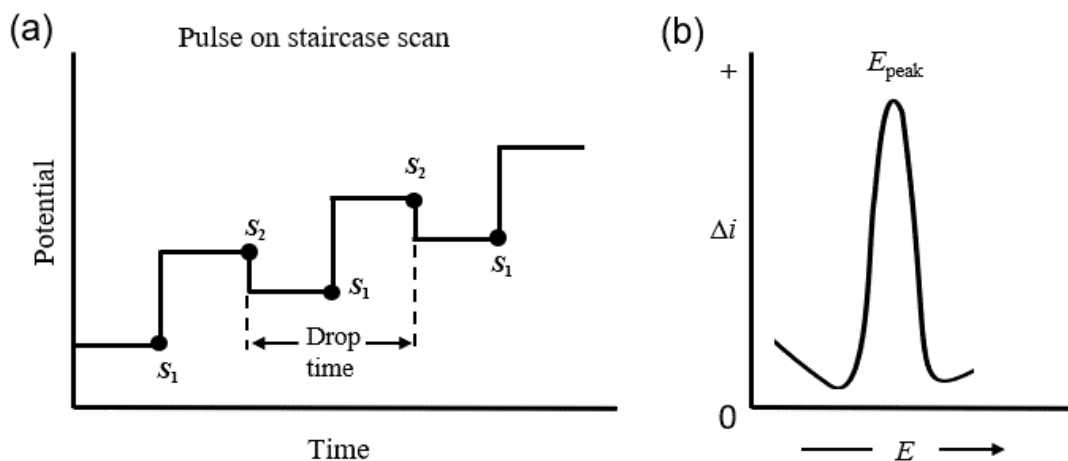


Figure 7. (a) Excitation signals and (b) voltammogram for a DPV experiment. Adapted from [36].

Although there are several voltammetric, undoubtedly all of them have characteristics of interest to be used in the development of biosensors.

An additional voltammetric technique is stripping voltammetry. A common technique used for preconcentration purposes is anodic stripping voltammetry, usually employed for trace metal ion determination. In this technique the preconcentration step consists of the application of a constant potential for the electrodeposition of the electroactive species. This step is followed by an equilibration time and a determination step. The latter consisting of stripping the previously electrodeposited species back in the solution. Thus, the three steps involved in anodic stripping voltammetry are: (i) preconcentration (deposition), (ii) equilibration, (iii) redissolution [29,36].

As an example, cadmium ion determination can be mentioned. Initially, the electrode potential is adjusted to a negative enough value to reduce cadmium ions to metallic cadmium, which is electrodeposited on the electrode. In the next step the potential is scanned to more positive (anodic) values, and the cadmium is redissolved returning to the solution due to its oxidation. When cadmium reoxidation occurs, the current will vary and the obtained i_p value is proportional to the cadmium concentration in the sample solution.

The preconcentration (electrochemical deposition) is a key step to achieve a higher analytical signal related to the concentration of the analyte in the solution, which also explains the increased sensitivity of the technique.

1.8 Electrochemical immunosensors and magnetic immunoassays

Electrochemical immunosensors and immunoassays are compact analytical tools that allow the detection of an antigen (e.g. cancer protein biomarker) in which the antigen-antibody interaction can be detected using a transducer that can convert the biochemical reaction into a measurable electrical signal that is then recorded and displayed [37]. When the recognition element or target analyte consists of an antibody or antigen as receptors, the event is denoted as immunosensing strategy. When an electrode is used to transduce the immunosensing strategy it can be classified as "electrochemical immunosensor". In addition, the interactions can occur either directly (biosensor) or indirectly (magnetic bioassay) on the transducer surface [32].

The procedure when an immunosensor is used consists of the sequential addition of biological components on the transducer surface, with appropriate washing steps between the incubation steps. In a magnetic immunoassay, effective separations and pre-concentrations of an antigen from large and complex samples can be achieved using an external magnetic field. In this assay type, the biological components are sequentially added to a microtube, where the immunological reactions occur. Like this, analyte isolation and purification are much easier and faster than with other methods [38], minimizing damage of biological materials and decreasing analysis times and costs [39,40]. The major drawbacks of the frequently used MPs for magnetic separation (MSep) are their particle size (100nm-micron) and the multiple steps required to improve bioconjugation. However, superparamagnetic and biocompatible platforms with high magnetization constitute a major advance. In this thesis, functionalized magnetic beads were used as biocompatible platforms to capture the selected biomarkers to develop magnetic immunoassays. The spherical MBs configuration results in a high surface area available to immobilize biomolecules, providing lower detection limits, and may lead to higher colloidal stability, improving their accessibility to the targets [41]. The high saturation magnetization and superparamagnetism enable faster and more efficient separations and prevent the particles' aggregation after the removal of the external magnetic field.

Among the distinct immunoassay formats (competitive, label-free, sandwich), the non-competitive (sandwich) assay is widely applied in electrochemical sensors. Contrary to non-competitive assays, the label-free assay usually does not require label, and detection is commonly performed using a redox pair as probe. Although in this strategy a short assay time is commonly reported, time-consuming transducer preparation or WE



functionalization (to enhance the electron transfer) is required. The non-competitive assay is vastly reported and consists of the binding of the antigen (target biomarker, present in the sample) to capture (Ab-C) and secondary/detection (Ab-D) antibodies, through the antibody's binding site (paratope). The Ab-C is immobilized on the WE, in the case of immunosensors, or on the magnetic particle surface, when magnetic assay is performed. The Ab-D is usually labelled (e.g. enzyme, electroactive compound) which allows the detection of the antibody/antigen interaction. In competitive assays the labels employed are similar to the ones reported for the sandwich assays. In this specific assay type, usually the antigens from the sample compete with labelled antigens (added to the sample) for the binding sites of the previously immobilized Ab-C on the electrode surface [27]. The common immobilization methods for the Ab-C are physical adsorption, covalent binding, matrix entrapment, cross-linking and affinity binding [32].

Figure 8 shows the schematic representation of an electrochemical immunosensor, the transducer connection and the signal processor.

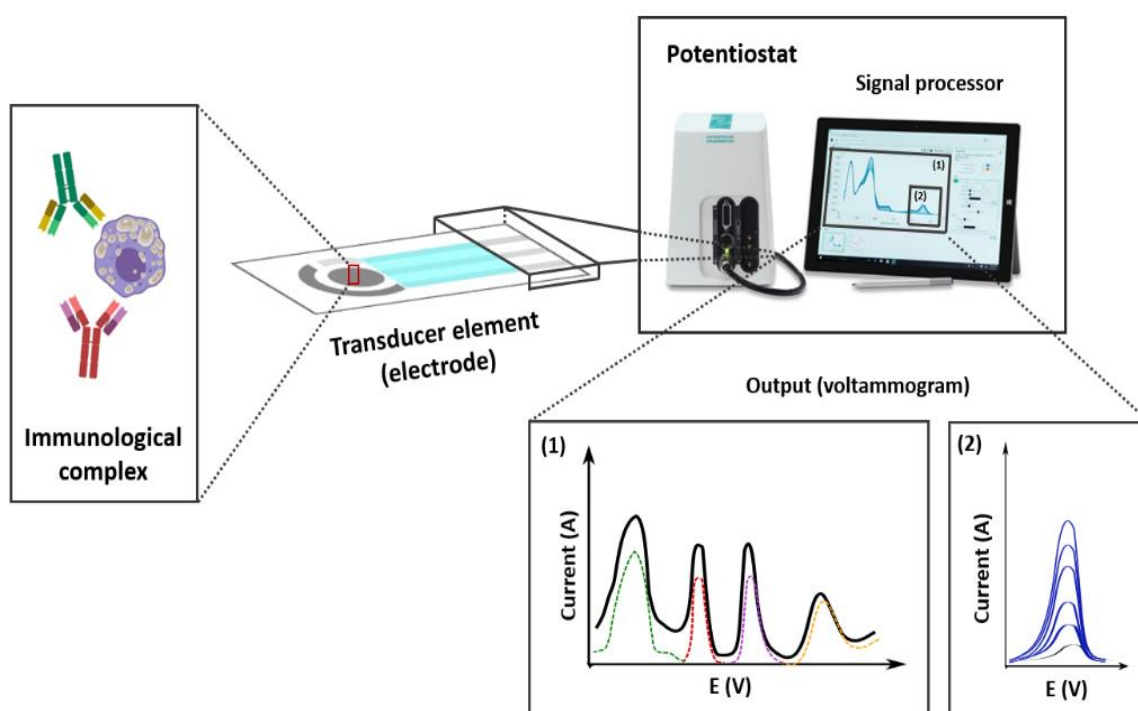


Figure 8. Scheme of an electrochemical immunosensor. Voltammetric signal is obtained for distinct analytes, which allows (1) simultaneous or (2) individual detection.

1.8.1 Metalloenzymatic detection

Figure 9 schematically represents one of the immunoassay's detection strategies used in the present thesis. This strategy is based on metalloenzymatic detection, in which, after the capture antibody's immobilization and the incubation with the antigen and the detection antibody (labelled with the enzyme alkaline phosphatase), the enzymatic substrate (3-indoxyl phosphate, 3-IP) combined with silver ions (silver nitrate) are added. In this step AP hydrolyzes 3-IP resulting in an indoxyl intermediate that reduces the silver ions in solution to metallic silver and indigo blue [42]. The electrochemical signal of the enzymatically generated metallic silver is then recorded by LSV.

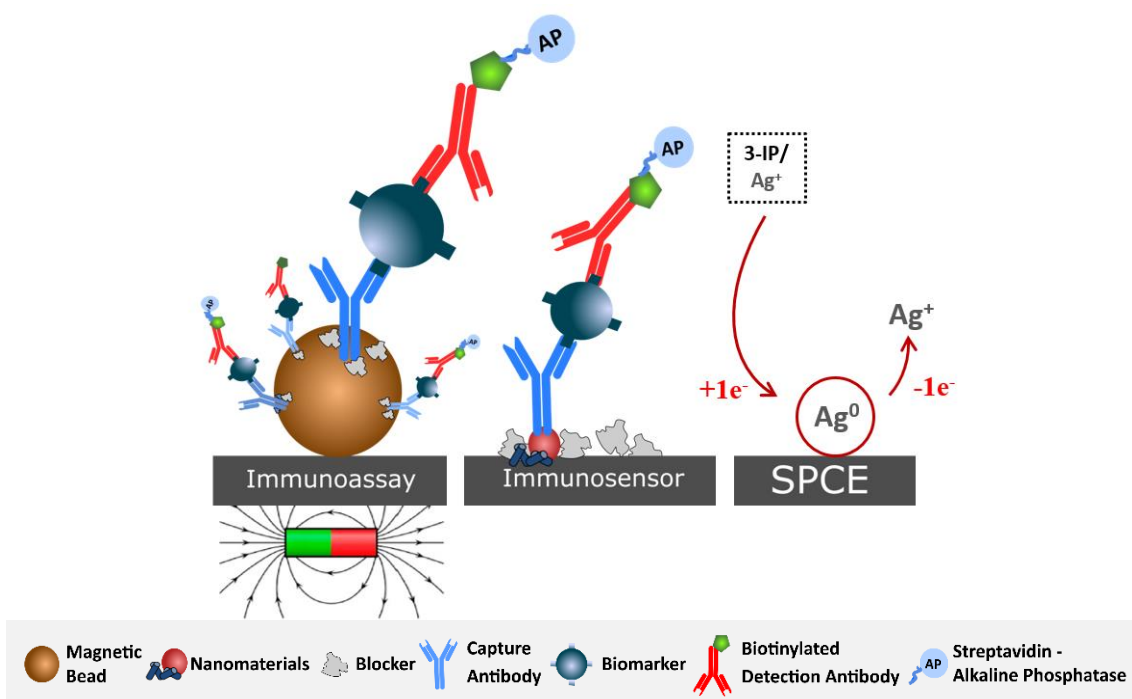


Figure 9. Schematic representation of the metalloenzymatic detection strategy.

Although enzymes are widely used as labels in bioassay practice due to their high selectivity and efficiency, they have some drawbacks, namely the low stability; the cross-reactivity with plasma constituents, etc. [43]. In fact, working with electroactive labels surpasses thermal instability aspects, intrinsic to the nature of enzymes, which are the main disadvantages in their use [44]. Compared to laborious enzymatic methodologies, the use of QDs eliminates the need for substrate addition, which can contribute for the reduction of the analysis time.

1.8.2 Metallic nanoparticles as electrochemical detection labels

Nanoparticle-based signal amplification has a huge interest since excellent stability, higher sensitivity, easy of mass production (large scale) and lower synthesis costs can be achieved. The high amplification and multiplexing properties of metallic nanoparticles (e.g. quantum dots (QDs)) make them ideal labels for immunoassays [45], resulting in more sensitive, faster and cheaper analysis [22]. Briefly, in the assay used in the present thesis, the antigen is linked to the Ab-C immobilized on the SPCE or MPs/MBs, followed by incubation with a secondary detection antibody (labelled with QDs), as can be observed in Figure 10. Then, the QDs are dissolved with a HCl solution. Subsequently, an aliquot of acetate buffer (pH 4-5) containing Bi(III) is added and the voltammetric procedure is applied (differential pulse anodic stripping voltammetry, DPASV). In this procedure a bismuth film is formed on the electrode and, simultaneously, the dissolved (ionic) metal label (Cd^{2+}), is reduced to its solid state by applying a constant negative potential and then stripped into solution using an anodic potential scan. The resulting current increases with increasing biomarker concentration.

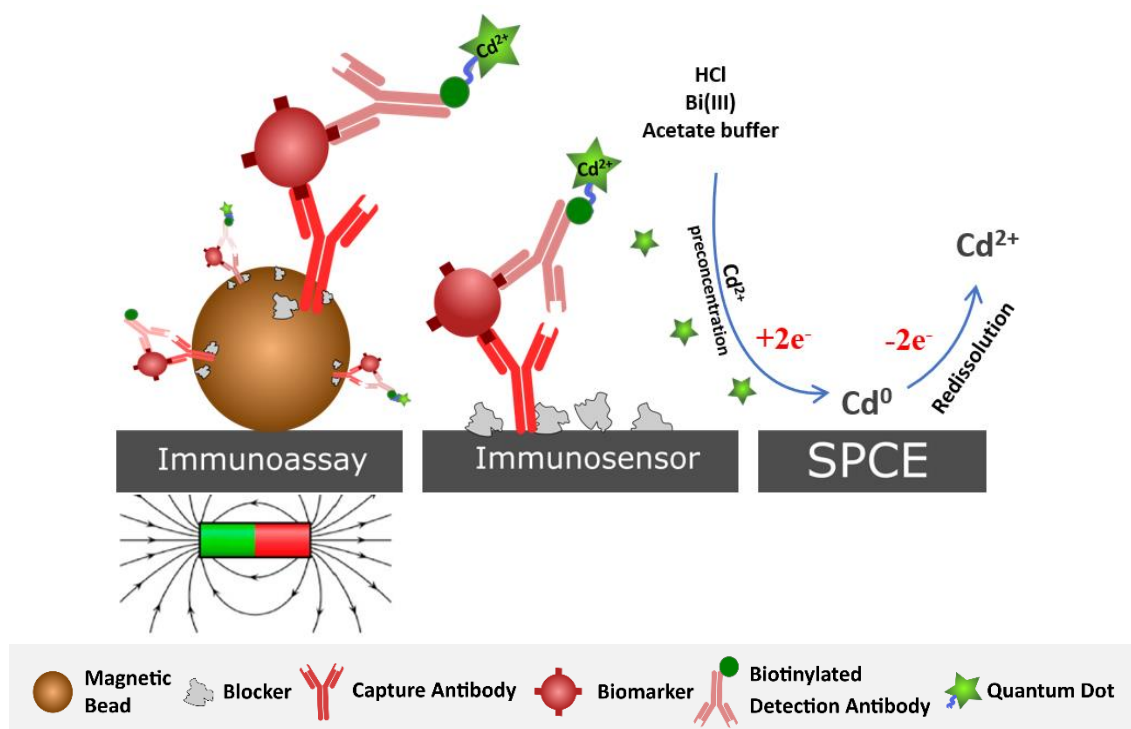


Figure 10. Schematic representation of the detection strategy using quantum dots.

References

- [1] World Health Organization. Cancer. **2018**. Available from: <https://www.who.int/en/news-room/fact-sheets/detail/cancer>.
- [2] International Agency for Research on Cancer. Cancer screening in the European Union (2017): report on the implementation of the council recommendation on cancer screening. **2017**. <https://screening.iarc.fr/EUreport.php>
- [3] J Ferlay, M Colombet, I Soerjomataram, T Dyba, G Randi, M Bettio, A Gavin, O Visser, F Bray. Cancer incidence and mortality patterns in Europe: Estimates for 40 countries and 25 major cancers in 2018. *European Journal of Cancer* **2018**, 103, 356-387. <https://doi.org/10.1016/j.ejca.2018.07.005>
- [4] F Bray, J Ferlay, I Soerjomataram, RL Siegel, LA Torre, A Jemal. Global cancer statistics 2018: GLOBOCAN estimates of incidence and mortality worldwide for 36 cancers in 185 countries. *CA: A Cancer Journal for Clinicians* **2018**, 68(6), 394-424. <https://doi.org/10.3322/caac.21492>
- [5] N Patani, L-A Martin, M Dowsett. Biomarkers for the clinical management of breast cancer: International perspective. *International Journal of Cancer*. **2013**, 133, 1-13. <https://doi.org/10.1002/ijc.27997>
- [6] GW Sledge, EP Mamounas, GN Hortobagyi, HJ Burstein, PJ Goodwin, AC Wolff. Past, present, and future challenges in Breast Cancer Treatment. *Journal of Clinical Oncology* **2014**, 32 (19), 1979-1986. <https://doi.org/10.1200/JCO.2014.55.4139>
- [7] X Dai, H Cheng, Z Bai, J Li. Breast Cancer Cell Line Classification and Its Relevance with Breast Tumor Subtyping. *Journal of Cancer* **2017**, 8(16), 3131-3141. <https://doi.org/10.7150/jca.18457>
- [8] S Mittal, H Kaur, N Gautam, AK Mantha. Biosensors for breast cancer diagnosis: A review of bioreceptors, biotransducers and signal amplification strategies. *Biosensors and Bioelectronics* **2017**, 88, 217–231. <https://doi.org/10.1016/j.bios.2016.08.028>
- [9] E Senkus, S Kyriakides, F Penault-Llorca, P Poortmans, A Thompson, S Zackrisson, F Cardoso, ESMO Guidelines Working Group. Primary breast cancer: ESMO Clinical Practice Guidelines for diagnosis, treatment and follow-up. *Annals of Oncology* **2015**, 26 (Supplement 5), v8–v30. <https://doi.org/10.1093/annonc/mdv298>
- [10] L Lam, N McAndrew, M Yee, T Fu, JC Tchou, H Zhang. Challenges in the clinical utility of the serum test for HER2 ECD. *Biochimica et Biophysica Acta* **2012**, 1826(1), 199-208. <https://doi.org/10.1016/j.bbcan.2012.03.012>
- [11] D Gioia, M Dresse, D Mayr, D Nagel, V Heinemann, P Stieber. Serum HER 2 in combination with CA 15-3 as a parameter for prognosis in patients with early breast cancer. *Clinica Chimica Acta* **2015**, 440, 16-22.



<https://doi.org/10.1016/j.cca.2014.11.001>

[12] IE Tothill. Biosensors for cancer markers diagnosis. *Seminars in Cell & Developmental Biology* **2009**, 20, 55-62. <https://doi.org/10.1016/j.semcd.2009.01.015>

[13] MJ Duffy, N Harbeck, M Nap, R Molina, A Nicolini, E Senkus, F Cardoso. Clinical use of biomarkers in breast cancer: Updated guidelines from the European Group on Tumor Markers (EGTM). *European Journal of Cancer* **2017**, 75, 284-298.

<https://doi.org/10.1016/j.ejca.2017.01.017>

[14] D Hanahan, RA Weinberg. Hallmarks of Cancer: The next generation. *Cell* **2011**, 144 (5), 646-674. <https://doi.org/10.1016/j.cell.2011.02.013>

[15] J Castle, H Shaker, K Morris, JD Tugwood, CC Kirwan. The significance of circulating tumour cells in breast cancer: A review. *The Breast* **2014**, 23 (5), 552-560.

<https://doi.org/10.1016/j.breast.2014.07.002>

[16] N Iqbal, N Iqbal. Human Epidermal Growth Factor Receptor 2 (HER2) in Cancers: Overexpression and Therapeutic Implications. *Molecular Biology International* **2014**, 2014, 852748. <https://doi.org/10.1155/2014/852748>

[17] AC Wolff, M Elizabeth, H Hammond, KH Allison, BE Harvey, PB Mangu, JMS Bartlett, M Bilous, IO Ellis, P Fitzgibbons, W Hanna, RB Jenkins, MF Press, PA Spears, GH Vance, G Viale, LM Mcshane, M Dowsett. Human epidermal growth factor receptor 2 testing in breast cancer: American society of clinical oncology/college of American pathologists clinical practice guideline focused update. *Journal of Clinical Oncology* **2018**, 36, 2105-2122. <https://doi.org/10.1200/JCO.2018.77.8738>

[18] CA Hudis. Trastuzumab-mechanism of action and use in clinical practice. *The New England Journal of Medicine* **2007**, 357, 39-51. <https://doi.org/10.1056/NEJMra043186>

[19] C Tsé, AS Gauchez, W Jacot, PJ Lamy. HER2 shedding and serum HER2 extracellular domain: biology and clinical utility in breast cancer. *Cancer treatment reviews* **2012**, 38, 133-142. <https://doi.org/10.1016/j.ctrv.2011.03.008>

[20] JL Hsu, M-C Hung. The role of HER2, EGFR, and other receptor tyrosine kinases in breast cancer. *Cancer metastasis reviews* **2016**, 35(4), 575-588.

<https://doi.org/10.1007/s10555-016-9649-6>

[21] P Autier, M Boniol. Mammography screening: A major issue in medicine. *European Journal of Cancer* **2018**, 90:34–62. <https://doi.org/10.1016/j.ejca.2017.11.002>

[22] M Labib, EH Sargent, SO Kelley. Electrochemical Methods for the Analysis of Clinically Relevant Biomolecules. *Chemical Reviews* **2016**, 116, 16, 9001-9090.

<https://doi.org/10.1021/acs.chemrev.6b00220>

- [23] S Campuzano, P Yáñez-Sedeño, JM Pingarrón. Current trends and challenges in bioelectrochemistry for non-invasive and early diagnosis. *Current Opinion in Electrochemistry* **2018**, 12:81–91. <https://doi.org/10.1016/j.coelec.2018.04.015>
- [24] E Primiceri, MS Chiriaco, FM Notarangelo, A Crocamo, D Ardissino, M Cereda, AP Bramanti, MA Bianchessi, G Giannelli, G Maruccio. Key Enabling Technologies for Point-of-Care Diagnostics. *Sensors (Basel)* **2018**, 18(11), E3607. <https://doi.org/10.3390/s18113607>
- [25] DR Thévenot, K Toth, RA Durst, GS Wilson. Electrochemical biosensors: recommended definitions and classification. *Biosensors and Bioelectronics* **2001**, 16(1-2), 121-31. [https://doi.org/10.1016/S0956-5663\(01\)00115-4](https://doi.org/10.1016/S0956-5663(01)00115-4)
- [26] V Velusamy, K Arshak, O Korostynska, K Oliwa, C Adley. An overview of foodborne pathogen detection: In the perspective of biosensors. *Biotechnology Advances* **2010**, 28 232-254. <https://doi.org/10.1016/j.biotechadv.2009.12.004>
- [27] M Freitas, HPA Nouws, C Delerue-Matos. Electrochemical biosensing in cancer diagnostics and follow-up. *Electroanalysis* **2018**, 30, 1576-1595. <https://doi.org/10.1002/elan.201800193>
- [28] MMPS Neves, MB González-García, D Hernández-Santos, P Fanjul-Bolado. Future trends in the market for electrochemical biosensing. *Current Opinion in Electrochemistry* **2018**, 10, 107–111. <https://doi.org/10.1016/j.coelec.2018.05.002>
- [29] DA Skoog, SR Crouch, FJ Holler, DM West. Fundamentals of Analytical Chemistry. *Published by Cengage Learning, Inc.* **2013**, pp. 1-1072. ISBN 9780495558286.
- [30] AJ Bard, LR Faulkner, Electrochemical Methods Fundamentals of Electrochemistry. *Published by John Wiley & Sons, Inc.* New York, USA. **2001**, pp. 1-850. ISBN 0-471-04372-9.
- [31] G Martínez-Paredes, MB González-García, A Costa-García. In situ electrochemical generation of gold nanostructured screen-printed carbon electrodes. Application to the detection of lead underpotential deposition. *Electrochimica Acta* **2009**, 54, 4801-4808. <https://doi.org/10.1016/j.electacta.2009.03.085>
- [32] W. Putzbach, NJ Ronkainen. Immobilization Techniques in the Fabrication of Nanomaterial-Based Electrochemical Biosensors: A Review. *Sensors (Basel)* **2013**, 13(4), 4811-4840. <https://doi.org/10.3390/s130404811>
- [33] P Yáñez-Sedeño, S Campuzano, JM Pingarrón. Magnetic particles coupled to disposable screen-printed transducers for electrochemical biosensing. *Sensors* **2016**, 16, 1585-1617. <https://doi.org/10.3390/s16101585>

- [34] I Diaconu, C Cristea, V Hârceagă, G Marrazza, I Berindan-Neagoe, Robert Săndulescu, Electrochemical immunosensors in breast and ovarian cancer. *Clinica Chimica Acta* **2013**, 425, 128-138. <https://doi.org/10.1016/j.cca.2013.07.017>
- [35] X Pei, B Zhang, J Tang, B Liu, W Lai, D Tang. Sandwich-type immunosensors and immunoassays exploiting nanostructure labels: A review. *Analytica Chimica Acta* **2013**, 758, 1-18. <https://doi.org/10.1016/j.aca.2012.10.060>
- [36] J Wang. Analytical Electrochemistry, Third Edition. *Published by John Wiley and Sons, Inc.* New York, USA. **2006**, pp. 1-250. ISBN 0-471-28272-3.
- [37] FS Felix, L Angnes. Electrochemical immunosensors – A powerful tool for analytical applications. *Biosensors and Bioelectronics* **2018**, 102, 470-478.
- [38] K Aguilar-Arteaga, JA Rodriguez, E Barrado. Magnetic solids in analytical chemistry: A review. *Analytica Chimica Acta* **2010**, 674, 157-165. <https://doi.org/10.1016/j.bios.2017.11.029>
- [39] I-M Hsing, Y Xu, W Zhao. Micro- and Nano- Magnetic Particles for Applications in Biosensing. *Electroanalysis* **2007**, 19, 755-768. <https://doi.org/10.1002/elan.200603785>
- [40] AA Ansari, M Alhoshan, MS Alsalhi, AS Aldwayyan. Prospects of Nanotechnology in Clinical Immunodiagnosics. *Sensors* **2010**, 10, 6535-6581. <https://doi.org/10.3390/s100706535>
- [41] R Ladj, A Bitar, M Eissa, Y Mugnier, R Le Dantec, H Fessia, A Elaissaria. Individual inorganic nanoparticles: preparation, functionalization and in vitro biomedical diagnostic applications. *Journal of Materials Chemistry B* **2013**, 1, 1381-1396. <https://doi.org/10.1039/C2TB00301E>
- [42] P Fanjul-Bolado, D Hernández-Santos, MB González-García, A Costa-García. Alkaline Phosphatase-Catalyzed Silver Deposition for Electrochemical Detection. *Analytical Chemistry* **2007**, 79, 5272-5277. <https://doi.org/10.1021/ac070624o>
- [43] MJ O'sullivan, JW Bridges, V Marks. Enzyme Immunoassay: A Review. *Annals of clinical biochemistry* **1979**, 16, 221-240. <https://doi.org/10.1177/000456327901600162>
- [44] Y Liu, L Zhang, Q Guo, H Hou, T You. Enzyme-free ethanol sensor based on electrospun nickel nanoparticle-loaded carbon fiber paste electrode. *Analytica Chimica Acta* **2010**, 663, 153-157. <https://doi.org/10.1016/j.aca.2010.01.061>
- [45] J Wang. Nanoparticle-Based Electrochemical Bioassays of Proteins. *Electroanalysis* **2007**, 19, 769-776. <https://doi.org/10.1002/elan.200603789>

CHAPTER 2

2

ELECTROCHEMICAL BIOSENSING IN CANCER – INSIGHTS AND CHALLENGES

2

Overview

This chapter presents a review article. An integral transcript of the published article is presented according to the journal rights and with requested permission (section 2.1). In addition, an update of the review work was carried out specifically for the biomarker studied in this thesis: HER2 (section 2.2).

Briefly, a literature revision related to electrochemical immunosensors and immunoassays in cancer diagnostics and follow-up was carried out with the aim of gathering information about the state-of-the-art.

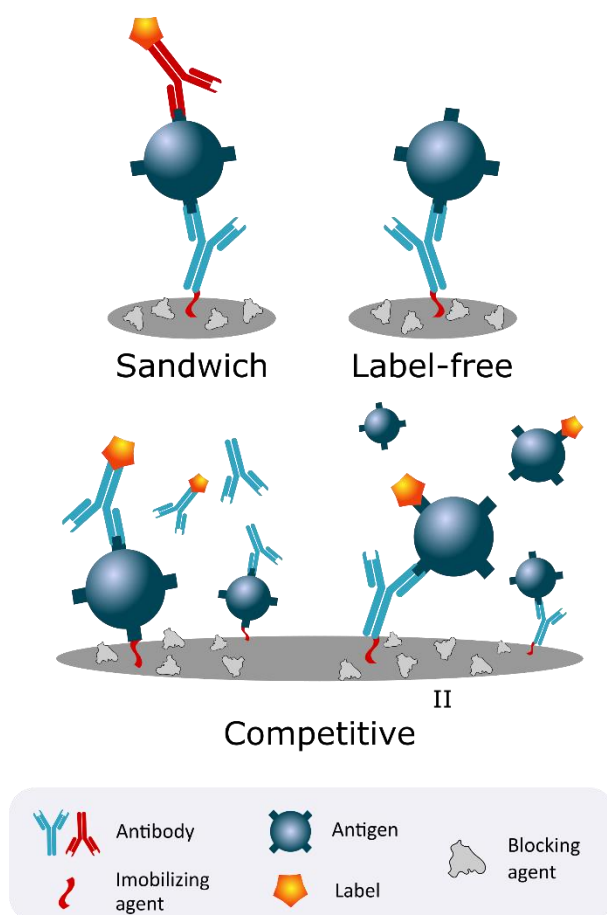
From the clinical point-of-view, although routine methodologies are adopted by local hospitals and oncological centers, there is a need for new analytical methodologies and point-of-care devices for non-invasive analysis of cancer biomarkers. Challenges regarding the analytical characteristics of electrochemical biosensors for detection and quantification of cancer biomarkers, as target analytes, of relevant cancer-types are highlighted in this bibliographic work.

A survey of the published studies shows the continuous progress and the evolution of analytical methodologies for an increasingly effective diagnosis. The attention in this research area is now mainly focussed on the increase of the sensitivity through different types of transducer modifications, sensing surface constructions and detection strategies. The low limits of detection achieved with the developed sensors allows the diagnosis of cancer in an early stage.

The first author contribution includes data compilation; tables construction; preparation and drawing of images and schemes; writing and editing the manuscript (original draft – Lead).

2.1 Electrochemical Biosensing in Cancer Diagnostics and Follow-up

Electroanalysis 30 (8) (2018) 1576-1595



Author Contributions:

Maria Freitas (investigation: Equal; Methodology: Equal; Writing – original draft: Lead); Henri Nouws (Conceptualization: Lead; Funding acquisition: Equal; Methodology: Lead; Project administration: Equal; Supervision: Equal; Validation: Equal; Writing – review & editing: Lead); Cristina Delerue-Matos (Funding acquisition: Equal; Methodology: Equal; Supervision: Equal; Validation: Equal; Writing – review & editing: Supporting)

DOI: 10.1002/elan.201800193

Electrochemical Biosensing in Cancer Diagnostics and Follow-up

Maria Freitas,^[a] Henri P. A. Nouws,^{*,[a]} and Cristina Delerue-Matos^[a]

Abstract: In cancer, screening and early detection are critical for the success of the patient's treatment and to increase the survival rate. The development of analytical tools for non-invasive detection, through the analysis of cancer biomarkers, is imperative for disease diagnosis, treatment and follow-up. Tumour biomarkers refer to substances or processes that, in clinical settings, are indicative of the presence of cancer in the body. These biomarkers can be detected using biosensors, that, because of their fast, accurate and point of care applicability, are prominent alternatives to the traditional methods. Moreover, the constant innovations in the biosensing field improve the determination of normal and/or elevated levels of tumour biomarkers in patients' biological fluids (such as serum, plasma, whole blood, urine, etc.). Although several biomarkers (DNA, RNA,

proteins, cells) are known, the detection of proteins and circulating tumour cells (CTCs) are the most commonly reported due to their approval as tumour biomarkers by the specialized entities and commonly accepted for diagnosis by medical and clinical teams. Therefore, electrochemical immunosensors and cytosensors are vastly described in this review, because of their fast, simple and accurate detection, the low sample volumes required, and the excellent limits of detection obtained. The biosensing strategies reported for the six most commonly diagnosed cancers (lung, breast, colorectal, prostate, liver and stomach) are summarized and the distinct phases of the sensors' constructions (surface modification, antibody immobilization, immunochemical interactions, detection approach) and applications are discussed.

Keywords: cancer biomarker • electrochemical biosensing • immunosensor • cytosensor • nanomaterial

1 Introduction

The International Agency for Research on Cancer (IARC) estimated that in 2012 there were 14.1 million new cancer cases, 8.2 million cancer deaths and 32.6 million people living with cancer (within 5 years of diagnosis) worldwide [1].

According to the World Health Organization (WHO) cancer is a generic term for a large group of diseases that can affect any part of the body. The major feature of cancer is the rapid creation of abnormal cells that grow beyond their usual boundaries, and can then spread to other organs, a process referred to as metastasis, which is the major cause of death from cancer [2].

The most commonly diagnosed cancers in 2012 were lung (1.82 million), breast (1.67 million), colorectal (1.36 million), prostate (1.1 million cases), stomach (951000 cases) and liver (782000 cases). These six cancers represent 55 percent of the global incidence burden in 2012 [1].

When cancer is present in the body the levels of several substances can be altered both in or on tumour cells as well as in biological fluids (blood, urine, etc.). These substances are produced by cancer cells or by other cells of the body in response to cancer or certain benign (noncancerous) conditions [3] and are referred to as biomarkers. This includes abnormalities in DNA (germline or somatic), RNA, proteins, metabolites, and abnormal cellular or tissue processes. A particular cancer type

can be detected through qualitative and/or quantitative analysis of a certain biomarker [4]. These biomarkers may also be used to monitor the response to treatment and allow patient follow-up. The identification of circulating (peripheral blood) biomarkers, analysed in so called "liquid biopsies", would have enormous implications in diagnosis and treatment [5] and avoid the traditional invasive biopsy.

2 Cancer Biomarkers

Currently, a wide range of specific biomolecules has been proposed as potential biomarkers for cancer detection. However, the vast majority still need to be validated for use in the clinical setting, mainly because of lack of specificity and/or sensitivity. Protein biomarkers can be detected in distinct cancer stages and are classified as prognostic, therapeutic or diagnostic biomarkers. The screening and evaluation of an individual's susceptibility to cancer can contribute and support the decisions of medical teams, underlying the risk of incidence or progression. The detection is normally conducted in bio-

[a] M. Freitas, H. P. A. Nouws, C. Delerue-Matos
REQUIMTE/LAQV, Instituto Superior de Engenharia do Porto, Politécnico do Porto, Rua Dr. António Bernardino de Almeida, 4200-072 Porto, Portugal
E-mail: han@isep.ipp.pt

Review

ELECTROANALYSIS

logical fluids, with serum being the most desirable testing matrix in clinical tests. This non-invasive practise has revitalized early detection [6].

The electrochemical analysis of circulating protein biomarkers is the main focus of this review because of their potential prognostic value. However, a detailed description of these biomarkers is beyond the scope of this review and the authors' expertise. Therefore, a short summary of the common protein biomarkers used for the development of electrochemical immunosensors related to the six most commonly diagnosed cancers in 2012 is presented in Table 1.

Table 1. Some protein cancer biomarkers.

Cancer	Protein Biomarker	Ref
Lung	Neuron-Specific Enolase (NSE)	[14–19] [20–22]
	Squamous Cell Carcinoma antigen (SCC)	
Breast	Human epidermal growth factor receptor 2 (HER2)	[23–30] [31–39]
	Cancer Antigen 15-3 (CA 15-3)	
Colorectal and Stomach	Cancer Antigen 19-9 (CA 19-9)	[40–43]
Prostate	Prostate-Specific Antigen (PSA)	[44–69]
Liver Stomach	α -1-Fetoprotein (AFP)	[70–99]
	Cancer Antigen 72-4 (CA 72-4)	[100–101] [102]
	Interleukin-6 (IL-6)	

(i) Lung cancer, the most incident cancer-type with the highest cancer mortality rate worldwide, is mainly divided into two broad categories: small-cell lung carcinoma (SCLC) and non-small cell lung carcinoma (NSCLC). Neuron specific enolase (NSE) is a specific protein marker in lung cancer detection and a high percentage of patients with SCLC have elevated serum NSE concentrations at diagnosis. On the other hand, cytokeratin fragment 21-1 (CYFRA 21-1), squamous cell carcinoma antigen (SCC) and carcinoembryonic antigen (CEA) have been associated with NSCLC cases, which represent the vast majority of lung cancer cases [7]; (ii) Breast cancer is a healthcare concern of women worldwide. The protein biomarkers with evidence of clinical utility for breast cancer include CEA, Human epidermal growth factor receptor 2 (HER2) and Cancer Antigen 15-3 (CA 15-3) [8]; (iii) Colorectal cancer (CRC) is the second most commonly diagnosed cancer among women and third among men worldwide. Two of the most widely known serum protein biomarkers for CRC are the Cancer Antigen 19-9 (CA 19-9) and CEA. Simultaneous detection of both biomarkers is beneficial in evaluating the therapeutic effect [9]; (iv) Prostate cancer is the most common cancer-type in men. Prostate specific antigen (PSA) is the classic and the most widely used protein biomarker for clinical diagnosis [10]; (v) Hepatocellular carcinoma (HCC) is the fifth most common cancer, representing more than 90% of primary liver cancer, and is frequently detected by α -fetoprotein (AFP). Nevertheless, three serum biomarkers are normally suggested to determine the risk of liver cancer: AFP, AFP-L3, and des-gamma-carboxy-prothrombin (DCP) [11]; (vi) Stomach cancer, also known as gastric cancer, remains one of the leading challenges in oncologic research because of its frequent occurrence and poor prognosis. Besides the



Maria Freitas obtained her degree in Biochemistry in 2010 from University of Trás-os-Montes and Alto Douro (Portugal) and her MSc degree in Quality Control in 2012 from Faculty of Pharmacy, University of Porto, Portugal. Currently she is a Ph. D. student in doctoral program on Sustainable Chemistry at REQUIMTE and her research interests include the development of electrochemical methodologies (immunosensors and MIPs) for the analysis of cancer biomarkers, and synthesis of nanomaterials, mainly magnetic core/shell nanoparticles.



Henri P.A. Nouws obtained his PhD in Chemistry in 2007 (Faculty of Sciences, University of Porto, Portugal). Currently he is an auxiliary professor at the Chemical Engineering Department of the School of Engineering, Polytechnic Institute of Porto (ISEP-IPP, Portugal). He is also an integrated research member of REQUIMTE and his present research interests include the



development of analytical (electrochemical) methodologies for pharmaceutical, clinical, and food analysis.

Cristina Delerue-Matos obtained her PhD in Chemical-Physics, specialty in electrochemistry, in 1990. She is principal coordinator professor at the School of Engineering of the Polytechnic Institute of Porto (ISEP-IPP, Portugal) and also coordinates the REQUIMTE/ISEP research group (www.graq.isep.ipp.pt). Her research interests include the development of analytical methodologies for environmental, food, pharmaceutical, biochemical and industrial control. She is co-author of more than 250 publications in scientific journals.

Review

classical serum-based protein biomarkers associated with stomach cancer (CEA, CA 19-9 and Cancer Antigen 72-4 (CA 72-4)), the interleukin IL6 is also considered a valuable biomarker for this type of cancer [12].

As referred previously, several classic biomarkers are eligible for cancer diagnosis. However, a careful and judicious decision is often necessary to avoid false results and thus a misdiagnosis. The simultaneous (multiplexed) detection of distinct biomarkers could avoid these problems. For example, CEA leads to effective cancer detection, but is non-specific (it is commonly used to monitor several cancer types, such as colorectal, lung, gastric, pancreas, liver and breast) So, its overexpression only indicates the presence of an elevated amount of cancer cells [13]. Therefore, the combination of CEA and other more specific biomarkers can greatly contribute to a more reliable diagnosis.

Throughout this review the state of the art of electrochemical immunosensors and immunoassays in the field of cancer analysis is discussed. Besides this, because of the large number of recent developments related to circulating tumor cells (CTCs), the detection of these cells using electrochemical devices is also included. For the selected analytical strategies included in this work the actual design, construction and detection approach are analysed and discussed. The most relevant topics related to the recently published electrochemical sensors are presented in summarized tables.

3 Electrochemical Biosensors

The established tests to determine cancer biomarkers are based on invasive methods, such as biopsies, followed by immunohistochemistry (IHC) and fluorescent in situ hybridization (FISH) analysis methods [103]. Although the detection of protein cancer biomarkers in blood or serum is not a routine practice, their analysis is possible and is mainly based on enzyme-linked immunosorbent assays (ELISA). However, some of these assays are not sufficiently sensitive for the detection of low biomarker concentrations [104] and in the prognostic detection, which is then susceptible to produce false results [105].

To overcome this problem major efforts have been made to develop more sensitive analytical techniques for biomarker detection, with a special emphasis on biosensors. The International Union of Pure and Applied Chemistry (IUPAC) defines a biosensor as “an integrated receptor-transducer device, which is capable of providing selective quantitative or semi-quantitative analytical information using a biological recognition element” [106]. The biological recognition element can be DNA, an antibody, an antigen, an enzyme, a whole cell, a cell organelle, etc. The transducer is used to convert the recognition event into an analytically useful signal. This signal transduction can be based on electrochemical, optical, piezoelectric and calorimetric principles. Biosensors are usually designed to provide highly selective and sensitive detection of target analytes through the use of

ELECTROANALYSIS

specific biological recognition elements combined with highly sensitive detection techniques. Among the several types of biosensors, the ones that employ electrochemical detection (voltammetry, amperometry, potentiometry, conductometry and electrochemical impedance spectroscopy) are the most widely studied. Electrochemical biosensors are outstanding candidates for inclusion in portable (point-of-care) systems because, besides their fast responses, simplicity and ease of use, the instrumentation needed to perform the analysis has been reduced to (low-cost) pocket-size dimensions. Furthermore, after the development of individual assays for the biomarkers, their combination to form multiplexed detection systems is possible. Therefore, they can provide fast recording of biomarker tumour profiles, which can play an important role in early diagnosis and personalized medicine.

4 Electrochemical Immunosensors for Protein Cancer Biomarker Analysis

Most of the electrochemical biosensors developed to date for the detection of cancer protein biomarkers are voltammetric or amperometric immunosensors. Therefore, only these types of sensors are included in this review. Furthermore, because of the large amount of published studies and the extension of this review, only a reduced number of these articles can be presented. The studies included were retrieved from the Clarivate Analytics Web of Science database (timespan: 2007–2017) by combining the following keywords: cancer, protein biomarker, biosensor and electrochemistry. Although studies without the application in real samples were excluded, a few studies in which these samples were not used were included because of the interest of the construction of the sensing phase or the detection label.

A summary of electrochemical immunosensors (EI) for the analysis of protein biomarkers of lung (Table 2), breast (Table 3), colorectal and stomach (Table 4), prostate (Table 5), liver (Table 6) and stomach (Table 7), cancer is presented. This summary focuses on several important features of the sensors: the transducer electrode and its surface modification, the immobilization strategy of the capture antibody, the assay type, the electrochemical detection technique, the species detected, the sample, and the limit of detection (LOD).

Promising new strategies have been implemented in the design and construction of immunosensors for early screening and cancer diagnosis. Voltammetric and amperometric sensors are especially interesting because of the high sensitivity that can be attained. Electrochemical biomarker detection has been carried out with distinct techniques (amperometry, cyclic voltammetry (CV), linear sweep voltammetry (LSV), differential pulse voltammetry (DPV), square wave voltammetry (SWV), stripping voltammetry and electrochemical impedance spectroscopy (EIS)). Amperometry, CV and DPV are the most commonly employed techniques because they provide low

Review

ELECTROANALYSIS

Table 2. Lung cancer biomarker analysis with electrochemical immunosensors.

Biomarker	Transducer	Surface modification	Immobilization	Assay	Label	Technique	Detection	Sample	LOD	Ref.
NSE	GCE	Hydrogel/Gold nanoparticles (AuNP)	Adsorption	Label-free	n/a	SWV	$[\text{Fe}(\text{CN})_6]^{3-/4-}$	Patient serum	0.26 pg/mL	[14]
	GCE	Thionine (TH)/Carbon nanosphere-functionalized graphene	Adsorption	Sandwich	Platinum nanoflower (PtNF)-labeled horseradish peroxidase (HRP)	DPV	H_2O_2	Spiked new-born cattle serum	5.0 pg/mL	[15]
	GCE	β -Cyclodextrin (CD)	Affinity	Sandwich	Guanine-decorated graphene nanostructures (GGN)	DPV	$\text{Ru}(\text{NH}_3)_6^{3+}$	Spiked new-born cattle serum	1.0 pg/mL	[16]
	GCE	Single-walled carbon nanotubes (SWCNTs)	Covalent (EDC/NHS)	Competitive	n/a	DPV	1-NP	Patient serum	33 pg/mL	[17]
	GCE	Gold nanocrystals (AuNC)/nickel hexacyanoferrate nanoparticles/Gold nanoparticle (AuNP)-functionalized graphene nanosheets (GS)	Adsorption	Label-free	n/a	CV	$[\text{Fe}(\text{CN})_6]^{3-/4-}$	Patient serum	0.3 pg/mL	[18]
	GCE	Prussian blue (PB)-silica dioxide/ β -aminopropyltriethoxysilane (APTES)/ Chitosan (CS)-AuNP	Adsorption	Label-free	n/a	CV	PB	Patient serum	80 pg/mL	[19]
SCC	GCE	Nitrogen-doped graphene sheets (N-GS)	Covalent (GA)	Sandwich	Sodium montmorillonites/polyaniline/AuNPs	Amperometry	H_2O_2	Human serum	0.33 pg/mL	[20]
	GCE	Reduced graphene oxide (rGO)-tetraethylene pentamine (TEPA)	Covalent (GA)	Sandwich	Gold-silver nanoclusters	Amperometry	H_2O_2	n/a	1.3 pg/mL	[21]
	GCE	N-GS	Covalent (GA)	Sandwich	Dumbbell-like Pt- Fe_3O_4 NPs	Amperometry	H_2O_2	Human serum	15.3 pg/mL	[22]

1-NP: 1-naphthol; CV: Cyclic voltammetry; DPV: Differential pulse voltammetry; EDC: 1-ethyl-3-(3-dimethylaminopropyl)-carbodiimide; GA: Glutaraldehyde; GCE: Glassy Carbon Electrode; H_2O_2 : Hydrogen Peroxide; NHS: N-hydroxysuccinimide; NSE: Neuron-Specific Enolase; PB: Prussian blue; SCC: Squamous Cell Carcinoma antigen; SWV: Square wave voltammetry.

Table 3. Breast cancer biomarker analysis with electrochemical immunosensors.

Biomarker	Transducer	Surface modification	Immobilization	Assay	Label	Technique	Detection	Sample	LOD	Ref.
HER2	8 × SPE	Streptavidin MBs (Strep-MBs) Protein A-MBs (ProtA-MBs)	Affinity	Sandwich	AP	DPV	1-NP	Spiked human serum	1.8 ng/mL 2.6 ng/mL	[23]
	CILE	Streptavidin MBs (Strep-MBs) Multi-walled carbon nanotubes (MWCNT)/Gold nanoparticles (AuNPs)	Adsorption	Label-free	n/a	EIS	1-NP	Patient serum	3.4 ng/mL 7.4 ng/mL	[24]
SPCE	GSPE	AuNPs	Adsorption	Label-free	n/a	EIS	[Fe(CN) ₆] ^{3-/4-}	Spiked human serum	6.0 ng/mL	[25]
	SPCE	-	Covalent (EDC/NHS)	Sandwich	HRP	Amperometry	HQ	Human cells lysates	1.0 µg/mL	[26]
AuE	SPCE	AuNPs	Adsorption	Sandwich	AP	LSV	Silver	Spiked human serum	4.4 ng/mL	[27]
	AuE	AuNP/3-Mercaptopropionic acid (MPA)/Cysteamine/Fe ₃ O ₄ NPs	Covalent (2-iminothiolane)	Label-free	n/a	DPV	[Fe(CN) ₆] ^{3-/4-}	Patient serum	0.995 pg/mL	[28]
CA 15-3	SPCE	Magnetic beads-Protein A (MBs-Protein A)	Affinity (Protein A)	Sandwich	AP	DPV	1-NP	Patient serum	6.0 ng/mL	[29]
	Au-NEEs	Polycarbonate	Adsorption	Sandwich	HRP	CV	MB	Cell lysates	n/a	[30]
GCE	AuE	Cys/Graphene oxide (GO)/Py	Covalent (EDC/NHS)	Sandwich	MWCNT-Ferritin	DPV	HQ	Spiked human serum	0.009 U/mL	[31]
	GCE	Ionic liquid (IL)-functionalized GS	Covalent (EDC/NHS)	Sandwich	Cd ²⁺ -functionalized nanoporous TiO ₂	SWV	Cadmium	n/a	0.008 U/mL	[32]
ITO	GCE	Graphene oxide (GO)	Affinity interaction (Avidin)	Sandwich	Tyrosinase (Tyr)	Chronocoulometry	o-Benzoquinone	Spiked human serum	0.100 U/mL	[33]
	GCE	AuNP/ferrocene (Fc)-rGO	Adsorption	Label-free	n/a	DPV	Fc	Patient serum	0.015 U/mL	[34]
GCE	GCE	Nitrogen-doped graphene sheets (N-GS)	Covalent (EDC/NHS)	Label-free	n/a	DPV	[Fe(CN) ₆] ^{3-/4-}	Spiked human serum	0.012 U/mL	[35]
	GCE	Nanoporous gold/Gra/TH	Covalent (GA)	Sandwich	HRP-encapsulated liposomes	DPV	TH	Patient serum	5 × 10 ⁻⁶ U/mL	[36]
AuE	GCE	CNTs-OrgSi@CS/PINCS/GOD	Adsorption	Label-free	n/a	CV	FADH ₂	Spiked human serum	0.040 U/mL	[37]
	AuE	Ferrocenecarboxylic (Fc-COOH)-doped silica nanoparticles (SNPs)	Covalent (GA)	Label-free	n/a	CV	Fc-COOH	Patient serum	0.640 U/mL	[38]
AuE	AuE	PB/AuNP/dsDNA/AuNP	Adsorption	Label-free	n/a	CV	PB	Patient serum	600 pg/mL	[39]

1-NP: 1-naphthol; 8 × SPE: eight screen-printed electrochemical cells; AuE: Gold electrode; AP: Alkaline phosphatase; CA 15-3: Cancer Antigen 15-3; CILE: carbon ionic liquid electrode; CV: Cyclic voltammetry; DPV: Differential pulse voltammetry; EDC: 1-ethyl-3-(3-dimethylaminopropyl)carbodiimide; EIS: Electrochemical impedance spectroscopy; Fc: ferrocene; GA: Glutaraldehyde; GCE: Glassy carbon electrode; GSPE: Graphite screen-printed electrodes; HER2: Human epidermal growth factor receptor 2; HQ: Hydroquinone; HRP: Horseradish peroxidase; ITO: Indium-tin oxide; LSV: linear sweep voltammetry; MB: Methylene blue; NEEs: Nanoelectrode ensembles; NHS: N-hydroxysuccinimide; PB: Prussian blue; SPCE: Screen-printed carbon electrode; SWV: Square wave voltammetry; TH: Thionine.



Review

ELECTROANALYSIS

Table 4. Colorectal and Stomach cancer biomarker analysis with electrochemical immunosensors.

Biomarker	Transducer	Surface modification	Immobilization	Assay	Label	Technique	Detection	Sample	LOD	Ref.
CA 19-9 (Colorectal and Stomach)	SPCE	Chitosan	Covalent (GA)	Sandwich	AuNP/poly(ami-damine) dimer (PAAD)	Amperometry	H ₂	Patient serum	0.0063 U/ mL	[40]
	GCE	AuNPs-porous GO	Adsorption	Sandwich	Au@Pd-Gra/TH/HRP	DPV	TH	Patient serum	0.006 U/ mL	[41]
	GCE	CS/MWCNTs/glucose oxidase/silica-protected magnetite particle-Gold-mesoporous silica (Fe ₃ O ₄ @SiO ₂ -Au@mSiO ₂)	Adsorption	Label-free	n/a	DPV	Glucose oxidase (GOD)	n/a	0.004 U/ mL	[42]
	AuE	MWCNTs-BSA/gold colloids	Adsorption	Sandwich	Nafion coated SiO ₂ NPs	CV	[Fe(CN) ₆] ^{3-/4-}	Patient serum	0.060 U/ mL	[43]

AuE: Gold electrode; CA 19-9: Cancer Antigen 19-9; CV: Cyclic voltammetry; DPV: Differential pulse voltammetry; GA: Glutaraldehyde; GCE: Glassy carbon electrode; HRP: Horseradish peroxidase; SPCE: Screen-printed carbon electrode; TH: Thionine.

limits of detection (LOD), in the order of pg/mL and/or fg/mL, for the cancer biomarkers reported in this review.

Voltammetric and amperometric sensors generally incorporate a three-electrode configuration, composed of working-, reference- and auxiliary electrodes, which are placed in contact with the sample. Then the potential of the working electrode (WE) is either varied within a predefined potential range (voltammetry) or fixed at a constant potential (amperometry) and the resulting current is measured. The analytical process thus occurs at the WE and therefore the recognition element is immobilized on the surface of this electrode. The WE is a small-size electrode or a screen-printed electrode (SPE) made of, for example, carbon, gold, or platinum. Other specific working electrodes such as indium tin oxide (ITO) or paper electrodes [33,53] are also employed depending on the specifications or characteristics of the electrochemical technique and the biosensor performance. Moreover, the WE can be modified with nanostructures and distinct materials such as carbon nanotubes, gold nanoparticles, nanoelectrode ensembles (NEEs) prepared in track-etched polycarbonate membranes [30], a multiwalled carbon nanotube-ionic liquid (MW-CILE) [24], and a three-dimensional Au nanowire array (3D AuNW) with electropolymerized polypyrrole [55].

5 Electrode Surface Modification

Sensor surfaces modified with nanostructures can provide an additional increment in the biosensor's performance and advanced development of portable devices that can support early cancer diagnosis [107]. The WE's surface is therefore frequently modified with (nano) materials such as metal (especially gold) nanoparticles or nanocomposites and carbon nanostructures to (i) improve the immobilization and the stability of the biological recognition element, (ii) increase the recognition element's load, (iii) enhance the sensor's sensitivity and/or (iv) change the detection potential to minimize interferences of other species. For the last two purposes, a redox mediator can also be included in the surface modification strategy.

Gold nanoparticles (AuNP) are an excellent nanomaterial with favourable biocompatibility, good conductivity, and a high surface-to-volume ratio. As examples of sensors using AuNPs, Ravalli et al. [25] developed a sensitive biosensor based on easy immobilization of the bioreceptor on AuNPs, electrodeposited on screen-printed graphite. Marques et al. [27] used screen-printed carbon electrodes, modified with AuNPs, for effective antibody immobilization. In this work, the formation of the AuNPs was achieved through electrodeposition of ionic gold by applying a constant current followed by applying a constant potential. Chu et al. [48] used AuNPs as a substrate material to immobilize the antibodies and to accelerate electron transfer. The AuNPs were prepared in accordance with the conventional citrate method that consists of reducing the gold nanoparticles with a

Review

ELECTROANALYSIS

Table 5. Prostate cancer biomarker analysis with electrochemical immunosensors.

Biomarker	Transducer	Surface modification	Immobilization	Assay	Label	Technique	Detection	Sample	LOD	Ref.
PSA	GCE	Graphene/CoS–Au	Adsorption	Sandwich	Toluidine blue/CeO ₂ mesoporous nanoparticles/ionic liquids doped carboxymethyl chitosan (TB/M–CeO ₂ /CMC/ILs)	DPV	TB	Spiked human serum	0.16 pg/mL	[44]
	GCE	Sulfo group functionalized multi-walled carbon nanotubes/Gold NP (MWCNTs–SO ₃ H@Au)	Adsorption	Sandwich	Mesoporous core-shell Pd@Pt NP-amino group functionalized graphene (M–Pd@Pt/NH ₂ –GS)	Amperometry	H ₂ O ₂	Spiked human serum	3.3 fg/mL	[45]
	AuE	CD/p-Toluenesulfonyl chloride (PTSC)/ethylenediamine	Covalent (GA)	Label-free	n/a	DPV	[Fe(CN) ₆] ^{3–/4–}	Human serum	0.3 pg/mL	[46]
	GCE	Graphene sheets–APTES–S@AuNPs (GS–APTES@Au)	Adsorption	Sandwich	APTES-cubic Cu ₂ O-ferrocene-carboxylic acid (APTES–Cu ₂ O@Fe–COOH)	DPV	H ₂ O ₂	Spiked human serum	0.05 pg/mL	[47]
	GCE	AuNPs	Adsorption	Sandwich	Palladium-doped cuprous oxide nanoparticles (Pd@Cu ₂ O NPs)	Amperometry	H ₂ O ₂	Spiked human serum	2.0 fg/mL	[48]
	8X SPCE	Streptavidin–MBs	Affinity (Streptavidin/Biotin)	Sandwich	HRP	Amperometry	TMB	Patient serum	1.86 ng/mL	[49]
	GCE	High molecular-weight silk peptide/Reduced graphene oxide (rGO)	Covalent (GA)	Label-free	n/a	DPV	[Fe(CN) ₆] ^{3–/4–}	Patient serum	53 pg/mL	[50]
	GCE	Multi-walled carbon nanotubes (MWCNTs)	Covalent (EDC/NHS)	Sandwich	AuNPs–6-ferrocenyl hexanethiol	DPV	6-ferrocenyl hexanethiol	Spiked human serum	5.4 pg/mL	[51]
	GCE	Gold–Pd@SnO ₂	Adsorption	Sandwich	Gold-mesoporous carbon nanoparticles–HRP–MB	DPV	MB	Spiked human serum	3.0 pg/mL	[52]
	Paper electrode	Gold nanorods (AuNRs)	Adsorption	Sandwich	Zinc oxide spheres–silver nanoparticles	Amperometry	H ₂ O ₂	Patient serum	1.5 pg/mL	[53]
	GCE	Fe-modified hydrogel/CS/AuNPs	Adsorption	Label-free	n/a	SWV	Fc	Spiked human serum	0.5 pg/mL	[54]
	3D AuNW	Polypyrrole(Ppy)	Entrapment	Label-free	n/a	DPV	[Fe(CN) ₆] ^{3–/4–}	Spiked human serum	0.3 fg/mL	[55]
	GCE	MWCNTs/L/CS/TH	Covalent (Phthaloyl chloride)	Sandwich	HRP	DPV	TH	Human serum	1.0 pg/mL	[56]
	ITO	Palladium NP–rGO	Covalent (EDC/NHS)	Label-free	n/a	Amperometry	[Fe(CN) ₆] ^{3–/4–}	Spiked human serum	10 pg/mL	[57]
	GCE	Graphene oxide (GO)	Covalent (EDC/NHS)	Sandwich	Fe-incorporated polystyrene spheres	SWV	Fc	Spiked human serum	1.0 pg/mL	[58]
	Vegetable parchment SPCE	Graphene	Covalent (GA)	Sandwich	AuNPs–HRP	LSV	H ₂ O ₂	Patient serum	0.46 pg/mL	[59]
	AuE	MWCNTs/AuNPs	Adsorption	Sandwich	MWCNT–HRP	SWV	[Fe(CN) ₆] ^{3–}	Spiked human serum	0.40 pg/mL	[60]



Review

ELECTROANALYSIS

Table 5. continued

Biomarker	Transducer	Surface modification	Immobilization	Assay	Label	Technique	Detection	Sample	LOD	Ref.
GCE	Nafion/Cross-linked starch-MWCNTs/AuNP	Adsorption	Label-free	n/a	CV	$[\text{Fe}(\text{CN})_6]^{3-/4-}$	Patient serum	7.0 pg/mL	[61]	
GCE	Graphene sheets – methylene blue – chitosan (GS-MB-CS)	Covalent (GA)	Label-free	n/a	Amperometry	MB	Patient serum	1.3 pg/mL	[62]	
GCE	GS/cobalt hexacyanoferrate NP	Covalent (PBSE)	Sandwich	CdS quantum dots-GS	SWV	Cadmium	Patient serum	3.0 pg/mL	[63]	
GCE	GS	Covalent (PBSE)	Label-free	n/a	Amperometry	Cobalt hexacyanoferrate NP	Patient serum	10 pg/mL	[64]	
GCE	Nanoporous Au	Covalent (EDC/NHS)	Sandwich	Dopamine-Fe ₃ O ₄ -Fe-monocarboxylic acid	SWV	Fe monocarboxylic acid	Spiked serum	2.0 pg/mL	[65]	
GCE	GS	Adsorption	Label-free	n/a	CV	$[\text{Fe}(\text{CN})_6]^{3-}$	Patient serum	3.0 pg/mL	[66]	
GCE	GS	Covalent (PBSE)	Sandwich	GS/TH/HRP	Amperometry	TH	Patient and spiked serum	1.0 pg/mL	[67]	
AuE	Cysteamine	Covalent (GA)	Sandwich	AP-encapsulated liposomes	LSV	Silver	Patient serum	7.0 pg/mL	[68]	
Dual-SPCE	AuNPs	Adsorption	Sandwich	AP	LSV	Silver	Human prostate tumour cell cultures	1.0 ng/mL	[69]	

AuE: Gold electrode; AP: Alkaline phosphatase; CV: Cyclic voltammetry; DPV: Differential pulse voltammetry; EDC: 1-ethyl-3-(3-dimethylaminopropyl)-carbodiimide; Fe: ferrocene; GA: Glutaraldehyde; GCE: Glassy carbon electrode; H₂O₂: Hydrogen Peroxide; HRP: Horseradish peroxidase; LSV: linear sweep voltammetry; MB: Methylene blue; NHS: N-hydroxysuccinimide; PBSE: 1-pyrenebutanoic acid, succinimidyl ester; PSA: Prostate-Specific Antigen; SPCE: Screen-printed carbon electrode; SWV: Square wave voltammetry; TB: Toluidine blue; TH: Thionine; TMB: 3,3',5,5'-Tetramethylbenzidine.

Review

ELECTROANALYSIS

Table 6. Liver cancer biomarker analysis with electrochemical immunosensors.

Biomarker	Transducer	Surface modification	Immobilization	Assay	Label	Technique	Detection	Sample	LOD	Ref.
AFP	MGCE	Fe ₃ O ₄ -ε-Polylysine-heparin nanoparticles (Fe ₃ O ₄ -ε-PL-Hep)	Adsorption	Label-free	n/a	DPV	[Fe(CN) ₆] ^{3-/4-}	Human blood	0.072 ng/mL	[70]
	GCE	Heparin-polyglutamic-polyproline nanoparticles (Hep-PGA-PPy)	Covalent (EDC/NHS)	Label-free	n/a	DPV	[Fe(CN) ₆] ^{3-/4-}	Human blood samples	0.099 ng/mL	[71]
	GCE	CS-Au/Hyperbranched polyester nanoparticles-nitrite groups	Electrostatic interaction	Label-free	n/a	DPV	[Fe(CN) ₆] ^{3-/4-}	Spiked human serum	0.055 ng/mL	[72]
	GCE	Graphene oxide (GO)	Covalent (EDC/NHS)	Sandwich	Hydroxyapatite nanoparticles (HAPNPs)	SWV	Molybdate	Human serum	50 fg/mL	[73]
	GCE	Cuprous oxide nanowires decorated graphene oxide nanosheets-toluidine blue (Cu ₂ O@GO-TB)	Covalent (EDC/NHS)	Label-free	n/a	SWV	TB	Spiked human serum	0.1 fg/mL	[74]
	GCE	PANI/AuNPs/PEG	Covalent (EDC/NHS)	Label-free	n/a	DPV	PANI	Spiked serum samples	0.007 pg/mL	[75]
	GCE	Graphene/Gold nanoparticles (Gr/AuNP)	Adsorption	Sandwich	Poly(MB)-Au nanocomposites	SWV	MB	Patient serum	19.6 fg/mL	[76]
	GCE	N-doped multi-walled carbon nanotube (N-MWCNT)/Poly-dopamine (PDA)	Adsorption	Sandwich	GS/Au@Pt nanodendrites	Amperometry	H ₂ O ₂	Spiked serum	0.05 pg/mL	[77]
	GCE	AuNPs	Adsorption	Sandwich	GS/CeO ₂ mesoporous nanoparticles (M-CeO ₂)/APTES/Pd octahedral nanoparticles (Pd)	Amperometry	H ₂ O ₂	Spiked human serum	3.0 fg/mL	[78]
	GCE	Molybdenum carbide nanotubes / Thiomine (Mo ₂ C/TH)	Covalent (GA)	Label-free	n/a	DPV	TH	Patient serum	3.0 pg/mL	[79]
	GCE	AuNPs	Adsorption	Sandwich	Biotin (B)-functionalized amine magnetic nanoparticle (APTES@Fe ₃ O ₄)	Amperometry	H ₂ O ₂	Spiked serum samples	0.33 pg/mL	[80]
	GCE	Carbon nanotubes/Gold nanorod (CNTs/Au NR)	Adsorption	Sandwich	HRP	DPV	TMB	Human serum	30 pg/mL	[81]
	GCE	β-Cyclodextrin – graphene (nano) sheets (β-CD-GS)	Covalent (EDC/NHS)	Sandwich	PdNi-NPs/N-doped Gra nanoribbons	Amperometry	H ₂ O	Human serum	0.03 pg/mL	[82]
	GCE	Gra/SnO ₂ /Au	Adsorption	Label-free	n/a	DPV	[Ru(NH ₃) ₆] ³⁺	Spiked serum samples	10 pg/mL	[83]
Paper-based microfluidic device		AuNW/GS	Adsorption	Sandwich	Copper sulfide/graphene oxide (CuS/GO)	Amperometry	H ₂ O ₂	Patient serum	0.5 pg/mL	[84]
GCE		AuNPs	Adsorption	Sandwich	Pb ²⁺ @Au@MWCNTs-Fe ₃ O ₄	Amperometry	H ₂ O ₂	Serum samples	3.3 fg/mL	[85]



Review

ELECTROANALYSIS

Table 6. continued

Biomarker	Transducer	Surface modification	Immobilization	Assay	Label	Technique	Detection	Sample	LOD	Ref.
GCE		MWCNTs	Covalent (EDC/NHS)	Sandwich	Carbon decorated Fe ₃ O ₄ magnetic microspheres @palladium (Fe ₃ O ₄ @C@Pd)	Amperometry	H ₂ O ₂	Human serum	0.16 pg/mL	[86]
GCE		AuNRs	Adsorption	Label-free	n/a	CV	[Fe(CN) ₆] ³⁻⁻⁴⁻	Patient serum	40 pg/mL	[87]
GCE		CD-GS	Adsorption	Sandwich	Pt@CuO-MWCNTs	Amperometry	[Fe(CN) ₆] ³⁻⁻⁴⁻	Patient serum	0.33 pg/mL	[88]
GCE		GS/copper oxide nanoflowers/AuNPs	Adsorption	Label-free	n/a	Amperometry	H ₂ O ₂	Human serum	5.3 fg/mL	[89]
3D AuE		3-mercaptopropionic acid (MPA)	Covalent (EDC/NHS)	Sandwich	HRP	Amperometry	TMB	Patient serum	3.0 pg/mL	[90]
GCE		CS-AuNPs	Adsorption	Label-free	n/a	LSV	H ₂ O ₂	Patient plasma	40 pg/mL	[91]
GCE		Pd-rGO	Adsorption	Label-free	n/a	DPV	H ₂ O ₂	Patient serum	5.0 pg/mL	[92]
GCE		AuNPs/multifunctional mesoporous silica/toluidine blue (TB)	Adsorption	Sandwich	Au@MCM-41/TB	DPV	TB	Patient serum	0.05 pg/mL	[93]
AuE		CS-SWCNTs/AuNPs	Affinity (Protein A)	Sandwich	Hollow AuNPs-HRP-TH	DPV	TH	Patient serum	8.3 pg/mL	[94]
GCE		Pd nanoplates	Adsorption	Label-free	n/a	SWV	[Fe(CN) ₆] ³⁻⁻⁴⁻	Patient serum	4.0 pg/mL	[95]
GCE		rGO/Nation/AuNPs	Adsorption	Sandwich	GOD-HPNPs-Fe ₃ O ₄ -TH	DPV	TH	Human serum	1.6 pg/mL	[96]
GCE		AuNPs/PDA/TH/GO	Adsorption	Label-free	n/a	DPV	TH	Human serum	30 pg/mL	[97]
Pt		Poly (3,4-ethylenedioxythiophene) (PEDOT)/AuNPs/Azure I/ZnSe quantum dots	Adsorption	Label-free	n/a	CV	Azure I	Patient serum	1.1 fg/mL	[98]
GCE		Polyamidoamine dendrimers/carbon dots/Au	Adsorption	Label-free	n/a	DPV	[Fe(CN) ₆] ³⁻⁻⁴⁻	Patient serum	25 fg/mL	[99]

AFP: α -1-Fetoprotein; AuE: Gold electrode; GCE: Glassy carbon electrode; CV: Cyclic voltammetry; DPV: Differential pulse voltammetry; EDC: 1-ethyl-3-(3-dimethylaminopropyl) carbodiimide; GA: Glutaraldehyde; GOD: Glucose oxidase; H₂O₂: Hydrogen Peroxide; HRP: Horseradish peroxidase; LSV: linear sweep voltammetry; MB: Methylene blue; MGCE: magnetic glassy carbon electrode; NHS: N-hydroxysuccinimide; PANI: Polyaniline; Pt: Platinum electrode; SWV: Square wave voltammetry; TB: Toluidine blue; TH: Thionine; TMB: 3,3',5,5'-Tetramethylbenzidine.

Review

ELECTROANALYSIS

Table 7. Stomach cancer biomarker analysis with electrochemical immunosensors.

Biomarker	Transducer	Surface modification	Immobilization	Assay	Label	Technique	Detection	Sample	LOD	Ref.
CA72-4	GCE	Nanoporous gold (NPG)	Adsorption	Sandwich	Polyamine-Au asymmetric multi-component nanoparticles (PANI-AuAMNPs)	Amperometry	H ₂ O ₂	Spiked serum samples	0.10 U/mL	[100]
	GCE	Reduced graphene oxide – tetraethylene pentamine (rGO-TEPA)	Covalent (EDC/NHS)	Sandwich	Dumbbell-like PtPd-Fe ₃ O ₄ NPs	Amperometry	H ₂ O ₂	Patient serum	0.3 mU/mL	[101]
IL-6	GCE	3-3'-Dithio-bis (propionic acid NHS)/Ferrocenyltethered dimer/AuNP	Adsorption	Sandwich	HRP	Amperometry	Ferrocenyl-tethered dimer	Patient serum	1.0 pg/mL	[102]

CA 72-4; Cancer Antigen 72-4; EDC: 1-ethyl-3-(3-dimethylaminopropyl)-carbodiimide; GCE: Glassy carbon electrode; HRP: Horseradish peroxidase; H₂O₂; Hydrogen Peroxide; IL-6: Interleukin-6; NHS: N-hydroxysuccinimide.

negatively charged ligand. Briefly, the synthesis involves a solution containing HAuCl₄ and ultrapure water that is refluxed at high temperature. Then, under magnetic stirring, the reducing agent sodium citrate is added. After adequate cooling of the solution, a drop of the obtained AuNPs was placed on the working electrode and allowed to disperse. Anti-PSA antibodies were immobilized by physical and chemical binding. Besides AuNPs, other subtypes of gold nanomaterials were also reported to improve the sensor performance: gold nanorods (AuNRs) [53,87] and nanoporous gold (NPG), that can also be used to efficiently immobilize the bioreceptor element. Wei et al. [66] prepared a NPG film with uniform pore size and large surface area by a dealloying method, which allowed the adsorption of the antibody into the pores of the film and provided a low detection limit.

On the other hand, carbon-based nanomaterials are also used in transducer surface modifications because of several reasons: (i) the increase of the surface area and subsequent increase of sensitivity; (ii) immobilization of a large amount of biomolecules, and (iii) their unique characteristics and properties, especially their excellent electrical conductivity [108]. Distinct dimensional carbon-based nanomaterials can be used, such as carbon nanotubes (CNTs) that contemplate single-walled carbon nanotubes (SWCNTs) [17] and multi-walled carbon nanotubes (MWCNTs) [51,86] or graphene (Gra) which contemplates graphene (nano) sheets (GS) [59,65,67], nitrogen-doped graphene sheets (N-GS) [20,22,35], graphene oxide (GO) [33,58] and reduced graphene oxide (rGO) [21,101]. Recent progress in the synthesis of graphene-based hybrid nanomaterials have made them even more appreciated, benefiting from the electrochemical catalytic properties and the higher electron transfer rate between the electrode and the detection molecules [15,109]. For example, Zhang et al. [15] reported a sandwich-type immunoassay using carbon nanosphere-functionalized graphene hybrid nanosheets on a glassy carbon electrode (GCE) as sensing platform. The use of functionalized graphene nanosheets increases the surface area for the immobilization of biomolecules.

Furthermore, the conjugation between gold- and carbon-based nanomaterials and/or ionic liquids offer multiple options in the sensor's construction. Improved performances were achieved using distinct combinations, such as AuNC/nickel hexacyanoferrate NPs/AuNP-GS [18], MWCNTs/AuNPs [24,60], AuNPs/Fc-rGO [34], AuNPs-porous GO [41], MWCNTs/gold colloids [43], Nafion/MWCNTs/AuNPs [61], AuNRs/CNTs [81], gold nanowires (AuNW)/GS [84], chitosan (CS)-SWCNTs/AuNPs [94], rGO/nafion/AuNPs [96], AuNPs/PDA/TH/GO [97].

For example, Yang et al. [41] reported a sensing platform composed of AuNPs functionalized porous graphene (Au-PGO). In this sandwich-type electrochemical immunosensor for the determination of CA 19-9, an Au-PGO nanohybrid structure provided a large accessible surface area for the immobilization of the antibodies,

Review

which also facilitated electron transfer, leading to a further enhancement of the sensor's sensitivity. In addition, Li et al. [84] reported an immunosensor for the detection of AFP using a hybrid nanostructure for effective antibody immobilization. The sensing platform was prepared by in situ solution-phase synthesis using non-covalent ultrathin gold nanowires (AuNWs) functionalized graphene sheets (GS). The water-soluble AuNWs/GS hybrid allowed efficient electrochemical sensing and combined the advantages of the carbon- and gold-based nanomaterials. The developed sensor was successfully applied to the analysis of serum samples from both healthy individuals and cancer patients.

Besides gold and carbon, other nanomaterials have also been used to easily conjugate nano- and biomaterials and biomolecules in the construction of disposable and sensitive immunosensors and immunoassays. Hong et al. [38] developed an electrochemical immunosensor for the detection of CA 15-3 using ferrocenecarboxylic acid (Fc-COOH)-doped silica nanoparticles (SNPs) as an affinity support on a AuE. The use of colloidal silica prevented the leakage of Fc-COOH which was easily modified with a trialkoxysilane. The NH_2 groups on the nanoparticles' surfaces allowed the covalent immobilization of CA 15-3 antibodies using glutaraldehyde as crosslinking agent. In another work, Yang et al. [52] electrodeposited AuNPs onto the surface of a Pd@flower-like SnO_2 nanocomposite for effective antibody immobilization, leading to an enhancement of the sensitivity of the immunosensor. In another approach, Li et al. [64] developed a label-free immunosensor for PSA detection based on the binding of the antibody to a thin film composed of graphene sheet (GS) and cobalt hexacyanoferrate nanoparticles (CoNP) on a GCE. The synergistic effect between the nanomaterials was investigated and showed that the electroactivity of CoNP was greatly improved in the presence of GS and that the formed composite film displayed high electroactivity and good stability.

Based on the unique characteristics of an graphene/ SnO_2 /Au nanocomposite, an immunosensor for AFP detection was developed through layer-by-layer self-assembly on a GCE [83]. The good biocompatibility of the nanocomposite provided suitable conditions for the interaction between antibody and antigen and the combination of graphene, SnO_2 and Au provided the efficient detection of the biomarker.

Xu et al. [71] reported an immunosensor that could be applied to the analysis of AFP in whole blood samples by using heparin-polyglutamic-polypyrrole (Hep-PGA-PPy) nanoparticles. The construction of the sensor was based on the immobilization of anti-AFP antibodies on the Hep-PGA-PPy nanoparticles that were then dropped on a GCE surface (previously modified with APTES) and fixed on the sensing surface through electrostatic bonding. The Hep-PGA-PPy nanoparticles improved the anti-biofouling effect of the electrode by combining the distinct characteristics of the nanoparticle components. The

developed immunosensor exhibited a low limit of detection (0.099 ng/mL).

Biomaterials have also been introduced in the surface modification strategy and are often coated with nanomaterials to improve the performance of the biosensor [54,62,91,99]. An interesting work developed by Gao et al. [99] was based on polyamidoamine dendrimers capped-carbon dots (PAMAM-CDs)/Au nanocrystal nanocomposites as an immobilization matrix on a GCE for sensitive immunosensing of AFP. The referred matrix offered the possibility to combine distinct nanomaterials to form nanocomposites, which exhibited excellent conductivity, stability and biocompatibility of the electrode's surface.

6 Antibody Immobilization

For the development of immunosensors, as for the majority of biosensors, the immobilization of the antibody on the sensor's surface is crucial to achieve adequate performance characteristics (e.g. high sensitivity and precision, short response times, etc.) and long-term stability. It is therefore important to minimize antibody denaturation and conformational changes during or after immobilization [110]. The orientation of the antibodies and the low non-specific adsorption on the sensing surface are critical factors for the effective detection of the antigen. In general, the antibodies' functional groups are allowed to react and bind with the functional groups available on the distinct (modified) sensing platforms. Thus, for the development of electrochemical immunosensors several antibody immobilization strategies have been explored, including: non-covalent (adsorption and entrapment), covalent and affinity approaches.

The adsorption strategy is the most easily performed and consists of casting an antibody solution on the electrode's surface or dipping the electrode in an antibody solution. Then, after an appropriate incubation time, the electrode is washed to remove non-adsorbed antibodies. The major drawbacks of this technique are the random orientation of the antibodies, which exhibit lower antigen binding capacities than properly orientated antibodies [110], and the formation of weak bonds between the antibody and the transducer, which can lead to the loss of antibody during analysis and storage. In the adsorption process, the interaction between the antibodies and the electrode surface can be classified as electrostatic or hydrophobic. In this strategy, distinct carbon- and gold-based nanomaterials are typically used as platforms for the efficient binding of antibodies. The interaction between antibodies and gold nanomaterials (mainly AuNPs) are usually achieved by chemisorption via thiol derivatives, involving a chemical adsorption process between the nanomaterial surface and the adsorbent surface, which causes the bond to be created [14,25,27,48,69,78,80,85,87]. As an example, Wang et al. [14] described the immobilization of antibodies through adsorption onto AuNPs electrodeposited on a hydrogel film, that

ELECTROANALYSIS

Review

ELECTROANALYSIS

was used as an electrochemical immunosensing substrate for the detection of NSE in serum samples.

Another type of non-covalent immobilization is entrapment. In this process, the biological recognition element can be immobilized within a suitable matrix. Normally, the biocomponent is mixed with the supporting (nano) material and then deposited on the electrode surface. Electropolymerization is also often used for biomolecule entrapment. Moon et al. [55], suggested a label-free immunosensor for PSA by incorporating the anti-PSA antibody into polypyrrole. The electropolymerization of polypyrrole on an Au nanowire array was the key strategy in this study where anti-PSA antibodies could simultaneously be immobilized on individual polypyrrole nanowires, without additional modification steps, resulting in enhanced molecular interactions. The nanowires served as an efficient reservoir for the incorporation of high concentrations of anti-PSA antibodies. Indeed, the large surface area and well-defined nanowire structure make them ideal for efficient antibody immobilization and thus, to enhance the loading capacity. In addition, the preferential electrostatic association between positive charges of the oxidized polypyrrole chains and negative carboxyl groups on the antibody allows strong immobilization while ensuring antigenic epitope conservation.

Very stable linkage of the antibody to the sensor surface can be achieved through covalent binding between functional groups present on the (chemically modified) transducer surface and the antibody. Nevertheless, care must be taken not to bind functional groups essential for antigen binding. Examples of compounds used for this purpose are the well-known combination of 1-ethyl-3-(3-dimethylaminopropyl)-carbodiimide and N-hydroxysuccinimide (EDC/NHS). Glutaraldehyde (GA), 1-pyrenebutanoic acid succinimidyl ester (PBSE), phthaloyl chloride and iminithiolane can also be used. Many immunosensors were described in which carbodiimide chemistry was employed for antibody immobilization [17,26,31,32,35,51,57,58,65,82,86,90,101]. In general, in this process the primary amine groups of the antibody are covalently bound to the carboxylic acid group present on the sensor surface, through reactive succinimide esters by amine coupling through EDC/NHS chemistry. On the other hand, aldehyde modification is a suitable strategy to use when the sensor's surface is functionalized with materials containing chemical groups such as amines or alcohols to form imines. Basically, the modified sensing surface is treated with glutaraldehyde (or other aldehydes) that is allowed to react with the antibodies' functional groups. Like this, the binding between the surface and the biological compound is accomplished through the cross-linking agent [20–22,36,38,40,46,50,59,68,79].

Antibodies can also be covalently immobilized onto the working electrode through PBSE, based on an amidation reaction between the available amine groups of the antibody and the succinimidyl ester group of PBSE [64,67]. Yang et al. [67] developed an immunosensor for

prostate cancer biomarker detection by immobilization of the primary antibody onto the surfaces of GS through PBSE which was adsorbed onto the nanomaterial through π - π stacking.

In addition, self-assembly provides a convenient and simple way of creating a highly ordered thin molecular film with tailored chemical properties. In this process, the thin molecular layer is formed by adsorption of molecules from solution onto a solid surface. Subsequently, the adsorbates spontaneously arrange themselves until a completely ordered molecular monolayer is formed, which is called the self-assembled monolayer (SAM) [111], and onto which antibodies can be immobilized. Qu et al. [68] used cysteamine to produce a SAM on the sensor platform and covalently bound the capture antibody through glutaraldehyde. Emami et al. [28] proposed the construction of a label-free immunosensor composed of distinct layers for HER2 detection. Firstly, AuNPs were electrodeposited on a gold electrode surface, followed by the immersion of the electrode in a 3-mercaptopropionic acid (MPA) solution to form the SAM. Then, ECD/NHS was added to activate the carboxyl groups of the MPA layer. Subsequently, cysteamine was added and bound via amide formation. Thereafter, pegylated magnetic iron nanoparticles bound to the thiolated antibodies were added to the previously formed layer-by-layer sensing surface.

Affinity as an immobilization process consists of the interaction between intermediate binding biomolecules (e.g. Protein A, Protein G, biotin, avidin or streptavidin) or carbohydrates (β -cyclodextrin) and a part of an antibody, known as the Fc region. These non-covalent interactions are usually very strong and are adequate to preferentially orient the antibodies and immobilize them successfully on the electrode platform.

Li et al. [94] reported a multi-step sensor platform approach by casting SWCNTs dispersed in chitosan (CSSH-SWCNTs) on the electrode. This process allowed the formation of a multitude of thiol groups ($-SH$) onto which AuNPs were immobilized. Subsequently the electrode was incubated with protein A (PA) which provided adequate orientation of antibodies on the electrode surface. Park et al. [33] compared the biosensing performance of electroreduction-based electrochemical-enzymatic redox-cycling schemes for the detection of cancer antigen CA 15-3 by using avidin in the surface modification. In this sensor, biotinylated anti-CA-15-3 IgG antibodies were placed on avidin-modified ITO electrodes for adequate orientation (Figure 1), and a detection limit of 0.100 U/mL was obtained.

7 Assay Formats (Immunochemical Interactions)

In EI, the most common immunochemical (antibody-antigen) assay formats are: non-competitive (sandwich), label-free and competitive assays, which are schematized in Figure 2.

Review

ELECTROANALYSIS

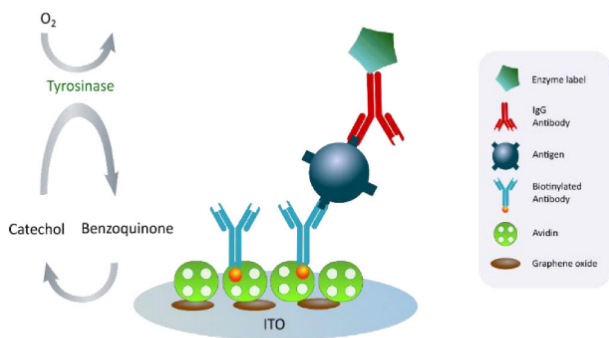


Fig. 1. Schematic Representation of an Electrochemical Immunosensor based on GO and Avidin modified sensing platform [33]. Re-drawn using Inkscape software.

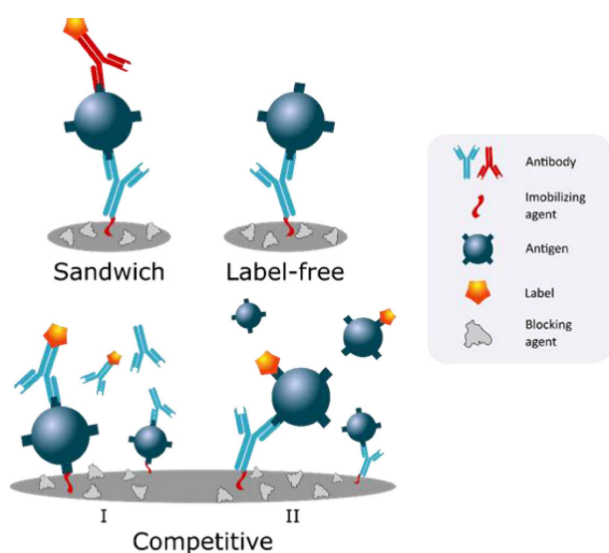


Fig. 2. Types of immunoassays (I – immobilized antibodies react with free antigens in competition with labelled antigens, II – immobilized antigens react with free and labelled antibodies).

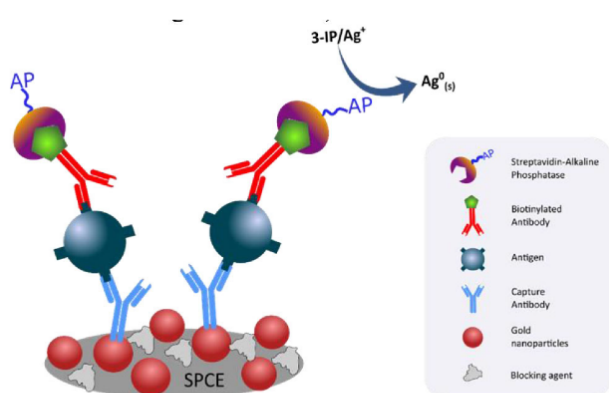


Fig. 3. Schematic representation of a sandwich immunosensor for breast cancer protein biomarker detection [27]. Re-drawn using Inkscape software.

In the non-competitive (sandwich) assay, a capture antibody is immobilized on the electrode's surface which is subsequently blocked using an inert protein (e.g. BSA or casein) to avoid non-specific adsorption. The sensor is then incubated with the sample, and the antigen (cancer biomarker) is bound to the antibody's binding site. Then a secondary antibody is added to complete the sandwich format. In this type of assays the secondary antibody is usually labelled to enable the detection of the antibody-antigen interaction and/or to enhance the analytical signal [27]. Enzymes such as alkaline phosphatase (AP), horseradish peroxidase (HRP) are classic examples of such labels. When enzymatic labels are used, the enzymatic substrate is placed on the sensor's surface after the incubation with the secondary antibody and one of the enzymatic reaction products can be monitored. In this case, the electrochemical signal is proportional to the concentration of the electroactive product which in turn is proportional to the amount of enzymatic label and subsequently to the concentration of the antigen in the sample. The use of enzyme labels provides significant signal amplification, resulting in extremely low detection limits [112]. In EI for the analysis of cancer biomarkers, the most frequently used enzymes are AP and HRP. Examples of immunosensors in which the AP label was used are: Marques et al. [27] for the detection of HER2 and Escamilla-Gomez et al. [69] for the detection of PSA. In these works, the antibody-antigen interaction was measured by using a combination of 3-indoxyl phosphate (3-IP), an enzymatic substrate of AP, and silver ions (Figure 3), leading to the formation of metallic silver which was detected by LSV. The use of silver ions increases the electrochemical signal when compared to the use of 3-IP alone, allowing detection limits below the cut-off values for the mentioned biomarkers (4.4 ng/mL for HER2 and 1.0 ng/mL for PSA).

In another approach, the use of liposomes, as carriers of the marker molecules, can also amplify the signal and improve the sensitivity of the immunosensor. A similar sandwich assay developed by Escamilla-Gomez et al. [69] for PSA detection was performed by Qu et al. [68]. However, in the latter study, AP was encapsulated in liposomes. After the immunological interactions, the bound liposomes were lysed with Triton X-100 to release the encapsulated AP, which converted ascorbic acid 2-phosphate (AA-p) into ascorbic acid and, in the presence of silver ions, led to deposition of the metallic silver.

Besides the use of AP, HRP is used in a wide range of sensor approaches. In the sensor developed by Mucelli et al. [30], secondary antibodies labelled with HRP and methylene blue (MB) were used to detect the interaction between the protein and the antibody. MB is extensively employed as mediator or electrochemically active agent in cancer biosensors. Here, the electrochemical signal is generated by MB (added as soluble mediator) which shuttles electrons from the electrode to HRP during the enzymatic reaction with its substrate, H₂O₂. In addition, Biscay et al. [49], Guo et al. [81] and Zhong et al. [90]

Review

used similar methodologies based on HRP as label and 3,3',5,5' tetramethylbenzidine (TMB) as co-substrate. The authors combined TMB and H_2O_2 to apply a less positive potential and thus avoid some interferences.

Enzymes can also be combined with metallic (nano) materials and/or with redox mediators to obtain more efficient electrochemical signal amplifications. In the work developed by Li et al. [94] a sandwich-type electrochemical immunoassay was constructed based on an efficient signal amplification strategy using hollow AuNPs, HRP NP bioconjugates and TH. Here, TH was used as mediator between HRP enzyme and the electrode surface, and then HRP could synergistically catalyse H_2O_2 . TH is highly redox active and improves the intensity of the signal (Figure 4).

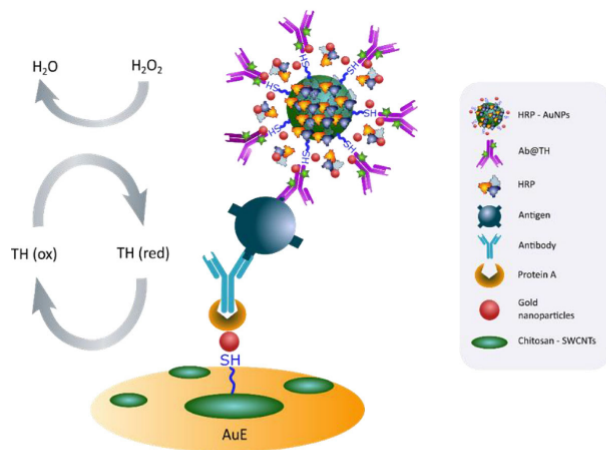


Fig. 4. Electrochemical signal amplification strategy [94]. Re-drawn using Inkscape software.

However, the drawbacks of loaded enzymes limit their use as labels in electrochemical immunosensors because of: (i) easy inactivation; (ii) costly preparation; (iii) laborious purification processes. Therefore, nanomaterials with electrocatalytic properties for the electrochemical detection of H_2O_2 are frequently employed to: (i) enhance the sensitivity achieved in the analysis, (ii) reduce the detection potential to minimize the interference of other species present in the sample. A disadvantage of H_2O_2 detection is the high detection potential, which can also lead to the oxidation of other substances present in the sample.

Jiang et al. [80] developed an amplification option for a sandwich-type immunosensor based on biotin-functionalized amination of a magnetic nanoparticle composite (B-APTES@ Fe_3O_4) as label for detection of AFP. The strategy was successfully implemented using a biotin-streptavidin-biotin (B-SA-B) network. Here, further signal amplification could be achieved as SA and BAPTES@ Fe_3O_4 are added layer by layer on the electrode. In addition, B-APTES@ Fe_3O_4 was used as label

of the secondary antibody, which catalysed the electrochemical reaction of H_2O_2 .

In the immunosensor for PSA detection developed by Chu et al. [48], Pd@ Cu_2O NPs were used as label and presented the excellent characteristics of palladium- (Pd NPs) and cuprous oxide nanoparticles (Cu_2O NPs).

An enzyme-free immunosensor for PSA detection was constructed by Sun et al. [53], using porous zinc oxide spheres-silver nanoparticles (ZnO_2 -AgNPs) nanocomposites as signal labels. The large surface area of ZnO_2 provided sites for the inclusion of AgNPs which improved their catalytic capacity toward H_2O_2 reduction. This allowed the construction of enzyme-free electrochemical sensors which are cheaper and simpler than enzyme-labelled immunosensors.

Moreover, metal ions and quantum dots (QDs) seem to be promising candidates as labels. Commercially available QDs are normally preferred because their preparation is complicated and tedious. However, the drawbacks of using QDs include the rather harsh conditions needed to dissolve QDs and the need for a highly sensitive stripping technique to obtain the signal [32]. Distinct sensing strategies for metal ions/QD-based biosensors can be performed by using several ions (e.g. Cd^{2+} , Pb^{2+} , Cu^{2+} , Zn^{2+}) for direct labelling, avoiding the above-mentioned problems. Zhao et al. developed an immunosensor for detection of the breast cancer biomarker CA 15-3 where Cd^{2+} -functionalized nanoporous TiO_2 (TiO_2 - Cd^{2+}) was used as label for the detection of the signal [32]. Nanoporous TiO_2 spheres were used because of its highly specific surface area (functionalized with abundant $-\text{NH}_2$ groups) which are favourable for the adsorption of high amount of Cd^{2+} which was subsequently detected by SWV, allowing to obtain a detection limit of 0.008 U/mL.

In the label-free approach the antibody-antigen interaction is detected directly without the need of a secondary antibody. This simplifies the immunoassay, allowing faster and cheaper analysis [113]. In these assays, like in the sandwich technique, an antibody is immobilized on the transducer's surface and the immunocomplex is formed after incubation with a sample. Then a redox probe is placed on the sensor and the analytical signal is recorded. The amplitude of this signal decreases with increasing antigen concentration because of the electron transfer hindrance caused by the formed immunocomplex. The most commonly employed redox probes in the label-free approach for cancer immunosensors are: $[\text{Fe}(\text{CN})_6]^{3-/4-}$ [18, 24, 25, 28, 35, 46, 50, 55, 57, 61, 66, 87, 95, 99], Prussian blue (PB) [19, 39], Ferrocene (Fc) [34, 54], Ferrocenecarboxylic acid (Fc-COOH) [38], Methylene Blue (MB) [62], Cobalt hexacyanoferrate NPs [64], thionine (TH) [79, 97], $[\text{Ru}(\text{NH}_3)_6]^{3+/2+}$ [83], H_2O_2 [89, 91, 92], Azure I [98]. As an example, the $[\text{Fe}(\text{CN})_6]^{3-/4-}$ redox probe was used by Deng et al. [46] in a label-free immunoassay for trace species analysis, based on the "gate-effect" of a β -cyclodextrin (β -CD) layer. In this work, the detection of PSA was carried out using a β -CD assembled layer, which created gates for

Review

ELECTROANALYSIS

the electron transfer of the probe. The monoclonal antibody labelled β -CD and the interspaces between β -CD molecules in the layer were formed on the electrode, which act as a channel for the electron transfer from the probe (Figure 5). By virtue of the “gate-effect”, signal amplification and enhancement of the signal-to-noise ratio was achieved.

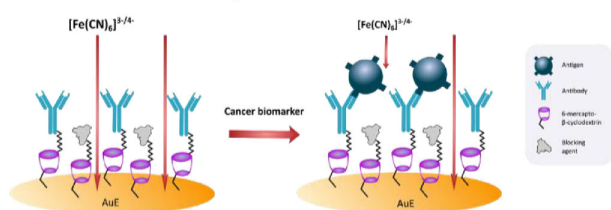


Fig. 5. Example of a label free assay, using $[\text{Fe}(\text{CN})_6]^{3-/4-}$ as redox probe [46]. Re-drawn using Inkscape software.

Moreover, Mao et al. [62] used Methylene Blue (MB) as the redox probe in a label-free EI based on a nanocomposite film composed of graphene sheets-methylene blue-chitosan (GS-MB-CS). The film was used as electrode material to immobilize the antibody because of the high nanocomposite film binding affinity to the electrode. Another example of a redox probe is $[\text{Ru}(\text{NH}_3)_6]^{3+}$ that was used in a label-free immunosensor for the detection of AFP by monitoring the peak current change [83]. In this work, a graphene/ SnO_2/Au nanocomposite sensor platform was used to immobilize the capture antibody. A decrease in the peak current intensity of $[\text{Ru}(\text{NH}_3)_6]^{3+}$ was related to the interaction between antibody and antigen.

Another assay type with a reduced number of applications in electrochemical immunosensing of cancer biomarkers is the competitive immunoassay. In this assay

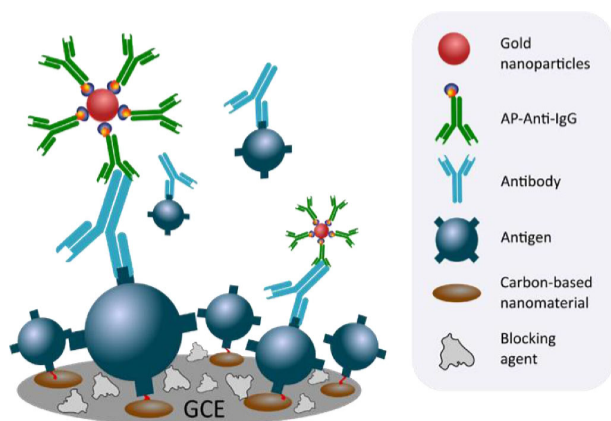


Fig. 6. Schematic representation of Competitive electrochemical immunosensor for NSE detection [17]. Re-drawn using Inkscape software.

(i) immobilized antibodies react with free antigens in competition with labelled antigens or (ii) immobilized antigens react with free and labelled antibodies [114]. The labels employed are identical to the ones used in non-competitive assays. Yu et al. [17] developed a competitive electrochemical immunosensor for the detection of NSE in serum. In the sensing phase construction, a drop of SWCNTs was cast onto a GCE electrode and EDC/NHS was added to activate the carboxyl groups, allowing efficient NSE binding. In this competitive format, the high loading of NSE on SWCNTs greatly extended the limit of the detectable range. For the competitive immunoreaction, the sensor was incubated with the sample (containing ‘free’ NSE) and anti-NSE antibodies. For the signal readout, AP-anti-IgG/AuNP was used, that exhibited high catalytic activity toward the hydrolysis of α -NP in DEA buffer (Figure 6).

8 Magnetic Immunoassays

In addition to the previously mentioned sensor surface modification based on nanomaterials and biomaterials, magnetic beads (MBs) are powerful tools for bioassays because of, for example, the increase of the surface area and the improvement of the sensitivity of the detection method [115]. Their use, combined with modified electrode surfaces improves biomolecule interactions and reduces or/and minimizes the matrix effect of the sample by efficient washing steps [116]. MBs can be manipulated with an external magnet that enables biological reaction events to be performed away from the electrode and can be retained on a sensor surface by an external magnetic field through, for example, the placement of small magnets below the surface of the working electrode (normally with the corresponding size of the WE). Therefore, the recognition element is not in direct contact with the electrode surface, which constitutes the major drawback related to the use of MBs [117]. MBs can be functionalized with distinct recognition elements generally through (i) affinity agents (e.g. Protein A, streptavidin) and (ii) covalent binding (e.g. EDC/NHS, GA, SAMs) (Figure 7).

Ikhani et al. [23] reported three simple magnetic bead-based approaches, combined with screen-printed arrays, for the analysis of HER2. The bioassays were based on a sandwich format in which affibody (Af) or antibody molecules were immobilized on streptavidin- or protein A-modified MBs (Strept-MBs or Prot A-MBs). Both types of MBs could be used for immuno-precipitation purposes.

Al-Khafaji et al. [29] reported a magnetic immunoassay for HER2 detection by using protein A-modified magnetic beads. The proposed assay was based on a sandwich format in which antibody-functionalised magnetic beads were used to capture the protein biomarker. Then, anti-HER2 antibodies labelled with AP were added to trace the affinity reaction, using 1-naphthyl-phosphate as enzymatic substrate and DPV for signal detection.

Review

ELECTROANALYSIS

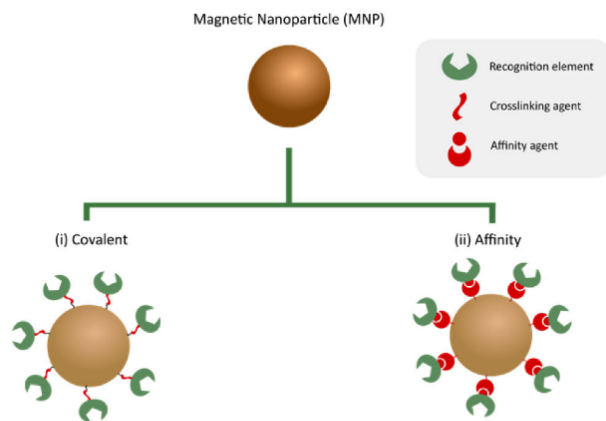


Fig. 7. Strategies on immobilization of recognition element onto the surface of magnetic particles.

Biscay et al. [49] investigated a screening device using magnetic beads as solid phase to develop an immunoassay for the detection of total PSA (tPSA) in serum. Here, the tPSA detection was performed by using superparamagnetic beads (1 mm) modified with streptavidin and an 8-channel screen printed electrode array. In this assay, a mixture of biotinylated antibodies and HRP-labelled antibodies were added to a previously prepared solution containing Strep-MBs and PSA, forming a sandwich complex. Then, TMB was added, which was subsequently oxidized in the reaction cascade and detected by chronoamperometry.

9 Simultaneous/Multiplex Detection

Screening and early diagnosis of cancer contributes to prognosis judgement and appropriate treatment of the patient. In clinical practice, the determination of a single specific biomarker is facing a great challenge and has limitations because of the poor specificity and sensitivity

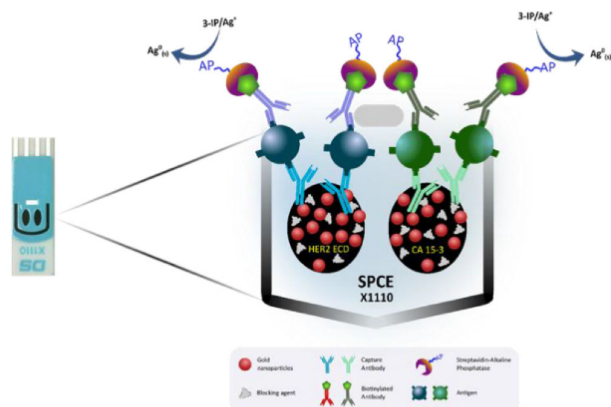


Fig. 8. Schematic representation of multiplexed detection of cancer biomarkers [118]. Re-drawn using Inkscape software.

between the tumour biomarker and the cancer type. Thus, simultaneous detection of multiple biomarkers is of utmost importance and may confer high diagnostic specificity of the disease. To address this, the design of (bio) sensors for the simultaneous detection of multiple tumour biomarkers has demonstrated significant improvements.

Multiplexed electrochemical immunoassays and/or immunosensors are feasible options to detect, identify and quantify two or more biomarkers in the same sample. A major issue in the development of these assays is related to the distinction between the signals of the multiple antigen–antibody interactions. One option is to use multi-working electrode sensors in which each WE is modified with a specific capture antibody. Another option is the use of antibodies with distinct labels (multi-labelling). In this last approach, the electrochemical detection based can be performed on single WE sensors.

Escamilla-Gomez et al. [69] reported the use of SPCEs that contain two carbon working electrodes for the simultaneous determination of prostate specific antigen (free PSA and total PSA). In this sensor, 8A6 anti-PSA and 5G6 anti-PSA antibodies were separately immobilized, through adsorption, on each of the WEs. Then, biotinylated antibodies and an S-AP conjugate were added, and the detection was accomplished using a substrate solution containing 3-IP and silver ions. The analytical signal was obtained by LSV and the results showed the feasibility of the simultaneous detection of fPSA and tPSA in human prostate tumour cells.

A similar approach with multi WE sensors was reported by Marques et al. [118]. In their strategy, a multiplexed electrochemical immunosensor for the simultaneous detection of two breast cancer biomarkers (CA 15-3 and HER2-ECD) was developed based on a customized dual screen-printed carbon electrode (bi-SPCE) nanostructured with in situ generated gold nanoparticles. The application of this bi-immunosensor was based on the antigen-antibody interactions, in which specific capture antibodies for these biomarkers were immobilized by adsorption on each nanostructured working electrode, and the electrochemical signals were detected by LSV analysis of enzymatically (AP) generated metallic silver (Figure 8). The immunosensor's limits of detection were 5.0 U/mL for CA 15-3 and 2.9 ng/mL for HER2-ECD.

10 Cytosensors

One of the major current challenges in cancer diagnostics and follow-up is the analysis of circulating tumour cells (CTCs). CTCs are cells that are shed from a primary tumour and circulate in the body. They contain a large amount of information on the tumour phenotype [119]. Due to the important information that can be obtained from CTCs, several detection methodologies have been developed that contribute to a more efficient diagnosis.

Therefore, cytosensors have emerged as an innovating area related to electrochemical (bio) sensors. Cytosensors

Review

are a class of biosensors that can detect specific cells through their recognition by, for example, antibodies, aptamers, DNA, that are immobilized on a transducer surface. Although the analysis of CTCs is important in diagnosis, no analytical devices are currently available that allow their effective detection with low costs, small sample volumes and in situ detection.

CTCs originating from epithelial tumours express the epithelial cell adhesion molecule EpCAM [119–121]. Recently, cytosensors for CTCs detection using EpCAM have been described [122, 123]. Shen et al. [122] developed a reusable cytosensor with self-assembled monolayers deposited onto an AuE to directionally insert the capture probe (EpCAM aptamer) which specifically binds to EpCAM over-expressed on the membrane of breast cancer MCF-7 cells. The electrochemical response of this label-free cytosensor towards MCF7 cells was recorded by EIS using the redox probe $[\text{Fe}(\text{CN})_6]^{3-/4-}$. Maltez-da Costa et al. [123] developed a strategy for a simple monitoring and rapid electrochemical biosensing for CTCs quantification using specific antibodies labelled with magnetic beads (MBs). Human colon adenocarcinoma cell line (Caco2) was chosen as a model CTC because, similarly to other adenocarcinomas, Caco2 have a strong expression of EpCAM. In this cytosensor, the authors combined anti-EpCAM antibody-functionalized MBs with antibody-modified AuNPs in liquid suspensions. The detection of the labelled Caco2 cells was performed by chronoamperometry through the hydrogen evolution reaction, using 1 M HCl, that was electrocatalyzed by the AuNP labels. In another work, HER2-overexpressing cells could be detected using a hydrazine-AuNP-aptamer bioconjugate [124]. The developed sensor could differentiate between HER2-positive and HER2-negative breast cancer cells and could be applied to diagnosis through either HER2 protein or SK-BR-3 breast cancer cell in human serum samples. In the detection process the sensor was placed in a silver nitrate solution where silver ions were selectively reduced to metallic silver by hydrazine which was then oxidized using square wave stripping voltammetry (SWSV). Lu et al. [125] developed an electrochemical cytosensor for lung cancer cell detection that could sensitively differentiate A549 cells from normal ones (AT II cells) using an epidermal growth factor (EGFR) antibody to recognize EGFR receptors that are over-expressed on the cancer cells. To avoid the drawbacks related to the use of extra immobilization agents and enzymes, AuNPs decorated m-aminophenol based resin microspheres were used to act as suitable immobilization carriers and to facilitate electron transfer. The detection strategy used in this approach was based on the electron transfer blockage of the immunocaptured A549 cells.

11 Conclusions

The continuous progress and the evolution of analytical methodologies allow an increasingly effective diagnosis and follow-up of cancer. In this review, a short summary

ELECTROANALYSIS

of recently developed voltammetric and amperometric immunoassays and cytosensors for the analysis of the six most commonly diagnosed cancer biomarkers is presented. A survey of the published studies shows that the attention in this research area is now mainly focussed on the increase of the sensitivity through different types of electrode surface modifications (carbon- and gold- based nanomaterials, nanoparticles, nanocomposites, SAMs and/or biomaterials) and detection labels of (secondary) antibodies. Magnetic immunoassays also constitute an adequate strategy because of the inherent advantages of using magnetic particles, since they enhance the interactions of the biomolecules and minimize the effect of the sample matrix. Moreover, the development of sensors that provide simultaneous or multiplexed detection contributes to a better prognosis and more efficient screening. The development of cytosensors is currently a challenge to improve cancer detection.

The low limits of detection attained with the developed sensors allows the detection of cancers in an early stage, which could prevent the deaths of millions of people and reduce the suffering of patients and their families and the cost to society. Furthermore, their high sensitivity enables the detection of only slight changes in the biomarker concentration. This could be an excellent additional tool for monitoring cancer patients during treatment and follow-up.

Acknowledgements

Maria Freitas is grateful to FCT-Fundação para a Ciência e a Tecnologia for her PhD grant (SFRH/BD/111942/2015), financed by POPH-QREN-Tipologia 4.1-Formação Avançada, subsidized by Fundo Social Europeu and Ministério da Ciência, Tecnologia e Ensino Superior. This work received financial support from the European Union (FEDER funds through COMPETE) and National Funds (FCT) through project UID/QUI/50006/2013.

References

- [1] J. Ferlay, I. Soerjomataram, R. Dikshit, S. Eser, C. Mathers, M. Rebelo, D. M. Parkin, D. Forman, F. Bray, *Int. J. Cancer* **2014**, *136*, E359–E386. Available from: <http://globocan.iarc.fr>.
- [2] WHO. Cancer, Fact sheet N°297. Available from: <http://www.who.int/mediacentre/factsheets/fs297/en/#>.
- [3] C. Paoletti, D. F. Hayes, *Annu Rev Med* **2014**, *65*, 95–110.
- [4] Z. Altintas, *I. Tothill. Sens. Actuator B-Chem* **2013**, *188*, 988–98.
- [5] S. A. Joosse, T. M. Gorges, K. Pantel. *EMBO Mol Med* **2015**, *7*, 1–11.
- [6] A. Mishra, M. Verma, *Cancers (Basel)* **2010**, *2*, 190–208.
- [7] C. S. Dela Cruz, L. T. Tanoue, R. A. Matthay, *Clin. Chest. Med.* **2011**, *32*, 605–644.
- [8] S. Mittal, H. Kaur, N. Gautam, A. K. Mantha, *Biosens. Bioelectron.* **2017**, *88*, 217–231.
- [9] K. Y. C. Fung, L. Purins, I. K. Priebe, C. Pompeia, G. V. Brierley, B. Tabor, T. Lockett, P. Gibbs, J. Tie, P.

Review

ELECTROANALYSIS

- McMurrick, J. Moore, A. Ruszkiewicz, A. Burgess, E. Nicc, L. J. Cosgrove, *J. Mol. Biomark Diagn.* **2014**, *S6*, 003.
- [10] C. A. K. Borrebaeck, *Nat. Rev. Cancer* **2017**, *17*, 199–204.
- [11] G. Ferrín, P. Aguilar-Melero, M. Rodríguez-Perálvarez, J. L. Montero-Álvarez, M. de la Mata, *Hepat. Med.* **2015**, *7*, 1–10.
- [12] L. Mi, X. Ji, J. Ji, *Transl. Gastrointest. Cancer* **2016**, *5*, 16–29.
- [13] S. Benchimol, A. Fuks, S. Jothy, N. Beauchemin, K. Shiota, C. P. Stanners, *Cell* **1989**, *57*, 327–334.
- [14] H. Wang, H. Han, Z. Ma, *Bioelectrochemistry* **2017**, *114*, 48–53.
- [15] Y. Zhang, W. Ren, *Anal. Methods* **2013**, *5*, 3379–3385.
- [16] G.-Z. Li, F. Tian, *Anal. Sci.* **2013**, *29*, 1195–1201.
- [17] T. Yu, W. Cheng, Q. Li, C. Luo, L. Yan, D. Zhang, Y. Yin, S. Ding, H. Ju, *Talanta* **2012**, *93*, 433–438.
- [18] J. Han, Y. Zhuo, Y. Q. Chai, Y. L. Yuan, R. Yuan, *Biosens. Bioelectron.* **2012**, *31*, 399–405.
- [19] Z. Zhong, J. Shan, Z. Zhang, Y. Qing, D. Wang, *Electroanalysis* **2010**, *22*, 2569–2575.
- [20] H. Jia, P. Gao, H. Ma, Y. Li, J. Gao, B. Du, Q. Wei, *Talanta* **2015**, *132*, 803–808.
- [21] X. Zhang, F. Li, Q. Wei, B. Du, D. Wu, H. Li, *Sens. Actuator B-Chem.* **2014**, *194*, 64–70.
- [22] D. Wu, H. Fan, Y. Li, Y. Zhang, H. Liang, Q. Wei, *Biosens. Bioelectron.* **2013**, *46*, 91–96.
- [23] H. Ilkhani, A. Ravalli, G. Marrazza, *Chemosensors* **2016**, *4*, 1–10.
- [24] E. Arkan, R. Saber, Z. Karimi, M. Shamsipur, *Anal. Chim. Acta.* **2015**, *874*, 66–74.
- [25] A. Ravalli, C. G. Rocha, H. Yamanaka, G. Marrazza, *Bioelectrochemistry* **2015**, *106*, 268–275.
- [26] S. Patris, P. De Pauw, M. Vandeput, J. Huet, P. V. Antwerpen, S. Muyldermans, J.-M. Kauffmann, *Talanta* **2014**, *130*, 164–170.
- [27] R. C. B. Marques, S. Viswanathan, H. P. A. Nouws, C. Delcruce-Matos, M. B. Gonzalez-Garcia, *Talanta* **2014**, *129*, 594–599.
- [28] M. Emami, M. Shamsipur, R. Saber, R. Irajirad, *Analyst* **2014**, *139*, 2858–2866.
- [29] Q. A. M. Al-Khafaji, M. Harris, S. Tombelli, S. Laschi, A. P. F. Turner, M. Mascini, G. Marrazza, *Electroanalysis* **2012**, *24*, 735–742.
- [30] S. P. Mucelli, M. Zamuner, M. Tormen, G. Stanta, P. Ugo, *Biosens. Bioelectron.* **2008**, *23*, 1900–1903.
- [31] R. Akter, B. Jcong, J.-S. Choi, M. A. Rahman, *Biosens. Bioelectron.* **2016**, *80*, 123–130.
- [32] L. Zhao, Q. Wei, H. Wu, J. Dou, H. Li, *Biosens. Bioelectron.* **2014**, *59*, 75–80.
- [33] S. Park, A. Singh, S. Kim, H. Yang, *Anal. Chem.* **2014**, *86*, 1560–1566.
- [34] C. Li, X. Qiu, K. Deng, Z. Hou, *Anal. Methods* **2014**, *6*, 9078–9084.
- [35] H. Li, J. He, S. Li, A. P. Turner, *Biosens. Bioelectron.* **2013**, *43*, 25–29.
- [36] S. Ge, X. Jiao, D. Chen, *Analyst* **2012**, *137*, 4440–4447.
- [37] W. Li, R. Yuan, Y. Chai, Y. Chen, *Biosens. Bioelectron.* **2010**, *25*, 2548–2552.
- [38] C. Hong, R. Yuan, Y. Chai, Y. Zhuo, *Anal. Chim. Acta* **2009**, *633*, 244–249.
- [39] Y. Yang, Z. Zhong, H. Liu, T. Zhu, J. Wu, M. Li, D. Wang, *Electroanalysis* **2008**, *20*, 2621–2628.
- [40] G. Sun, H. Liu, Y. Zhang, J. Yu, M. Yan, X. Song, W. He, *New J. Chem.* **2015**, *39*, 6062–6067.
- [41] F. Yang, Z. Yang, Y. Zhuo, Y. Chai, R. Yuan, *Biosens. Bioelectron.* **2015**, *66*, 356–362.
- [42] F. Hu, S. Chen, R. Yuan, *Sens. Actuator B-Chem.* **2013**, *176*, 713–722.
- [43] Y. Zhuo, R. Yuan, Y. Q. Chai, C. L. Hong, *Analyst* **2010**, *135*, 2036–2042.
- [44] Y. Wei, X. Li, X. Sun, H. Ma, Y. Zhang, Q. Wei, *Biosens. Bioelectron.* **2017**, *94*, 141–147.
- [45] M. Li, P. Wang, F. Li, Q. Chu, Y. Li, Y. Dong, *Biosens. Bioelectron.* **2017**, *87*, 752–759.
- [46] H. Deng, J. Li, Y. Zhang, H. Pan, G. Xu, *Anal. Chim. Acta* **2016**, *926*, 48–54.
- [47] H. Ma, Y. Li, Y. Wang, L. Hu, Y. Zhang, D. Fa, T. Yan, Q. Wei, *Biosens. Bioelectron.* **2016**, *78*, 167–173.
- [48] Y. Chu, H. Wang, H. Ma, D. Wu, B. Du, Q. Wei, *RSC Adv.* **2016**, *6*, 84698–84704.
- [49] J. Biscay, M. B. G. García, A. C. García, *Electroanalysis* **2015**, *27*, 2773–2777.
- [50] Y. Wang, Y. Qu, G. Liu, X. Hou, Y. Huang, W. Wu, K. Wu, C. Li, *Microchim. Acta* **2015**, *182*, 2061–2067.
- [51] J. Yang, W. Wen, X. Zhang, S. Wang, *Microchim. Acta* **2015**, *182*, 1855–1861.
- [52] L. Yang, H. Zhao, G. Deng, X. Ran, Y. Li, X. Xie, C.-P. Li, *RSC Adv.* **2015**, *5*, 74046–74053.
- [53] G. Sun, H. Liu, Y. Zhang, J. Yu, M. Yan, X. Song, W. He, *New J. Chem.* **2015**, *39*, 6062–6067.
- [54] Y. Huang, Y. Ding, T. Li, M. Yang, *Anal. Methods* **2015**, *7*, 411–415.
- [55] J. M. Moon, Y. H. Kim, Y. Cho, *Biosens. Bioelectron.* **2014**, *57*, 157–161.
- [56] B. Kavosi, A. Salimi, R. Hallaj, K. Amani, *Biosens. Bioelectron.* **2014**, *52*, 20–28.
- [57] V. Kumar, S. Srivastava, S. Umrao, R. Kumar, G. Nath, G. Sumana, P. S. Saxena, A. Srivastava, *RSC Adv.* **2014**, *4*, 2267–2273.
- [58] L. Ding, J. You, R. Kong, F. Qu, *Anal. Chim. Acta* **2013**, *793*, 19–25.
- [59] M. Yan, D. Zang, S. Ge, L. Ge, J. Yu, *Biosens. Bioelectron.* **2012**, *38*, 355–361.
- [60] R. Akter, M. A. Rahman, C. K. Rhee, *Anal. Chem.* **2012**, *84*, 6407–6415.
- [61] J. Tian, J. Huang, Y. Zhao, S. Zhao, *Microchim. Acta* **2012**, *178*, 81–88.
- [62] K. Mao, D. Wu, Y. Li, H. Ma, Z. Ni, Yu H, C. Luo, Q. Wei, B. Du, *Anal. Biochem.* **2012**, *422*, 22–27.
- [63] M. Yang, A. Javadi, S. Gong, *Sens. Actuator B-Chem.* **2011**, *155*, 357–360.
- [64] T. Li, M. Yang, H. Li, *J. Electroanal. Chem.* **2011**, *655*, 50–55.
- [65] H. Li, Q. Wei, J. He, T. Li, Y. Zhao, Y. Cai, B. Du, Z. Qian, M. Yang, *Biosens. Bioelectron.* **2011**, *26*, 3590–3595.
- [66] Q. Wei, Y. Zhao, C. Xu, D. Wu, Y. Cai, J. He, H. Li, B. Du, M. Yang, *Biosens. Bioelectron.* **2011**, *26*, 3714–3718.
- [67] M. Yang, A. Javadi, H. Li, S. Gong, *Biosens. Bioelectron.* **2010**, *26*, 560–565.
- [68] B. Qu, L. Guo, X. Chu, D. H. Wu, G. L. Shen, R. Q. Yu, *Anal. Chim. Acta* **2010**, *663*, 147–152.
- [69] V. Escamilla-Gomez, D. Hernandez-Santos, M. B. Gonzalez-Garcia, J. M. Pingarron-Carrazon, A. Costa-Garcia, *Biosens. Bioelectron.* **2009**, *24*, 2678–2683.
- [70] T. Xua, B. Chia, F. Wub, S. Mab, S. Zhanb, M. Yib, H. Xua, C. Mao, *Biosens. Bioelectron.* **2017**, *95*, 87–93.
- [71] T. Xu, B. Chi, J. Gao, M. Chu, W. Fan, M. Yi, H. Xu, C. Mao, *Anal. Chim. Acta* **2017**, *977*, 36–43.
- [72] Y. Niu, T. Yang, S. Ma, F. Peng, M. Yi, M. Wan, C. Mao, J. Shen, *Biosens. Bioelectron.* **2017**, *92*, 1–7.
- [73] Y. Huang, C. Tang, J. Liu, J. Cheng, Z. Si, T. Li, M. Yang, *Microchim. Acta* **2017**, *184*, 855–861.

Review

ELECTROANALYSIS

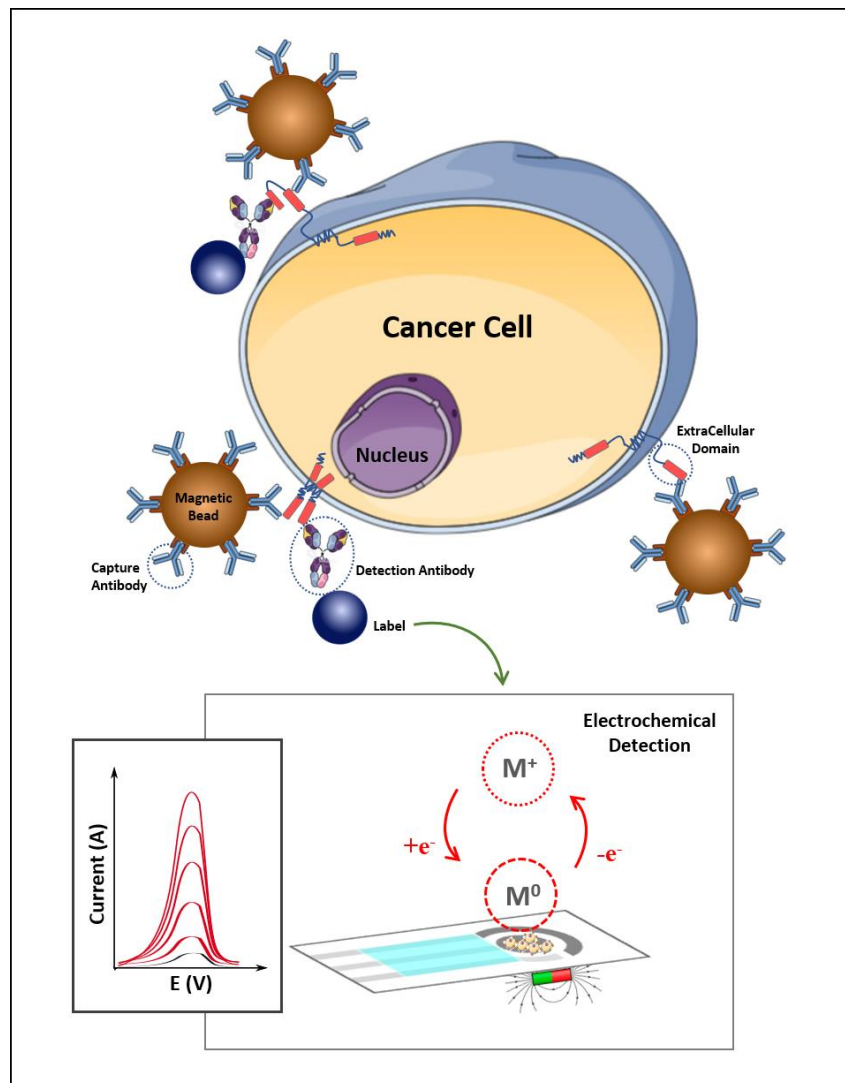
- [74] H. Wang, Y. Zhang, Y. Wang, H. Ma, B. Du, Q. Wei, *Biosens. Bioelectron.* **2017**, *87*, 745–751.
- [75] N. Hui, X. Sun, Z. Song, S. Niu, X. Luo, *Biosens. Bioelectron.* **2016**, *86*, 143–49.
- [76] J. Shan, L. Wang, Z. Ma, Z. Ma, *Sens. Actuator B-Chem.* **2016**, *237*, 666–671.
- [77] L. Jiao, Z. Mu, C. Zhu, Q. Wei, H. Li, D. Du, Y. Lin, *Sens. Actuator B-Chem.* **2016**, *231*, 513–519.
- [78] Y. Wei, Y. Li, N. Li, Y. Zhang, T. Yan, H. Man, Q. Wei, *Biosens. Bioelectron.* **2016**, *79*, 482–487.
- [79] Q. Zhai, X. Zhang, J. Li, E. Wang, *Nanoscale* **2016**, *8*, 15303–15308.
- [80] L. Jiang, F. Li, J. Feng, P. Wang, Q. Liu, Y. Li, Y. Dong, Q. Wei, *RSC Adv.* **2016**, *6*, 24373–24380.
- [81] J. Guo, X. Han, J. Wang, J. Zhao, Z. Guo, Y. Zhang, *Anal. Biochem.* **2015**, *491*, 58–64.
- [82] N. Li, H. Ma, W. Cao, D. Wu, T. Yan, B. Du, Q. Wei, *Biosens. Bioelectron.* **2015**, *74*, 786–791.
- [83] J. Liu, G. Lin, C. Xiao, Y. Xue, A. Yang, H. Ren, W. Lu, H. Zhao, X. Li, Z. Yuan, *Biosens. Bioelectron.* **2015**, *71*, 82–87.
- [84] L. Li, L. Zhang, J. Yu, S. Ge, X. Song, *Biosens. Bioelectron.* **2015**, *71*, 108–114.
- [85] F. Li, J. Han, L. Jiang, Y. Wang, Y. Li, Y. Dong, Q. Wei, *Biosens. Bioelectron.* **2015**, *68*, 626–632.
- [86] L. Ji, Z. Guo, T. Yan, H. Ma, B. Du, Y. Li, Q. Wei, *Biosens. Bioelectron.* **2015**, *68*, 757–762.
- [87] C. Zhou, D. Liu, L. Xu, Q. Li, J. Song, S. Xu, R. Xing, H. Song, *Sci. Rep.* **2015**, *5*, 1–7.
- [88] L. Jiang, J. Han, F. Li, J. Gao, Y. Li, Y. Dong, Q. Wei, *Electrochim. Acta* **2015**, *160*, 7–14.
- [89] Y. Wang, D. Wu, Y. Zhang, X. Ren, Y. Wang, H. Ma, Q. Wie, *RSC Adv.* **2015**, *5*, 56583–56589.
- [90] G. Zhong, R. Lan, W. Zhang, F. Fu, Y. Sun, H. Peng, T. Chen, Y. Cai, A. Liu, J. Lin, X. Lin, *Int. J. Nanomedicine* **2015**, *10*, 2219–2228.
- [91] M. C. Tu, H. Y. Chen, Y. Wang, S. M. Moochhala, P. Alagappan, B. Liedberg, *Anal. Chim. Acta* **2015**, *853*, 228–233.
- [92] T. Qi, J. Liao, Y. Li, J. Peng, W. Li, B. Chu, H. Li, Y. Wei, Z. Qian, *Biosens. Bioelectron.* **2014**, *61*, 245–250.
- [93] Y. Wang, X. Li, W. Cao, Y. Li, H. Li, B. Du, Q. Wei, *Talanta* **2014**, *129*, 411–416.
- [94] Y. Li, R. Yuan, Y. Chai, Y. Zhuo, H. Su, Y. Zhang, *Microchim. Acta* **2014**, *181*, 679–685.
- [95] H. Wang, H. Li, Y. Zhang, Q. Wei, H. Ma, D. Wu, Y. Li, Y. Zhang, B. Du, *Biosens. Bioelectron.* **2014**, *53*, 305–309.
- [96] Z. Yang, Y. Chai, R. Yuan, Y. Zhuo, Y. Li, J. Han, N. Liao, *Sens. Actuator B-Chem.* **2014**, *193*, 461–66.
- [97] H. P. Peng, Y. Hu, A. L. Liu, W. Chen, X. H. Lin, X.-B. Yu, *J. Electroanal. Chem.* **2014**, *712*, 89–95.
- [98] K. Liu, J. Zhang, Q. Liu, H. Huang, *Electrochim. Acta* **2013**, *114*, 448–454.
- [99] Q. Gao, J. Han, Z. Ma, *Biosens. Bioelectron.* **2013**, *49*, 323–328.
- [100] H. Fan, Z. Guo, L. Gao, Y. Zhang, D. Fan, G. Ji, B. Du, Q. Wei, *Biosens. Bioelectron.* **2015**, *64*, 51–56.
- [101] D. Wu, Z. Guo, Y. Liu, A. Guo, W. Lou, D. Fan, Q. Wei, *Talanta* **2015**, *134*, 305–309.
- [102] J. Liao, D. Tang, *Curr. Pharm. Anal.* **2009**, *5*, 164–170.
- [103] C. Tsé, A. S. Gauchez, W. Jacot, P. J. Lamy, *Cancer Treat. Rev.* **2012**, *38*, 133–142.
- [104] I. E. Tothill, *Semin. Cell Dev. Biol.* **2009**, *20*, 55–62.
- [105] L. Lam, N. McAndrew, M. Yee, T. Fu, J. C. Tchou, H. Zhang, *Biochim. Biophys. Acta* **2012**, *1826*, 199–208.
- [106] D. R. Thevenot, K. Tóth, R. A. Durst, G. S. Wilson, *Biosens. Bioelectron.* **2001**, *16*, 121–131.
- [107] M. Oliverio, S. Perotto, G. C. Messina, L. Lovato, F. De Angelis, *ACS Appl. Mater. Interfaces* **2017**, *9*, 29394–29411.
- [108] L. Tan, Y. Chen, H. Yang, Y. Shi, J. Si, G. Yang, Z. Wu, P. Wang, X. Lu, H. Bai, Y. Yang, *Sens. Actuator B-Chem.* **2009**, *142*, 316–320.
- [109] R. I. Jafri, T. Arockiadoss, N. Rajalakshmi, S. Ramaprabhu, *J. Electrochem. Soc.* **2010**, *157*, B874–B879.
- [110] Y. Jung, J. Y. Jeong, B. H. Chung, *Analyst* **2008**, *133*, 697–701.
- [111] A. Ulman, *Chem. Rev.* **1996**, *96*, 1533–1554.
- [112] N. J. Ronkainen, S. L. Okon, *Materials* **2014**, *7*, 4669–4709.
- [113] H. D. Jang, S. K. Kim, H. Chang, J. W. Choi, *Biosens. Bioelectron.* **2015**, *63*, 546–551.
- [114] F. Ricci, G. Adornetto, G. Palleschi, *Electrochim. Acta* **2012**, *84*, 74–83.
- [115] P. Yáñez-Sedeño, S. Campuzano, J. M. Pingarrón, *Sensors* **2016**, *16*, 1585–1617.
- [116] E. Paleček, M. Fojta, *Talanta* **2007**, *74*, 276–290.
- [117] V. Mani, B. V. Chikkaveeraiah, J. F. Rusling, *Expert. Opin. Med. Diagn.* **2011**, *5*, 381–391.
- [118] R. C. B. Marques, E. Costa-Rama, S. Viswanathan, H. P. A. Nouws, A. Costa-García, C. Delerue-Matos, M. B. González-García, *Sens. Actuator B-Chem.* **2018**, *255*, 918–925.
- [119] A. Dasgupta, A. R. Lim, C. M. Ghajar, *Mol. Oncol.* **2017**, *11*, 40–61.
- [120] M. Perfézou, A. Turner, A. Merkoçi, *Chem. Soc. Rev.* **2012**, *41*, 2606–2622.
- [121] P. T. H. Went, A. Lugli, S. Meier, M. Bundi, M. Mirlacher, G. Sauter, S. Dirnhofer, *Hum. Pathol.* **2004**, *35*, 122–128.
- [122] H. Shen, J. Yang, Z. Chen, X. Chen, L. Wang, J. Hu, F. Ji, G. Xie, W. Feng, *Biosens. Bioelectron.* **2016**, *81*, 495–502.
- [123] M. Maltez-da Costa, A. Escosura-Muñiz, C. Nogués, L. Barrios, E. Ibáñez, A. Merkoçi, *Nano Lett.* **2012**, *12*, 4164–4171.
- [124] Y. Zhuo, R. Yuan, Y. Q. Chai, C. L. Hong, *Anal. Chem.* **2013**, *85*, 1058–1064.
- [125] W. Lu, H.-Y. Wang, M. Wang, Y. Wang, L. Tao, W. Qian, *RSC Adv.* **2015**, *5*, 24615–24624.

Received: March 9, 2018

Accepted: March 30, 2018

Published online on April 30, 2018

2.2 Electrochemical strategies for HER2 detection: an update



The present section includes an update to the review work, specifically for the biomarker under study in this thesis: HER2.

2.2 Electrochemical strategies for HER2 detection: an update

The progress of electrochemical biosensors for the detection of breast cancer biomarkers has increased over the past decade. The state of art of electrochemical immunosensors, immunoassays and bioassay-based procedures for HER2 is discussed. A summary of the relevant topics and the main characteristics of the sensor development are presented in tables. The studies included were retrieved from the Clarivate Analytics Web of Science database (timespan: 2008–2020).

2.2.1 Electrochemical immunosensors for HER2 detection

Since the first reported electrochemical immunosensor for HER2 detection, in 2008, great improvements in the area have been reported and over 15 scientific publications can be found in the literature. Table 1 summarizes the main analytical parameters of the developed immunosensors [1-16]. Transducers include conventional electrodes such as glassy carbon electrode (GCE) [2] and gold electrode (AuE) [3,13]; miniaturized SPE [4-6,9-12,14,16]; carbon ionic liquid electrode (CILE) [7]; indium tin oxide (ITO) [15]; and microarrays [8]. Transducer surface modifications were mainly performed with carbon- and gold nanomaterials, self-assembled monolayers or a zwitterionic hydrogel.

Label-free assays were reported with excellent assay times, however with expensive and time-consuming transducer surface modifications. Ferricyanide/ferrocyanide ($[\text{Fe}(\text{CN})_6]^{3-/4-}$) was commonly used as redox probe [3,6,7,9,11,15]. On the other hand, the majority of the reported studies consists of sandwich-type assays. Distinct labels were employed, such as enzymes (horseradish peroxidase (HRP) [1,5,13], alkaline phosphatase (AP) [4,12]), QDs (lead sulfide (PbS) [14], cadmium/selenium (CdSe) [16]) and hydrazine [2]. In addition, detection strategies were achieved using 3,3',5,5'-tetramethylbenzidine (TMB) [10,13], hydroquinone (HQ) [5,8], methylene blue (MB) [1] or metal ions (silver, lead and cadmium) [2,4,12,14,16]. No competitive assays were found in the research data. Despite the strategies described for the immunosensor's development, with several ranges under study, only one reports a detection limit above the cut-off value established for this biomarker (15 ng/mL) [5]. Furthermore, two distinct works have a longer assay time (> 6 h) [1,10], compared to the remaining works that report sample analysis in less than 3 h, demonstrating that the developed immunosensors as rapid methodologies for breast cancer detection. Long-term stability shows that the reported sensors were stable, at least, for one week. Spiked human serum, patient serum or cells were included in all studies, demonstrating their applicability.

Table 1. Electrochemical immunosensors for analysis of HER2 breast cancer biomarker.

Breast cancer analyte	Sensing surface			Sample	Detection strategy			LOD	Ref		
	Transducer	Transducer preparation time*	Modification with the biorecognition element*		Label	Technique	Detection			Assay time	
HER2	NEEs	n.d.	2 h	n.d.	Cell lysates	HRP	CV	MB	7 h 10 min	40 ng/mL	[1]
HER2	GCE/poly-DPB(AuNP)	> 4 h	~ 12 h	n.d.	Cancer cells	Hydrazin	SWASV	Silver	1 h 10 min	0.037 pg/mL	[2]
HER2	AuE/AuNP-MPA-Cys	> 22 h	~ 12 h	3 weeks	Patient serum	n.a.	DPV	[Fe (CN) ₆] ^{3-/4-}	30 min	0.995 pg/mL	[3]
HER2-ECD	SPCE/AuNP	~ 10 min	~ 12 h	n.d.	Spiked human serum	AP	LSV	Silver	2 h 50 min	4.4 ng/mL	[4]
HER2	SPE	1 h	1 h	3 weeks	Cell lysates	HRP	Amperometry	HQ	22 min	1 µg/mL	[5]
HER2	GSPE/AuNP	~ 10 min	~ 12 h	2 weeks	Spiked human serum	n.a.	EIS	[Fe (CN) ₆] ^{3-/4-}	2 h	6.0 ng/mL	[6]
HER2	CILE-MWCNT/AuNP	> 30 h	6 h	n.d.	Patient serum	n.a.	EIS	[Fe (CN) ₆] ^{3-/4-}	35 min	7.2 ng/mL	[7]
HER2	8 WEAMPA	> 24 h	~ 12 h	14 days	Spiked human serum	HRP	Amperometry	HQ	1 h 15 min	12 pg/mL	[8]
HER2	SPCE/Cys-AuNP	> 2 h	~ 12 h	22 days	Spiked human serum	n.a.	EIS	[Fe (CN) ₆] ^{3-/4-}	1 h	0.01 ng/mL	[9]
HER2	SPCE	–	2 h	7 days	Patient serum	HRP	CV	TMB	6 h 05 min	4 ng/mL	[10]
HER2	SPCE/zwitterionic hydrogel	> 12 h	15 min	3 weeks	Patient serum	n.a.	EIS	[Fe (CN) ₆] ^{3-/4-}	n.d.	5 pg/mL	[11]
HER2-ECD	SPCE/MWCNT-AuNP	~ 15 min	~ 12 h	n.d.	Spiked human serum	AP	LSV	Silver	2 h 20 min	0.16 ng/mL	[12]
HER2	AuE/Cys	13 h	1 h	n.d.	Spiked human serum	HRP	Chronoamperometry	TMB	3 h 12 min	1.0 ng/mL	[13]
HER2	SPCE	1 h	45 min	n.d.	Spiked human serum	PbS QDs	SWASV	Lead	2 h 20 min	0.28 ng/mL	[14]
HER2	ITO/MoO ₃ -RGO-APTES	> 2 h	~ 5 h	9 weeks	Patient serum	n.a.	DPV	[Fe (CN) ₆] ^{3-/4-}	15 min	0.001 ng/mL	[15]
HER2-ECD	SPCE	–	~ 12 h	7 days	Spiked human serum	QDs	SWV	Cadmium	1 h 30 min	2.1 ng/mL	[16]

* Overnight incubations were considered as a 12 h period for comparison purposes.
 AuE – gold electrode; AP – alkaline phosphatase; AuNP – gold nanoparticles; APTES – 3-aminopropyltriethoxysilane; CILE – carbon ionic liquid electrode; Cys – cysteamine; CV – cyclic voltammetry; DPB – 2,5-bis(2-thienyl)-1H-pyrole-1-(p-benzoic acid); DPV – differential pulse voltammetry; EIS – electrochemical impedance spectroscopy; ECD – extracellular domain; GCE – glassy carbon electrode; GSPE – graphite screen-printed electrode; HER2 – human epidermal growth factor receptor 2; HQ – hydroquinone; HRP – horseradish peroxidase; ITO – indium tin oxide; LSV – linear sweep voltammetry; MB – methylene blue; MoO₃ – molybdenum trioxide; MPA – 3-mercaptopropionic acid; MWCNT – multiwalled carbon nanotube; n.d. – no data; n.a. – not applicable; NEEs – nanoelectrode ensembles; PbS – lead sulfide; RGO – reduced graphene oxide; QDs – quantum dots; SPCE – screen-printed carbon electrode; SPE – screen-printed electrode; SWASV – square wave voltammetry; SWV – square wave voltammetry; TMB – 3,3',5,5'-Tetramethylbenzidine; WEA – working electrode array.

2.2.2 Magnetic electrochemical immunoassays for HER2 detection

Although few magnetic immunoassays are reported for HER2, excellent analytical characteristics and assay performances were described. Table 2 summarizes the experimental parameters of these procedures [17-23].

In 2012 Al-Khafaji *et al.* [17] described an electrochemical immunoassay for HER2 detection using a sandwich format in which anti-HER2 antibodies were immobilized on protein A-modified MBs. DPV was used to obtain the analytical signal, employing alkaline phosphatase (AP) as detection label and 1-naphthyl-phosphate (1-NP) as the enzymatic substrate. In another study the detection of ErbB2, also based on a sandwich format, involved the covalent immobilization of the capture antibody on carboxylic acid-functionalized MBs. The modified beads were incubated with a solution containing the antigen and HRP-labelled secondary antibodies with detection performed through amperometry using hydroquinone/H₂O₂ [18].

In a distinct work, three electrochemical bioassays were developed using affibodies (Af) or antibodies (Ab), immobilized on streptavidin-MBs or protein A-modified MBs, respectively. Detection of the antibody-antigen interaction by DPV was achieved through the use of AP and 1-NP [19].

Magnetite nanoparticles coated with 3-aminopropyltrimethoxysilane (Fe₃O₄-APTMS) were used as sensing platform for efficient capture of HER2 in biological fluids [20]. Silver signal enhancement strategy was applied using hydrazine (label) and detection was accomplished by DPV.

In another strategy, streptavidin-MBs were employed to a cellulase-linked sandwich assay. MBs were applied onto a graphite electrode modified with nitrocellulose film in which the cellulase label digests the film. This changes the electrical properties that were recorded by chronocoulometry (CC) [21].

Two distinct works were developed by Freitas *et al.*, using carboxylic acid-modified magnetic beads (HOOC-MBs), using a sandwich format, however using distinct labels and detection strategies: metalloenzymatic detection, using AP as label, 3-IP as enzymatic substrate and silver ions detection was performed by LSV [22]; using quantum dots as nanolabels with cadmium detection performed through DPV [23].

Table 2. Electrochemical immunoassays for analysis of HER2 breast cancer biomarker.

Breast cancer analyte	Sensing surface			Sample	Detection strategy			LOD	Ref		
	Transducer	Transducer preparation time*	Modification with biorecognition element*		Long-term stability	Label	Technique			Detection	Assay time
HER2	SPCE/ProtA-MBs	~ 15 min	40 min	10 days	Patient serum	AP	DPV	1-NP	2 h 05 min	6.0 ng/mL	[17]
ErbB2	SPCE/HOOC-MBs	~ 40 min	1 h	n.d.	Patient serum and cell lysates	HRP	Amperometry	HQ	1 h	25 pg/mL	[18]
HER2	8× SPE/Strep-MBs or ProtA-MBs	~ 15 min	~ 12 h 45 min	1 week	Spiked human serum	AP	DPV	1-NP	2 h 51 min 1 h 51 min	1.8, 2.6 and 3.4 ng/mL	[19]
HER2	GCE/Fe ₃ O ₄ -APTMS	> 3 h	2 h	10 days	Patient serum	Hydrazin	DPV	Silver	2 h	2.0×10 ⁻⁵ ng/mL	[20]
HER2	GrE/nitrocellulose/Strep-MBs	1 h	1 h	n.d.	Spiked human serum	Cellulase	Chronocoulometry	Nitrocellulose digestion	3 h	1 fM	[21]
HER2-ECD	SPCE/HOOC-MBs	~ 15 min	1 h	60 days	Spiked human serum	AP	LSV	Silver	1 h 50 min	2.8 ng/mL	[22]
HER2-ECD	SPCE/HOCC-MBs	~ 15 min	1 h	60 days	Spiked human serum	QDs	SWV	Cadmium	1 h 30 min	0.29 ng/mL	[23]

*Overnight incubations were considered as a 12 h period for comparison purposes.

1-NP – 1-naphthol; AP – alkaline phosphatase; APTMS – (3-Aminopropyl)triethoxysilane; DPV – differential pulse voltammetry; ECD – extracellular domain; Fe₃O₄ – magnetite nanoparticles; GCE – glassy carbon electrode; GrE – graphite electrode; HER2/ErbB2 – human epidermal growth factor receptor 2; HOOC-MBs – carboxylic acid functionalized MBs; HRP – horseradish peroxidase; HQ – hydroquinone; LSV – linear sweep voltammetry; MBs – magnetic beads; n.d. – no data; n.a. – not applicable; ProtA – protein A; QDs – quantum dots; SPE – streptavidin; SPC – screen-printed carbon electrode; SPCE – screen-printed carbon electrode; SWV – Square wave voltammetry.

2.2.3 Electrochemical bioassay-based procedures for HER2-expressing breast cancer cell lines

Circulating tumour cells (CTCs) enumeration and characterization have gained importance since the ability of cell invasion and metastization can be responsible for a large number of deaths. Only a few scientific works reported electrochemical immunoassay-based protocols for HER2-expressing breast cancer cell line enumeration. Details of analytical parameters related to the published assays for the detection of HER2 in cancer cell lines are presented in Table 3 [1,2,18,22-27].

HER2-positive (HER2(+)) and HER2-negative (HER2(-)) tumour cells or cell lysates were tested throughout the works to evaluate the assays and to test the selectivity. Mucelli *et al.* [1] developed nanoelectrode ensembles to detect small amounts of HER2. Then, HER2 overexpressing cell lysates (SK-BR-3) and HER2(-) MCF-7 lysates were tested and the sensor demonstrate to be selective for different HER2 amounts in the tumour lysates. In a different approach, Zhu *et al.* [2] proposed a sensor capable of differentiating between HER2(+) SK-BR-3, HER2(-) MCF-7 and normal breast cell line MCF 10A. For the selectivity studies, cancer cell line Hela was tested. The direct attachment of hydrazine onto the AuNP catalyst ensures the reduction and deposition of silver that allow the detection of HER2 protein and the HER2(+) cancer cells.

In a distinct format, an immunomagnetic sensor developed by Eletxigerra *et al.* [18] reported carboxylic acid-modified MBs used for the assessment of ErbB2 directly in intact breast cancer cells. A significantly higher amperometric response was obtained for the SK-BR-3 cells, whereas a low response was reported for the MCF-7 and MDA-MB-436 (HER2(-)) breast cancer cells. In the reported magnetic immunoassays developed by Freitas *et al.* [22,23] after detection of HER2 levels in human serum, breast cancer cells SK-BR-3, MCF-7 and MDA-MB-231 were tested.

A label-free approach was proposed for rapid detection of HER2 using $[\text{Fe}(\text{CN})_6]^{3-/4-}$ as redox probe [24]. To assess the selectivity of the developed nano-biosensor distinct cancer cells were tested: HER2-expressing SK-BR-3; HER2(+) with middle expression level ZR-75-1; low expression level of HER2 MDA-MB-231; normal MCF10A breast cell line and colon cancer cell line SW742. In a distinct concept, Boriacheck *et al.* [25] reported the detection of HER2(+) breast cancer cell lines BT-474 and FAM134B(+), and colon cancer cell line SW-48, both isolated from tumor-derived exosomes. For the assay construction, streptavidin-modified MBs, CdSe quantum dot (CdSe QD) and a bare GCE were used. Anodic stripping voltammetry was carried out for the quantification of Cd^{2+} . Following the same concept, however in a label-free assay-type, Yadav *et al.* [26]

reported an approach that exhibit an excellent specificity for HER2(+) BT-474 cell-derived exosomes in which DPV allows to monitor the analyses in the presence of the redox pair $[\text{Fe}(\text{CN})_6]^{3-/4-}$. The electrochemical signal generated from HER2(+) exosome was compared to the control experiment performed with MDA-MB-231 exosomes.

In a different approach, an aptamer-based label-free assay was described, using $[\text{Fe}(\text{CN})_6]^{3-/4-}$ as probe [27]. In the sensor construction, a composite of bimetallic MnFe Prussian blue analogue coupled to gold nanoparticles (MnFePBA@AuNP) was placed on an AuE electrode, used for the determination of trace levels of HER2 and living MCF-7 cells. To assess the selectivity, normal L929 cells were used.

Table 3. Electrochemical bioassay-based analysis of HER2-expressing breast cancer cell lines.

HER2 ⁺ Cell type	Sensing surface			Sample	Detection strategy			LOD (cell/mL)	Selectivity	Ref
	Transducer preparation time*	Transducer preparation time*	Modification with biorecognition element*		Label	Technique	Detection			
SK-BR-3	n.a.	2 h	n.d.	Buffer	HRP	CV	MB	6 h	MCF-7	[1]
SK-BR-3	> 4 h	~ 12 h	n.d.	Human serum	Hydrazin	SWASV	Silver	1 h 10 min	MCF10, MCF7, Hela	[2]
SK-BR-3	~40 min	1 h	n.d.	Cell lysates	HRP	Amperometry	HQ	1 h	MDA-MB-434, MCF-7	[18]
SK-BR-3	15 min	1 h	60 days	Human serum	AP	LSV	Silver	1 h 50 min	MDA-MB-231	[22]
SK-BR-3	15 min	1 h	60 days	Human serum	QDs	SWV	Cadmium	1 h 30 min	MDA-MB-231, MCF-7	[23]
SK-BR-3	> 4 h	~ 12 h	45 days	Whole blood	n.a.	DPV	[Fe (CN) ₆] ^{3-/4-}	30 min	ZR-75-1, MDA- MB-231, SW- 742, MCF-10A	[24]
BT-474	n.a.	30 min	n.d.	Patient serum	QDs	SWASV	Cadmium	1 h 50 min	100 exosome/ μ L SW-48	[25]
BT-474	n.a.	20 min	n.d.	Human serum	n.a.	DPV	[Fe (CN) ₆] ^{3-/4-}	2 h	MDA-MB-231	[26]
MCF-7	5 h	2 h	15 days	Human serum	n.a.	EIS	[Fe (CN) ₆] ^{3-/4-}	1 h	L929	[27]

* Overnight incubations were considered as a 12 h period for comparison purposes.

AgNP – silver nanoparticles; AuE – gold electrode; AuNP – gold nanoparticles; CV – cyclic voltammetry; DPB – 2,5-bis(2-thienyl)-1H-pyrrole-1-(p-benzoic acid); DPV – differential pulse voltammetry; EIS – electrochemical impedance spectroscopy; FTO – fluorine doped tin oxide; GCE – glassy carbon electrode; HER2 – human epidermal growth factor receptor 2; HOOC-MBs – carboxylic acid functionalized magnetic beads; HRP – horseradish peroxidase; HQ – hydroquinone; MB – methylene blue; MnFePBA – bimetallic MnFe Prussian blue analogue; n.d. – no data; n.a. – not applicable; NEES – nanoelectrode ensembles; NFG – nitrogen-doped graphene; PANI – polyaniline; QDs – quantum dots; Strep-MBs – streptavidin modified magnetic beads; SPCE – screen-printed carbon electrode; SPCE/E – extraavidin modified screen printed carbon electrodes; SWASV – square wave anodic stripping voltammetry; SWV – Square wave voltammetry.

References

- [1] SP Mucelli, M Zamuner, M Tormen, G Stanta, P Ugo. Nanoelectrode ensembles as recognition platform for electrochemical immunosensors. *Biosensors and Bioelectronics* **2008**, 23, 1900-1903. <https://doi.org/10.1016/j.bios.2008.02.027>
- [2] Y Zhu, P Chandra, YB Shim. Ultrasensitive and selective electrochemical diagnosis of breast cancer based on a hydrazine-Au nanoparticle-aptamer bioconjugate. *Analytical Chemistry* **2013**, 85, 1058-1064. <https://doi.org/10.1021/ac302923k>
- [3] M Emami, M Shamsipur, R Saber, R Irajirad. An electrochemical immunosensor for detection of a breast cancer biomarker based on antiHER2–iron oxide nanoparticle bioconjugates. *Analyst* **2014**, 139, 2858-2866. <https://doi.org/10.1039/C4AN00183D>
- [4] RCB Marques, S Viswanathan, HPA Nouws, C Delerue-Matos, M.B. González-García. Electrochemical immunosensor for the analysis of the breast cancer biomarker HER2 ECD. *Talanta* **2014**, 129, 594-599. <https://doi.org/10.1016/j.talanta.2014.06.035>
- [5] S Patris, P De Pauw, M Vandeput, J Huet, P Van Antwerpen, S Muyldermans, JM Kauffmann. Nanoimmunoassay onto a screen-printed electrode for HER2 breast cancer biomarker determination. *Talanta* **2014**, 130, 164-170. <https://doi.org/10.1016/j.talanta.2014.06.069>
- [6] A Ravalli, CG da Rocha, H Yamanaka, G Marrazza. A label-free electrochemical affisensor for cancer marker detection: The case of HER2. *Bioelectrochemistry* **2015**, 106, 268-275. <https://doi.org/10.1016/j.bioelechem.2015.07.010>
- [7] E Arkan, R Saber, Z Karimi, M Shamsipur. A novel antibody-antigen based impedimetric immunosensor for low level detection of HER2 in serum samples of breast cancer patients via modification of a gold nanoparticles decorated multiwall carbon nanotube-ionic liquid electrode. *Analytica Chimica Acta* **2015**, 874, 66-74. <https://doi.org/10.1016/j.aca.2015.03.022>
- [8] S Carvajal, SN Fera, AL Jones, TA Baldo, IM Mosa, JF Rusling, CE Krause. Disposable inkjet-printed electrochemical platform for detection of clinically relevant HER-2 breast cancer biomarker. *Biosensors and Bioelectronics* **2018**, 104, 158-162. <https://doi.org/10.1016/j.bios.2018.01.003>
- [9] S Sharma, J Zapatero-Rodríguez, R Saxena, R O'Kennedy, S Srivastava. Ultrasensitive direct impedimetric immunosensor for detection of serum HER2. *Biosensors and Bioelectronics* **2018**, 106, 78-85. <https://doi.org/10.1016/j.bios.2018.01.056>
- [10] SD Tallapragada, K Layek, R Mukherjee, KK Mistry, M Ghosh. Development of screen-printed electrode based immunosensor for the detection of HER2 antigen in human serum samples. *Bioelectrochemistry* **2017**, 118, 25-30.

<https://doi.org/10.1016/j.bioelechem.2017.06.009>

[11] E Chocholova, T Bertok, L Lorencova, A Holazova, P Farkas, A Vikartovska, V Bella, D Velicova, P Kasak, AA Eckstein, J Mosnacek, D Hasko, J Tkac. Advanced antifouling zwitterionic layer based impedimetric HER2 biosensing in human serum: glycoprofiling as a novel approach for breast cancer diagnostics. *Sensors and Actuators B Chemical* **2018**, 272, 626-633. <https://doi.org/10.1016/j.snb.2018.07.029>

[12] M Freitas, HPA Nouws, C Delerue-Matos, Electrochemical sensing platforms for HER2-ECD breast cancer biomarker detection. *Electroanalysis* **2019**, 31, 121-128. <https://doi.org/10.1002/elan.201800537>

[13] M Jarczewska, A. Trojan, M. Gągała, E Malinowska. Studies on the Affinity-based Biosensors for Electrochemical Detection of HER2 Cancer Biomarker. *Electroanalysis* **2019**, 31, 1125-1134. <https://doi.org/10.1002/elan.201900041>

[14] ZMANH Lah, SAA Ahmad, MS Zainic, MA Kamarudin. An Electrochemical Sandwich Immunosensor for the Detection of HER2 using Antibody-Conjugated PbS Quantum Dot as a label. *Journal of Pharmaceutical and Biomedical Analysis* **2019**, 174, 608-617. <https://doi.org/10.1016/j.jpba.2019.06.024>

[15] S Augustine, P Kumar, BD Malhotra. Amine-Functionalized MoO₃@RGO Nanohybrid-Based Biosensor for Breast Cancer Detection. *ACS Applied Bio Materials* **2019**, 2,12, 5366–5378. <https://doi.org/10.1021/acsabm.9b00659>

[16] M Freitas, MMPS Neves, HPA Nouws, C Delerue-Matos. Quantum dots as nanolabels for breast cancer biomarker HER2-ECD analysis in human serum. *Talanta* **2020**, 208, 120430. <https://doi.org/10.1016/j.talanta.2019.120430>

[17] QAM Al-Khafaji, M Harris, S Tombelli, S Laschi, APF Turner, M Mascini, G Marrazza. An electrochemical immunoassay for HER2 detection. *Electroanalysis* **2012**, 24, 735-742. <https://doi.org/10.1002/elan.201100501>

[18] U Eletxigerra, J Martinez-Perdiguero, S Merino, R Barderas, RM Torrente-Rodríguez, R Villalonga, JM Pingarrón, S Campuzano. Amperometric magnetoimmunosensor for ErbB2 breast cancer biomarker determination in human serum, cell lysates and intact breast cancer cells. *Biosensors and Bioelectronics* **2015**, 70, 34-41. <https://doi.org/10.1016/j.bios.2015.03.017>

[19] H Ilkhani, A Ravalli, G Marrazza. Design of an affibody-based recognition strategy for human epidermal growth factor receptor 2 (HER2) detection by electrochemical biosensors. *Chemosensors* **2016**, 4, 23. <https://doi.org/10.3390/chemosensors4040023>

[20] M Shamsipur, M Emami, L Farzin, R Saber. A sandwich-type electrochemical immunosensor based on in situ silver deposition for determination of serum level of HER2 in breast cancer patients. *Biosensors and Bioelectronics* **2018**, 103, 54-61.

<https://doi.org/10.1016/j.bios.2017.12.022>

[21] K Malecka, D Pankratov, EE Ferapontova. Femtomolar electroanalysis of a breast cancer biomarker HER-2/neu protein in human serum by the cellulase-linked sandwich assay on magnetic beads. *Analytica Chimica Acta* **2019**, 1077, 24, 140-149.

<https://doi.org/10.1016/j.aca.2019.05.052>

[22] M Freitas, HPA Nouws, E Keating, C Delerue-Matos. High-performance electrochemical immunomagnetic assay for breast cancer analysis. *Sensors and Actuators: B. Chemical* **2020**, 308, 127667. <https://doi.org/10.1016/j.snb.2020.127667>

[23] M Freitas, HPA Nouws, E Keating, VC Fernandes, C Delerue-Matos. Immunomagnetic-beads-based assay for voltammetric analysis of HER2-ECD breast cancer biomarker and tumour cells using Quantum Dots as nanolabels. *Microchimica Acta* **2020**, 187 (3), 184. doi.org/10.1007/s00604-020-4156-4

[24] R Salahandish, A Ghaffarinejad, SM Naghi, K Majidzadeh-A, H Zargartalebi, A Sanati-Nezhad. Nano-biosensor for highly sensitive detection of HER2 positive breast cancer. *Biosensors and Bioelectronics* **2018**, 117, 104-111.

<https://doi.org/10.1016/j.bios.2018.05.043>

[25] K Boriachek, Md. N Islam, V Gopalan, AK Lam, N-T Nguyen, MJA Shiddiky. Quantum dot-based sensitive detection of disease specific exosome in serum. *Analyst* **2017**, 142, 2211-2219. <https://doi.org/10.1039/C7AN00672A>

[26] S Yadav, K Boriachek, M N Islam, R Lobb, A Möller, MM Hill, MSA Hossain, N-T Nguyen, MJA Shiddiky. An Electrochemical Method for the Detection of Disease Specific Exosomes. *ChemElectroChem* **2016**, 3, 1-6. <https://doi.org/10.1002/celec.201600391>

[27] N Zhou, F Su, Z Li, X Yan, C Zhang, B Hu, L He, M Wang, Z Zhang. Gold nanoparticles conjugated to bimetallic manganese(II) and iron(II) Prussian Blue analogues for aptamer-based impedimetric determination of the human epidermal growth factor receptor-2 and living MCF-7 cells. *Microchimica Acta* **2019**, 186(2), 75.

<https://doi.org/10.1007/s00604-018-3184-9>

CHAPTER 3

ELECTROCHEMICAL IMMUNOASSAYS WITH METALLOENZYMATIC DETECTION



3

Overview

This chapter comprises two original scientific publications in international peer-reviewed journals (sections 3.1 and 3.2).

An integral transcript of the published articles is presented according to the journal rights and with requested permission.

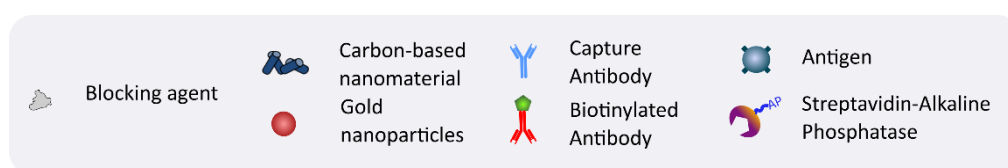
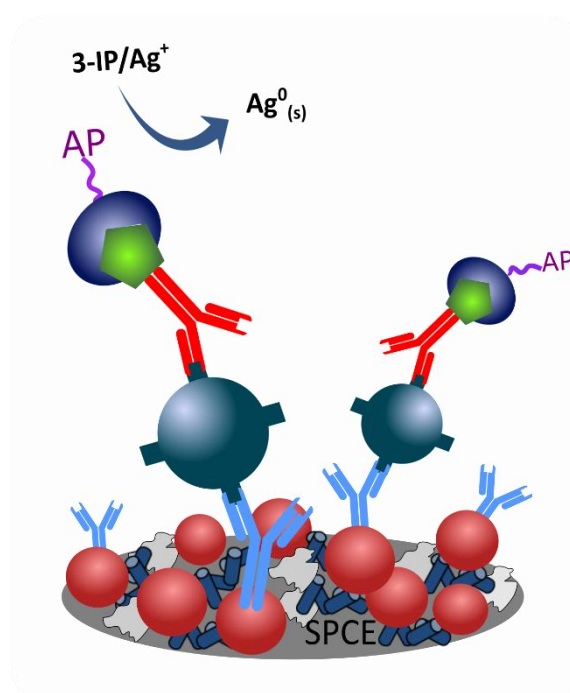
Distinct electrochemical transducer platforms were tested and characterized (electrochemical and microscopy techniques) and used for the detection of HER2-ECD, in a sandwich-type assay format.

Screen-printed carbon electrodes (SPCEs) were firstly modified with: (i) reduced graphene oxide (rGO), (ii) carboxylic acid functionalized single-walled carbon nanotubes (SWCNT-COOH), (iii) carboxylic acid functionalized multiwalled carbon nanotubes (MWCNT-COOH), and their conjugation with gold nanoparticles (AuNP): (iv) rGO/AuNP, (v) SWCNT/AuNP, (vi) MWCNT/AuNP. In addition, (vii) carboxylic acid functionalized magnetic beads (HOOC-MBs) were used for the construction of an immunomagnetic assay. Metalloenzymatic detection, fully described in the chapter 1 (general introduction), was employed for HER2-ECD detection and cancer cell analysis.

The first author's contributions contemplated the preparation and characterization of nano- and micro materials, used for the efficient modification of SPCE; subsequent preparation, optimization and application of the developed assay in human serum; cancer cell-lines preparation and application; data compilation, writing and editing the manuscripts (original draft – Lead).

3.1 Electrochemical Sensing Platforms for HER2-ECD Breast Cancer Biomarker Detection

Electroanalysis 31 (1) (2019) 121-128



Author Contributions:

Maria Freitas (investigation: Equal; Methodology: Equal; Writing – original draft: Lead); Henri Nouws (Conceptualization: Lead; Funding acquisition: Equal; Methodology: Lead; Project administration: Equal; Supervision: Equal; Validation: Equal; Writing – review & editing: Lead); Cristina Delerue-Matos (Funding acquisition: Equal; Methodology: Equal; Supervision: Equal; Validation: Equal; Writing – review & editing: Supporting)

DOI: 10.1002/elan.201800537

Electrochemical Sensing Platforms for HER2-ECD Breast Cancer Biomarker Detection

Maria Freitas,^[a] Henri P. A. Nouws,^{*,[a]} and Cristina Delerue-Matos^[a]

Abstract: Screening and early diagnosis are crucial to increase the success of cancer patients' treatments and improve the survival rate. To contribute to this success, distinct electrochemical immunosensing platforms were developed for the analysis of the ExtraCellular Domain of the Human Epidermal growth factor Receptor 2 (HER2-ECD) through sandwich assays on nanomaterial-modified screen-printed carbon electrodes (SPCEs). The most promising platforms showed to be SPCEs modified with (i) gold nanoparticles (AuNPs) and (ii) multiwalled carbon nanotubes combined with AuNPs. The antibody-

antigen interaction was detected using a secondary antibody labelled with alkaline phosphatase and 3-indoxyl phosphate and silver ions as the enzymatic substrate. The electrochemical signal of the enzymatically generated metallic silver was recorded by linear sweep voltammetry. Under the optimized conditions, linear calibration plots were obtained between 7.5 and 50 ng/mL and the total assay time was 2 h 20 min, achieving LODs of 0.16 ng/mL (SPCE-MWCNT/AuNP) and 8.5 ng/mL (SPCE-AuNP), which are well below the established cut-off value of 15 ng/mL for this cancer biomarker.

Keywords: Biomarker · Biosensor · Breast cancer · Electrochemistry · Immunoassay

1 Introduction

Breast cancer, one of the major life-threatening diseases in woman, is still one of the leading causes of oncological deaths [1]. Diagnostic techniques for its detection are in constant development but are yet far from ideal. Currently medical strategies for screening and early detection are based on imaging tools, namely mammography. Although detection is usually achieved with high efficiency, it only allows the visualization of the tumour and cannot predict its biological behaviour and evolution [2,3]. Nevertheless, the evolution of clinical methods for effective detection of breast cancer along with the development of non-invasive and low-cost in situ techniques can improve survival rates and allow personalized patient follow-up [2,4]. These non-invasive methods are a prominent alternative not only regarding response time but also to minimize the patients' suffering. For this purpose, biosensors have been developed because they provide fast analysis and specific recognition. Therefore, their development is in continuous expansion and they have widely been applied in point-of-care detection [4,5]. Current innovations in the field of biosensing lead to accurate results in the analysis of tumour biomarkers in patients' biological fluids such as serum, plasma, whole blood, urine, etc. A tumour biomarker is a substance or process indicative of the presence of cancer in the body [6]. Breast cancer biomarkers can be divided into prognostic, therapeutic and diagnostic, and can be detected according to the stage of the cancer [7]. Among the variety of biomolecules that are approved as tumour biomarkers and accepted for diagnosis by medical and clinical teams, there are many biological fluid-based biomarkers of interest for the development of electro-

chemical biosensors. The main protein breast cancer biomarkers for non-invasive clinical tests are the Human Epidermal growth factor Receptor 2 (HER2, ErbB2 or CD340), Cancer Antigen 15-3 (CA 15-3) and Carcinoembryonic Antigen (CEA). In addition, Circulating Tumour Cells (CTCs) can also provide prognostic or predictive information [8,9]. In serum analysis biomarkers that shed extracellular domains in the peripheral blood (e.g. HER2) are important analytes that can be used as a source of information on the status of the tumour. HER2-ECD is a protein breast cancer biomarker that presents serum levels below 15 ng/mL for healthy individuals and can be important for patients' screening and early detection. HER2 is overexpressed in 20–30% of invasive breast cancer and HER2-positive breast cancer is particularly more aggressive than others [7–9].

A few electrochemical immunosensing strategies for the detection of HER2 in serum have been reported. These strategies are generally based on the modification of the electrode surface with nano- or micromaterials that can provide improved performances like the promotion of electron transfer, signal amplification and the decrease of the limit of detection. Furthermore, the use of small-size transducers, the reasonably short assay times and the low reagent/sample volumes are key features for the development of point-of-care devices. Marques et al. (2014) developed a sandwich-type assay on screen-printed carbon

[a] M. Freitas, H. P. A. Nouws, C. Delerue-Matos
REQUIMTE/LAQV, Instituto Superior de Engenharia do
Porto, Politécnico do Porto, Rua Dr. António Bernardino de
Almeida 431, 4200-072 Porto, Portugal
E-mail: han@isep.ipp.pt

Full Paper

ELECTROANALYSIS

electrodes (SPCEs) which were nanostructured with gold nanoparticles (AuNP) to efficiently immobilize anti-HER2-ECD capture antibodies through chemisorption [10]. In a different approach Ravalli et al. developed a label-free impedimetric biosensor based on the immobilization of a terminal cysteine-modified affibody on gold nanostructured graphite screen-printed electrodes. AuNPs were used in these studies to enhance the capture antibody's immobilization and to retain its immunoreactivity on the electrode [11]. Furthermore, the use of nanomaterials, with excellent and reliable physicochemical properties, in the sensor's construction increases the electrode's surface area with a subsequent increase of sensitivity [12]. Arkan et al. proposed an immunosensor based on multiwalled carbon nanotubes (MWCNTs) and AuNPs contained in a carbon ionic liquid electrode (CILE). Pre-synthesized AuNPs were grown on the MWCNT-CILE surface through electrodeposition, to form AuNP/MWCNT-CILE, which is a suitable surface for antibody attachment [13]. In a distinct approach, Emami et al. employed magnetic iron nanoparticles for efficient antibody immobilization on an electrode surface that was previously modified with AuNPs/3-mercaptopropionic acid/cysteamine/poly(ethylene glycol)-maleimide-3-aminopropyltrimethoxysilane [14]. Moreover, in an analogous but simpler methodology, Shamsipur et al. reported the use of 3-aminopropyltrimethoxysilane coated magnetite nanoparticles combined with an antibody (antiHER2/APTMS-Fe₃O₄ NPs) as a platform for efficient HER2 detection [15]. The easy manipulation, washing and collection of the magnetic nanoparticles using simple magnets or magnetic bars are major advantages compared to non-magnetic assays, reducing cross-reactivity and matrix effects. Efficient bioconjugation is largely achieved by using magnetic particles comprising a magnetite core (Fe₃O₄ MNPs) with a non-magnetic coating [5]. Al-Khafaji et al. and Ilkhani et al. used magnetic beads functionalized with Protein A to improve the affinity interaction between the biomolecules and to construct faster electrochemical bioassays [16,17]. Eletxigerra et al. developed a magnetoimmunosensor based on carboxylic acid-modified magnetic beads. Horseradish peroxidase-labelled secondary antibodies were used and detection was performed through amperometry using the hydroquinone (HQ)/H₂O₂ system [18]. Recently, Tallapragada et al. proposed a sandwich-type immunosensor based on the biotin-avidin chemistry for accurate detection of HER2 by using home-made SPEs [19]. Although unmodified electrodes were also used for the sensor construction, the total assay time was longer than for the previously reported electrochemical immunosensors.

In this work distinct sensing platforms were studied for the detection of HER2-ECD: (i) SPCEs modified with AuNP, graphene, single- or multiwalled carbon nanotubes (SWCNT, MWCNT) and (ii) SPCEs modified with graphene, SWCNT- or MWCNT in combination with AuNPs, forming hybrid nanostructures. These approaches combined the advantages of the nanomaterials' biocompa-

ibilities and the high binding affinity. The use of carbon nanomaterials allows better coverage of the SPCEs and the electrodeposition of the gold nanoparticles provides a large accessible surface area for effective antibody immobilization. The sensing platforms were characterized by scanning electron microscopy (SEM) and the electrochemical signals were recorded by linear sweep voltammetry (LSV). The detection of the antibody-antigen interaction in the sandwich assay was possible by using a secondary antibody labelled with alkaline phosphatase; the electrochemical signal was generated through the oxidation of enzymatically deposited metallic silver (a mixture of 3-indoxyl phosphate (enzymatic substrate) and silver ions). In this study the use of different carbon nanomaterials, and their combination with AuNPs, with the above-mentioned detection strategy for the detection of HER2-ECD is reported for the first time.

2 Experimental

2.1 Instrumentation

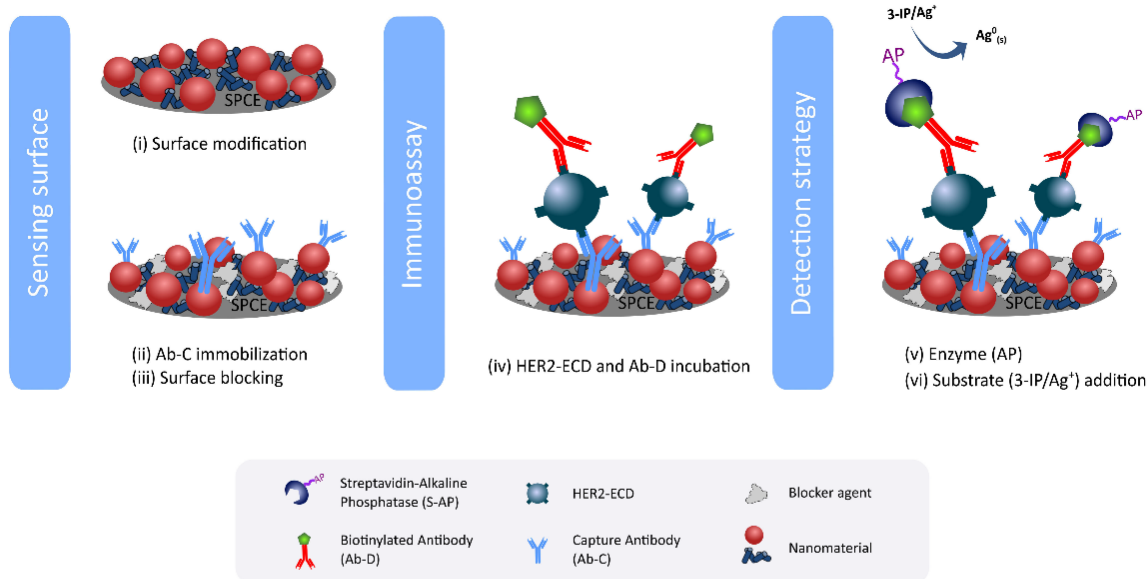
The electrochemical measurements were carried out using a potentiostat/galvanostat (Autolab PGSTAT101, Metrohm Autolab) controlled by the NOVA software package (v.1.9; Metrohm Autolab). Screen-printed carbon electrodes (SPCE, DRP-110) and a specific connector (DRP-CAC) to interface the electrodes and the potentiostat/galvanostat were supplied by DropSens. The SPCEs consisted of working (d=4 mm) and counter electrodes made of carbon inks and a silver pseudoreference electrode. All the electrodes were discarded after use. The SEM images were obtained by using FEI Quanta 400FEG ESEM/EDAX Genesis X4 M equipment, at the "Centro de Materiais da Universidade do Porto (CEMUP)". The histograms were obtained using SPSS software, version 20.0 (SPSS Inc., Chicago, Illinois).

2.2 Reagents

Albumin from human serum (HSA), albumin from bovine serum (BSA), β -casein from bovine milk, reduced graphene oxide (rGO), carboxylic acid functionalized multiwalled carbon nanotubes (MWCNT-COOH), carboxylic acid functionalized single-walled carbon nanotubes (SWCNT-COOH), 3-indoxyl phosphate (3-IP), N,N-dimethylformamide (DMF), ethanolamine, hydrochloric acid, magnesium nitrate hexahydrate, nitric acid, streptavidin-alkaline phosphatase (S-AP) from *Streptomyces avidinii*, human serum (from male AB clotted whole blood), tetrachloroauric(III) acid and tris(hydroxymethyl)aminomethane (Tris), were obtained from Sigma-Aldrich. Silver nitrate was purchased from Alfa Aesar. Rabbit IgG monoclonal anti-human-HER2-ECD (clone 002) antibody (capture antibody), mouse IgG2a monoclonal biotinylated anti-human-HER2-ECD (clone 8B5DAC1) antibody (detection antibody), and a recombinant HER2-ECD protein (antigen) were obtained from Sino Biological Inc.

Full Paper

ELECTROANALYSIS



Scheme 1. Schematic representation of the electrochemical immunoassay.

Ultra-pure water (resistivity = 18.2 M Ω cm) was used and was obtained from a Millipore (Simplicity 185) water purification system. The tetrachloroauric(III) acid solution (0.10 mM) for the electrodeposition of AuNPs was prepared in 0.1 M HCl. Working solutions of the capture (C) and detection (D) antibodies and the antigen were prepared in 0.1 M Tris-HNO₃ pH 7.4 (buffer 1). The S-AP solutions were prepared in 0.1 M Tris-HNO₃ pH 7.4 containing 1 % BSA (buffer 2). The solution containing 3-IP (1×10^{-3} M) and silver nitrate (4×10^{-4} M) was prepared in 0.1 M Tris-HNO₃ pH 9.8 containing Mg(NO₃)₂ (2×10^{-2} M) (buffer 3) and stored at 4 °C protected from light. All the buffers and solutions were prepared daily.

2.3 Sensor/Assay Development and Procedure

Scheme 1 elucidates the different steps of the used sandwich assay.

2.3.1 Surface Modification

Several SPCE-based immunosensors were tested using different nanomaterials: rGO, SWCNT-COOH, MWCNT-COOH and AuNPs and combinations of these materials.

For the carbon nanotubes, (i) the surface of the SPCE was modified by dropping a 1- μ L aliquot of an rGO, SWCNT-COOH or MWCNT-COOH suspension (dispersed in DMF) on the working electrode (WE) of the SPCE which was then dried for 5 minutes at 50 °C.

The modification of the WE (with or without the carbon nanomaterials) with AuNPs was carried out by electrodeposition of gold from 40 μ L of a 0.10 mM [AuCl₄]⁻ (in 0.1 M HCl) solution according to the procedure described by Martínez-Paredes et al.: first a

constant current (-100 μ A) was applied for 240 s, and subsequently a constant potential (+0.1 V) was applied for 120 s [20]. The obtained AuNP-modified electrodes were rinsed with water and dried with nitrogen before use.

2.3.2 Capture Antibody Immobilization

The immobilization of the capture antibody on the modified SPCE surfaces was performed based on a previous work: (ii) incubation of the SPCE with 10 μ L of the capture antibody solution (optimized concentration: 25 μ g/mL), overnight at 4 °C in a humidified chamber. Then the SPCE was washed with buffer 1 before (iii) blocking the free surface sites with β -casein (2 % (m/V) in buffer 1, 40 μ L, 30 min) [10].

2.3.3 Immunoassay

The optimized assay consisted of the following steps: after washing with buffer 1, (iv) a previously prepared mixture (5 min before use) containing the detection antibody (2 μ g/mL), HER2-ECD and BSA 0.5 % (m/V) was added (40 μ L) and left to incubate for 30 min. The washing step was then repeated with buffer 1, and (v) an aliquot (40 μ L) of S-AP solution (5×10^{-10} M) was added for 60 min. Subsequently, a washing step was carried out firstly with buffer 1, and then with buffer 3.

For the electrochemical measurements, (vi) a 40- μ L aliquot of the mixture containing the enzymatic substrate (3-IP, 1.0×10^{-3} M) and silver nitrate (4.0×10^{-4} M) was placed on the SPCE and after 20 min the electrochemical signal was obtained by LSV using the following parameters: potential range: -0.03 V – +0.4 V; scan rate: 50 mV/s.

Full Paper

ELECTROANALYSIS

2.4 Sample Preparation

Male human serum was stored at -20°C and was used as obtained, i.e. serum samples were spiked with HER2-ECD at different concentrations and analysed without further treatments. The electrochemical measurements were performed using the above-mentioned conditions.

3 Results and Discussion

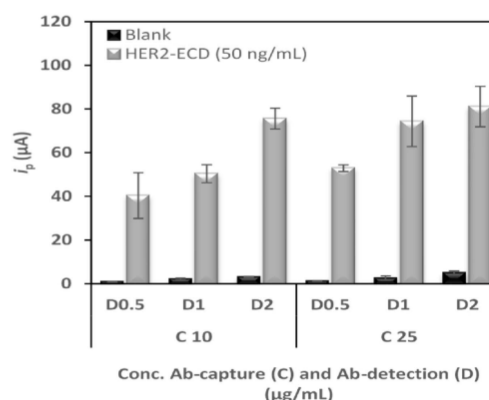
3.1 Sensor/Assay Optimization

3.1.1 Antibody Concentrations

The immobilization of the capture antibody on the sensor's surface and the detection approach are some of the key features to guarantee the adequate performance of immunosensors. According to a previously reported immunosensor for HER2-ECD detection developed in our group [10], AuNPs constitute a good nanomaterial to be used for immobilization through chemisorption of monoclonal anti-human HER2-ECD antibodies (Ab-C). This allowed stable immobilization of the antibodies and led to a high sensitivity. In the present study the same procedure was adopted, and the Ab-C and Ab-D concentrations were studied using SPCE-AuNP and the following conditions: Ab-C: 10 and 25 $\mu\text{g}/\text{mL}$; casein: 2% (m/V); HER2-ECD: 0 and 50 ng/mL; BSA: 0.5% (m/V); Ab-D: 0.5; 1 and 2 $\mu\text{g}/\text{mL}$; S-AP: 2.0×10^{-10} M with BSA 1% (m/V). The obtained peak current intensities are presented in Figure 1(a). As can be observed, the lowest Ab-C concentration (10 $\mu\text{g}/\text{mL}$) led to the lowest peak current intensities and the increase of the Ab-D concentration led to an increase of the electrochemical signal. However, the results also showed that the peak current intensity was similar when the highest Ab-D concentration (2 $\mu\text{g}/\text{mL}$) was used for both Ab-C concentrations (10 and 25 $\mu\text{g}/\text{mL}$), revealing the importance of the Ab-D concentration on the immunosensor's performance. The result can be explained based on the high amount of S-AP that binds to the detection antibody (Ab-D), leading to the signal amplification. Although a good result was achieved with the combination of Ab-C 10 $\mu\text{g}/\text{mL}$ and Ab-D 2 $\mu\text{g}/\text{mL}$, the best performance was obtained when Ab-C 25 $\mu\text{g}/\text{mL}$ and Ab-D 2 $\mu\text{g}/\text{mL}$ were used. Therefore, these concentrations were chosen to proceed with the optimization of the immunoassay.

We previously reported an immunosensor for HER2-ECD detection, using a gold nanoparticle-modified SPCE as transducer, but using Ab-C 50 $\mu\text{g}/\text{mL}$ and Ab-D 1 $\mu\text{g}/\text{mL}$ [10]. Comparing the results with the ones obtained in the present study, it can be concluded that lower Ab-C concentrations (10 and 25 $\mu\text{g}/\text{mL}$) and a higher Ab-D concentration (2 $\mu\text{g}/\text{mL}$) lead to higher peak current intensities.

(a)



(b)

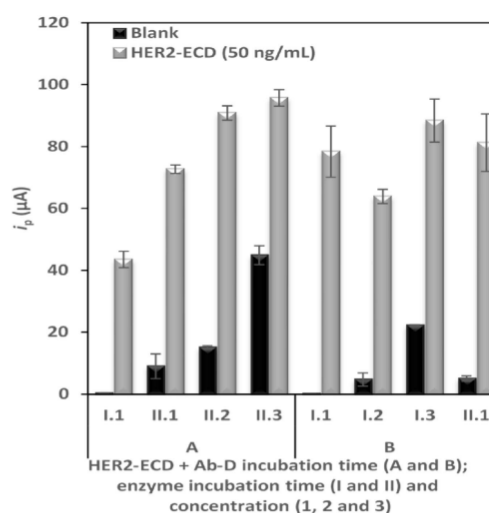


Fig. 1. Optimization of (a) Ab-C and Ab-D concentrations and (b) incubation time of HER2+Ab-D (A – 30 min and B – 60 min), enzyme incubation time (I – 30 min and II – 60 min) and concentration (1 – 2×10^{-10} M; 2– 5×10^{-10} M and 3– 1×10^{-9} M). (Ab-C (25 $\mu\text{g}/\text{mL}$), Ab-D (2 $\mu\text{g}/\text{mL}$), casein (2%), HER2-ECD (0 (blank) and 50 ng/mL), BSA (0.5%), 3-IP (1×10^{-3} M) and Ag^+ (4×10^{-4} M)).

3.1.2 Incubation Times and Enzyme Concentration

The influence of the incubation time of the mixture HER2-ECD + Ab-D (containing 0.5% BSA) was studied using two different times: 30 min (A) and 60 min (B). In addition, three concentrations of S-AP were tested: (1) 2×10^{-10} M; (2) 5×10^{-10} M and (3) 1×10^{-9} M, which were incubated for: 30 min (I) and 60 min (II). The influence of these parameters was studied using the previously optimized antibody concentrations (Ab-C 2 $\mu\text{g}/\text{mL}$ and Ab-D 2 $\mu\text{g}/\text{mL}$). The different combinations between the incubation times of the mixture and the incubation time and concentrations of S-AP are shown in Figure 1(b). The sequence of the tested parameters is presented according to the incubation time of the HER2-ECD + Ab-D

Full Paper

ELECTROANALYSIS

mixture: I.1, II.1, II.2 and II.3 for A and I.1, I.2, I.3 and II.1 for B.

The results for the shortest incubation times combined with the lowest S-AP concentration (A – I.1) showed a considerable decrease of the peak current intensity. On the other hand, the longest incubation times combined with the lowest S-AP concentration (B – II.1) resulted in a considerable improvement of the electrochemical signal. Nevertheless, in the latter assay an increase of the blank signal was observed because of the increase of non-specific adsorption on the electrode surface. Regarding the assays in which longer incubation of the enzyme (II – 60 min) was used higher signals were observed (A – II.1, A – II.2 and A – II.3), but an increase of the enzyme concentration increased the blank signal because of the adsorption of S-AP on the electrode's surface, indicating that a large amount of enzyme does not bind specifically to the Ab-D. This was also observed in B – I.3, although the enzyme incubation time was only 30 min.

Thus, regardless of the analysis time, the increase of the S-AP concentration leads to higher signal intensity. The combination of the lowest S-AP concentration and incubation time (B – I.1) resulted in a higher analytical signal and a lower blank signal. As a compromise between sensitivity and analysis time assay A – II.2 was used in the subsequent studies.

In this work a higher analytical signal and a shorter assay time (2 h 20 min) were obtained when compared to the previous work [10].

3.1.3 Sensing Platform Modification and Characterization

Distinct gold- and carbon-based nanomaterials can be used in the electrode surface modification procedure for HER2-ECD detection to obtain high sensitivities with reduced interferences and low detection limits [10,11,13]. To compare the results obtained with SPCE-AuNPs as transducer, three carbon-based nanomaterials were tested: (i) rGO, (ii) SWCNT-COOH and (iii) MWCNT-COOH. In addition, the combination of rGO, SWCNT-COOH or MWCNT-COOH with AuNPs were also studied.

For the surface modification of the SPCEs the carbon nanomaterials' concentrations were optimized (0.5 $\mu\text{g}/\mu\text{L}$, 1 $\mu\text{g}/\mu\text{L}$, 2 $\mu\text{g}/\mu\text{L}$ and 4 $\mu\text{g}/\mu\text{L}$) and 1 $\mu\text{g}/\mu\text{L}$ was chosen because of the better sensitivity and precision of the analysis (data not shown).

The signals obtained using a 50-ng/mL HER2-ECD solution were compared with the ones obtained with the SPCE-AuNP (Figure 2).

Between the distinct carbon nanomaterial types, either individually or combined with AuNPs, the use of MWCNTs led to the highest signal. However, only when the MWCNT-AuNP combination was used an increase of the signal compared with the SPCE-AuNP was observed. Furthermore, the use of the carbon-based nanomaterials provided lower blank signals because coating the surface of the electrode with these materials is generally more effective, thereby reducing the interference of the sample

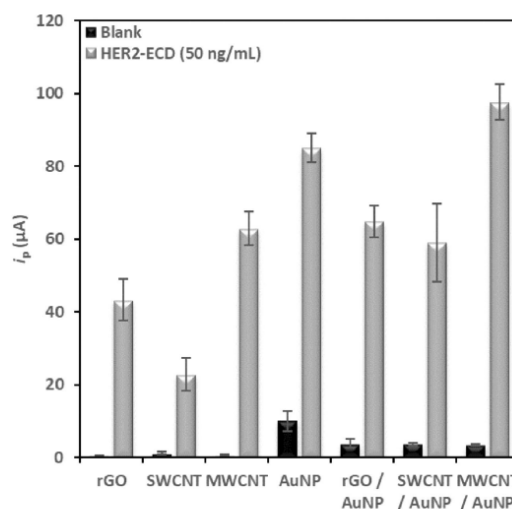


Fig. 2. Peak current intensities obtained using the tested sensing platforms.

matrix or the excess of antibodies and/or enzymes which have not been effectively removed in the washing step and which have no binding affinity to these materials. On the other hand, gold nanomaterials allow a more efficient immobilization of biomolecules, as can be observed by the increase of the signal.

Scanning electron microscopy (SEM) was used to characterize the modifications of the SPCE surfaces that provided the highest electrochemical signals. The electro-deposited AuNPs presented a normal distribution and a circular shape with an average diameter of 17.9 ± 4.2 nm (Figure 3(a)). When the AuNPs were electrodeposited on the SPCE previously modified with carbon nanotubes an increase in their size was observed (average diameter: 26.1 ± 5.6 nm) because the surface of the SPCE was completely covered with the carbon nanotubes (Figure 3(b)).

3.2 Analytical Performance and Applicability

The analytical responses toward different HER2-ECD concentrations using the best surface modifications (AuNP and MWCNT/AuNP) were first tested in buffer. Solutions of HER2-ECD (concentrations between 7.5 and 100 ng/mL) were analysed and the working ranges were established (data not shown). Then the sensing strategies were tested in spiked human serum samples. The linear relationship between i_p and [HER2 ECD] (7.5–50 ng/mL) was established for SPCE-AuNP ($i_p = 1.22 \pm 0.07$ [HER2-ECD] + 27.6 \pm 2.1, $r = 0.995$) and for the SPCE-MWCNT/AuNP ($i_p = 2.31 \pm 0.13$ [HER2-ECD] + 9.03 \pm 4.27, $r = 0.997$). This shows that the SPCE-MWCNT/AuNP provided the highest sensitivity. The limits of detection (LOD) and quantification (LOQ) were calculated from the respective calibration plots using the equations: $\text{LOD} = 3 s_{\text{blank}}/m$ and $\text{LOQ} = 10 s_{\text{blank}}/m$ where s_{blank} is the

Full Paper

ELECTROANALYSIS

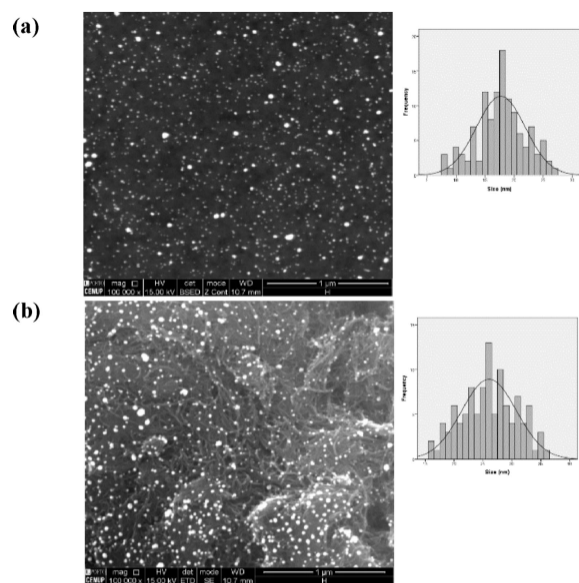


Fig. 3. SEM images and respective histograms of (a) SPCE-AuNP and (b) SPCE-MWCNT/AuNP.

standard deviation of the blank signal and m is the slope of the calibration plot. The LODs were 8.5 ng/mL for the SPCE-AuNP and 0.16 ng/mL for the SPCE-MWCNT/AuNP. Considering the cut-off value for HER2-ECD (15 ng/mL), the sensing strategies provided LODs that were below this value, indicating their usefulness for HER2-ECD detection in the initial stage of the cancer. Representative voltammograms in the linear range and the calibration plots are presented in Figure 4. Additional figures of merit are presented in Table 1.

The precision of the results, in terms of repeatability and intermediate precision, using the distinct sensing platforms was tested by analysing a 50-ng/mL HER2-ECD solution in triplicate on the same day and different days. Relative standard deviations (RSD) of 2.8% and 6.5% for the SPCE-AuNP, 2.5% and 7.6% for the SPCE-

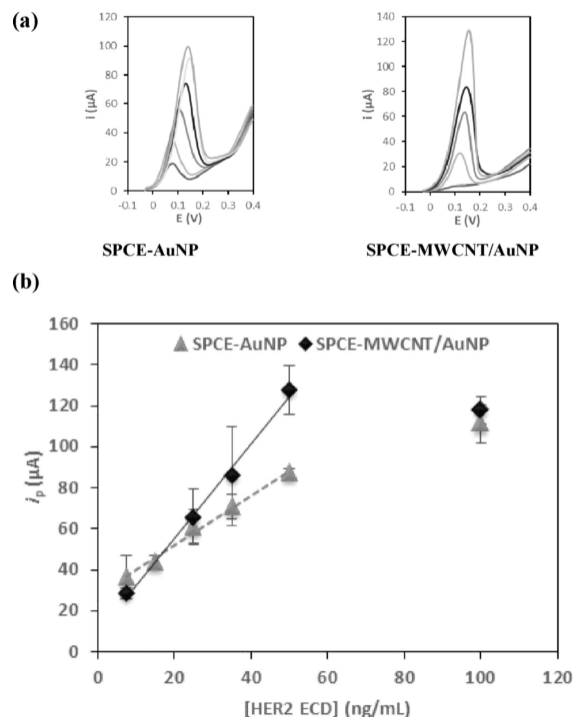


Fig. 4. (a) Examples of linear sweep voltammograms for the analysis of HER2-ECD: 0, 7.5, 15, 25, 35 and 50 ng/mL, (b) calibration plots in spiked human serum using SPCE-AuNP and SPCE-MWCNT/AuNP.

MWCNT/AuNP were obtained, indicating that all the sensing platforms provided precise results.

Because the SPCE-MWCNT/AuNP provided the highest sensitivity, recovery studies with this platform were performed using spiked serum samples. The results for three replicates of added 7.5, 15 and 50 ng/mL HER2-ECD were found to be 8.25 ± 0.67 ng/mL, 12.4 ± 0.98 ng/mL and 45.6 ± 1.34 ng/mL, with average recoveries of 110%, 83% and 91%, respectively. These values indicated that the SPCE-MWCNT/AuNP provided accurate results.

Table 1. Analytical characteristics of the developed electrochemical biosensors for the analysis of HER2-ECD in Human serum samples.

Figure of merit	SPCE-AuNP	SPCE-MWCNT/AuNP
Concentration interval (ng/mL)	7.5–50	7.5–50
Correlation coefficient (r)	0.995	0.997
Slope (m) ($\mu\text{A}/(\text{ng/mL})$)	1.22	2.31
Standard deviation of the slope (S_m) ($\mu\text{A}/(\text{ng/mL})$)	0.07	0.13
Intercept (b) (μA)	27.6	9.03
Standard deviation of the intercept (S_b) (μA)	2.1	4.27
Standard deviation of the linear regression ($S_{y/x}$)	2.30	3.97
Standard deviation of the method (S_m)	1.9	1.7
Coefficient of variation of the method (V_{s0}) (%)	7.1	5.8
Limit of detection (LOD) (ng/mL)	8.5	0.16
Limit of quantification (LOQ) (ng/mL)	28	0.54

Full Paper

ELECTROANALYSIS

Table 2. Characteristics of electrochemical immunosensors and immunoassays for HER2 analysis.

Transducer	Surface modification	Assay	Technique	Sample	Assay time	Linear range (ng/mL)	LOD (ng/mL)	Ref.
SPCE	AuNPs	Sandwich	LSV	Spiked human serum	2 h 20 min	7.5–50	8.5	This work
	MWCNT(–COOH)/AuNPs						0.16	
SPCE	AuNPs	Sandwich	LSV	Spiked human serum	2 h 50 min	15–100	4.4	[10]
GSPE	AuNPs	Label-free	EIS	Spiked human serum	2 h	5.0–40	6.0	[11]
CILE	MWCNT/AuNPs	Label-free	EIS	Patient serum	35 min	10–110	7.4	[13]
AuE	AuNP/3-Mercaptopropionic acid (MPA)/Cysteamine/ Fe ₃ O ₄ NPs	Label-free	DPV	Patient serum	1 h 15 min	0.01–10	0.995	[14]
GCE	APTMS-Fe ₃ O ₄ NPs	Sandwich	DPV	Spiked human serum	1 h 50 min	5.0×10^{-4} –50	2.0×10^{-5}	[15]
SPCE	Protein A-MBs (ProtA-MBs)	Sandwich	DPV	Patient serum	2 h 05 min	2.5–15	6.0	[16]
8 × SPE	Protein A-MBs (ProtA-MBs)	Sandwich	DPV	Spiked human serum	1 h 51 min	2.5–20	2.6	[17]
	Streptavidin MBs (Strep-MBs)			Human serum	2 h 51 min		3.4	
SPCE	Carboxylic acid-modified MBs(HOOC-MBs)	Sandwich	Amperometry	Human serum and cell lysates	2 h	0.1–32	26×10^{-3}	[18]
SPE	–	Sandwich	CV	Patient serum	6 h 05 min	5.0–20	4.0	[19]
						20–200		

The selectivities of the SPCE-AuNP and SPCE-MWCNT/AuNP were tested through the analysis of other biomarkers and possible serum interferences: another breast cancer biomarker (CA 15-3), a biomarker of kidney function (cystatin C) and human serum albumin (HSA). Solutions of these proteins of 30 U/mL (CA 15-3), 565 ng/mL (cystatin C) and 35 mg/mL (HSA) were tested. These concentrations were chosen based on the values that can be expected in real situations (except for CA 15-3, which can vary greatly in the case of cancer patients). The peak current intensities obtained for these non-target proteins are shown in Figure 5. As can be observed, the signals were significantly different from the ones obtained for HER2-ECD, confirming the selectivity of the different sensing platforms.

In Table 2 some characteristics of electrochemical immunosensors and immunoassays reported for HER2 analysis in serum samples are presented. Although in label-free assays the analysis times are shorter than in the sandwich-type assays, the time required for the electrode surface modification and subsequent incubation of the capture antibody is considerably higher. From the comparison of the analytical performances of the immunomagnetic assays [14–18] with the immunosensors [10, 11, 13, 19] can be concluded that when magnetic beads are used as sensing platform, shorter linear ranges and slightly lower LODs were obtained. This indicates that the use of magnetic particles and the detection strategy optimized in this work is promising. Nevertheless, all the reported sensing strategies provide limits of detection below the cut-off value for HER2 (15 ng/mL), which means that they could be useful in the clinical setting.

In the strategies studied in our work generally similar linear ranges and analysis times were obtained and the

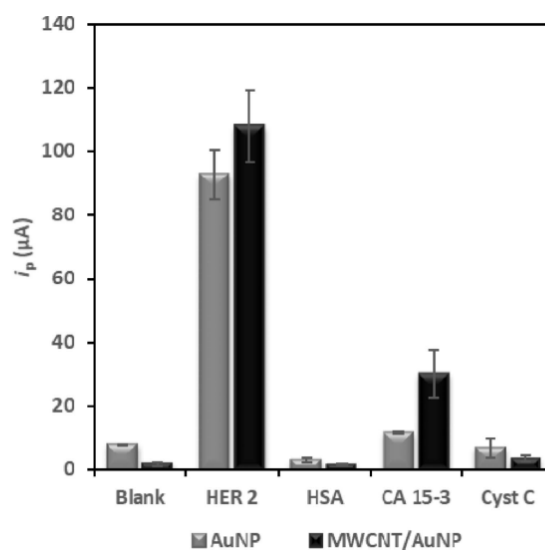


Fig. 5. Results obtained in the selectivity studies using the developed sensing strategies.

LODs were comparable with the ones reported in the previous works, except for the studies in which magnetic particles were applied. Nevertheless, the best sensitivity was obtained for the SPCE-MWCNT/AuNP which is probably due to the good electrode surface coverage of the carboxylic acid functionalized MWCNTs and subsequent electrodeposition of gold, which allows suitable antibody immobilization.

Full Paper

ELECTROANALYSIS

4 Conclusions

To improve the electrochemical analysis of HER2-ECD, the modification of the surface of SPCEs with gold (AuNPs) and carbon nanomaterials (rGO, SWCNT-COOH and MWCNT-COOH) and combinations of these materials were tested. Among the carbon-based nanomaterials, MWCNT-COOH provided the highest sensitivity. The combination of MWCNT-COOH with AuNPs revealed the highest sensitivity. The antibody concentrations were optimized and used to develop biosensing strategies on SPCE-AuNP and SPCE-MWCNT/AuNP, achieving limits of detection well below the cut-off value for this breast cancer biomarker.

Spiked human serum samples were used to test the sensing platforms' applicability and the selectivity was confirmed through the analysis of other biomarkers and possible serum interferents: Human Serum Albumin (HSA), Cancer Antigen 15-3 (CA 15-3) and Cystatin C, observing no significant interference of these proteins in the analysis.

Like this, the developed sensing strategies could be an alternative for the analysis of HER2-ECD.

Acknowledgements

Maria Freitas is grateful to FCT-Fundação para a Ciência e a Tecnologia for her PhD grant (SFRH/BD/111942/2015), financed by POPH-QREN-Tipologia 4.1-Formação Avançada, subsidized by Fundo Social Europeu and Ministério da Ciência, Tecnologia e Ensino Superior. This work received financial support from the European Union (FEDER funds through COMPETE) and National Funds (FCT) through project UID/QUI/50006/2013.

References

- [1] J. Ferlay, I. Soerjomataram, R. Dikshit, S. Esler, C. Mathers, M. Rebelo, D. M. Parkin, D. Forman, F. Bray, *Int. J. Cancer* **2015**, *136*, E359–E386.
- [2] A. Ravelli, J.M. Reuben, F. Lanza, S. Anfossi, M. R. Cappelletti, L. Zanotti, A. Gobbi, C. Senti, P. Brambilla, M.

- Milani, D. Spada, P. Pedrazzoli, M. Martino, A. Bottini, D. Generali, *Tumor Biol.* **2015**, *36*, 6653–6665.
- [3] A. M. Berghuis, H. Koffijberg, J. Prakash, L. W. Terstappen, M. J. IJzerman, *Int. J. Mol. Sci.* **2017**, *18*, 363–408.
- [4] S. Campuzano, M. Pedrero, J. M. Pingarrón, *Sensors* **2017**, *17*, 1993–2016.
- [5] M. Freitas, H. P. A. Nouws, C. Delerue-Matos, *Electroanalysis* **2018**, *30*, 1–21.
- [6] Biomarkers Definitions Working Group, *Clin. Pharmacol. Ther.* **2001**, *69*, 89–95.
- [7] S. Mittal, H. Kaur, N. Gautam, A. N. Mantha, *Biosens. Bioelectron.* **2017**, *15*, 217–231.
- [8] M. Hasanzadeh, N. Shadjou, M. de la Guardia, *TrAC Trends Anal. Chem.* **2017**, *91*, 67–76.
- [9] A. Mishra, M. Verma, *Cancers* **2010**, *2*, 190–208.
- [10] R. C.B. Marques, S. Viswanathan, H. P. A. Nouws, C. Delerue-Matos, M. B. González-García, *Talanta* **2014**, *129*, 594–599.
- [11] A. Ravalli, C. G. Rocha, H. Yamanaka, G. Marrazza, *Bioelectrochemistry* **2015**, *106*, 268–275.
- [12] B. Wang, U. Akiba, J. I. Anzai, *Molecules* **2017**, *22*, 1048–1068.
- [13] E. Arkan, R. Saber, Z. Karimi, M. Shamsipur, *Anal. Chim. Acta* **2015**, *874*, 66–74.
- [14] M. Emami, M. Shamsipur, R. Saber, R. Irajirad, *Analyst* **2014**, *139*, 2858–66.
- [15] M. Shamsipur, M. Emami, L. Farzin, R. Saber, *Biosens. Bioelectron.* **2018**, *103*, 54–61.
- [16] Q. A. M. Al-Khafaji, M. Harris, S. Tombelli, S. Laschi, A. P. F. Turner, M. Mascini, G. Marrazza, *Electroanalysis* **2012**, *24*, 735–742.
- [17] H. Ilkhani, A. Ravalli, G. Marrazza, *Chemosensors* **2016**, *4*, 1–10.
- [18] U. Elettigerra, J. Martínez-Perdiguero, S. Merino, R. Barderas, R. M. Torrente-Rodríguez, R. Villalonga, J. M. Pingarrón, S. Campuzano, *Biosens. Bioelectron.* **2015**, *70*, 34–41.
- [19] S. D. Tallapragada, K. Layek, R. Mukherjee, K. K. Mistry, M. Ghosh, *Bioelectrochemistry* **2017**, *118*, 25–30.
- [20] G. Martínez-Paredes, M. B. González-García, A. Costa-García, *Electrochim. Acta* **2009**, *54*, 4801–4808.

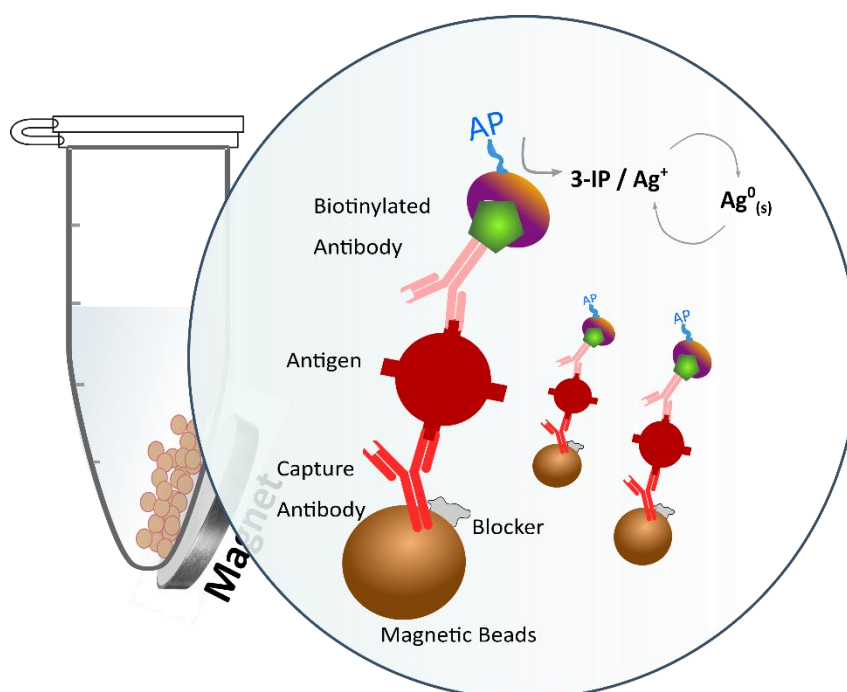
Received: August 1, 2018

Accepted: October 26, 2018

Published online on November 27, 2018

3.2 High-performance electrochemical immunomagnetic assay for breast cancer analysis

Sensors and Actuators: B. Chemical 308 (2020) 127667



Author Contributions:

Maria Freitas (investigation: Equal; Methodology: Equal; Writing – original draft: Lead); Henri Nouws (Conceptualization: Lead; Funding acquisition: Equal; Methodology: Lead; Project administration: Equal; Supervision: Equal; Validation: Equal; Writing – review & editing: Lead); Elisa Keating (Cell-lines acquisition and culture); Cristina Delerue-Matos (Funding acquisition: Equal; Methodology: Equal; Supervision: Equal; Validation: Equal; Writing – review & editing: Supporting)

Highlights

- Detection of cancer biomarkers in biological fluids is useful for early diagnosis.
- An electrochemical immunomagnetic bioassay was developed for HER2-ECD detection.
- Magnetic beads constitute a versatile tool for the construction of the assay.
- The assay was selective towards the target protein and live breast cancer cells.
- The assay was successfully tested in the analysis of human serum.



Contents lists available at ScienceDirect

Sensors and Actuators B: Chemical

journal homepage: www.elsevier.com/locate/snb

High-performance electrochemical immunomagnetic assay for breast cancer analysis

Maria Freitas^a, Henri P.A. Nouws^{a,*}, Elisa Keating^{b,c}, Cristina Delerue-Matos^a^a REQUIMTE/LAQV, Instituto Superior de Engenharia do Porto, Politécnico do Porto, Rua Dr. António Bernardino de Almeida 431, 4200-072 Porto, Portugal^b Department of Biomedicine – Unit of Biochemistry, Faculty of Medicine, University of Porto, Al. Prof. Hernâni Monteiro, 4200-319 Porto, Portugal^c CINTESIS – Center for Health Technology and Services Research, Rua Dr. Plácido da Costa, 4200-450 Porto, Portugal

ARTICLE INFO

Keywords:

Breast cancer
HER2-ECD
SK-BR-3
Electrochemical immunoassay
Magnetic beads
Screen printed electrodes

ABSTRACT

Despite the evolution of targeted therapies in oncology, some challenges such as screening and early diagnosis of cancer-related biomarkers still remain. The analysis of the Human Epidermal growth factor Receptor 2 (HER2) in biological fluids provides essential information for effective treatments. In this work we report the development of an electrochemical immunomagnetic bioassay for the analysis of the extracellular domain of HER2 (HER2-ECD) in human serum and cancer cells. Biomodified carboxylic acid functionalized magnetic beads (COOH-MBs) were used as the capture probe and an antibody labelled with alkaline phosphatase (AP) as the signalling probe. In the presence of HER2-ECD a sandwich complex was formed on the MBs, which were magnetically attracted to the surface of a screen-printed carbon electrode (SPCE). After the addition of 3-indoxyl phosphate and silver ions, used as the enzymatic substrate, the immunological interaction was detected by linear sweep voltammetry. Two linear concentration ranges were established: one between 5.0 and 50 ng/mL and another between 50 and 100 ng/mL. The developed assay provided a clinically useful detection limit (2.8 ng/mL) and has an adequate precision ($V_{x0} < 5\%$). The assay provided accurate results and was selective towards the target biomarker. Additionally, CTCs were analysed in human serum and a detection limit of 3 cells/mL was achieved for the HER⁺ breast cancer cell line SK-BR-3.

1. Introduction

Screening and early-stage diagnosis of oncological diseases and an adequate follow-up are critical for successful patient management. This promotes general public health and increases the survival rate [1,2]. The gold standard procedures established for screening and detection of breast cancer are based on imaging tools. However, these techniques have limitations such as the decrease of sensitivity when breast tissue density increases. In addition, invasive techniques (e.g. biopsies) are required to confirm the presence of the tumour [3,4]. Technological advances in this field include (bio)sensors/assays that provide rapid and accurate diagnosis and point-of-care detection possibilities by combining the selectivity of biomolecule interactions with the high sensitivity of modern analytical techniques for non-invasive analysis [5,6]. Therefore, electrochemical biosensors were already widely employed for tumour marker recognition and detection [7–9].

Human Epidermal growth factor Receptor 2 (HER2) is a specific cancer related biomarker used in clinical settings. Abnormal HER2 levels are particularly significant since its overexpression is related to

invasive and aggressive breast cancer-types [10]. HER2 is reported as a biomarker of interest in the development of non-invasive tests for diagnosis in serum samples by the European Group on Tumor Markers (EGTM) [11] and the Food and Drug Administration (FDA) [12]. Besides this, the analysis of circulating tumour cells has risen attention since biomarkers present on the cell surface can be detected through the analysis of their extracellular domains (ECDs) [13].

A wide diversity of electrochemical immunosensors for the analysis of HER2 in serum samples have been published [14–29]. Although simple strategies with non-modified transducers have been reported [14–18], versatile and innovative transducing platforms, modified and/or functionalized with nanomaterials [19–22], self-assembled monolayers [23,24], polymers [25] or sequential layer deposition [26–29] are also part of the described methodologies. However, this diversity leads to time-consuming sensor surface construction strategies. A variety of new smart materials, particularly nano- and micro materials, can vastly improve screening and diagnosis because they increase the assay's performance, including the reduction of the analysis time and the enhancement of the sensitivity and/or selectivity [30]. Therefore,

* Corresponding author.

E-mail address: han@isep.ipp.pt (H.P.A. Nouws).<https://doi.org/10.1016/j.snb.2020.127667>

Received 12 November 2019; Received in revised form 30 December 2019; Accepted 3 January 2020

Available online 07 January 2020

0925-4005/ © 2020 Elsevier B.V. All rights reserved.

magnetic nanoparticles (MNPs) and magnetic beads (MBs) have gained great interest as sensing platforms in electrochemical immunomagnetic assays for cancer diagnosis [1]. When using magnetic particles biomolecular interactions are improved, matrix effects are minimized through efficient washing steps [31] and preconcentration of the analyte is easily achieved. Thus, by immobilizing antibodies on their surfaces, the effective magnetic separation and the pre-concentration of an antigen from complex samples can be achieved. In the case of electrochemical magnetoassays an additional advantage is the fact that the assay is mostly performed away from the electrode (in microtubes), reducing possible electrode fouling. Only the detection strategy is carried out on the electrode surface using small magnets with the size of the working electrode for efficient magnetic attraction before the electrochemical measurement [32,33].

Because of the above-mentioned advantages, some electrochemical immunomagnetic assays have already been reported. These assays were based on the use of 'self-made' nanoparticles or commercially available MBs as sensing platforms, containing distinct functional groups or recognition elements on their surfaces [34–38]. In these works, modification of the magnetic particles' surfaces with the biorecognition element was achieved, either through covalent binding or affinity processes, in a short time (1 h) when compared to the reported immunosensors in which the immobilization procedure usually occurs overnight.

To avoid the misclassification of HER2-positive patients, the evaluation of circulating tumour cell overexpression is of utmost importance. Detection of HER2-positive cell-lines can greatly contribute to early status assessment and to monitor the patients' treatments. In this work we report the development of an electrochemical immunomagnetic assay for the detection of HER2-ECD in human serum using carboxylic acid functionalized magnetic beads (HOOC-MBs) and screen-printed carbon electrodes (SPCEs). The HOOC-MBs constituted a versatile tool for the construction of the magnetic immunosensing platform and stable immobilization of a large amount of antibodies was achieved through covalent binding. After this step, the sandwich assay consisted of the addition of HER2-ECD and biotinylated detection antibodies, which were then labelled with (streptavidin)-alkaline phosphatase (AP). This resulted in a bioconjugate that was attracted to the surface of the SPCE by placing a magnet ($d = 4$ mm) below its WE. The combination of 3-indoxyl phosphate (the enzymatic substrate) and silver nitrate allowed the detection of the immunological interaction by linear sweep voltammetry (LSV) (Scheme 1). Additionally, the assay was also tested for the analysis of live breast cancer cells (HER2⁺: SK-BR-3; HER2⁻: MDA-MB-231). This is the first electrochemical immunomagnetic assay for HER2-ECD and cancer cell analysis using this detection strategy.

2. Materials and methods

2.1. Reagents and solutions

Albumin from bovine serum (BSA), 3-indoxyl phosphate (3-IP), ethanolamine (EA), streptavidin-alkaline phosphatase (S-AP) from *Streptomyces avidinii*, N-(3-dimethylaminopropyl)-n'-ethylcarbodiimide hydrochloride (EDC), N-Hydroxysuccinimide (NHS), MES monohydrate, Tween[®] 20, and tris(hydroxymethyl)aminomethane (Tris) were obtained from Sigma-Aldrich. Monoclonal capture and detection antibodies and recombinant HER2-ECD were purchased from Sino Biological Inc. Dynabeads[™] MyOne[™] Carboxylic Acid (MBs, 10 mg/mL) were acquired from Life Technologies.

The following solutions were used: 0.1 M MES pH 6 (buffer 1, B1), for MBs activation (200 mM EDC and 50 mM NHS) and to prepare the capture antibody (Ab-C) solution; PBS pH 8.3 (buffer 2, B2) to prepare the blocking solution (EA, 1 M); 0.1 M Tris-HNO₃ pH 7.4 (buffer 3, B3) to prepare working solutions of the detection (Ab-D) antibodies and the antigen (HER2-ECD); 0.1 M Tris-HNO₃ pH 7.4 with 1% BSA (m/v)

(buffer 4, B4) to prepare the S-AP solution; 0.1 M Tris-HNO₃ pH 9.8 containing Mg(NO₃)₂ (2.0×10^{-2} M) (buffer 5, B5) to prepare the solution containing 3-IP (1.0×10^{-3} M) and silver nitrate (4.0×10^{-4} M) (stored at 4 °C and protected from light). For the washing steps 0.01% of Tween 20 (T) was added to the distinct buffers. These buffers were used according to the specifications of the suppliers of the biomolecules and the MBs.

All solutions were prepared in Type I purified water (resistivity = 18.2 MΩ cm).

2.2. Modification of the HOOC-MBs and immunoassay

All the steps of the immunomagnetic assay were performed at room temperature, under continuous vortex stirring (950 rpm) and protected from light. The washing steps consisted of the addition of 100 μL of the adequate buffer containing Tween-20 and subsequent continuous stirring for 2 min. After each washing step, the MBs were attracted using a magnetic rack and the supernatant was discarded after 1 min. A 6-μL aliquot of the HOOC-MBs suspension (10 mg/mL) was placed in a 1.5-mL tube and the MBs were washed once with B1 (100 μL, 5 min) before proceeding.

The main steps of the assay are represented in Scheme 1.

The MBs' biomodification consisted of the following steps: (i) activation of the MBs by adding EDC/NHS (100 μL, 15 min), followed by a single washing step with B1-T; (ii) addition of 100 μL of a Ab-C solution (25 μg/mL, 60 min) (this leads to an average amount of 0.047 μg antibody per MB, which is in accordance with the amount recommended by the MBs supplier) followed by washing with B1-T and B2-T; (iii) incubation of the MBs with EA (100 μL, 10 min) after washing steps with B2-T and B3-T. The MBs were resuspended in B3-T and stored at 4 °C until use.

For the optimized immunoassay (iv) HER2-ECD or cancer cells (variable concentration) and Ab-D (2 μg/μL) were previously mixed and a 100-μL aliquot of this mixture was added for 60 min. Then, the MBs were washed with B3-T. Afterwards, the MBs were incubated with (v) a S-AP solution (5.0×10^{-10} M in B4, 100 μL, 30 min), and finally washed twice with B5-T and resuspended in 50 μL of B5.

2.3. Electrochemical measurements

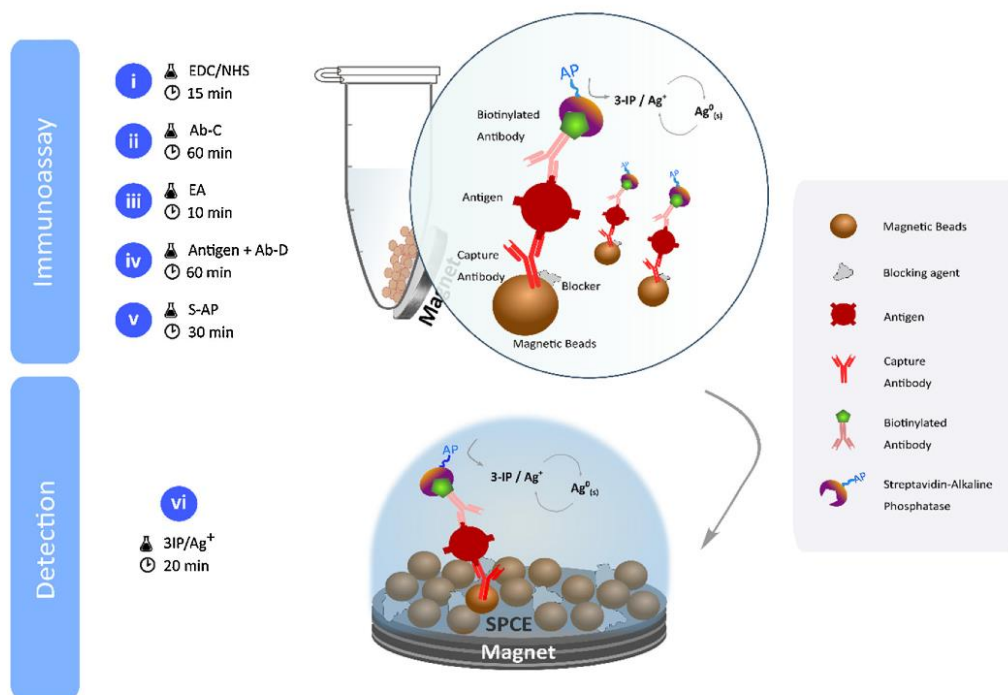
The MBs were attracted to the WE of the SPCE (DRP-110, DropSens) using a 4-mm magnet. A 25-μL aliquot of the re-suspended MBs (corresponding to 30 μg of MBs) was placed on the SPCE and the MBs were magnetically attracted for 2 min. The solution was then removed and (vi) 40 μL of the enzymatic substrate solution (3-IP, 1.0×10^{-3} M) containing silver nitrate (4.0×10^{-4} M) was added for 20 min. The detection was performed by linear sweep voltammetry (LSV) through the analysis of the deposited silver (potential range: -0.03 V to $+0.4$ V, scan rate: 50 mV/s). A potentiostat/galvanostat (PGSTAT101, Metrohm Autolab) and the NOVA software package (v.1.9; Metrohm Autolab) were used to record the voltammograms.

2.4. Analyses of human serum samples

To evaluate the applicability of the developed assay, Human serum (from male AB clotted whole blood, Sigma-Aldrich) was spiked with HER2-ECD (1 μL of a HER2-ECD standard solution was added to 49 μL of serum) and analysed without any pre-treatment or further dilution. The results were compared with the ones obtained with a commercial Human ErbB2 (HER2) ELISA kit (Thermo Scientific, Invitrogen).

2.5. Cell culture and detection

The breast cancer cell line MDA-MB-231 (HER2-negative cancer cells) was obtained from ATCC[®] and SK-BR-3 cells (HER2-positive cancer cells) were provided by the Department of Biomedicine — Unit



Scheme 1. Representation of the immunoassay.

of Biochemistry of the Faculty of Medicine of the University of Porto. The cells were cultured in RPMI medium. For detection experiments, cells were seeded on 21 cm² plastic cell culture dishes (TPP®). On the day of the experiment, the cells were harvested with Trypsin-EDTA 0.25% and counted using an automated cell counter (Countess™, Thermo Scientific, Invitrogen). A trypan-blue exclusion assay was performed using automatic cell counting to confirm cell viability, which was between 91% and 96%. The distinct cells concentrations (1×10^2 – 1×10^5 cells/mL) were prepared in human serum and analysed using the optimized immunoassay (Sections 2.2 and 2.3).

2.6. Magnetic bead and cell analysis

FEI Quanta 400FEG ESEM/EDAX Genesis X4M equipment was used to obtain the SEM images. ImageJ open source software was used to determine the particles' average size and histograms were obtained with SPSS (v.20.0; SPSS Inc.). The cell lines used in this study were imaged by a Nikon TMS microscope.

3. Results and discussion

3.1. Electrode surface characterization

The MBs were magnetically attracted to the SPCE and the electrode surface was characterized by SEM (Fig. 1). In the obtained images no agglomeration of the magnetic particles was observed, and they were perfectly distributed on the electrode surface. The average size was 1094 ± 32.5 nm which is in agreement with the size indicated by the supplier. The organization and linear distribution of the MBs on the electrode's surface are excellent features for the detection of the biomarker.

3.2. Optimization of the experimental parameters of the immunoassay

The effect of the amount of MBs used in the assay was evaluated

between 7.5 and 90 µg using the following conditions: Ab-C: 25 µg/mL; EA: 1 M; HER2-ECD: 0 (blank) and 50 ng/mL; Ab-D: 2 µg/mL; S-AP: 5.0×10^{-10} M with BSA 1% (m/V). The obtained results are presented in Fig. 2A. With the increase of the amount of MBs, from 7.5 to 45 µg, an increase of the analytical signal (peak current intensity (i_p)) was observed, after which it slightly decreased. The lowest amount of MBs (7.5 µg) led to the lowest i_p due to the reduced amount of capture antibodies. However, for the highest amount of MBs (90 µg) a slight decrease of the peak current intensity was observed, which can be due to a higher electron transfer resistance and thus lower current intensity. The best signal-to-blank ratio (S/B) was verified for 30 µg of MBs. This amount was used for the optimization of the other experimental parameters.

The Ab-C and Ab-D concentrations were subsequently optimized using the following conditions: HOOC-MBs: 30 µg; Ab-C: 10 and 25 µg/mL; HER2: 0 (blank) and 50 ng/mL; Ab-D: 1, 2 and 4 µg/mL; S-AP: 5.0×10^{-10} M with BSA 1% (m/V). As can be seen in Fig. 2B, the highest i_p was obtained for Ab-C 25 µg/mL and Ab-D 4 µg/mL, however with a lower precision when compared to the other tested combinations. Although the combination of Ab-C 25 µg/mL and Ab-D 2 µg/mL provided a slightly lower sensitivity, a better precision of the results was achieved. Therefore, this combination was used in the subsequent optimizations.

To improve the total assay time, the incubation times of the several reagents were tested using the 'step-by-step' approach (SI Fig. S1): (1) HER2-ECD 30 min, Ab-D 30 min, S-AP 30 min; (2) HER2-ECD 30 min, Ab-D 60 min, S-AP 60 min; (3) HER2-ECD 60 min, Ab-D 60 min, S-AP 60 min; (4) HER2-ECD 30 min, Ab-D 60 min, S-AP 30 min. The alternatives 3 and 4 led to the highest sensitivity, however, in approach 4 the shorter incubation time of the enzyme led to a lower blank signal. To further reduce the blank signal, and using alternative 4, 0.5% (m/V) of BSA was added to the following solutions: (i) antigen (HER2-ECD), (ii) Ab-D and (iii) both the antigen and the Ab-D, with the purpose of blocking nonspecific adsorption. The addition of BSA 0.5% (m/V) to the Ab-D solution (alternative (ii)) clearly reduced the blank signal while

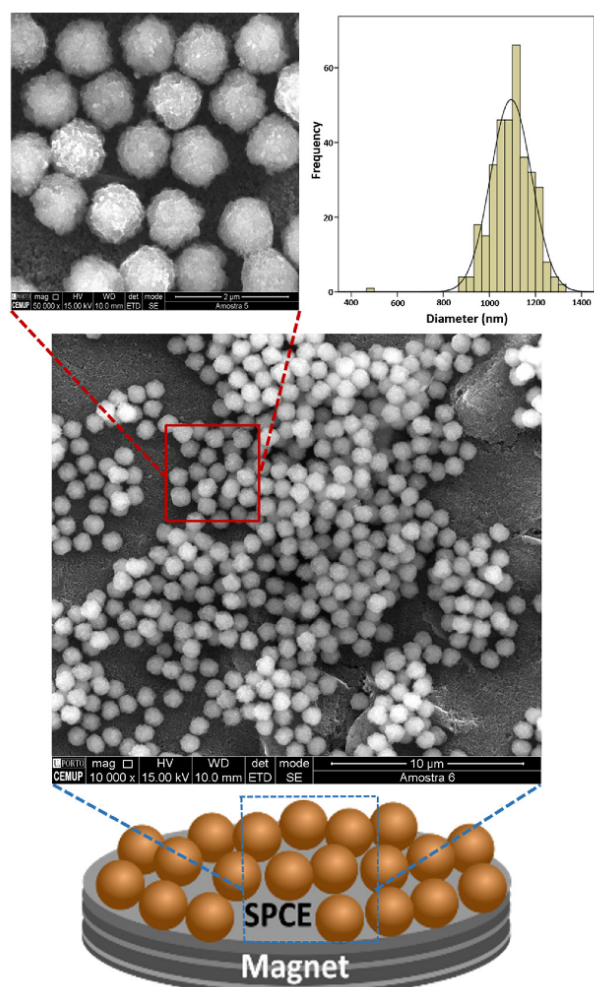


Fig. 1. SEM image of the SPCE covered with HOOC-MBs and the respective size distribution.

maintaining the signal for the analyte (50 ng/mL), leading to the best S/B ratio (SI Fig. S2).

Furthermore, in immunoassay protocols where enzyme conjugates are used, the addition of a blocking agent is usually advantageous to improve the S/B ratio. For this purpose, DEA 0.1 M and BSA 1% (m/V) were tested, according to previously published works [19,37]. As can be seen in SI Fig. S3A, although the use of both blockers resulted in excellent blank values, the highest analytical signal was obtained when BSA 1% (m/V) was used. Subsequently, four different S-AP solutions (with BSA 1% (m/V)) were tested: 2.0×10^{-10} ; 5.0×10^{-10} ; 1.0×10^{-9} and 5.0×10^{-9} M (SI Fig. S3B). As can be observed, higher S-AP concentrations led to higher i_p values. The 5.0×10^{-10} M concentration was chosen because it provided the best S/B ratio.

In order to reduce the analysis time of the immunoassay even further, a combination of several steps, by pre-incubation of the reagents, was studied. The tested alternatives were: (A) step-by-step assay, (B) pre-incubation of HER2-ECD + Ab-D during 60 min and (C) 120 min; (D) pre-incubation of Ab-D + S-AP (60 min); and (E) pre-incubation of HER2-ECD + Ab-D + S-AP (60 min). The obtained i_p values are presented in Fig. 3. Alternatives B and C led to the highest analytical signals, with alternative B providing a better precision among these two alternatives. On the other hand, the results obtained for alternatives D and E revealed a low signal and are not suitable for appropriate HER2-

ECD detection. Thus, the pre-incubation of HER2-ECD and Ab-D (containing BSA 0.5% (m/V)) for 60 min was used for the analysis of HER2-ECD in Human serum. To complete the optimization of the experimental parameters, the assay was tested at different temperatures (20, 25 and 30 °C). As can be seen in SI Fig. S4A the optimum temperature was 30 °C. The affinity of the MBs to the antigen, i.e. without the use of capture antibody, was also tested and no significant interaction was observed (SI Fig. S4B). Table S1 presents the main experimental variables, the tested range and the selected values.

3.3. Analytical characteristics of the assay

The analytical performance of the assay was evaluated under the optimized conditions. After verification of the suitability of the magnetic immunoassay to detect HER2-ECD in buffer solutions (0.1 M Tris-HNO₃ pH 7.4 (buffer 3); linear range 7.5–75 ng/mL ($n = 5$), $i_p = 1.05 \pm 0.08$ [HER2-ECD] + 55.2 ± 3.5 , $r = 0.993$ (SI Fig. S5)), experiments using Human serum as the matrix were carried out. The precision of the assay was evaluated for the analysis of 50 ng/mL HER2-ECD using three different SPCEs, on the same day and different days. Relative standard deviations (RSDs) of 4.0% and 3.4% were obtained, indicating that the developed assay provided precise results.

For calibration purposes, the electrochemical signal for different HER2-ECD concentrations (5–100 ng/mL) were studied (Fig. 4). The peak current intensity increased proportionally to the HER2-ECD concentration in two distinct ranges: between 5.0 and 50 ng/mL (1) and between 50 and 100 ng/mL. At the lower HER2-ECD concentrations the sensitivity was higher, which implies that the developed method can detect small variations in the cancer biomarker concentrations at the early stage of the disease. For the higher concentration range a different analytical behaviour was observed which can be explained by the near saturation of the antibody binding sites. The figures of merit for both ranges are indicated in Table 1. The linear relationship between i_p and [HER2-ECD] were: (1) $i_p = 0.81 \pm 0.03$ [HER2-ECD] + 2.46 ± 0.94 ($r = 0.997$) and (2) $i_p = 0.19 \pm 0.01$ [HER2-ECD] + 32.6 ± 1.1 ($r = 0.997$). The limits of detection (LOD) and quantification (LOQ) were calculated using the respective calibration data, using the equations: $LOD = 3 s_b/m$ and $LOQ = 10 s_b/m$, where s_b is the standard deviation of the blank and m is the slope of the calibration plot. The obtained LODs were 2.8 ng/mL and 11.8 ng/mL and the LOQs were 9.3 ng/mL and 39.2 ng/mL, for concentration ranges 1 and 2, respectively. For both ranges the LODs were clearly lower than the established cut-off value (15 ng/mL). The analytical characteristics are better for range 1, however, the usefulness for both ranges are evident since they allow primary diagnosis (screening and/or early detection) and the evolution of the patient's treatment (follow-up). The coefficient of variation of the method ($V_{x,0}$) was 1.20% and 0.29% for the ranges 1 and 2 respectively, demonstrating adequate precision of the method ($V_{x,0} < 5\%$).

When the calibration plot was constructed in serum a clear matrix effect was observed. The slopes of the calibration plots in serum were 1.3 (range 1) and 5.6 (range 2) times lower than the slope obtained with the measurements in buffer. This could be due to globulins, especially immunoglobulins G (IgG) present in the serum [39,40].

To evaluate the accuracy of the developed immunoassay, spiked sera with 15 and 50 ng/mL HER2-ECD were tested and recoveries were found to be 98.7% and 95.3%, respectively. The recovery obtained with the ELISA kit was 111.3% for 15 ng/mL (Table 2) (note: the sample containing 50 ng/mL could not be analysed using the ELISA kit because the measured absorbance was outside the calibration range). When comparing the results of both assays a relative deviation of -11.4% was obtained, which confirmed that the developed assay provides accurate results.

The storage stability of the MBs, modified with the capture antibody and blocked with ethanolamine, was also tested. The anti-HER2-ECD-MBs were stored at 4 °C in 100 μ L of PBS-T. The immunomagnetic assay

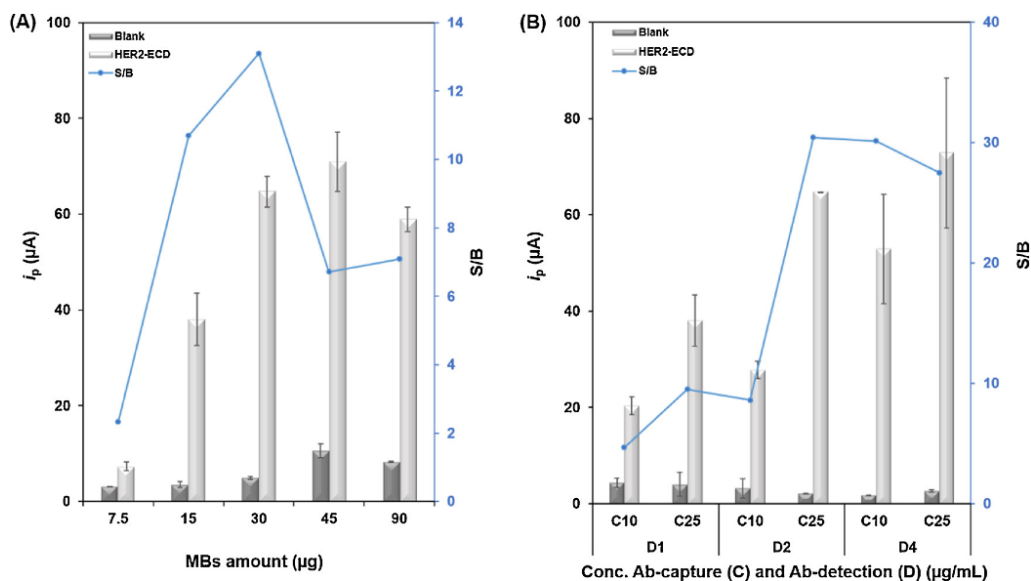


Fig. 2. Optimization of (A) the amount of magnetic beads and (B) the Ab-C and Ab-D concentrations (HER2-ECD: 0 and 50 ng/mL).

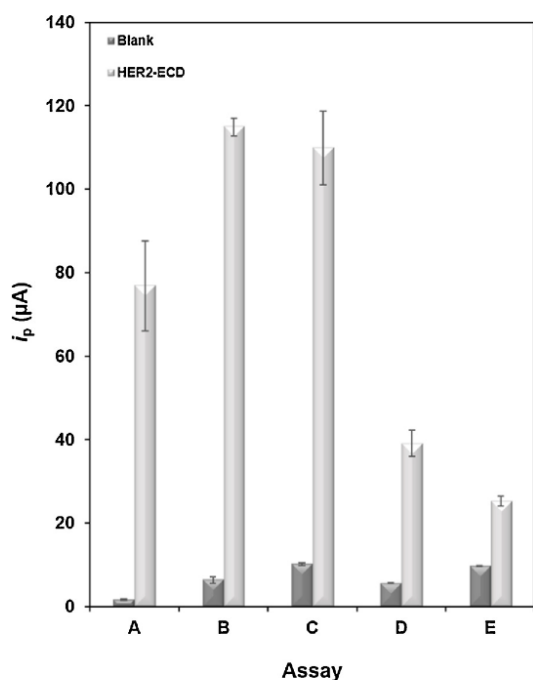


Fig. 3. Results of different assay strategies. (A) step-by-step assay, (B) pre-incubation of HER2 + Ab-D (60 min) and (C) pre-incubation of HER2 + Ab-D (120 min); (D) pre-incubation of Ab-D + S-AP (60 min); and (E) pre-incubation of HER2 + Ab-D + S-AP (60 min).

(in buffer solution) was performed on the same day and after 1, 7, 15, 21, 30 and 60 days using 0 and 50 ng/mL HER2-ECD. No significant difference in the measured blank and analytical signals was apparent over 60 days, obtaining 99.7% of the initial signal (SI Fig. S6), which indicates the stability of the MBs during this period. Furthermore, the use of these previously prepared MBs reduces the time required for the biomarker detection to 110 min.

The selectivity of the assay towards HER2-ECD was tested with

distinct human proteins (analysed in human serum): an analogous breast cancer biomarker (CA 15-3, 30 U/mL), a kidney function biomarker (cystatin C, 565 ng/mL) and Human serum albumin (HSA, 35 mg/mL). As can be seen in Fig. 5, the tested proteins showed an extremely low electrochemical signal, even at higher concentrations, confirming the selectivity of the assay towards HER2-ECD. In addition, this study allowed to confirm the specificity of the monoclonal antibodies.

3.4. Analysis of live breast cancer cells

Monitoring HER2-overexpressed cancer cells is actually a huge challenge from the clinical point of view. To test the performance of our immunoassay, two distinct breast cancer cell-lines were used: the HER2⁺ SK-BR-3 cell line and the HER2⁻MDA-MB-231 cell line. As can be observed in Fig. 6, HER2⁺ cancer cells provided a concentration-dependent signal which was 5x higher than the signal obtained with HER2⁻ cells, confirming the high selectivity of the optimized assay for the detection of HER2 biomarkers. The calibration curve (i_p vs. \log [cells]) for SK-BR-3 cells was established in the linear range between 1×10^2 – 1×10^5 cells/mL ($i_p = 3.38 \pm 0.15 \log[\text{SK-BR-3}] - 2.81 \pm 0.55$, $r = 0.996$). The coefficient of variation of the method (V_{x_0}) was found to be 2.4% and a limit of detection of 3 cells/mL was achieved.

3.5. Comparison with other electrochemical immunomagnetic assays

The developed immunomagnetic assay was compared with other electrochemical methodologies for cancer biomarker analysis (HER2, ErbB2, EGFR, CA 15-3, exosomes and α -LA) using a wide variety of functionalized MBs (e.g. protein A functionalized MBs (ProtA-MBs), streptavidin functionalized MBs (Strep-MBs), carboxylic acid functionalized MBs (HOOC-MBs) or 'self-made' iron nanoparticles (Fe_3O_4 NPs) [34–38,41–45] (Table 3). The 'self-made' magnetic particles required a time-consuming procedure and expensive characterization techniques leading to lengthy and costly preparation of the material. This is a key factor in favouring the use of commercially available MBs, enabling not only a faster but also a cheaper and more sustainable sensor preparation. Moreover, compared with the construction of immunosensors, magnetic assays can improve the antibody orientation on

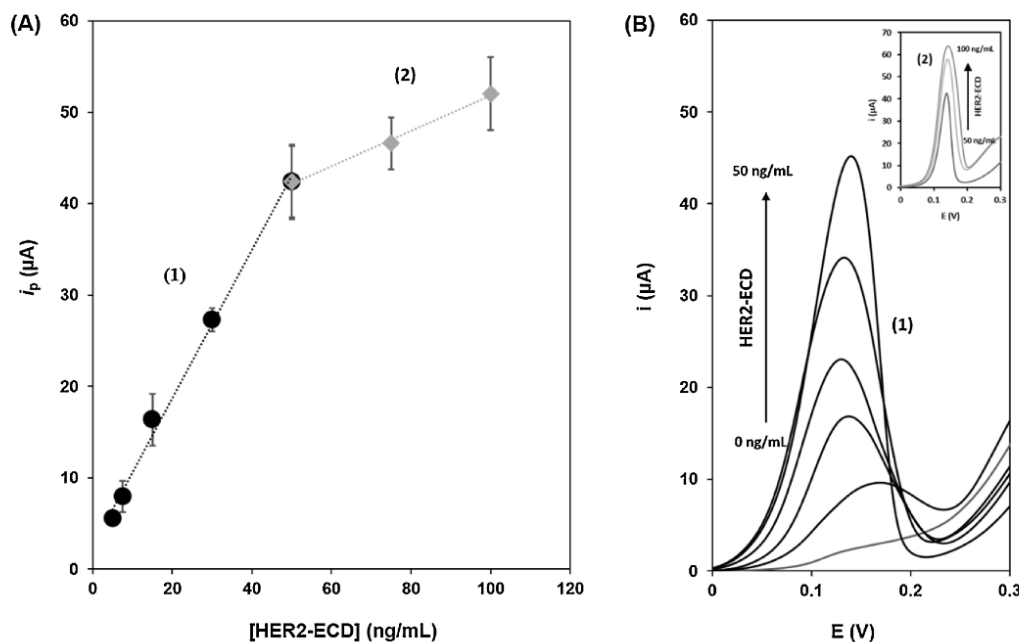


Fig. 4. Analysis of HER2-ECD in undiluted Human serum (A) Calibration plots and (B) Representative linear sweep voltammograms ([HER2-ECD] (ng/mL): (1) 0, 5, 7.5, 15, 30 and 50; (2) 50, 75 and 100).

Table 1

Figures of merit of the developed magnetic immunoassay for the analysis of HER2-ECD in Human serum.

Figure of merit	1	2
Concentration interval (ng/mL)	5.0–50	50–100
Correlation coefficient (r)	0.997	0.997
Slope (m) ($\mu\text{A} / (\text{ng}/\text{mL})$)	0.81	0.19
Standard deviation of the slope (S_m) ($\mu\text{A} / (\text{ng}/\text{mL})$)	0.03	0.01
Intercept (b) (μA)	2.46	32.6
Standard deviation of the intercept (S_b) (μA)	0.94	1.09
Standard deviation of the linear regression ($S_{y/x}$)	1.29	0.49
Standard deviation of the method ($S_{x,0}$)	0.26	0.16
Coefficient of variation of the method ($V_{x,0}$) (%)	1.20	0.29
Limit of detection (LOD) (ng/mL)	2.8	11.8
Limit of quantification (LOQ) (ng/mL)	9.3	39.2

the particles' surfaces in a rapid manner (1 h), allowing appropriate antigen binding. In addition, the described assays allow studies to be carried out using (extremely) low volumes and concentrations, and, due to the efficient washing steps and analyte pre-concentration, reliable analysis in serum samples can be achieved with excellent limits of detection. Although only a few studies concerning cell analysis were reported [38,44], CTC analyses for the evaluation of HER2-positive patients are of utmost importance to help the decisions of clinical teams for effective personalized therapy. The immunomagnetic assay developed in this work can effectively contribute to distinguish positive and negative HER2 cell-types with a competitive assay time that is

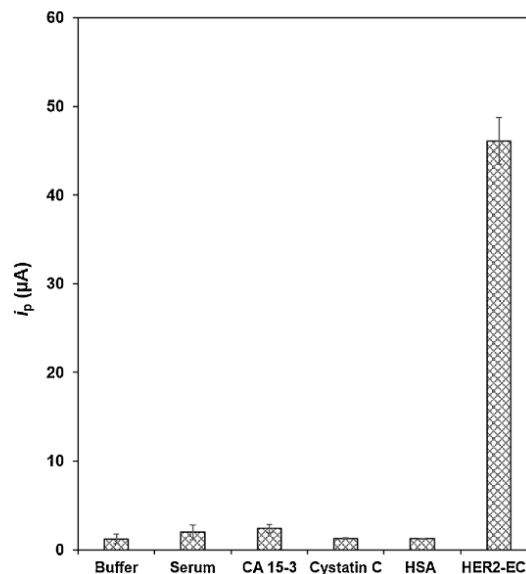


Fig. 5. Selectivity studies using non-target proteins (the signal for HER2-ECD is included for comparison).

Table 2

Recovery values, relative standard deviations (RSD) and relative deviation obtained in the analysis of HER2-ECD using the developed immunoassay and a commercial ELISA kit.

Technique	Added (ng/mL)	Found (ng/mL)	Recovery (%)	RSD (%)	Relative deviation (%)	Sample dilution
Elisa Kit	15	16.7	111.3	0.033	-11.4	4-fold
Electrochemical immunoassay	50	47.6	95.3	3.7	*	Undiluted

* The absorbance value for 50 ng/mL obtained using the ELISA kit was outside of the calibration range.

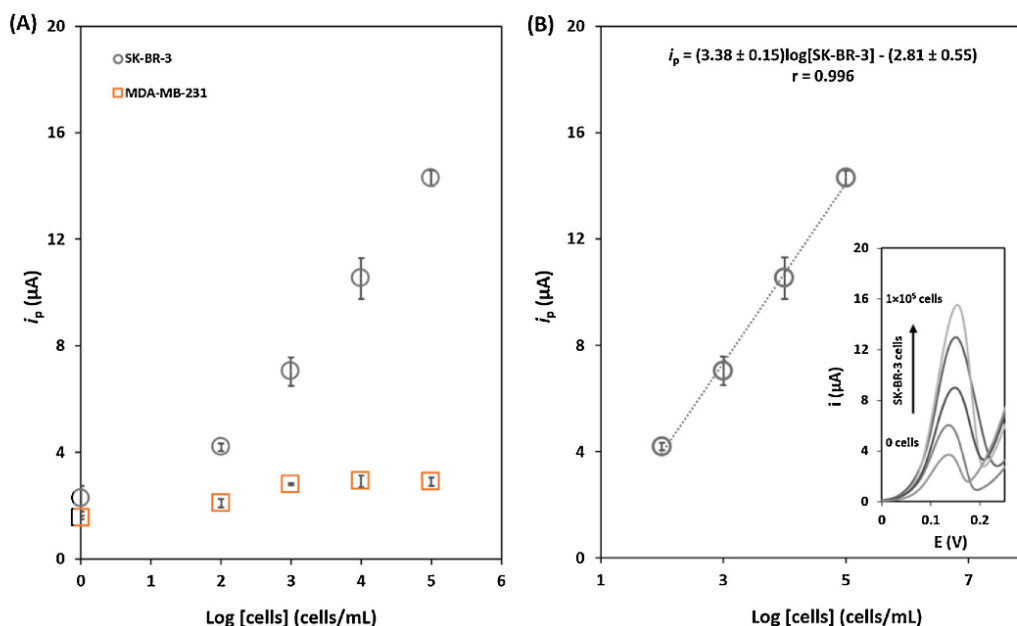


Fig. 6. (A) Calibration plots for the analysis of SK-BR-3 and MDA-MB-231 breast cancer cell lines in human serum; (B) Calibration straight for the analysis of SK-BR-3 (HER2⁺ cancer cells): 1×10^2 , 1×10^3 , 1×10^4 and 1×10^5 cells/mL. Inset: Examples of linear sweep voltammograms.

surpassed only by two works [38,41]. However, one of these works [38] didn't include a stability study and the other showed a much shorter stability [41].

As far as we know, to date no electrochemical immunomagnetic assays were reported for the detection of HER2-ECD using screen-printed carbon electrodes, MBs-COOH, 3-indoxyl phosphate (3-IP) and silver ions (Ag^+). Only the magnetic bioassay for the assessment of ErbB2 status directly in intact breast cancer cells employed SPCE and HOOC-MBs, achieving an excellent limit of detection [38]. The assay construction and the simplicity of this method can be compared with the present work and allows the use of a small-size (portable) equipment. This allows in situ analysis, requiring reduced reagent/sample volumes. Like this, the assay developed in this work could allow non-invasive screening and follow-up, according to the requirements of the clinical teams, and facilitates the monitoring of patients with reduced mobility or difficult access locations.

The FDA-approved HER2 diagnostic tests and the recently updated guidelines from the European Group on Tumor Markers (EGTM) reported that the main tests available to measure HER2 gene amplification/protein overexpression are immunohistochemistry (IHC), in situ hybridisation (ISH) and ELISA [11,12]. These tests are mostly performed by clinical professionals from oncological centres or specialized clinics, which makes their accessibility limited to the availability of specific technicians and / or equipment. Despite the evolution in this area and the significant investments and continuous development, it is still verified that the available tests have high costs for the national healthcare systems. Furthermore, only three biomarkers are mandatory to be analysed for all patients with breast cancer (oestrogen receptor (ER) and progesterone receptor (PR) for endocrine therapy and HER2 for the anti-HER2 therapy). Recommendations for further research not only involve the identification of additional markers but also analytical techniques capable of detecting the disease. Therefore, the constant development of electrochemical biosensors/assays could contribute to this field of research.

4. Conclusions

An electrochemical magnetic immunoassay, using HOOC-MBs and a

disposable SPCE as transducer, for the detection of HER2-ECD, a breast cancer biomarker, was developed. Sensitive and precise detection of the biomarker and an LOD well below the cut-off value was achieved in a total assay time of 110 min (actual hands-on-time: 20 min). The applicability and selectivity of the bioassay was demonstrated through the analysis of spiked human serum samples and distinct non-target proteins and possible serum interferents: Cancer Antigen 15-3 (CA 15-3), Cystatin C and Human Serum Albumin (HSA). The storage stability of the MBs was at least 60 days, which is much better than previously reported. The immunomagnetic assay exhibited an excellent analytical performance and was successfully applied to spiked serum samples and may be applicable in the clinical practice. Additionally, the assay was also tested for the analysis of live breast cancer cells (HER2⁺: SK-BR-3; HER2⁻: MDA-MB-231) and it was possible to distinguish the different HER2 expression levels, showing high selectivity for HER2-positive cells.

Declaration of interests

The authors declare that they have no known competing financial interests or personal relationships that could have appeared to influence the work reported in this paper.

Acknowledgements

The authors are grateful for the financial support from the Fundação para a Ciência e a Tecnologia (FCT)/the Ministério da Ciência, Tecnologia e Ensino Superior (MCTES) through national funds (Portugal) (LAQV - UID/QUI/50006/2019 and CINTESIS - UID/IC/4255/2019). Maria Freitas is grateful to FCT for her PhD grant (SFRH/BD/111942/2015), financed by POPH-QREN-Tipologia 4.1-Formação Avançada, subsidized by Fundo Social Europeu and the MCTES. The authors are also thankful to Rui Rocha and CEMUP "Centro de Materiais da Universidade do Porto" for the SEM work.

Appendix A. Supplementary data

Supplementary material related to this article can be found, in the

Table 3
Electrochemical immunoassays for breast cancer detection using magnetic beads (MBs).

Sensing surface construction		Analyte	Assay strategy	LOD	Cell analysis	Ref
Transducer	Preparation time*	Stability	Detection scheme	Assay time		
SPCE/ HOOC-MBs	1 h 15 min	60 days	LSV performed after addition of 3-IP/Ag ⁺ . AP used as label	1 h 50 min 2.8 ng/mL	SK-BR-3; MDA-MB-231	This work
GrE/ Nitrocellulose- Strep-MBs	2 h	n.d.	CC recorded before and after the nitrocellulose-modified electrode exposure to cellulase	1 hM	–	[34]
GCE/ Fe ₃ O ₄ -APTMS	> 5 h	10 days	Hyd-AuNPs/Fe ₃ O ₄ NPs used as label. Silver detection by DPV	2 h 2.0 × 10 ⁻⁵ ng/mL	–	[35]
8 × SPE/ Strep-MBs or ProtA-MBs	12 h 15 min 1 h	1 week	Hydrolysis of 1-NP catalysed by AP and detected by DPV	2 h 51 min 1.8; 2.6; 3.4 ng/mL 1 h 51 min	–	[36]
SPCE/ ProtA-MBs	1 h	10 days	Detection of 1-NP performed by DPV. AP used as label.	2 h 05 min	–	[37]
SPCE/ HOOC-MBs	1 h 40 min	n.d.	HRP used as label. HQ allow to obtain the amperometric response	1 h 6.0 ng/mL 26 pg/mL	SK-BR-3; MCF-7; MDA-MB-436	[38]
GCE/ Strep-MBs	1 h	7 days	AuNPs used as signalling probe. Detection accomplished by DPV	1 h 50 pg/mL	–	[41]
Au microelectrodes/ Strep	> 24 h	15 days	Strep-MBs conjugated with bio-HRP. HQ measured by SWV	5 h 15 × 10 ⁻⁶ U/mL	–	[42]
SPCE/ P(1,5DAN)-PPy NWS	> 14 h	n.d.	Strep-MBs used as carriers and HRP as label. DPV performed to measure HQ	1 h 30 min 0.02 U/mL	–	[43]
GCE/ Strep-MBs	30 min	n.d.	Cd ²⁺ detection carried out by SWASV. CdSe QDs used as label	1 h 50 min 100 exosomes/ μ L	BT474; SW-48	[44]
SPCE/ Lys-Fe ₃ O ₄ NPs	13 h	1 month	Ferrocene-modified AuNPs used to obtain the amperometric response	4 h 0.07 ng/mL	–	[45]

α -LA – α -lactalbumin; 1-NP – 1-naphthol; 3-IP – 3-indoxyl phosphate; Ag⁺ – silver ions; AP – alkaline phosphatase; APTMS – 3-aminopropyltrimethoxysilane; AuNPs – gold nanoparticles; CA 15-3 – cancer antigen 15-3; CC – chronocoulometry; CdSe QDs – Cadmium selenide quantum dots; Cd²⁺ – cadmium ions; DPV – differential pulse voltammetry; ECD – extracellular domain; EGFR – epidermal growth factor receptor; Fe₃O₄ – magnetic nanoparticles; GCE – glassy carbon electrode; GrE – graphene electrode; HER2, ErbB2 – human epidermal growth factor receptor 2; Hyd – hydrazine; HOOC-MBs – carboxylic acid functionalized magnetic beads; HQ – hydroquinone; HRP – horseradish peroxidase; Lys – lysozyme; LSV – linear sweep voltammetry; n.a. – not applicable; P(1,5DAN) – poly(1,5-diaminonaphthalene); PPy – NWS polypyrrole nanowires; ProtA-MBs – Protein A-modified magnetic beads; SPE – screen-printed electrode; n.d. – no data; SPCE – screen-printed carbon electrode; Strep-MBs – streptavidin-modified magnetic beads; SWV – Square wave voltammetry; SWASV – square wave anodic stripping voltammetry.

* Overnight incubations were considered as a 12 h period for comparison purposes.

M. Freitas, et al.

Sensors & Actuators: B. Chemical 308 (2020) 127667

online version, at doi:<https://doi.org/10.1016/j.snb.2020.127667>.

References

- [1] M. Freitas, H.P.A. Nows, C. Delerue-Matos, Electrochemical biosensing in cancer diagnostics and follow-up, *Electroanalysis* 30 (2018) 1576–1595, <https://doi.org/10.1002/elan.201800193>.
- [2] F. Puglisi, C. Fontanella, G. Numico, V. Sini, L. Evangelista, F. Monetti, S. Gori, L. Del Mastro, Follow-up of patients with early breast cancer: is it time to rewrite the story? *Crit. Rev. Oncol. Hematol.* 91 (2014) 130–141, <https://doi.org/10.1016/j.critrevonc.2014.03.001>.
- [3] A. Ravelli, J.M. Reuben, F. Lanza, S. Anfossi, M.R. Cappelletti, L. Zanotti, A. Gobbi, C. Senti, P. Brambilla, M. Milani, D. Spada, P. Pedrazzoli, M. Martino, A. Bottini, D. Generali, Breast cancer circulating biomarkers: advantages, drawbacks, and new insights, *Tumor Biol.* 36 (2015) 6653–6665, <https://doi.org/10.1007/s13277-015-3944-7>.
- [4] S. Mittal, H. Kaur, N. Gautam, A.K. Mantha, Biosensors for breast cancer diagnosis: a review of bioreceptors, biotransducers and signal amplification strategies, *Biosens. Bioelectron.* 88 (2017) 217–231, <https://doi.org/10.1016/j.bios.2016.08.028>.
- [5] S. Campuzano, M. Pedrero, J.M. Pingarrón, Non-invasive breast cancer diagnosis through electrochemical biosensing at different molecular levels, *Sensors (Switzerland)* 17 (2017) 1993, <https://doi.org/10.3390/s17091993>.
- [6] M. Iabih, F.H. Sargent, S.O. Kelley, Electrochemical methods for the analysis of clinically relevant biomolecules, *Chem. Rev.* 116 (2016) 9001–9090, <https://doi.org/10.1021/acs.chemrev.6b00220>.
- [7] A.J. Wang, X.Y. Zhu, Y. Chen, X. Luo, Y. Xue, J.J. Feng, Ultrasensitive label-free electrochemical immunoassay of carbohydrate antigen 15-3 using dendritic Au@Pt nanocrystals/ferrocene-grafted-chitosan for efficient signal amplification, *Sens. Actuators B Chem.* 292 (2019) 164–170, <https://doi.org/10.1016/j.snb.2019.04.128>.
- [8] R. Wang, J.J. Feng, Y. Xue, L. Wu, A.J. Wang, A label-free electrochemical immunosensor based on AgPt nanorings supported on reduced graphene oxide for ultrasensitive analysis of tumor marker, *Sens. Actuators B Chem.* 254 (2018) 1174–1181, <https://doi.org/10.1016/j.snb.2017.08.009>.
- [9] Y. Chen, P.X. Yuan, A.J. Wang, X. Luo, Y. Xue, L. Zhang, J.J. Feng, A novel electrochemical immunosensor for highly sensitive detection of prostate-specific antigen using 3D open-structured PtCu nanoframes for signal amplification, *Biosens. Bioelectron.* 126 (2019) 187–192, <https://doi.org/10.1016/j.bios.2018.10.057>.
- [10] A.C. Wolff, M. Elizabeth Hale Hammond, K.H. Allison, B.E. Harvey, P.B. Mangu, J.M.S. Bartlett, M. Bilous, I.O. Ellis, P. Fitzgibbons, W. Hanna, R.B. Jenkins, M.F. Press, P.A. Spears, G.H. Vance, G. Viale, L.M. McShane, M. Dowsett, Human epidermal growth factor receptor 2 testing in breast cancer: American society of clinical oncology/college of American pathologists clinical practice guideline focused update, *J. Clin. Oncol.* 36 (2018) 2105–2122, <https://doi.org/10.1200/JCO.2018.77.8738>.
- [11] M.J. Duffy, N. Harbeck, M. Nap, R. Molina, A. Nicolini, E. Senkus, F. Cardoso, Clinical use of biomarkers in breast cancer: updated guidelines from the European Group on Tumor Markers (EGTM), *Eur. J. Cancer* 75 (2017) 284–298, <https://doi.org/10.1016/j.ejca.2017.01.017>.
- [12] A.K. Füszéry, J. Levin, M.M. Chan, D.W. Chan, Translation of proteomic biomarkers into FDA approved cancer diagnostics: issues and challenges, *Clin. Proteomics* 10 (2013) 13, <https://doi.org/10.1186/1559-0275-10-13>.
- [13] M. Hasanzadeh, N. Shadjou, M. de la Guardia, Early stage screening of breast cancer using electrochemical biomarker detection, *Trends Anal. Chem.* 91 (2017) 67–76, <https://doi.org/10.1016/j.trac.2017.04.006>.
- [14] M. Freitas, M.M.P.S. Neves, H.P.A. Nows, C. Delerue-Matos, Quantum dots as nanolabels for breast cancer biomarker HER2-ECD analysis in human serum, *Talanta* 208 (2020) 120430, <https://doi.org/10.1016/j.talanta.2019.120430>.
- [15] Z.M.A.N.H. Lah, S.A.A. Ahmad, M.S. Zaini, M.A. Kamarudin, An electrochemical sandwich immunosensor for the detection of HER2 using antibody-conjugated PbS quantum dot as a label, *J. Pharm. Biomed. Anal.* 174 (2019) 608–617, <https://doi.org/10.1016/j.jpba.2019.06.024>.
- [16] S.D. Tallapragada, K. Layek, R. Mukherjee, K.K. Mistry, M. Ghosh, Development of screen-printed electrode based immunosensor for the detection of HER2 antigen in human serum samples, *Bioelectrochemistry* 118 (2017) 25–30, <https://doi.org/10.1016/j.bioelechem.2017.06.009>.
- [17] S. Patris, P. De Pauw, M. Vandepuit, J. Huet, P. Van Antwerpen, S. Muyldermans, J.M. Kauffmann, Nanoimmunoassay onto a screen printed electrode for HER2 breast cancer biomarker determination, *Talanta* 130 (2014) 164–170, <https://doi.org/10.1016/j.talanta.2014.06.069>.
- [18] S.P. Mucelli, M. Zamuner, M. Tormen, G. Stanta, P. Ugo, Nanoelectrode ensembles as recognition platform for electrochemical immunosensors, *Biosens. Bioelectron.* 23 (2008) 1900–1903, <https://doi.org/10.1016/j.bios.2008.02.027>.
- [19] M. Freitas, H.P.A. Nows, C. Delerue-Matos, Electrochemical sensing platforms for HER2-ECD breast cancer biomarker detection, *Electroanalysis* 31 (2019) 121–128, <https://doi.org/10.1002/elan.201800537>.
- [20] E. Arkan, R. Saber, Z. Karimi, M. Shamsipur, A novel antibody-antigen based impedimetric immunosensor for low level detection of HER2 in serum samples of breast cancer patients via modification of a gold nanoparticles decorated multiwall carbon nanotube-ionic liquid electrode, *Anal. Chim. Acta* 874 (2015) 66–74, <https://doi.org/10.1016/j.aca.2015.03.022>.
- [21] A. Ravalli, C.G. da Rocha, H. Yamanaka, G. Marrazza, A label-free electrochemical affensor for cancer marker detection: the case of HER2, *Bioelectrochemistry* 106 (2015) 268–275, <https://doi.org/10.1016/j.bioelechem.2015.07.010>.
- [22] R.C.B. Marques, S. Viswanathan, H.P.A. Nows, C. Delerue-Matos, M.B. González-García, Electrochemical immunosensor for the analysis of the breast cancer biomarker HER2 ECD, *Talanta* 129 (2014) 594–599, <https://doi.org/10.1016/j.talanta.2014.06.035>.
- [23] M. Jarczewska, A. Trojan, M. Gagala, E. Malinowska, Studies on the affinity-based biosensors for electrochemical detection of HER2 cancer biomarker, *Electroanalysis* 31 (2019) 1125–1134, <https://doi.org/10.1002/elan.201900041>.
- [24] S. Carvajal, S.N. Fera, A.L. Jones, T.A. Baldo, I.M. Mosa, J.F. Rusling, C.E. Krause, Disposable inkjet-printed electrochemical platform for detection of clinically relevant HER-2 breast cancer biomarker, *Biosens. Bioelectron.* 104 (2018) 158–162, <https://doi.org/10.1016/j.bios.2018.01.003>.
- [25] E. Chochołova, T. Bertok, L. Lorencova, A. Holazova, P. Farkas, A. Vikartovska, V. Bella, D. Velicova, P. Kasak, A.A. Eckstein, J. Mosnacek, D. Hasko, J. Tkac, Advanced antifouling zwitterionic layer based impedimetric HER2 biosensing in human serum: glycoprofiling as a novel approach for breast cancer diagnostics, *Sens. Actuators B Chem.* 272 (2018) 626–633, <https://doi.org/10.1016/j.snb.2018.07.029>.
- [26] S. Augustine, P. Kumar, B.D. Malhotra, Amine-Functionalized MoO₃@RGO Nanohybrid-based biosensor for breast cancer detection, *ACS Appl. Bio Mater.* 2 (2019) 5366–5378, <https://doi.org/10.1021/acsabm.9b00659>.
- [27] S. Sharma, J. Zapatero-Rodríguez, R. Saxena, R. O’Kennedy, S. Srivastava, Ultrasensitive direct impedimetric immunosensor for detection of serum HER2, *Biosens. Bioelectron.* 106 (2018) 78–85, <https://doi.org/10.1016/j.bios.2018.01.056>.
- [28] M. Emami, M. Shamsipur, R. Saber, R. Irajirad, An electrochemical immunosensor for detection of a breast cancer biomarker based on antiHER2-iron oxide nanoparticle bioconjugates, *Analyst* 139 (2014) 2858–2866, <https://doi.org/10.1039/c4an00183d>.
- [29] Y. Zhu, P. Chandra, Y.B. Shim, Ultrasensitive and selective electrochemical diagnosis of breast cancer based on a hydrazine-Au nanoparticle-aptamer bioconjugate, *Anal. Chem.* 85 (2013) 1058–1064, <https://doi.org/10.1021/ac302923k>.
- [30] P. Yáñez-Sedeño, S. Campuzano, J.M. Pingarrón, Magnetic particles coupled to disposable screen printed transducers for electrochemical biosensing, *Sensors (Switzerland)* 16 (2016) 1585, <https://doi.org/10.3390/s16101585>.
- [31] E. Paleček, M. Fojta, Magnetic beads as versatile tools for electrochemical DNA and protein biosensing, *Talanta* 74 (2007) 276–290, <https://doi.org/10.1016/j.talanta.2007.08.020>.
- [32] V. Mami, B.V. Chikkaveeraiiah, J.F. Rusling, Magnetic particles in ultrasensitive biomarker protein measurements for cancer detection and monitoring, *Expert Opin. Med. Diagn.* 5 (2011) 381–391, <https://doi.org/10.1517/17530059.2011.607161>.
- [33] F. Ricci, G. Adornetto, G. Palleschi, A review of experimental aspects of electrochemical immunosensors, *Electrochim. Acta* 84 (2012) 74–83, <https://doi.org/10.1016/j.electacta.2012.06.033>.
- [34] K. Malecka, D. Pankratov, E.E. Ferapontova, Femtomolar electroanalysis of a breast cancer biomarker HER-2/ncu protein in human serum by the cellulose-linked sandwich assay on magnetic beads, *Anal. Chim. Acta* 1077 (2019) 140–149, <https://doi.org/10.1016/j.aca.2019.05.052>.
- [35] M. Shamsipur, M. Emami, L. Farzin, R. Saber, A sandwich-type electrochemical immunosensor based on in situ silver deposition for determination of serum level of HER2 in breast cancer patients, *Biosens. Bioelectron.* 103 (2018) 54–61, <https://doi.org/10.1016/j.bios.2017.12.022>.
- [36] H. Ilkhani, A. Ravalli, G. Marrazza, Design of an antibody-based recognition strategy for human epidermal growth factor receptor 2 (HER2) detection by electrochemical biosensors, *Chemosensors* 4 (2016) 23, <https://doi.org/10.3390/chemosensors4040023>.
- [37] Q.A.M. Al-Khafaji, M. Harris, S. Tombelli, S. Laschi, A.P.F. Turner, M. Mascini, G. Marrazza, An electrochemical immunoassay for HER2 detection, *Electroanalysis* 24 (2012) 735–742, <https://doi.org/10.1002/elan.201100501>.
- [38] U. Elrtigerra, J. Martínez-Perdigueró, S. Merino, R. Barderas, R.M. Torrente-Rodríguez, R. Villalonga, J.M. Pingarrón, S. Campuzano, Amperometric magneto-immunosensor for ErbB2 breast cancer biomarker determination in human serum, cell lysates and intact breast cancer cells, *Biosens. Bioelectron.* 70 (2015) 34–41, <https://doi.org/10.1016/j.bios.2015.03.017>.
- [39] S.E.F. Melanson, M.J. Tanasijevic, P. Jarolim, Cardiac troponin assays: a view from the clinical chemistry laboratory, *Circulation* 116 (2007) e501–e504, <https://doi.org/10.1161/CIRCULATIONAHA.107.722975>.
- [40] J.T. Busher, Serum albumin and globulin, in: H.K. Walker, W.D. Hall, J.W. Hurst (Eds.), *Clinical Methods: The History, Physical, and Laboratory Examinations*, third ed., Butterworths, Boston (USA), 1990 (Chapter 101), <http://www.ncbi.nlm.nih.gov/pubmed/21250048>.
- [41] H. Ilkhani, M. Sarparast, A. Noori, S.Z. Bathaie, M.F. Mousavi, Electrochemical aptamer/antibody based sandwich immunosensor for the detection of EGFR, a cancer biomarker, using gold nanoparticles as a signaling probe, *Biosens. Bioelectron.* 74 (2015) 491–497, <https://doi.org/10.1016/j.bios.2015.06.063>.
- [42] S. Akbari Nakhjavani, B. Khalilzadeh, P. Samadi Pakchin, R. Saber, M.H. Ghahremani, Y. Omid, A highly sensitive and reliable detection of CA15-3 in patient plasma with electrochemical biosensor labeled with magnetic beads, *Biosens. Bioelectron.* 122 (2018) 8–15, <https://doi.org/10.1016/j.bios.2018.08.047>.
- [43] V.A. Nguyen, H.L. Nguyen, D.T. Nguyen, Q.P. Do, L.D. Tran, Electro synthesized poly(1,5-diaminonaphthalene)/polypyrrole nanowires bilayer as an immunosensor platform for breast cancer biomarker CA 15-3, *Curr. Appl. Phys.* 17 (2017) 1422–1429, <https://doi.org/10.1016/j.cap.2017.08.002>.
- [44] K. Boriachek, M.N. Islam, V. Gopalan, A.K. Lam, N.T. Nguyen, M.J.A. Shiddiky, Quantum dot-based sensitive detection of disease specific exosome in serum, *Analyst* 142 (2017) 2211–2219, <https://doi.org/10.1039/c7an00672a>.

M. Freitas, et al.

Sensors & Actuators: B. Chemical 308 (2020) 127667

- [45] A. Mars, S. Ben jaafar, A.B.A. El Gaicd, N. Raouafi, Electrochemical immunoassay for lactalbumin based on the use of ferrocene-modified gold nanoparticles and lysozyme-modified magnetic beads, *Microchim. Acta* 185 (2018) 449, <https://doi.org/10.1007/s00604-018-2986-0>.

Maria Freitas obtained her degree in Biochemistry in 2010 from the University of Trás-os-Montes and Alto Douro (Portugal) and her MSc degree in Quality Control in 2012 from the Faculty of Pharmacy, University of Porto (Portugal). Currently she is a Ph.D. student in the doctoral program on Sustainable Chemistry at REQUIMTE and her research interests include the development of electrochemical methodologies (immunosensors and MIPs) for the analysis of cancer biomarkers, and synthesis of nanomaterials, mainly magnetic core/shell nanoparticles.

Henri P.A. Nouws obtained his PhD in Chemistry in 2007 (Faculty of Sciences, University of Porto, Portugal). Currently he is an auxiliary professor at the Chemical Engineering Department of the School of Engineering, Polytechnic Institute of Porto (ISEP-IPP, Portugal). He is also an integrated research member of REQUIMTE and his

present research interests include the development of analytical (electrochemical) methodologies for pharmaceutical, clinical, and food analysis.

Elisa Keating obtained her PhD from the Faculty of Medicine, University of Porto (Portugal). Currently she is an Assistant Professor of the Department of Biomedicine and a member of the Pedagogical Council of the Faculty of Medicine of the University of Porto. She is the principal investigator of the ProNutri Group at CINTESIS, where she focuses on nutrition throughout life and metabolic programming.

Cristina Delerue-Matos obtained her PhD in Chemical-Physics, specialty in electrochemistry, in 1990. At the moment she is principal coordinator professor at the Chemical Engineering Department of the School of Engineering, Polytechnic Institute of Porto (ISEP-IPP, Portugal) and also coordinates the REQUIMTE/ISEP research group (www.grad.issep.ipp.pt). Her research interests include the development of analytical methodologies for environmental, food, pharmaceutical, biochemical and industrial control. She is co-author of more than 250 publications in scientific journals.

Supplementary Material

High-performance electrochemical immunomagnetic assay for breast cancer analysis

Maria Freitas¹, Henri P.A. Nouws^{1*}, Elisa Keating^{2,3}, Cristina Delerue-Matos¹

¹REQUIMTE/LAQV, Instituto Superior de Engenharia do Porto, Politécnico do Porto, Rua Dr. António Bernardino de Almeida 431, 4200-072 Porto, Portugal, ² Department of Biomedicine – Unit of Biochemistry, Faculty of Medicine, University of Porto, Al. Prof. Hernâni Monteiro, 4200-319 Porto, Portugal, ³CINTESIS – Center for Health Technology and Services Research, Rua Dr. Plácido da Costa, 4200-450 Porto, Portugal

* corresponding author: han@isep.ipp.pt

Contents

Table S1	S2
Figure S1	S2
Figure S2	S3
Figure S3	S3
Figure S4	S4
Figure S5	S4
Figure S6	S5

Table S1. Optimization of the experimental parameters of the magnetic immunoassay.

Experimental variable	Tested range	Selected value
MBs amount (μg)	7.5 – 90	30
[Ab-C] ($\mu\text{g/mL}$)	10 – 25	25
[Ab-D] ($\mu\text{g/mL}$)	1.0 – 4.0	2.0
[S-AP] (nmol/L)	0.2 – 5.0	0.50
Temperature ($^{\circ}\text{C}$)	20 – 30	30
t (mixture HER2-ECD and Ab-D) (min)	0 – 120	60

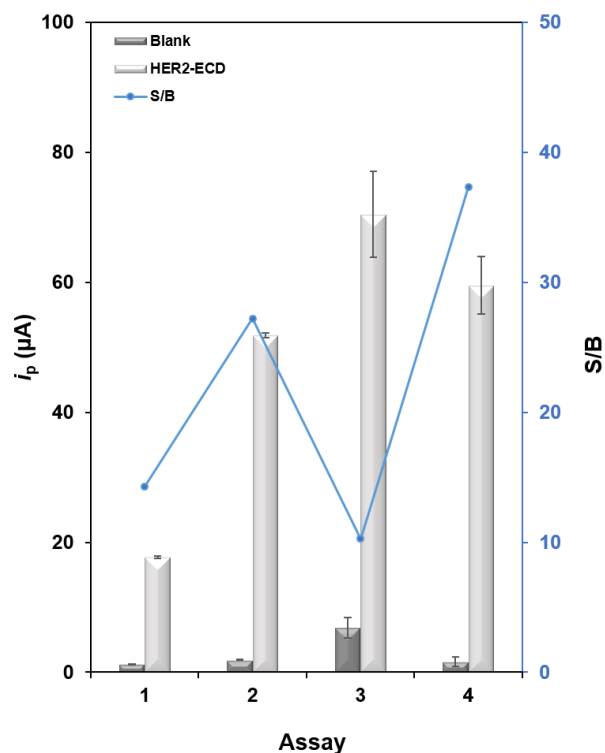


Figure S1. Optimization of the incubation time for the step-by-step assay: (1) HER2-ECD 30 min, Ab-D 30 min, S-AP 30 min; (2) HER2-ECD 30 min, Ab-D 60 min, S-AP 60 min; (3) HER2-ECD 60 min, Ab-D 60 min, S-AP 60 min; (4) HER2-ECD 30 min, Ab-D 60 min, S-AP 30 min. (Ab-C: 25 $\mu\text{g/mL}$, HER2-ECD: 0 and 50 ng/mL, Ab-D: 2 $\mu\text{g/mL}$).

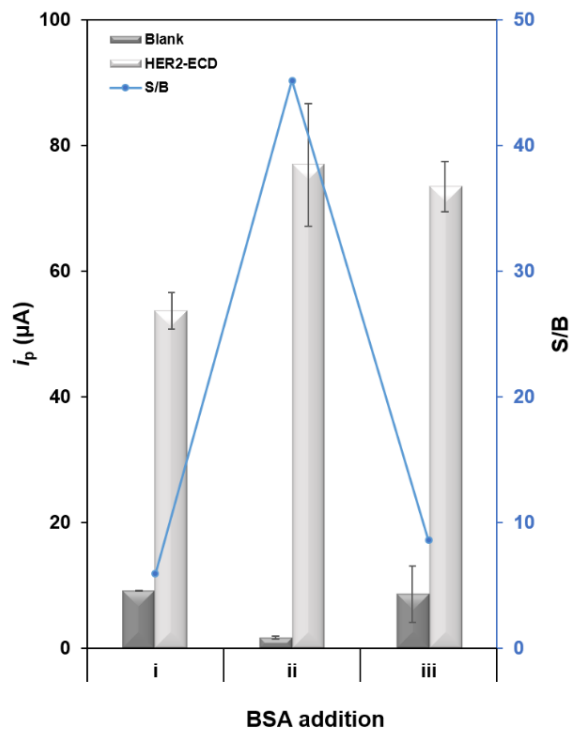


Figure S2. Addition of BSA 0.5% (m/V) to (i) HER2-ECD, (ii) Ab-D or (iii) in both solutions (antigen and Ab-D). (Ab-C: 25 $\mu\text{g/mL}$, HER2-ECD: 0 and 50 ng/mL , Ab-D: 2 $\mu\text{g/mL}$).

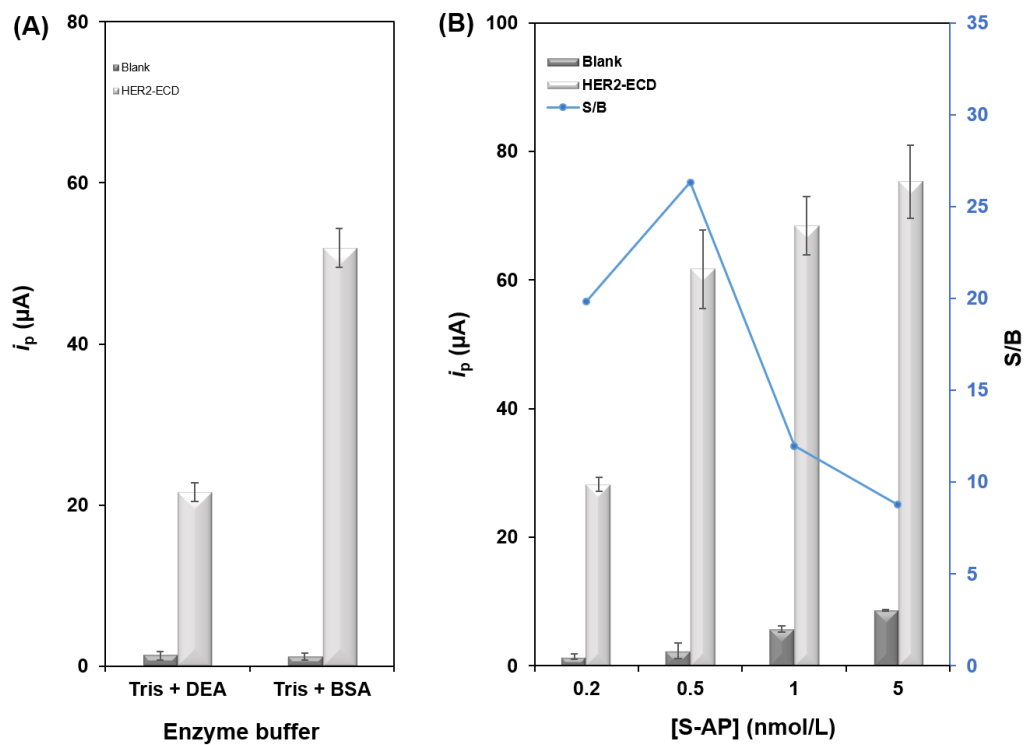


Figure S3. (A) Effect of the addition of DEA 0.1 M or BSA 1% (m/V) to the S-AP solution and (B) Variation of S-AP concentration (including BSA 1% (m/V)). (Ab-C: 25 $\mu\text{g/mL}$, HER2-ECD: 0 and 50 ng/mL , Ab-D: 2 $\mu\text{g/mL}$).

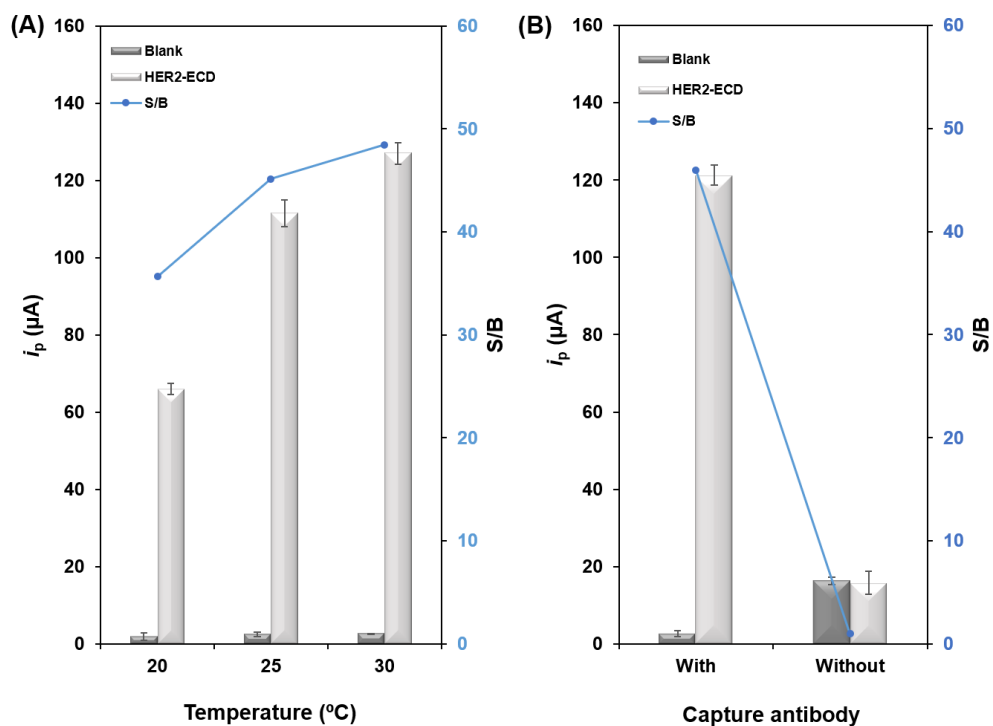


Figure S4. Optimization of experimental parameters. (A) Temperature, and (B) Affinity of the MBs with the antigen, i.e. with and without capture antibody.

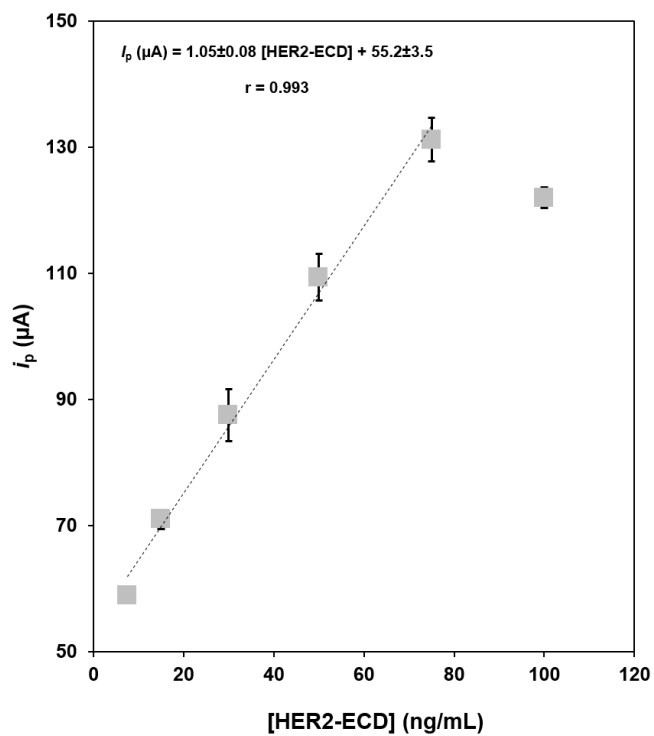


Figure S5. Calibration plot in 0.1M Tris-HNO₃ buffer (pH 7.4) for the analysis of HER2-ECD: 7.5, 15, 30, 50, 75 and 100 ng/mL. Experimental conditions: Ab-C: 25 $\mu\text{g}/\text{mL}$, BSA: 2% (m/V), Ab-D: 2 $\mu\text{g}/\text{mL}$.

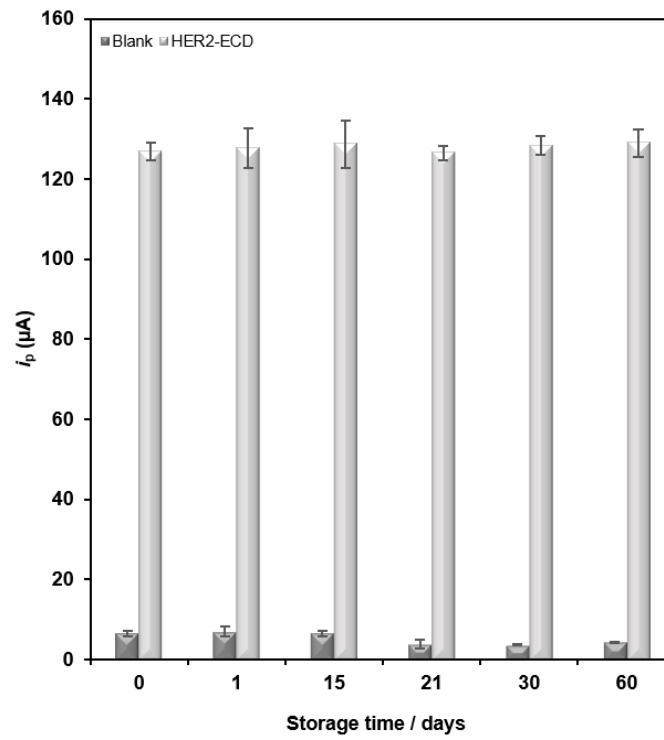


Figure S6. Obtained current intensities in the stability studies. (Ab-C: 25 $\mu\text{g}/\text{mL}$, HER2-ECD: 0 and 50 ng/mL, Ab-D: 2 $\mu\text{g}/\text{mL}$).

CHAPTER 4

ELECTROCHEMICAL IMMUNOASSAYS USING QUANTUM DOTS AS DETECTION LABELS

4

Overview

This chapter comprises two original scientific publications in international peer-reviewed journals (sections 4.1 and 4.2).

An integral transcript of the published articles is presented according to the journal rights and with requested permission.

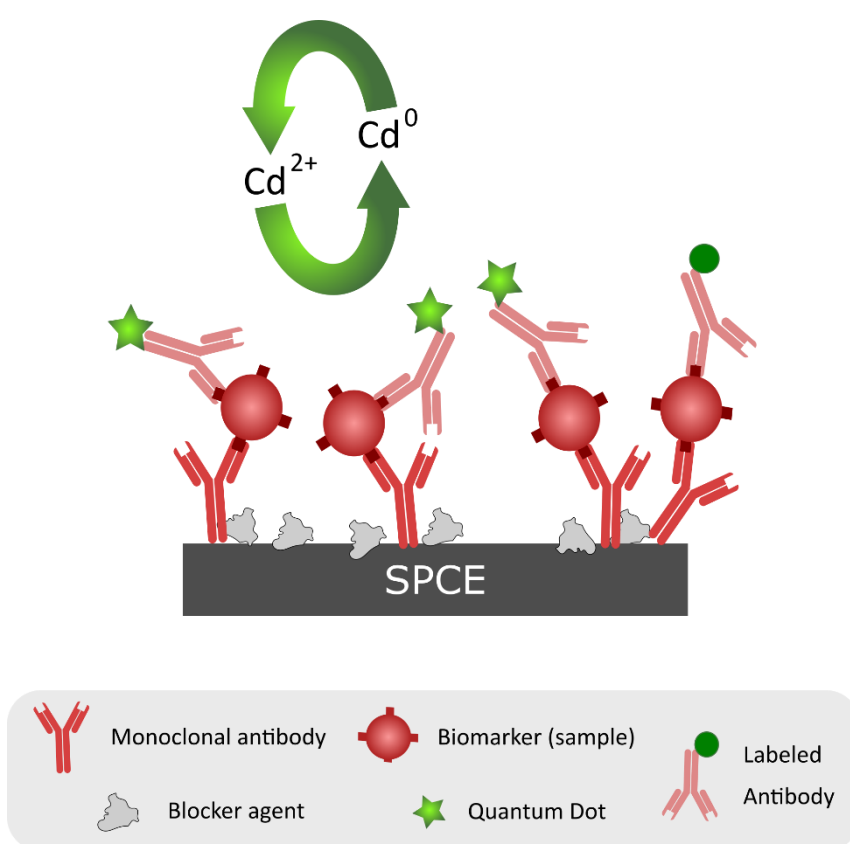
Sustainable alternatives to a more appealing dynamics in the detection strategy and the reduction of the assay time are the main perspectives considered in this chapter. The use of Quantum Dots (QDs) is an alternative to the commonly used redox probes or the enzymatic systems traditionally employed in the development of biosensors in healthcare.

In this chapter the detection strategy is based on the use of QDs as electroactive labels. Unlike the previous chapter where additional steps were required for the enzymatic reaction, here the addition of QDs and subsequent preconcentration and redissolution allows the detection of the metal ion (cadmium). For an adequate perception of analyte detection based on this detection strategy, this chapter presents the development, optimization and construction of an immunosensor and a magnetic immunoassay. Bare SPCEs were used as transducers (without modifications or functionalizations) for the immunosensor construction, and the magnetic immunoassay was developed using carboxylic acid-functionalized magnetic beads.

The first author contributions comprise the preparation of the transducer surface for efficient modification with the biorecognition element; assay preparation, optimization and application in human serum; cancer cell-lines preparation and application; data compilation; writing and editing the manuscript (original draft – Lead).

4.1 Quantum Dots as Nanolabels for Breast Cancer Biomarker HER2-ECD Analysis

Talanta 208 (2020) 120430



Author Contributions:

Maria Freitas (investigation: Equal; Methodology: Equal; Writing – original draft: Lead); Marta Neves (Methodology: Equal; Writing – review & editing: Supporting); Henri Nouws (Conceptualization: Lead; Funding acquisition: Equal; Methodology: Lead; Project administration: Equal; Supervision: Equal; Validation: Equal; Writing – review & editing: Lead); Cristina Delerue-Matos (Funding acquisition: Equal; Methodology: Equal; Supervision: Equal; Validation: Equal; Writing – review & editing: Supporting)

Highlights

- Detection of cancer biomarkers in biological fluids is useful for early diagnosis.
- An electrochemical immunosensor was developed for HER2-ECD.
- Quantum dots were used as detection label.
- The assay was selective towards the target biomarker.
- The assay was successfully tested in the analysis of human serum.

Talanta 208 (2020) 120430



Contents lists available at ScienceDirect

Talanta

journal homepage: www.elsevier.com/locate/talanta

Quantum dots as nanolabels for breast cancer biomarker HER2-ECD analysis in human serum



Maria Freitas, Marta M.P.S. Neves, Henri P.A. Nouws*, Cristina Delerue-Matos

REQUIMTE/LAQV, Instituto Superior de Engenharia do Porto, Politécnico do Porto, Rua Dr. António Bernardino de Almeida 431, 4200-072, Porto, Portugal

ARTICLE INFO

Keywords:

Electrochemical immunosensor
Breast cancer
HER2-ECD
Quantum dots
Screen-printed electrodes

ABSTRACT

Early detection of cancer increases the possibility for an adequate and successful treatment of the disease. Therefore, in this work, a disposable electrochemical immunosensor for the front-line detection of the ExtraCellular Domain of the Human Epidermal growth factor Receptor 2 (HER2-ECD), a breast cancer biomarker, in a simple and efficient manner is presented. Bare screen-printed carbon electrodes were selected as the transducer onto which a sandwich immunoassay was developed. The affinity process was detected through the use of an electroactive label, core/shell CdSe@ZnS Quantum Dots, by differential pulse anodic stripping voltammetry in a total time assay of 2 h, with an actual hands-on time of less than 30 min. The proposed immunosensor responded linearly to HER2-ECD concentration within a wide range (10–150 ng/mL), showing acceptable precision and a limit of detection (2.1 ng/mL, corresponding to a detected amount (sample volume = 40 µL) of 1.18 fmol) which is about 7 times lower than the established cut-off value (15 ng/mL). The usefulness of the developed methodology was tested through the analysis of spiked human serum samples. The reliability of the presented biosensor for the selective screening of HER2-ECD was confirmed by analysing another breast cancer biomarker (CA15-3) and several human serum proteins.

1. Introduction

The incidence of cancer has increased considerably worldwide, and affects the general population, resulting in significant mortality rates [1,2]. Screening and early detection allow appropriate treatments according to the stage of the disease and the availability of healthcare resources. Most European countries have national cancer screening programmes for colorectal [3,4], cervical [5,6] and breast [7,8] cancer. Breast cancer is an important public health concern with considerable impact for the patients, families and society as a whole. Its incidence and prevalence reveals slight differences among developed and developing countries, with the former presenting a global reduction in mortality due to a combination of improvements in prevention, detection and treatment [1,9]. In fact, some studies indicate that mortality rates have been diminishing in places where active screening programmes (e.g. mammography) were implemented [7–10]. Therefore, new analytical tools for the point-of-care (POC) detection of this disease at the early stages, as well as during its management and follow-up, are widely demanded. Moreover, the development of portable equipment for *in situ* breast cancer analysis could also be very useful in less developed regions, remote access areas or even for patients with reduced mobility.

The guidelines established by the European Group on Tumor Markers (EGTM) on the use of breast cancer biomarkers for decision-making regarding the treatments to be administered were recently updated. Despite the large number of new biomarkers that have been reported, only three are mandatory for all patients diagnosed with invasive breast cancer: oestrogen receptor (ER), progesterone receptor (PR) and human epidermal growth factor receptor 2 (HER2) [11]. The latter is established as an important diagnostic biomarker and is recommended for testing since this protein is overexpressed in 15–20% of primary invasive breast cancers and is related with the most aggressive phenotypes [12,13]. HER2 is a transmembrane protein located on the cell surface and has distinct domains: an extracellular domain (ECD), an intracellular tyrosine kinase domain and a transmembrane lipophilic segment. ECD can be cleaved by metalloproteases and released into the bloodstream. Consequently, HER2 can be measured in serum, which is key for the development of quantitative analytical strategies for breast cancer detection [14,15].

Currently, the two main types of tests accepted for the evaluation of HER2 overexpression in clinical use are immunohistochemistry and *in situ* hybridisation (ISH), which are not suited for POC diagnostics [11]. Hence, a considerable effort in the development of new alternative methodologies has been carried out. The use of “lab-on-a-chip” and

* Corresponding author.

E-mail address: han@isep.ipp.pt (H.P.A. Nouws).

<https://doi.org/10.1016/j.talanta.2019.120430>

Received 14 June 2019; Received in revised form 24 September 2019; Accepted 1 October 2019

Available online 03 October 2019

0039-9140/ © 2019 Elsevier B.V. All rights reserved.

biosensor technologies are currently providing remarkable tools for POC analysis. The possibility of miniaturization, portability, fast response and low cost are some of the electrochemical biosensors' features that make them attractive for the development of new analytical devices [16,17]. Electrochemical-based approaches for the detection of HER2-positive breast cancer have already been proposed. Different biosensing strategies were reported, which include nanomaterial-based sensing- and/or detection platforms [18–24], nanoelectrode ensembles (NEEs) [25], magnetic-based immunoassays [26,27], a sandwich-type immunoassay based on nanobodies [28], sensing strategies based on affibody/antibody recognition events [29], a MIP-based sensor [30], an impedimetric biosensor based on a zwitterionic hydrogel [31], an impedimetric immunosensor based on the use of single-chain fragment variable antibody fragments [32], a cellulase-linked sandwich assay [33], an inkjet-printed electrochemical platform [34], a polycytosine DNA-based immunosensor [35], and a microfluidic device based on a nanoshearing method [36]. While all of these methods have demonstrated suitable analytical performances, their application is still limited because of extensive and laborious protocols. The use of screen-printed electrodes (SPE) as the biosensor's transducer, without any surface modification prior to the functionalization with the biorecognition element, would considerably simplify the methodology. To date, only one electrochemical immunosensor for HER2 detection without prior modification of the electrode surface has been published [37]. In this work, a sandwich assay with enzymatic labelling allowed to achieve a low detection limit (4 ng/mL). However, a total assay time of 8 h revealed to be its major disadvantage because it is incompatible with a POC sensing strategy.

Nanoparticle-based signal amplification has attracted considerable interest in the development of electrochemical methods. Distinct signal amplification methodologies can be achieved using nanomaterials. Their application as labels can greatly improve the signal transduction and simplify the detection strategy. Quantum Dots (QDs) revealed to be promising candidates as such labels, since they can be conjugated to antibodies and other proteins [38–41]. In addition, they can be synthesized with different compositions or with distinct core-shell structures, which can be useful for multiplexed sensing. The commonly used QDs are composed of a CdS or CdSe core with an external shell to provide functional groups for bioreceptor immobilization with inert and biocompatible coatings [38–40]. Comparing to laborious enzymatic methodologies, the use of QDs eliminates the need for substrate addition, which can contribute to the reduction of the analysis time by applying a straightforward process consisting of: QD dissolution to release the metal ions, electrochemical deposition (preconcentration) of the released ions and a potential (stripping) scan to detect the deposited metal. The obtained electrochemical signal can then quantitatively be related to the analyte concentration. Furthermore, working with electroactive labels also surpasses thermal instability aspects inherent to the nature of enzymes, the main difficulties in their use as labels [42,43].

To the best of our knowledge, this is the first electrochemical immunosensing strategy based on QDs as electrochemical label for *in situ* detection of HER2-ECD.

2. Material and methods

2.1. Apparatus and electrodes

Electrochemical measurements were carried out with a potentiostat/galvanostat (Autolab PGSTAT204, Metrohm Autolab) controlled by the NOVA software package v.1.10 (Metrohm Autolab). Disposable screen-printed carbon electrodes (with a 4-mm working electrode, a silver pseudoreference electrode and a carbon counter electrode, all made of conducting ink (SPCE, DRP-110)) as well the specific connector to interface the electrodes (DRP-CAC) were supplied by Metrohm DropSens.

2.2. Reagents and solutions

Rabbit IgG monoclonal anti-human-HER2-ECD (clone 002) antibody (capture antibody – Ab-C), mouse IgG2a monoclonal biotinylated anti-human-HER2-ECD (clone 8B5DAC1) antibody (detection antibody – Ab-D), and a recombinant human HER2/ErBb2 protein (antigen) were obtained from Sino Biological Inc. Qdot® 655 streptavidin conjugate (QD-Strep) was purchased from Invitrogen - ThermoFisher Scientific. Bismuth ICP standard, acetic acid and sodium hydroxide were acquired from Merck. Human serum (from male AB clotted whole blood), albumin from bovine serum (BSA), nitric acid (HNO₃) and tris(hydroxymethyl)aminomethane (Tris) were obtained from Sigma-Aldrich.

Working solutions of BSA, the antibodies, antigen and QD-Strep were prepared in 0.1 M Tris-HNO₃ pH 7.2 buffer (Tris Buffer). The Bi(III) solution (1 mg/L) was prepared in acetate buffer (0.1 M, pH 4.5). Ultra-pure water was obtained from a Millipore (Simplicity 185) water purification system. Buffers and solutions were prepared daily.

The male human serum was stored at –20 °C. Serum samples (diluted 1:1 in Tris buffer) were spiked with HER2-ECD at different concentrations and analysed without further treatments. To evaluate the selectivity of the sensor, non-target proteins (possible interferents) were added to the serum solution.

2.3. Immunosensor development and detection strategy

Scheme 1 elucidates the immunosensor's construction and detection strategy according to the following optimized protocol:

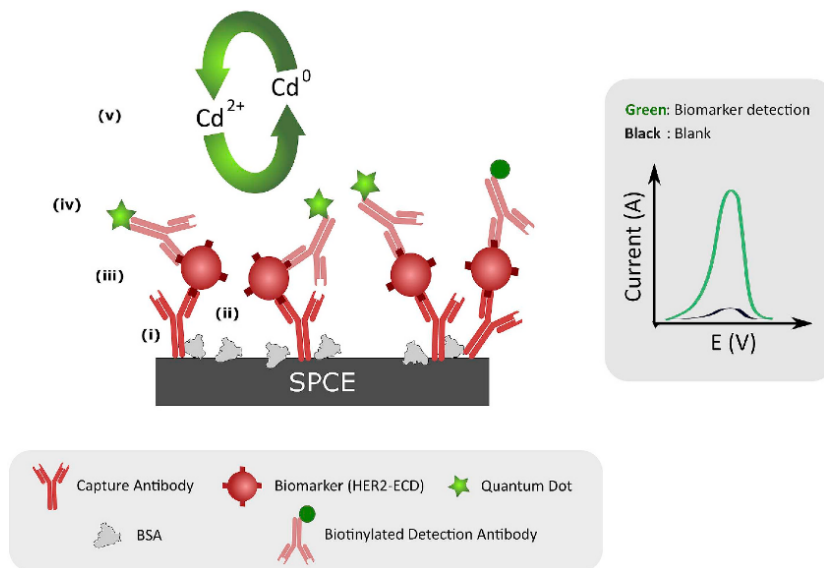
- (i) the Ab-C was immobilized on the SPCE surface by drop-casting a 10- μ L aliquot of a 25- μ g/mL Ab-C solution, which was left overnight in a humidified chamber at 4 °C. Then, the SPCE was washed with Tris buffer before the (ii) incubation with BSA ((2% (m/V), 40 μ L), for 30 min. After the free surface sites were efficiently blocked, (iii) 40 μ L of a previously prepared mixture (10 min before use) containing the Ab-D (2 μ g/mL), HER2-ECD and BSA 0.5% (m/V), was placed on the SPCE for 60 min. Afterwards, the washing step was repeated with Tris buffer and (iv) a 30- μ L aliquot of QDs-Strep solution (5 nM, containing BSA 0.5% (m/V)) was placed on the sensor surface and left to incubate during 30 min.

Prior to the measurements, a last washing step was performed with ultra-pure water. The analytical signal was obtained by differential pulse anodic stripping voltammetry (DPASV) based on a procedure described elsewhere [44]. Briefly, (v) 5 μ L of HCl (1.0 M) was added to fully cover the working electrode and to release Cd²⁺ from the QDs. This was followed by the addition of 40 μ L of an acetate buffer (0.1 M, pH 4.5) containing Bi(III) (1.0 mg/L). To activate the working electrode, a constant potential of +1.00 V was applied during 60 s. Then, the released cadmium ions were pre-concentrated by applying a potential of –1.10 V for 300 s. At the same time a bismuth film was formed. Finally, the potential was swept from –1.0 V to –0.7 V to strip the cadmium into the solution, recording the analytical signal (DPV parameters: pulse amplitude: 0.05 V; step potential: 0.01 V; modulation time: 0.01 s; interval time: 0.1 s).

3. Results and discussion

3.1. Optimization of experimental conditions

Non-invasive analysis of cancer biomarkers can be performed in biological fluids such as serum. Bearing in mind the complex matrices of biological samples, it is mandatory to ensure that background interferences, due to the nonspecific adsorption of biomolecules, are minimized. Hence, the blockage of nonspecific adsorptions on the sensor platform after the modification with the Ab-C is of great importance for efficient and specific biomarker detection. The Ab-C



Scheme 1. Representation of the immunosensor construction and detection strategy.

concentration (25 $\mu\text{g/mL}$) was selected in accordance with our previous study [18] and was used throughout the work. Casein (2% m/V) and bovine serum albumin (BSA) (2% m/V) were the two tested blocking agents. When casein was used as the blocking agent no electrochemical signal was obtained. This was possibly due to an excessive blocking effect (Fig. S1 I). When BSA was used this behaviour was not verified. Nevertheless, and as can be seen in Fig. S1 (II), the difference between the blank signal and the signal obtained for the analyte was very low. Thus, BSA was added in other steps of the assay: (III) BSA 0.5% (m/V) in both the HER2-ECD and the Ab-D solutions and (IV) BSA 0.5% (m/V) in the HER2-ECD- and 1% (m/V) in the Ab-D solution. The obtained peak current intensities (i_p) shown in Fig. S1 demonstrated that alternative III efficiently blocked nonspecific adsorption, leading to the highest signal-to-blank ratio.

Promising new approaches to improve the detection strategy in the development of electrochemical immunosensors have been aligned with nanotechnology through the use of nanolabels, such as QDs. Moreover, the functionalization of these nanomaterials with biomolecules such as streptavidin allows a strong binding to biotinylated antibodies. To optimize the conjugation between the biotinylated Ab-D and the QD-streptavidin conjugate (QD-Strep), different concentrations of Ab-D were tested (1, 2 and 4 $\mu\text{g/mL}$). The obtained i_p values are presented in Fig. 1, and although this value increased significantly between 1 and 2 $\mu\text{g/mL}$, only a slightly increase was observed between 2 and 4 $\mu\text{g/mL}$, which indicates that the latter Ab-D concentration is close to saturation. Therefore, 2 $\mu\text{g/mL}$ was chosen as the best compromise between the Ab-D concentration and the signal-to-blank ratio.

In this work QDs were used to enhance the electrochemical detection, to simplify the methodology and to reduce the assay time. Thus, after the optimization of the surface blocking and the antibodies' concentrations, three different QD concentrations were tested: 5, 10 and 20 nM (in terms of QDs) (Fig. 2A). The i_p increased with the increase of the QD concentration both in the absence and presence of the analyte (50 ng/mL). Accordingly, 5 nM was selected because it provided the highest signal-to-blank ratio. BSA 0.5% (m/V) was added to the QDs solution to further minimize nonspecific adsorption, which also led to a much higher signal-to-blank ratio and a better precision of the results (Fig. 2B).

Regarding the optimization of the assay, several formats were evaluated: step-by-step assays (A, B, C, D) and combined assays (E, F, G). The tested alternatives were: (A) antigen 60 min, Ab-D 60 min, QD

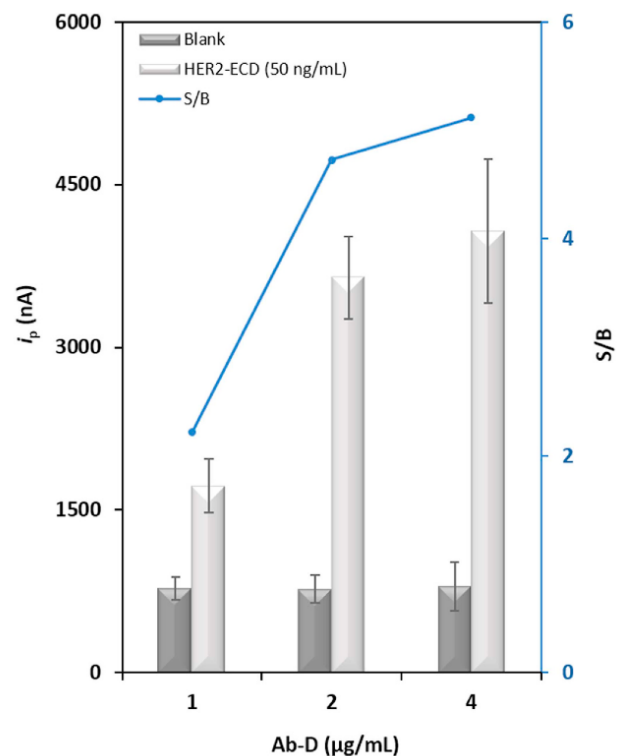


Fig. 1. Optimization of Ab-D concentration (1; 2 and 4 $\mu\text{g/mL}$). Experimental conditions: BSA (2% (m/V)), Ab-C 25 $\mu\text{g/mL}$, HER2-ECD (0 and 50 ng/mL), QD 5 nM.

60 min (control assay, used during optimization studies), (B) antigen 60 min, Ab-D 60 min, QD 30 min, (C) antigen 30 min, Ab-D 60 min, QD 30 min, (D) antigen 60 min, Ab-D 30 min, QD 30 min; and the combined steps, which involve the pre-incubation of reagents: (E) antigen + Ab-D 60 min, QD 60 min, (F) antigen + Ab-D 60 min, QD 30 min, (G) antigen 60 min, Ab-D + QD 60 min (Fig. 3). The alternatives B and F provided the best signal-to-blank ratios. In both assays,

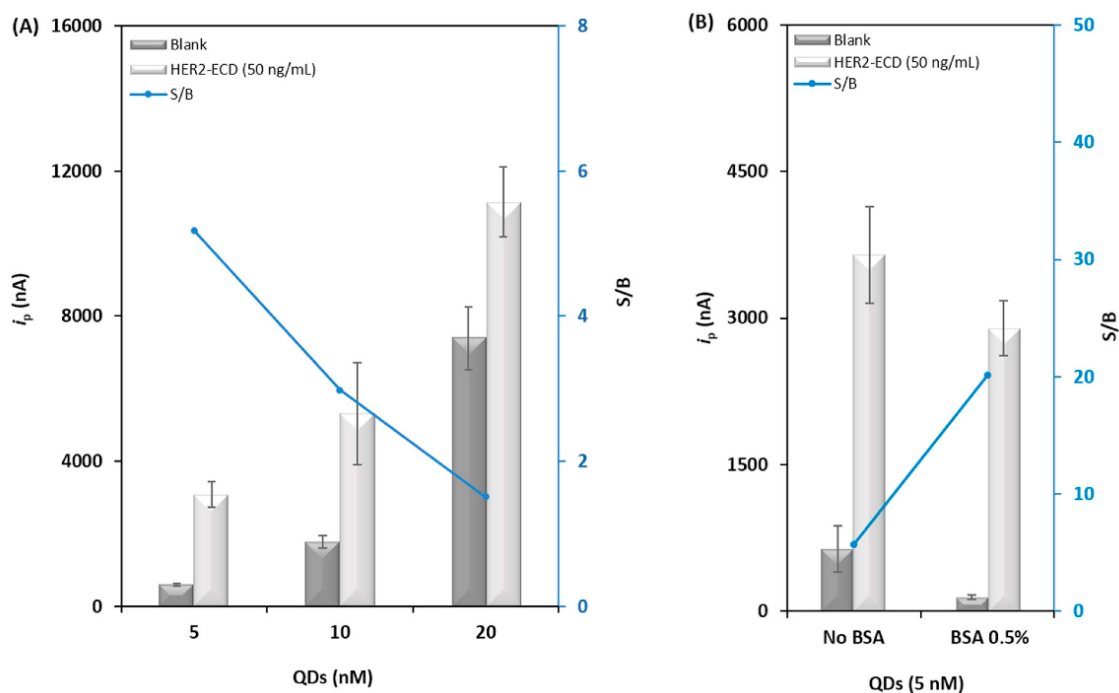


Fig. 2. (A) Optimization of QDs concentration (5; 10 and 20 nM) and (B) Current intensities obtained with QDs 5 nM in the absence and in the presence of BSA (0.5% (m/V)) in the solution. Experimental conditions: BSA (2% (m/V)), Ab-C (25 µg/mL), HER2-ECD (0 and 50 ng/mL), Ab-D (2 µg/mL).

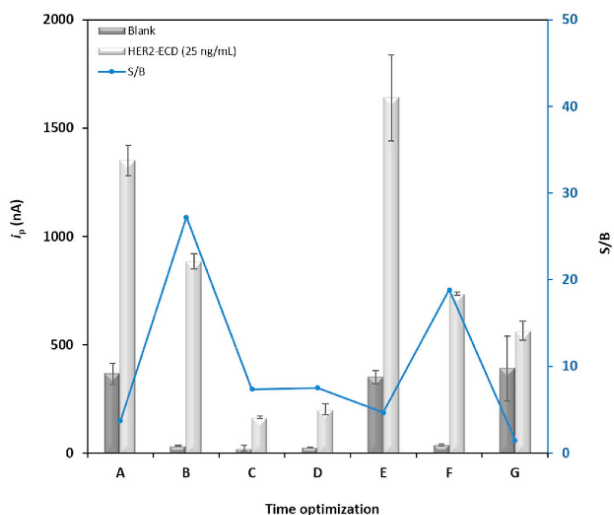


Fig. 3. Influence of the incubation time for step-by-step assay (A, B, C and D), and joining steps assay: HER2-ECD + Ab-D (E and F) and Ab-D + QDs (G). Experimental conditions: BSA (2% (m/V)), Ab-C (25 µg/mL), HER2-ECD (25 ng/mL), Ab-D (2 µg/mL), QDs (5 nM + BSA 0.5% (m/V)).

the QD incubation time was 30 min, which resulted in a reduction of both the blank and analytical signal and an increase of the signal-to-blank ratio. The sensor's response to increasing concentrations of HER2-ECD was assessed for both alternatives (B and F), obtaining similar sensitivities. Therefore, alternative F was chosen to proceed with the studies since the total time assay (120 min) was 60 min shorter than the one of alternative B. The combination of two steps not only allowed the increase of the precision of the results but also led to a more user-friendly assay.

3.2. Analytical performance for HER2-ECD determination in human serum

The analytical performance of the developed immunosensor was tested using the previous optimized parameters. Initially, distinct HER2-ECD concentrations, in buffer solution, were analysed and a linear range was established between 5 and 150 ng/mL (Fig. S2). Then, male human serum samples (diluted 1:1 in Tris buffer) were spiked with HER2-ECD from 5.0 to 400 ng/mL. A linear relationship between the analyte concentration and i_p was found between 10 and 150 ng/mL, according to the following equation: $i_p = (5.07 \pm 0.14) [\text{HER2-ECD}] + (18.4 \pm 11.8)$, $r = 0.9989$, $n = 5$. The corresponding calibration plot as well typical voltammograms within the linear range are presented in Fig. 4. When comparing the calibration plots constructed in buffer solution and serum, a clear matrix effect was observed; the slope of the calibration plot in serum was 5 times lower than the slope obtained with the measurements in buffer. This could be due to human serum albumin, which is the most abundant protein in human blood, and globulins, especially immunoglobulins G (IgG) [45,46]. To avoid excessive blocking of the transducer's surface, BSA was not added to the antigen - Ab-D solution. The limits of detection (LOD) and quantification (LOQ) were calculated as the concentration corresponding to $3 \times S_{\text{blank}}/m$ for the LOD and $10 \times S_{\text{blank}}/m$ for the LOQ (S_{blank} : standard deviation of the blank signal; m : slope of the calibration plot). The obtained limit of detection (2.1 ng/mL) was far below the cut-off value established for HER2-ECD (15 ng/mL), which corroborates the adequacy and practical utility of the developed sensor. Table 1 summarizes the figures of merit of the developed sensor.

3.3. Selectivity, stability, precision and recovery studies

The selectivity of the immunosensor was tested through the analysis of other proteins that could be found in serum. In this study, the sensor's response towards cancer antigen 15-3, another breast cancer protein (CA15-3, 50 U/mL) and cystatin C, a biomarker of kidney function (550 ng/mL) was tested. Blank and HER2-ECD (50 ng/mL) solutions

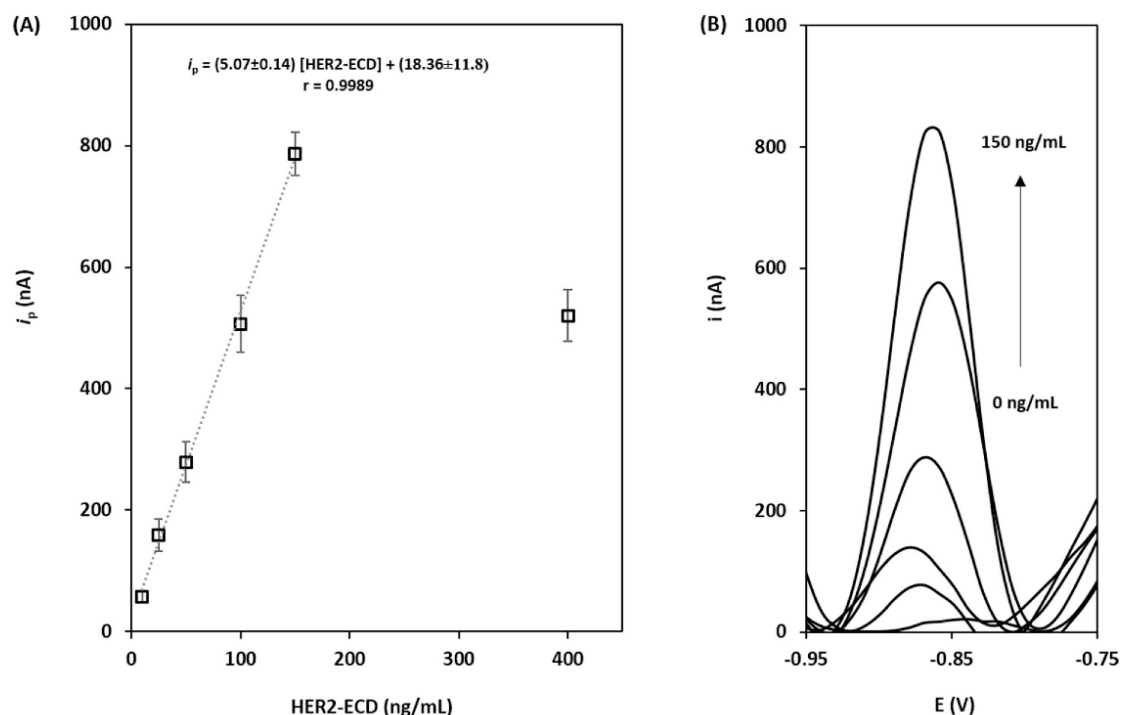


Fig. 4. (A) Calibration plot using the developed immunosensor in the presence of growing concentrations of HER2-ECD in human serum and (B) examples of typical differential pulse voltammograms obtained within the established linear range (0, 10, 25, 50, 100 and 150 ng/mL). Experimental conditions: Ab-capture: 25 $\mu\text{g/mL}$, BSA: 2% (m/V), Ab-D: 2 $\mu\text{g/mL}$, QDs: 5 nM with addition of BSA 0.5% (m/V).

Table 1

Figures of merit of the developed biosensor for the analysis of the cancer biomarker HER2-ECD in Human Serum samples.

Figure of merit	
Concentration interval (ng/mL)	10–150
Correlation coefficient (r)	0.9989
Slope (m) (nA/(ng/mL))	5.07
Standard deviation of the slope (S_m) (nA/(ng/mL))	0.14
Intercept (b) (nA)	18.4
Standard deviation of the intercept (S_b) (nA)	11.8
Standard deviation of the linear regression ($S_{y/x}$)	16.1
Standard deviation of the method ($S_{2\sigma}$)	3.2
Coefficient of variation of the method (V_{x0}) (%)	5.6
Limit of detection (LOD) (ng/mL)	2.1
Limit of quantification (LOQ) (ng/mL)	7.1

were also assayed for comparison purposes. All the proteins were added to male human serum and their concentrations were chosen based on the values that can be expected in real clinical environments. The obtained i_p values are presented in Fig. 5. In comparison to the analytical signal obtained for HER2-ECD, the other proteins did not show a significant response; the obtained i_p values were very similar to the blank signal, which confirmed the sensor's selectivity towards HER2-ECD.

The stability of the immunosensor was also studied. The as-prepared sensor was stored at 4 °C and measurements were performed during a month (Fig. S3). It was concluded that the sensor was stable for up to a week. So, the sensing phase of the proposed biosensor should be prepared on a weekly basis to guarantee a sensitive analysis.

The intermediate precision and the reproducibility of the results were assessed by analyzing a 50-ng/mL HER2-ECD solution (in human serum) on the same day and on three different days, obtaining relative standard deviation (RSD) of 7.1% and 4.9%, respectively, which indicates that the optimized sensor provided precise results.

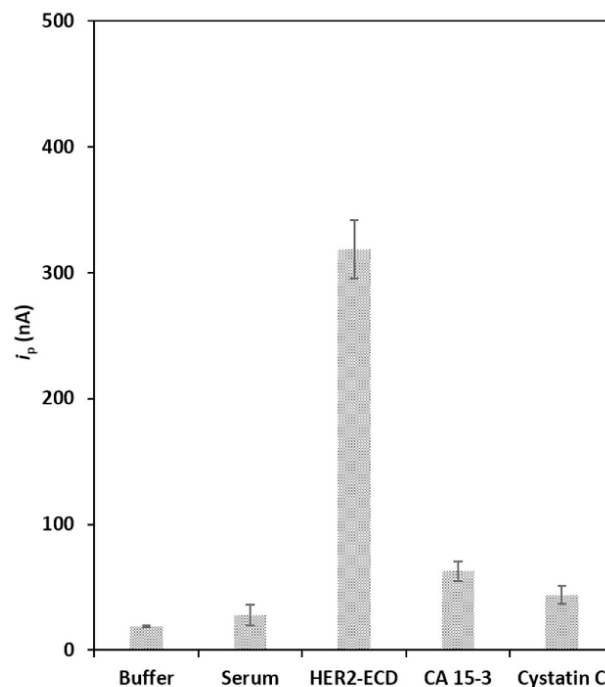


Fig. 5. Evaluation of the selectivity of the HER2-ECD sensor against other serum proteins. Experimental conditions: Ab-C: 25 $\mu\text{g/mL}$, BSA: 2% (m/V), Ab-D: 2 $\mu\text{g/mL}$, QDs: 5 nM with addition of BSA 0.5% (m/V). Serum proteins concentration: HER2-ECD: 50 ng/mL, CA 15-3: 50 U/mL, Cystatin C: 550 ng/mL.

Table 2
Summary of experimental parameters of electrochemical immunoassay-based procedures for HER2 analysis.

Breast cancer analyte	Sensing surface		Transducer preparation time ^a	Modification with the biorecognition element ^b	Long-term stability	Label	Technique	Detection	Assay time	LOD	Sample	Ref
	Transducer	Transducer										
HER2-ECD	Bare SPCE		–	~12 h	7 days	CdSe@ZnS QDs	DPV	Cadmium	2 h	2.1 ng/mL	Spiked human serum	[118]
HER2-ECD	SPCE/MWCNT-AuNP		~15 min	~12 h	n.d.	AP	LSV	Silver	2 h	0.16 ng/mL	Spiked human serum	[19]
SK-BR-3	FTO/NFG/AgNP/PANI		> 4 h	~12 h	45 days	n.a.	DPV	[Fe(CN) ₆] ^{3-/4-}	30 min	2 cells/mL	Whole blood	[20]
HER2	GCE/Fe ₃ O ₄ -APTMS		> 3 h	2 h	10 days	Hydrazin	DPV	Silver	2 h	2.0 × 10 ⁻⁵ ng/mL	Patient serum	[21]
HER2	CILE-MWCNT/AuNP		> 30 h	6 h	n.d.	n.a.	EIS	[Fe(CN) ₆] ^{3-/4-}	35 min	7.2 ng/mL	Patient serum	[22]
HER2-ECD	SPCE/AuNP		~10 min	~12 h	n.d.	AP	LSV	Silver	2 h	4.4 ng/mL	Spiked human serum	[23]
HER2	AuE/AuNP-MPA-Cys		> 22 h	~12 h	3 weeks	n.a.	DPV	[Fe(CN) ₆] ^{3-/4-}	30 min	0.995 pg/mL	Patient serum	[24]
HER2	GCE/poly-DPB(AuNP)		> 4 h	~12 h	n.d.	Hydrazin	SWSV	Silver	1 h	0.037 pg/mL	Cancer cells	[25]
HER2	NEEs		n.d.	2 h	n.d.	HRP	CV	MB	7 h	40 ng/mL	Cell lysates	[26]
HER2	SPCE/MBs		~15 min	40 min	10 days	AP	DPV	1-NP	2 h	6.0 ng/mL	Patient serum	[27]
Erbb2	SPCE/MBs		~40 min	1 h	n.d.	HRP	Amperometry	HQ	1 h	26 pg/mL	Patient serum and cell lysates	[28]
HER2	SPE		1 h	1 h	3 weeks	HRP	Amperometry	HQ	22 min	1 µg/mL	Cell lysates	[29]
HER2	8 × SPE/Strep-MBs or ProA-MBs		~15 min	~12 h	1 week	AP	DPV	1-NP	2 h	1.8, 2.6 and 3.4 ng/mL	Spiked human serum	[29]

1-NP – 1-naphthol; AgNP – silver nanoparticles; AP – alkaline phosphatase; APTMS – (3-Aminopropyl)triethoxysilane; AuE – gold electrode; AuNPs – gold nanoparticles; Cys – cysteamine; CV – cyclic voltammetry; CILE – carbon ionic liquid electrode; FTO – fluorine doped tin oxide; GCE – glassy carbon electrode; DPB – 2,5-bis(2-thienyl)-1H-pyrylo-1-(p-benzoic acid); DPV – differential pulse voltammetry; HER2 – human epidermal growth factor receptor 2; HRP – horseradish peroxidase; HQ – hydroquinone; LSV – linear sweep voltammetry; MBs – magnetic beads; MB – methylene blue; MPA – 3-mercaptopropionic acid; MWCNT – multilayered carbon nanotube; NEEs – nanoelectrode ensembles; NFG – nitrogen-doped graphene; n.d. – no data; n.a. – not applicable; PANI – polyaniline; QDs – quantum dots; SPCE – screen-printed carbon electrode; SWASV – square wave anodic stripping voltammetry; SWV – Square wave voltammetry.

^a Overnight incubations were considered as a 12-h period for comparison purposes.

M. Freitas, et al.

Talanta 208 (2020) 120430

To demonstrate the potential clinical utility of the immunosensor, recovery studies were performed using serum samples spiked with three different HER2-ECD concentrations: 25, 75 and 125 ng/mL. The average recoveries were found to be 105.6, 105.0 and 103.5% with RSDs of 5.6, 5.0 and 3.5%, respectively (n = 3). This indicates that the developed sensor provided both precise and accurate results.

3.4. Comparison with previous reported electrochemical immunosensors and immunoassays

The proposed immunosensor was compared with previously published immunosensors and immunoassays with electrochemical detection for HER2 analysis. As can be seen in Table 2, distinct configurations with comparable performances were described. The immunosensor developed in this work has a competitive assay time that is only surpassed by the label-free sensors [19,21,23] and by three works in which an enzymatic label was employed [24,27,28]. However, some of these shorter assay times are preceded by complex modifications of the electrode surface, as well as time-consuming procedures, which appears as a major drawback [19,21,23,24]. Moreover, the work developed by Patris et al. presented a good compromise between assay time and LOD, considering the complexity of the sample (cell lysates) [28]. The electrochemical magneto-immunoassay described by Eletxigerra et al. [27] demonstrated an exceptional LOD and assay time. Nevertheless, the dependence on an enzymatic substrate and the production of a substantial amount of waste, due to the volume of mediator needed for the measurement step, are the major drawbacks of the reported work. The remaining works did not improve the assay time of our assay. Accordingly, the immunosensor developed in this work presents a user-friendly straightforward 3-step assay protocol, within a highly competitive assay time, and achieving a low LOD (< reference cut-off value).

Furthermore, an additional overview of the use of metallic and carbon-based QDs for the immunosensing of different breast cancer biomarkers is summarized in Table SI 1. In some works, the QDs were used as detection label while in others they were employed in the modification of the transducer surface. Most of these works imply laborious protocols [38,40,47,48] and longer assay times [41,49]. Additionally, our immunosensor is the first one that employs QDs for the development of an electrochemical immunosensor for HER2-ECD.

4. Conclusions

A novel and efficient electrochemical immunosensor for the analysis of the breast cancer biomarker HER2-ECD, with a total time assay of 2 h, was developed. This work highlights the simplicity of the assay, with an actual hands-on-time of less than 30 min, without resorting to laborious electrode surface modifications. An electroactive QD label was employed and a limit of detection of 2.1 ng/mL was achieved, corresponding to the detection of 1.18 fmol of the analyte (sample volume = 40 µL). The analytical performance was tested in spiked human serum samples, demonstrating an excellent performance in a wide linear range with a high sensitivity, stability, precision and accuracy. The applicability and selectivity of the proposed methodology was tested and confirmed through the analysis of distinct serum proteins in human serum.

Acknowledgements

The authors are grateful for the financial support from the Fundação para a Ciência e a Tecnologia (FCT)/the Ministério da Ciência, Tecnologia e Ensino Superior (MCTES) through national funds (Portugal) (UID/QUI/50006/2019). This work was also supported by the European Union through projects Norte-01-0145-FEDER-000024 and Norte-01-0145-FEDER-000011, co-funded by FEDER in the scope of CCDR-N and NORTE2020 Partnership Agreement. Maria Freitas is

financially supported by FCT through the doctoral research Grant financed by fellowship SFRH/BD/111942/2015.

Appendix A. Supplementary data

Supplementary data to this article can be found online at <https://doi.org/10.1016/j.talanta.2019.120430>.

References

- [1] F. Bray, J. Ferlay, I. Soerjomataram, R.L. Siegel, L.A. Torre, A. Jemal, Global cancer statistics 2018: GLOBOCAN estimates of incidence and mortality worldwide for 36 cancers in 185 countries, *CA Cancer J. Clin.* 68 (2018) 394–424, <https://doi.org/10.3322/caac.21492>.
- [2] J. Ferlay, I. Soerjomataram, R. Dikshit, S. Eser, C. Mathers, M. Rebelo, D.M. Parkin, D. Forman, F. Bray, Cancer incidence and mortality worldwide: sources, methods and major patterns in GLOBOCAN 2012, *Int. J. Cancer* 136 (2015) E359–E386, <https://doi.org/10.1002/ijc.29210>.
- [3] E. Altobelli, A. Lattanzi, R. Paduano, G. Varassi, F. di Orio, Colorectal cancer prevention in Europe: burden of disease and status of screening programs, *Prev. Med.* 62 (2014) 132–141, <https://doi.org/10.1016/j.ypmed.2014.02.010>.
- [4] E. Altobelli, F. D'Aloisio, P.M. Angeletti, Colorectal cancer screening in countries of European Council outside of the EU-28, *World J. Gastroenterol.* 22 (2016) 4946–4957, <https://doi.org/10.3748/wjg.v22.i20.4946>.
- [5] G. Ronco, J. Dillner, K.M. Elfström, S. Tunesi, P.J.F. Snijders, M. Arbyn, H. Kitchener, N. Segnan, C. Gilham, P. Giorgi-Rossi, J. Berkhof, J. Peto, C.J.L.M. Meijer, J. Cuzick, M. Zappa, F. Carozzi, M. Confortini, P. Dalla Palma, M. Zorzi, A. Del Mistro, A. Gillio-Tos, C. Naldoni, D. Rijkaart, F. Van Kemenade, N. Bulkmans, D. Heideman, R. Rozendaal, G. Kenter, M. Almonte, C. Roberts, M. Desai, A. Sargent, W. Ryd, P. Nauciler, Efficacy of HPV-based screening for prevention of invasive cervical cancer: follow-up of four European randomised controlled trials, *Lancet* 383 (2014) 524–532, [https://doi.org/10.1016/S0140-6736\(13\)62218-7](https://doi.org/10.1016/S0140-6736(13)62218-7).
- [6] E. Altobelli, A. Lattanzi, Cervical carcinoma in the European Union, *Int. J. Gynecol. Cancer* 25 (2015) 474–483, <https://doi.org/10.1097/igc.0000000000000374>.
- [7] E. Altobelli, L. Rapacchieta, P.M. Angeletti, L. Barbante, F.V. Profeta, R. Fagnano, Breast cancer screening programmes across the WHO European region: differences among countries based on national income level, *Int. J. Environ. Res. Public Health* 14 (2017), <https://doi.org/10.3390/ijerph14040452>.
- [8] International Agency for Research on Cancer, Cancer Screening in the European Union: Report on the Implementation of the Council Recommendation on Cancer Screening, (2017).
- [9] J. Ferlay, M. Colombet, I. Soerjomataram, T. Dyba, G. Randi, M. Bettio, A. Gavin, O. Visser, F. Bray, Cancer incidence and mortality patterns in Europe: estimates for 40 countries and 25 major cancers in 2018, *Eur. J. Cancer* 103 (2018) 356–387, <https://doi.org/10.1016/j.ejca.2018.07.005>.
- [10] M.J.M. Broeders, P. Allgood, S.W. Duffy, S. Hofvind, I.D. Nagtegaal, E. Paci, S.M. Moss, L. Bucci, The impact of mammography screening programmes on incidence of advanced breast cancer in Europe: a literature review, *BMC Canc.* 18 (2018) 860, <https://doi.org/10.1186/s12885-018-4666-1>.
- [11] M.J. Duffy, N. Harbeck, M. Nap, R. Molina, A. Nicolini, E. Senkus, F. Cardoso, Clinical use of biomarkers in breast cancer: updated guidelines from the European group on tumor markers (EGTM), *Eur. J. Cancer* 75 (2017) 284–298, <https://doi.org/10.1016/j.ejca.2017.01.017>.
- [12] A.C. Wolff, M. Elizabeth, H. Hammond, K.H. Allison, B.E. Harvey, P.B. Mangu, J.M.S. Bartlett, M. Bilous, I.O. Ellis, P. Fitzgibbons, W. Hanna, R.B. Jenkins, M.F. Press, P.A. Spears, G.H. Vance, G. Viale, L.M. Mcshane, M. Dowssett, Human epidermal growth factor receptor 2 testing in breast cancer: American society of clinical oncology/college of American pathologists clinical practice guideline focused update, *J. Clin. Oncol.* 36 (2018) 2105–2122, <https://doi.org/10.1200/JCO.2018.01.0008>.
- [13] F.B. De Abreu, G.N. Schwartz, W.A. Wells, G.J. Tsongalis, Personalized therapy for breast cancer, *Clin. Genet.* 86 (2014) 62–67, <https://doi.org/10.1111/cge.12381>.
- [14] C. Tse, A.S. Gauchez, W. Jacot, P.J. Lamy, HER2 shedding and serum HER2 extracellular domain: biology and clinical utility in breast cancer, *Cancer Treat Rev.* 38 (2012) 133–142, <https://doi.org/10.1016/j.ctrv.2011.03.008>.
- [15] A. Perrier, J. Gligorov, G. Lefèvre, M. Boissan, The extracellular domain of Her2 in serum as a biomarker of breast cancer, *Lab. Invest.* 98 (2018) 696–707, <https://doi.org/10.1038/s41374-018-0033-8>.
- [16] M.A. Huaman, C.T. Fiske, T.F. Jones, J. Warkentin, B.E. Shepherd, F. Maruri, T.R. Sterling, Exercise altered the skeletal muscle MicroRNAs and gene expression profiles in burn rats with hindlimb unloading, *J. Burn Care Res.* 143 (2015) 951–959, <https://doi.org/10.1017/S0950268814002131.Tuberculosis>.
- [17] I.E. Tothill, Biosensors for cancer markers diagnosis, *Semin. Cell Dev. Biol.* 20 (2009) 55–62, <https://doi.org/10.1016/j.semcdb.2009.01.015>.
- [18] M. Freitas, H.P.A. Nouns, C. Delerue-Matos, Electrochemical sensing platforms for HER2-ECD breast cancer biomarker detection, *Electroanalysis* 31 (2019) 121–128, <https://doi.org/10.1002/elan.201800537>.
- [19] R. Salahandish, A. Ghaffarinejad, S.M. Naghib, K. Majidzadeh-A, H. Zargartalebi, A. Sanati-Nezhad, Nano-biosensor for highly sensitive detection of HER2 positive breast cancer, *Biosens. Bioelectron.* 117 (2018) 104–111, <https://doi.org/10.1016/j.bios.2018.05.043>.
- [20] M. Shamsipur, M. Emami, L. Farzin, R. Saber, A sandwich-type electrochemical immunosensor based on in situ silver deposition for determination of serum level of

- HER2 in breast cancer patients, *Biosens. Bioelectron.* 103 (2018) 54–61, <https://doi.org/10.1016/j.bios.2017.12.022>.
- [21] E. Arkan, R. Saber, Z. Karimi, M. Shamsipur, A novel antibody-antigen based impedimetric immunosensor for low level detection of HER2 in serum samples of breast cancer patients via modification of a gold nanoparticles decorated multiwall carbon nanotube-ionic liquid electrode, *Anal. Chim. Acta* 874 (2015) 66–74, <https://doi.org/10.1016/j.aca.2015.03.022>.
- [22] R.C.B. Marques, S. Viswanathan, H.P.A. Nows, C. Delerue-Matos, M.B. González-García, Electrochemical immunosensor for the analysis of the breast cancer biomarker HER2 ECD, *Talanta* 129 (2014) 594–599, <https://doi.org/10.1016/j.talanta.2014.06.035>.
- [23] M. Emami, M. Shamsipur, R. Saber, R. Iradjirad, An electrochemical immunosensor for detection of a breast cancer biomarker based on antiHER2-iron oxide nanoparticle bioconjugates, *Analyst* 139 (2014) 2858–2866, <https://doi.org/10.1039/c4an00183d>.
- [24] Y. Zhu, P. Chandra, Y.B. Shim, Ultrasensitive and selective electrochemical diagnosis of breast cancer based on a hydrazine-Au nanoparticle-aptamer bioconjugate, *Anal. Chem.* 85 (2013) 1058–1064, <https://doi.org/10.1021/ac302923k>.
- [25] S.P. Mucelli, M. Zamuner, M. Tormen, G. Stanta, P. Ugo, Nanoelectrode ensembles as recognition platform for electrochemical immunosensors, *Biosens. Bioelectron.* 23 (2008) 1900–1903, <https://doi.org/10.1016/j.bios.2008.02.027>.
- [26] Q.A.M. Al-Khafaji, M. Harris, S. Tombelli, S. Laschi, A.P.F. Turner, M. Mascini, G. Murrizza, An electrochemical immunoassay for HER2 detection, *Electroanalysis* 24 (2012) 735–742, <https://doi.org/10.1002/elan.201100501>.
- [27] U. Eletxigerra, J. Martínez-Perdiguero, S. Merino, R. Barderas, R.M. Torrente-Rodríguez, R. Villalonga, J.M. Pingarrón, S. Campuzano, Amperometric magnetite immunosensor for ErbB2 breast cancer biomarker determination in human serum, cell lysates and intact breast cancer cells, *Biosens. Bioelectron.* 70 (2015) 34–41, <https://doi.org/10.1016/j.bios.2015.03.017>.
- [28] S. Patris, P. De Pauw, M. Vandepuit, J. Huet, P. Van Antwerpen, S. Muyldermans, J.M. Kauffmann, Nanoimmunoassay onto a screen printed electrode for HER2 breast cancer biomarker determination, *Talanta* 130 (2014) 164–170, <https://doi.org/10.1016/j.talanta.2014.06.069>.
- [29] H. Ilkhani, A. Ravalli, G. Murrizza, Design of an antibody-based recognition strategy for human epidermal growth factor receptor 2 (HER2) detection by electrochemical biosensors, *Chemosensors* 4 (2016) 23, <https://doi.org/10.3390/chemosensors4040023>.
- [30] J.G. Pacheco, P. Rebelo, M. Freitas, H.P.A. Nows, C. Delerue-Matos, Breast cancer biomarker (HER2-ECD) detection using a molecularly imprinted electrochemical sensor, *Sens. Actuators B Chem.* 273 (2018) 1008–1014, <https://doi.org/10.1016/j.snb.2018.06.113>.
- [31] E. Chocholova, T. Bertok, L. Lorencova, A. Holazova, P. Farkas, A. Vikartovska, V. Bella, D. Velicova, P. Kasak, A.A. Eckstein, J. Mosnacek, D. Hasko, J. Tkac, Advanced antifouling zwitterionic layer based impedimetric HER2 biosensing in human serum: glycoprofiling as a novel approach for breast cancer diagnostics, *Sens. Actuators B Chem.* 272 (2018) 626–633, <https://doi.org/10.1016/j.snb.2018.07.029>.
- [32] S. Sharma, J. Zapatero-Rodríguez, R. Saxena, R. O'Kennedy, S. Srivastava, Ultrasensitive direct impedimetric immunosensor for detection of serum HER2, *Biosens. Bioelectron.* 106 (2018) 78–85, <https://doi.org/10.1016/j.bios.2018.01.056>.
- [33] K. Malecka, D. Pankratov, E.E. Ferapontova, Femtomolar electroanalysis of a breast cancer biomarker HER-2/neu protein in human serum by the cellulase-linked sandwich assay on magnetic beads, *Anal. Chim. Acta* (2019), <https://doi.org/10.1016/j.aca.2019.05.052>.
- [34] S. Carvajal, S.N. Fera, A.L. Jones, T.A. Baldo, I.M. Mosa, J.F. Rusling, C.E. Krause, Disposable inkjet-printed electrochemical platform for detection of clinically relevant HER-2 breast cancer biomarker, *Biosens. Bioelectron.* 104 (2018) 158–162, <https://doi.org/10.1016/j.bios.2018.01.003>.
- [35] X. Li, C. Shen, M. Yang, A. Rasooly, Polycytosine DNA electric-current-generated immunosensor for electrochemical detection of human epidermal growth factor receptor 2 (HER2), *Anal. Chem.* 90 (2018) 4764–4769, <https://doi.org/10.1021/acs.analchem.8b00023>.
- [36] R. Vaidyanathan, S. Rauf, M.J.A. Shiddiky, M. Trau, Tuneable surface shear forces to physically displace nonspecific molecules in protein biomarker detection, *Biosens. Bioelectron.* 61 (2014) 184–191, <https://doi.org/10.1016/j.bios.2014.03.061>.
- [37] S.D. Tallapragada, K. Layek, R. Mukherjee, K.K. Mistry, M. Ghosh, Development of screen-printed electrode based immunosensor for the detection of HER2 antigen in human serum samples, *Bioelectrochemistry* 118 (2017) 25–30, <https://doi.org/10.1016/j.bioelectrochem.2017.06.009>.
- [38] X. Wu, T. Xiao, Z. Luo, R. He, Y. Cao, Z. Guo, W. Zhang, Y. Chen, A micro-/nanochip and quantum dots-based 3D cytosensor for quantitative analysis of circulating tumor cells, *J. Nanobiotechnol.* 16 (2018) 65, <https://doi.org/10.1186/s12951-018-0390-x>.
- [39] K. Boriachek, M.N. Islam, V. Gopalan, A.K. Lam, N.T. Nguyen, M.J.A. Shiddiky, Quantum dot-based sensitive detection of disease specific exosome in serum, *Analyst* 142 (2017) 2211–2219, <https://doi.org/10.1039/c7an00672a>.
- [40] J.A.A. Ho, Y.C. Lin, L.S. Wang, K.C. Hwang, P.T. Chou, Carbon nanoparticle-enhanced immunoelectrochemical detection for protein tumor marker with cadmium sulfide biotracers, *Anal. Chem.* 81 (2009) 1340–1346, <https://doi.org/10.1021/ac801832h>.
- [41] Y. Luo, Y. Wang, H. Yan, Y. Wu, C. Zhu, D. Du, Y. Lin, SWCNTs@GQDs composites as nanocarriers for enzyme-free dual-signal amplification electrochemical immunoassay of cancer biomarker, *Anal. Chim. Acta* 1042 (2018) 44–51, <https://doi.org/10.1016/j.aca.2018.08.023>.
- [42] Y. Liu, L. Zhang, Q. Guo, H. Hou, T. You, Enzyme-free ethanol sensor based on electrospun nickel nanoparticle-loaded carbon fiber paste electrode, *Anal. Chim. Acta* 663 (2010) 153–157, <https://doi.org/10.1016/j.aca.2010.01.061>.
- [43] M. Freitas, H.P.A. Nows, C. Delerue-Matos, Electrochemical biosensing in cancer diagnostics and follow-up, *Electroanalysis* 30 (2018) 1576–1595, <https://doi.org/10.1002/elan.201800193>.
- [44] D. Martín-Yerga, M.B. González-García, A. Costa-García, Electrochemical immunosensor for anti-tissue transglutaminase antibodies based on the in situ detection of quantum dots, *Talanta* 130 (2014) 598–602, <https://doi.org/10.1016/j.talanta.2014.07.010>.
- [45] J.T. Busher, Serum albumin and globulin, in: H.K. Walker, W.D. Hall, J.W. Hurst (Eds.), *Clinical Methods: the History, Physical, and Laboratory Examinations*, third ed., Butterworths, Boston (USA), 1990 (Chapter 101).
- [46] S.E.F. Melanson, M.J. Tanasijevic, P. Jarolim, Cardiac troponin assays: a view from the clinical chemistry laboratory, *Circulation* 116 (2007) e501–e504, <https://doi.org/10.1161/CIRCULATIONAHA.107.722975>.
- [47] M. Hasanzadeh, S. Rahimi, E. Solhi, A. Mokhtarzadeh, N. Shadjou, J. Soleymani, S. Mahboob, Probing the antigen-antibody interaction towards ultrasensitive recognition of cancer biomarker in adenocarcinoma cell lysates using layer-by-layer assembled silver nano-cubics with porous structure on cysteamine capped GQDs, *Microchem. J.* 143 (2018) 379–392, <https://doi.org/10.1016/j.microc.2018.08.028>.
- [48] M. Hasanzadeh, S. Tagi, E. Solhi, N. Shadjou, A. Jouyban, A. Mokhtarzadeh, Immunosensing of breast cancer prognostic marker in adenocarcinoma cell lysates and unprocessed human plasma samples using gold nanostructure coated on organic substrate, *Int. J. Biol. Macromol.* 118 (2018) 1082–1089, <https://doi.org/10.1016/j.ijbiomac.2018.06.091>.
- [49] M. Hasanzadeh, H.N. Baghban, N. Shadjou, A. Mokhtarzadeh, Ultrasensitive electrochemical immunosensing of tumor suppressor protein p53 in unprocessed human plasma and cell lysates using a novel nanocomposite based on poly-cysteine/graphene quantum dots/gold nanoparticle, *Int. J. Biol. Macromol.* 107 (2018) 1348–1363, <https://doi.org/10.1016/j.ijbiomac.2017.11.006>.

Supplementary material

Quantum Dots as Nanolabels for Breast Cancer Biomarker HER2-ECD Analysis in Human Serum

Maria Freitas, Marta M.P.S. Neves, Henri P.A. Nouws*, Cristina Delerue-Matos
REQUIMTE/LAQV, Instituto Superior de Engenharia do Porto, Politécnico do Porto,
Rua Dr. António Bernardino de Almeida 431, 4200-072 Porto, Portugal

* corresponding author: han@isep.ipp.pt, tel.: +351-228340500

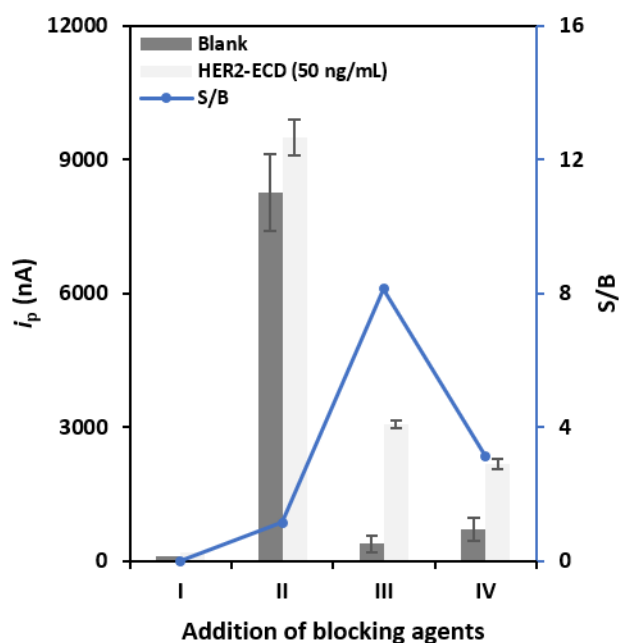


Figure S 1. Study of non-specific adsorptions. Evaluation of the blocking agents (I) Casein 2% and (II) BSA 2% in the blocking surface step, and evaluation of BSA effect in different incubation steps: (III) BSA 0.5% (m/V) for both the antigen and the detection antibody solutions (Ab-D), and (IV) BSA 0.5% (m/V) to the antigen and 1% (m/V) to the Ab-D solutions. Experimental conditions: Ab-C (25 $\mu\text{g/mL}$), HER2-ECD (0 and 50 ng/mL), Ab-D (2 $\mu\text{g/mL}$), QDs (10 nM).

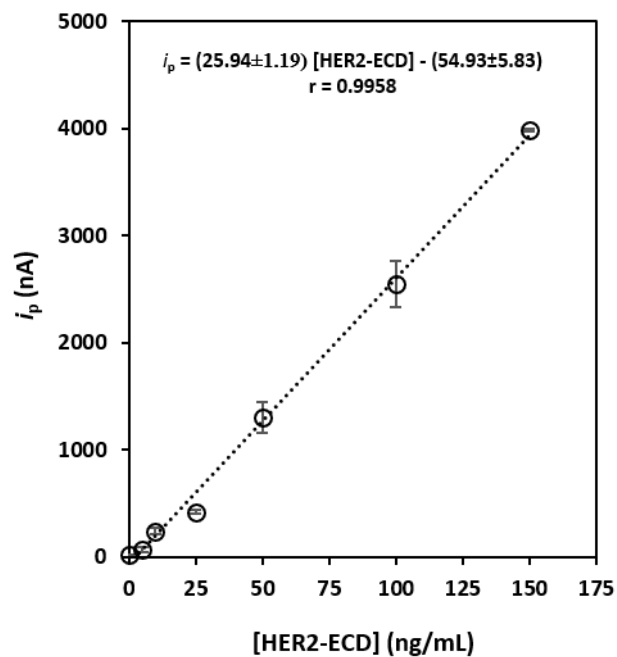


Figure S 2. Calibration plot in Tris buffer for the analysis of HER2-ECD: 0, 5, 10, 25, 50 and 100 ng/mL. Experimental conditions: Ab-C: 25 $\mu\text{g/mL}$, BSA: 2% (m/V), Ab-D: 2 $\mu\text{g/mL}$, QDs: 5 nM with addition of BSA 0.5% (m/V)).

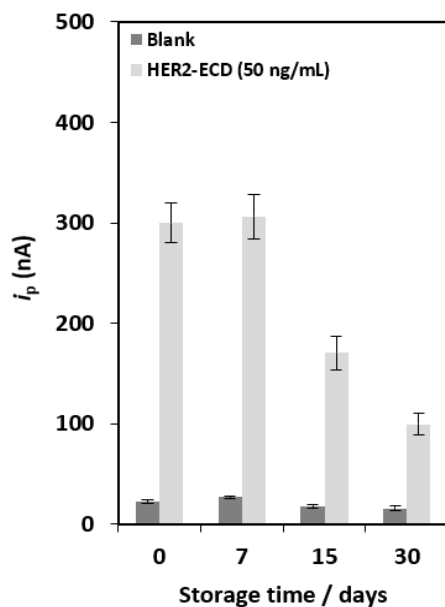


Figure S 3. Obtained current intensities for stability studies. Experimental conditions: Ab-C: 25 $\mu\text{g/mL}$, BSA: 2% (m/V), Ab-D: 2 $\mu\text{g/mL}$, QDs: 5 nM with addition of BSA 0.5% (m/V)).

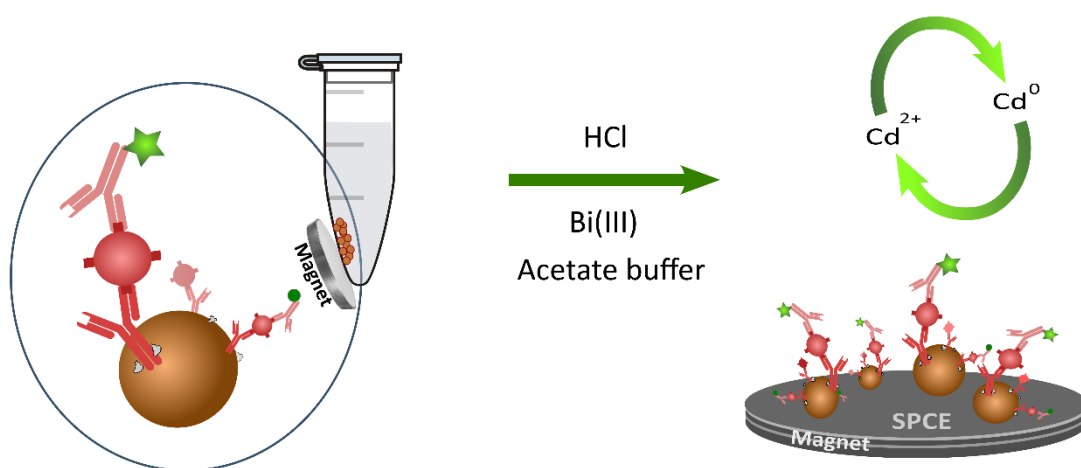
Table SI 1. Summary of experimental parameters of electrochemical immunoassay-based procedures for breast cancer biomarkers using Quantum Dots.

Breast cancer biomolecule	Sensing surface				Label	Technique	Detection	Assay time	LOD	Sample	Ref
	Transducer	Transducer preparation time*	Modification with the biorecognition element*	Long-term stability							
CTCs	ITO/3D Ni/PLGA micro-/nano-chip	~ 36 h	–	n.d.	CdSe@ZnS QDs	DPV	Cadmium	2 h	8 cells/mL	MCF7 cells	[38]
Exosomes	GCE/MB	–	20 min	n.d.	CdSe QDs	SWASV	Cadmium	1 h 50 min	100 exosome per μ L	Human serum	[39]
CEA	SPGE/PEI-CNP	~ 37 h	30 min	n.d.	CdS QDs	SWASV	Cadmium	35 min	32 pg/mL	Spiked human urine	[40]
CEA	GCE/rGO-AuNPs	~ 2 h	~ 12 h	n.d.	Graphene QDs	SWV	Thionine	2 h 50 min	5.3 pg/mL	Spiked human serum	[41]
p53	AuE/P-Cys/GQDs/AuNPs	~ 5 h	~ 10 h	8 days	HRP	DPV	Thionine	2 h 10 min	0.065 fM	Human Plasma	[49]
CA 15-3	GCE/GQDs/CysA/AgNCs	n.d.	1 h	7 days	n.a.	SWV	[Fe (CN) ₆] ^{3-/4-}	20 min	0.019 U/mL	Human plasma and cell lysates	[47]
CA 15-3	GCE/Au NSs/CysA /GQDs	n.d.	5 h	1 month	n.a.	SWV	[Fe (CN) ₆] ^{3-/4-}	2 h	0.011 U/mL	Cancer cell lysates	[48]
HER2-ECD	Bare SPCE	–	~ 12 h	7 days	CdSe@ZnS QDs	DPV	Cadmium	2 h	2.1 ng/mL	Spiked human serum	This study


* Overnight incubations were considered as a 12 h period for comparison purposes
 AgNCs – silver nanocubics; AuE – gold electrode; AuNPs – gold nanoparticles; Au NSs – gold nano-shrub; CEA – carcinoembryonic antigen; CA 15-3 – cancer antigen 15-3; CNP – carbon nanoparticle; CTCs – circulating tumor cells; CysA – cysteamine; GCE – glassy carbon electrode; GQDs – graphene quantum dots; DPV – differential pulse voltammetry; HRP – horseradish peroxidase; ITO – indium tin oxide; LSV – linear sweep voltammetry; MB – magnetic beads; n.d. – no data; n.a. – not applicable; P-Cys – poly L-cysteine; PEI – poly(ethylene imine); PLGA – poly (lactic-co-glycolic acid); QDs – quantum dots; rGO – reduced graphene oxide; SPCE – screen-printed carbon electrode; SPGE – screen-printed graphite electrode; SWASV – square wave anodic stripping voltammetry; SWV – Square wave voltammetry.

4.2 Immunomagnetic bead-based bioassay for the voltammetric analysis of the breast cancer biomarker HER2-ECD and tumour cells using quantum dots as detection labels

Microchimica Acta 187 (3) (2020) 184




 Blocker agent

 Monoclonal Antibody

 Biomarker

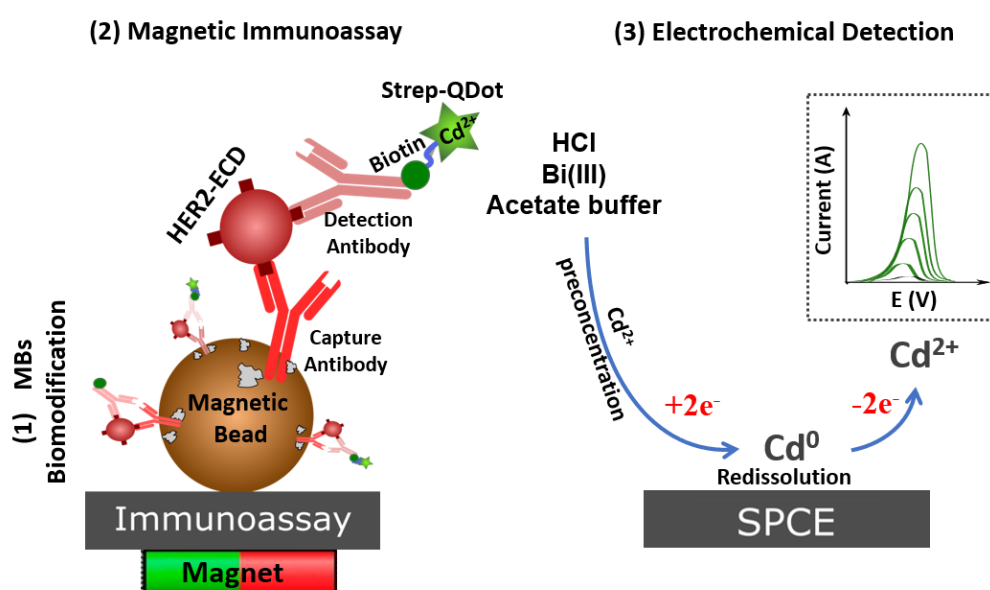
 Labeled Antibody

 Quantum Dot

Author Contributions:

Maria Freitas (investigation: Lead; Methodology: Equal; Writing – original draft: Lead); Henri Nouws (Conceptualization: Lead; Funding acquisition: Equal; Methodology: Lead; Project administration: Equal; Supervision: Equal; Validation: Equal; Writing – review & editing: Lead); Elisa Keating (Cell acquisition and culture); Virgínia C. Fernandes (Cell culture); Cristina Delerue-Matos (Funding acquisition: Equal; Methodology: Equal; Supervision: Equal; Validation: Equal; Writing – review & editing: Supporting)

Graphical Abstract



Schematic representation of an electrochemical immunomagnetic assay developed using MBs and SPCE as transducer surface and QDs as electroactive label. HER2-ECD breast cancer biomarker was determined, and the assay was successfully applied for detection of HER2-positive and HER2-negative cancer cell-lines.

Microchimica Acta (2020) 187:184
<https://doi.org/10.1007/s00604-020-4156-4>

ORIGINAL PAPER



Immunomagnetic bead-based bioassay for the voltammetric analysis of the breast cancer biomarker HER2-ECD and tumour cells using quantum dots as detection labels

Maria Freitas¹ · Henri P. A. Nouws¹ · Elisa Keating^{2,3} · Virginia Cruz Fernandes¹ · Cristina Delerue-Matos¹

Received: 16 September 2019 / Accepted: 11 February 2020
© Springer-Verlag GmbH Austria, part of Springer Nature 2020

Abstract

An electrochemical magnetic immunosensing strategy was developed for the determination of HER2-ECD, a breast cancer biomarker, and breast cancer cells in human serum. A sandwich assay was performed on carboxylic acid-functionalized magnetic beads (MBs) using a screen-printed carbon electrode (SPCE) as transducer surface. The affinity process was detected using electroactive labels; core/shell streptavidin-modified CdSe@ZnS Quantum Dots (QDs). Cd²⁺ ions, released from the QDs, were determined by differential pulse anodic stripping voltammetry (DPASV). An assay time of 90 min, with an actual hands-on time of about 20 min, a linear range between 0.50–50 ng·mL⁻¹ of HER2-ECD and a limit of detection of 0.29 ng·mL⁻¹ were achieved. Analysis of live breast cancer cells was also performed using the optimized assay. Breast cancer cell lines SK-BR-3 (a HER2-positive cell line), MDA-MB-231 (a HER2-negative cell line) and MCF-7 (a cell line with low HER2 expression) were tested. The selectivity of the assay towards SK-BR-3 cells was confirmed. A concentration-dependent signal that was 12.5× higher than the signal obtained for the HER2-negative cells (MDA-MB-231) and a limit of detection of 2 cells·mL⁻¹ was obtained.

Keywords Breast cancer · Cancer cells · Electrochemical immunoassay · HER2-ECD · Magnetic beads · Quantum dots

This article is part of the Topical Collection on *IX NyNA 2019. International Congress on Analytical Nanoscience and Nanotechnology*

This work was presented at the IX NyNA 2019, International Congress on Analytical Nanoscience and Nanotechnology at Zaragoza (Spain) from 2 - 4 July, 2019. Chairman: Dr. Juan R. Castillo.

Electronic supplementary material The online version of this article (<https://doi.org/10.1007/s00604-020-4156-4>) contains supplementary material, which is available to authorized users.

✉ Henri P. A. Nouws
han@isep.ipp.pt

¹ REQUIMTE/LAQV, Instituto Superior de Engenharia do Porto, Politécnico do Porto, R. Dr. António Bernardino de Almeida 431, 4200-072 Porto, Portugal

² Department of Biomedicine – Unit of Biochemistry, Faculty of Medicine, University of Porto, Al. Prof. Hernâni Monteiro, 4200-319 Porto, Portugal

³ CINTESIS – Center for Health Technology and Services Research, Rua Dr. Plácido da Costa, 4200-450 Porto, Portugal

Introduction

Cancer screening programs are implemented at the national level to reduce mortality rates [1]. Nevertheless, the limited sensitivity and the lack of specific results in the traditional diagnosis can significantly lead to unfavourable clinical outcomes [2]. The absence of non-invasive methodologies for accurate determination of carcinogenic biomarkers in the bloodstream is a real concern. Human epidermal growth factor receptor 2 (HER2) is a cancer biomarker overexpressed in primary cancer cases [3]. The tumour expression is dichotomized into HER2-positive and HER2-negative groups [4]. In this field, nanotechnological devices can be used to measure the protein expression in biological fluids (serum, plasma) from screening to follow-up. The assessment of the concentration of the extracellular domain of HER2 (HER2-ECD) in serum samples is a prominent alternative since this domain can be cleaved from the surface of cancer cells by matrix metalloproteases and released into the bloodstream [5]. In addition, the

assessment of HER2-positive circulating tumour cells (CTCs) is fundamental for patients that can benefit from personalized therapies and adjuvant treatment [6].

Electrochemical strategies for the determination of HER2 in human serum have been reported using distinct and elaborate electrode surface modifications based on sumptuous structures (nano, micro- and/or magnetic-based materials) to improve the transducer's performance [7]. Nevertheless, the synthesis of these materials and their functionalization require extensive and time-consuming procedures. In contrast, less innovation has been focused on the detection strategy. Distinct probes or labels to amplify the electrochemical signal are required since the redox pair $[\text{Fe}(\text{CN})_6]^{3-/4-}$ is still one of the most reported [8–12]. Although silver [13–16], 1-Naphtol (1-NP) [17], 3,3',5,5'-Tetramethyl[1,1'-biphenyl]-4,4'-diamine (TMB) [18] and molybdate [19, 20] were employed for the determination of HER2, the use of nanomaterials has not extensively been studied.

Nanoparticle-based signal amplification has attracted considerable attention in immunosensing strategies, since higher sensitivity and lower limits of detection can be achieved [21]. Quantum dots (QDs) are crystalline nanoparticles that revealed to be promising candidates as electrochemical detection labels in breast cancer assays due to the good electroactivity of the employed metals [22–24]. QDs can be analysed by stripping voltammetry after preconcentration of the metal on the electrode surface. The obtained signal can then be related to the analyte concentration [25, 26].

Bioassays using QDs as semiconductor nanolabels and magnetic particles as a platform for the targeted immobilization of antibodies constitute a versatile solution for the analysis of biomarkers in clinical practice. In the present work a magnetic immunoassay was developed using carboxylic acid-functionalized magnetic beads (COOH-MBs) onto which capture antibodies were covalently bound, allowing their oriented immobilization. This was followed by the addition of a solution containing the analyte (HER2-ECD or cancer cells) and a biotinylated detection antibody. Then streptavidin-coated core/shell CdSe@ZnS QDs were linked to the previously formed immunocomplex, and the determination was performed by differential pulse anodic stripping voltammetry (DPASV) on a screen-printed carbon electrode (SPCE). This is the first electrochemical magnetic bioassay for the analysis of HER2-ECD using a MB platform and core/shell CdSe@ZnS QDs as electroactive labels. The electrochemical analysis of HER2-positive (SK-BR-3), HER2-negative (MDA-MB-231) and low-expression HER2 cancer cells (MCF-7) using the present methodology is also new.

Experimental

Apparatus

The SEM images were obtained using FEI Quanta 400FEG ESEM/EDAX Genesis X4 M equipment at the “Centro de Materiais da Universidade do Porto (CEMUP)”. Cancer cells were imaged by a Nikon TMS microscope and counted using an automated cell counter (Countess™, ThermoFisher Scientific - Invitrogen, USA, www.thermofisher.com/invitrogen). Screen-printed carbon electrodes (with a 4-mm working electrode (WE) (electroactive area: 0.079 cm²), a silver pseudoreference electrode and a carbon counter electrode (SPCE, DRP-110)) and the specific connector (DRP-CAC) were supplied by Metrohm DropSens (Spain, www.dropsens.com). Electrochemical measurements were carried out with a potentiostat/galvanostat (Autolab PGSTAT204, Metrohm Autolab, The Netherlands, www.metrohm-autolab.com) controlled by the NOVA software package v.1.10 (Metrohm Autolab). Magnetic separations were carried out using a DynaMag™-2 magnet (ThermoFisher Scientific, USA, www.thermofisher.com). Ultra-pure water (resistivity = 18.2 MΩ.cm) used throughout the work was obtained from a Millipore water purification system (Simplicity 185) (Germany, www.merckmillipore.com).

Reagents and solutions

The chemical and biological reagents are indicated in the Electronic Supporting Material (ESM, Section S1). Buffers and working solutions of the antibodies, antigens and QD-Strep were prepared daily. The following buffers were used: MES buffer (0.1 M, pH 6) for the ECD/NHS (200 mM/50 mM) and the capture antibody (Ab-C, various concentrations) solutions, PBS buffer (0.02 M, pH 8) for the EA (1 M) solution, Tris buffer (0.1 M, pH 7.4) for the QD-strep (various concentrations), containing BSA (0.5% m/V), solutions, and acetate buffer (0.1 M, pH 4.5) to prepare the Bi(III) (1.0 mg·L⁻¹) solution. Tween 20 (0.01%) was added to the distinct buffers to be used in the washing steps.

Cell culture and CTC analysis

Breast cancer cell lines MDA-MB-231, MCF-7 and SK-BR-3 were cultured in RPMI medium supplemented with 10 and 15% inactivated FBS, respectively, and 1% antibiotic/antimycotic solution. Cells were incubated at 37 °C in a humidified atmosphere of 5% CO₂–95% air. The culture medium was changed every 2–3 days, and the culture was split every 7 days. For analysis, cells were seeded on 21-cm² plastic cell culture dishes (TPP®,

Trasadingen) and were used after 2–5 days in culture (90–100% confluence). On the day of the experiment, the cells were harvested with Trypsin-EDTA 0.25% and counted using the automated cell counter. A trypan-blue exclusion assay was performed to confirm cell viability, which was between 87 and 96% for all the cell lines. The distinct solutions of the cells (1×10^2 – 1×10^5 cells·mL⁻¹) were prepared in human serum and analysed using the optimized immunoassay.

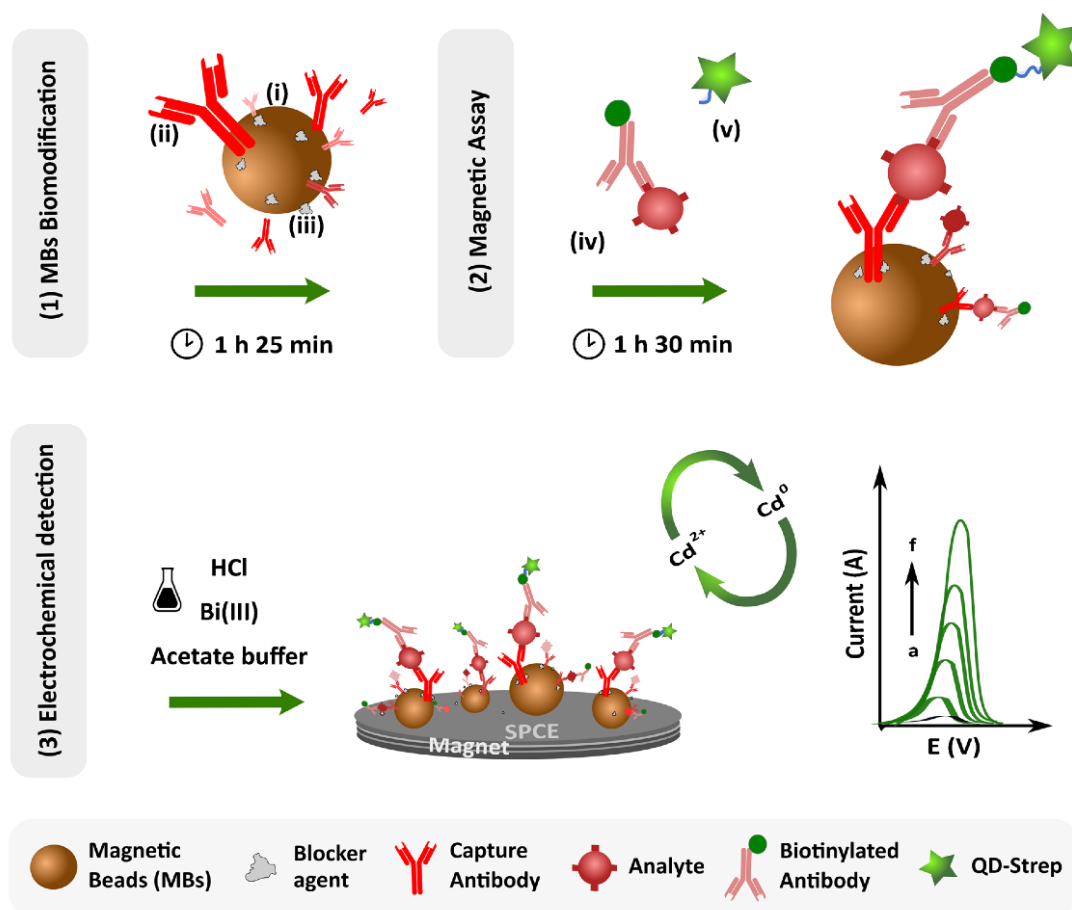
Electrochemical immunomagnetic bioassay for the analysis of HER2-ECD and living cells

A schematic representation of the sandwich immunoassay (Scheme 1) elucidates the distinct steps of the experimental procedure (note that steps (i) to (v) were performed in 0.5-mL

microtubes). All the steps of the assay were performed protected from light at room temperature using vortex stirring (950 rpm). Magnetic separations were carried out using the DynaMag™-2 magnet.

Prior to the biomodification, the MBs stock solution was washed with MES-T for 2 min.

- (1) The biomodification consisted of the following steps: (i) a 1.5- μ L aliquot of the MBs solution (containing 7.5 μ g of MBs) was resuspended in the EDC/NHS solution (100 μ L, 15 min) and (ii) incubated with Ab-C (25 μ g·mL⁻¹, 100 μ L, 1 h). After a washing step with MES-T and PBS-T (2 min each), the particles' free surfaces were (iii) blocked with EA (100 μ L, 10 min). The biomodified particles were resuspended in 100 μ L PBS-T and kept at 4 °C until use.



Scheme 1 Schematic representation of the magnetic immunoassay. **1** The MBs are first biomodified (i activation with EDC/NHS, ii addition of capture antibody, iii blocking with EA). **2** The magnetic assay is performed through the addition of iv a mixture containing the antigen (HER2-ECD or cancer cells) and the biotinylated antibody, followed by

the addition of v a QD-strep solution. The magnetic beads are magnetically attracted to the working electrode. **3** Electrochemical determination of the released Cd²⁺ is performed. Voltammograms of increasing HER2-ECD concentrations are exemplified.

- (2) The magnetic immunoassay consisted of the following:
 - (iv) The analyte solution (protein biomarker or cancer cells) was previously mixed with Ab-D ($2.0 \mu\text{g}\cdot\text{mL}^{-1}$) in human serum (10 min before use). The prepared mixture was then added to the biomodified MBs ($100 \mu\text{L}$, 1 h). Afterwards, a washing step with Tris-T was performed and (v) the MBs were incubated with a QD-strep solution (5.0 nM , $70 \mu\text{L}$, 30 min).
- (3) Electrochemical analysis: prior to the measurements, a washing step was performed with ultra-pure water. Then, a $10\text{-}\mu\text{L}$ aliquot of the final solution was placed on the WE of an SPCE under which a magnet ($d = 4 \text{ mm}$) was placed. The SPCE was totally dried with a nitrogen flow, and $5 \mu\text{L}$ of the HCl (1 M) and $40 \mu\text{L}$ of the Bi(III) ($1.0 \text{ mg}\cdot\text{L}^{-1}$) solutions were added to the electrode surface to release Cd^{2+} from the QDs. DPASV voltammograms were recorded using the following conditions: constant potential of $+1.00 \text{ V}$ during 60 s, followed by a potential of -1.10 V for 300 s (in this phase the released cadmium ions were pre-concentrated and a bismuth film was formed). The potential was swept from -1.00 V to -0.70 V to strip the cadmium into the solution, recording the electrochemical signal. (DPV parameters, pulse amplitude, 0.05 V ; step potential, 0.01 V ; modulation time, 0.01 s ; interval time, 0.1 s).

Results and discussion

Electrochemical behaviour of the quantum dots on distinctly modified SPCE surfaces

To elaborate the immunomagnetic assay, prior measurements were performed to study the electrochemical behaviour of cadmium (released from the QDs) using DPASV. In the tested procedure, cadmium was deposited simultaneously with a bismuth film which is considered an adequate alternative to the traditional mercury film [27]. Distinct carboxylic acid-functionalized materials were tested using an SPCE as transducer: multi-walled carbon nanotubes (HOOC-MWCNT, $1 \mu\text{g}\cdot\text{mL}^{-1}$), PEG gold-coated magnetic nanoparticles (HOOC- Fe_3O_4 @AuNP, $30 \mu\text{g}$) and magnetic beads (HOOC-MBs, $30 \mu\text{g}$). The sensing platforms were employed to analyse a $50\text{-ng}\cdot\text{mL}^{-1}$ HER2-ECD solution, and the obtained signals were compared with the ones obtained with a bare SPCE, using concentrations of Ab-C $25 \mu\text{g}\cdot\text{mL}^{-1}$, Ab-D $2.0 \mu\text{g}\cdot\text{mL}^{-1}$, QD 10 nM , HCl 1 M and Bi(III) $1.0 \text{ mg}\cdot\text{L}^{-1}$. The respective SEM images and obtained voltammograms are presented in Fig. 1. The functionalization of nano- and micromaterials with carboxylic acid groups commonly

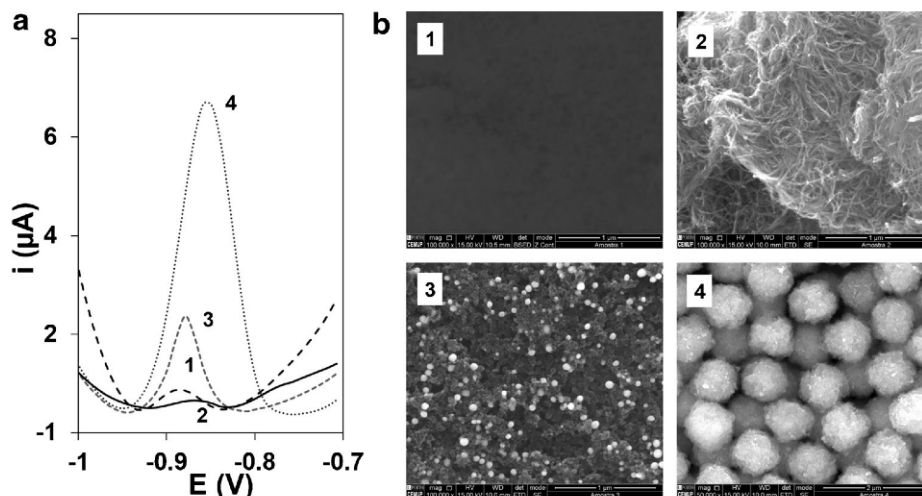
leads to an efficient and well-organized attachment of the antibody, allowing the construction of a stable and functional immunoassay [7, 28]. However, when the SPCE is modified with MWCNTs, the obtained peak current intensity was considerably lower than for the unmodified (bare) electrode, as can be seen in Fig. 1a (1 and 2). Despite the wide application of carbon-based nanomaterials in the construction of electrochemical immunosensors, in this work, the modification of the transducer with MWCNT proved to be inappropriate. As described in the literature, the electrode modification with carbon nanomaterials leads to higher adsorption of proteins on the transducer's surface, increasing the effect of the electrical double layer [29]. On the other hand, the use of both magnetic nano- and micro-particles leads to an increase in the current intensity. This is probably due to an efficient immobilization of the capture antibodies on these particles, as well as the specific orientation, which is not as effective on the SPCE-MWCNT surface. Although other studies report the construction of interesting magnetic assays using core/shell nanoparticles, in the present work, the electrochemical signal is noticeably higher when (micro-sized) MBs were used (Fig. 1a (3 and 4, respectively)). In fact, the SEM images (Fig. 1b (3 and 4)) support the results since it is observed that the MBs are arranged in an organized layer that can contribute to a more sensitive method. In contrast, the core/shell nanoparticles are not as homogeneous in size and are dispersed on the electrode's surface.

Thus, considering that the MBs are the best sensing surface, further studies were carried out to evaluate the possibility of improving the detection strategy. The electrochemical response of the QDs was verified by adding HCl and Bi(III) in four different strategies (ESM, Section S2). The best results were obtained by placing the biomodified-MBs on the WE followed by the addition of the HCl and Bi(III) solutions.

Optimization of the immunosensing strategy

The following experimental parameters that affect the immunoassay's performance were optimized: (a) assay format, (b) QD concentration, (c) MB amount and (d) Ab concentrations. Respective text and figures regarding the optimizations are included in the ESM (Section S3). The parameters selected to test the immunomagnetic assay for the analysis of HER2-ECD and cancer cells in human serum are presented in Table S1. In short, the following experimental conditions were found to give the best results: MBs $7.5 \mu\text{g}$, Ab-C $25 \mu\text{g}\cdot\text{mL}^{-1}$, Ab-D $2.0 \mu\text{g}\cdot\text{mL}^{-1}$ and QDs 5.0 nM , using a previously prepared mixture of the antigen and Ab-D (Format B). Under these conditions, the average amount of antibody per MB was 0.188 pg .

Fig. 1 **a** Study of the electrochemical behaviour of cadmium (released from a 10-nM QD solution) with distinct nano- and micromaterials used on SPCEs. **b** Respective SEM images: 1 – bare SPCE; 2 – SPCE-MWCNT; 3 – SPCE-Fe₃O₄@Au nanoparticles; 4 – SPCE-MBs



Analytical performance and stability of the modified magnetic beads

The optimized method was used to analyse the cancer biomarker in human serum. The precision of the results was evaluated using a 50-ng·mL⁻¹ HER2-ECD solution. Relative standard deviations (RSD) for the repeatability and reproducibility ($n = 3$) were 2.7 and 3.1%, respectively, demonstrating that the immunomagnetic assay provides precise results.

For calibration purposes, HER2-ECD solutions with increasing concentrations were prepared in human serum (0.50, 1.0, 2.5, 5.0, 10, 25, 50 and 100 ng·mL⁻¹) and analysed with the magnetic immunoassay. The linear range was established between 0.50 and 50 ng·mL⁻¹ ($i_p = 0.75 \pm 0.03$ [HER2-ECD] + 4.99 ± 0.58 , $r = 0.997$) with a sensitivity of $9.5 \mu\text{A}\cdot\text{mL}\cdot\text{ng}^{-1}\cdot\text{cm}^{-2}$. The calibration plot and examples of differential pulse anodic stripping voltammograms in the linear range are shown in Fig. 2. Limits of detection (LOD = 3 s/m) and quantification (LOQ = 10 s/m) were calculated from the calibration straight: “s” is the standard deviation of the blank and “m” is the slope. The values obtained were LOD = $0.29\text{ ng}\cdot\text{mL}^{-1}$ and LOQ = $0.96\text{ ng}\cdot\text{mL}^{-1}$. The obtained LOD was more than 50× lower than the cut-off value ($15\text{ ng}\cdot\text{mL}^{-1}$) established for HER2-ECD. The coefficient of variation of the method (V_{x0}) was 1.27%, demonstrating that the precision of the method is adequate ($V_{x0} < 5\%$). Additional figures of merit of the magnetic immunoassay are indicated in Table S2.

To assess the selectivity of the bioassay, other cancer protein biomarkers were tested, including breast cancer antigen 15–3 (CA15–3, $100\text{ U}\cdot\text{mL}^{-1}$), liver cancer biomarker alpha-Fetoprotein (AFP, $1\text{ }\mu\text{g}\cdot\text{mL}^{-1}$) and a possible serum interferent, human serum albumin (HSA, $100\text{ mg}\cdot\text{mL}^{-1}$). Concentrations were chosen based on values that

can be expected in real situations. The results demonstrated the high selectivity of the assay for HER2-ECD since the signals of the tested interferents are similar to the blank signal (Fig. 3a).

To assess the accuracy of the assay’s results both recovery experiments and the use of a reference method (ELISA)

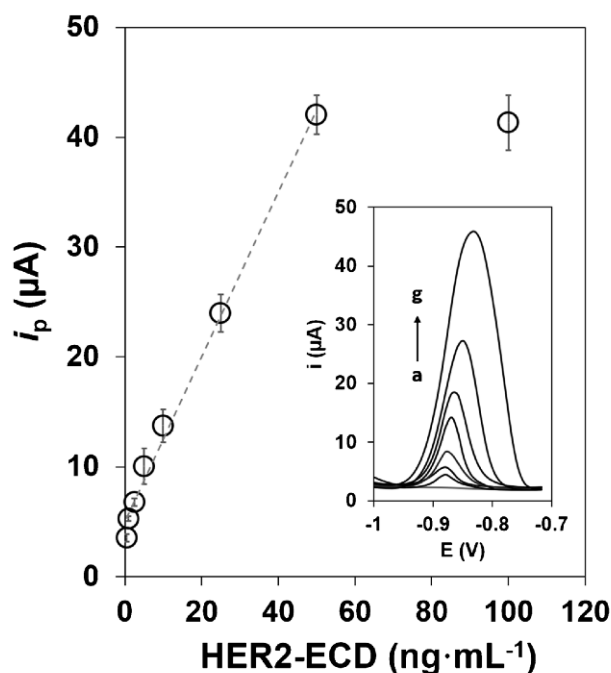
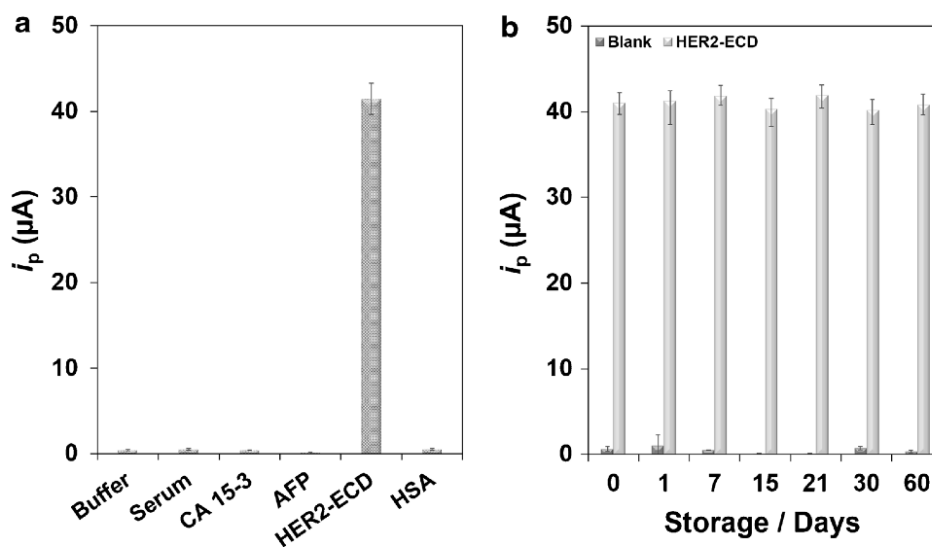


Fig. 2 Calibration plot for the analysis of HER2-ECD in human serum (i_p vs. HER2-ECD concentration) using the magnetic immunoassay. Inset: Differential pulse anodic stripping voltammograms of [HER2-ECD] (a–g); 0, 0.50, 1.0, 2.5, 5.0, 10, 25 and 50 ng·mL⁻¹. (Ab-C $25\text{ }\mu\text{g}\cdot\text{mL}^{-1}$; Ab-D $2.0\text{ }\mu\text{g}\cdot\text{mL}^{-1}$; QDs 5.0 nM. DPASV parameters: preconcentration + 1.00 V for 60 s and -1.10 V for 300 s; potential scan -1.00 V to -0.70 V; pulse amplitude 0.05 V; step potential 0.01 V; modulation time 0.01 s; interval time 0.1 s)

Fig. 3 **a** Responses for HER2-ECD, buffer, serum and possible interferents (CA15-3 100 U·mL⁻¹; AFP 1 μg·mL⁻¹ and HSA 100 mg·mL⁻¹). **b** Storage stability of the modified MBs, [HER2-ECD] 0 and 50 ng·mL⁻¹



were performed. For the recovery tests non-diluted human serum was spiked with distinct HER2-ECD concentrations (1.0, 2.5, 10, 20 and 50 ng·mL⁻¹). Recoveries between 99.8 and 108.0% were obtained (Table 1), indicating that the assay provides accurate results and can successfully be applied to real samples. Experimental specifications of the ELISA are provided in the ESM (Section S.1.2). Spiked serum samples with HER2-ECD concentrations between 0.5 and 50 ng·mL⁻¹ were analysed. A 4-fold dilution was required for the ELISA to ensure that the HER2-ECD was within the linear range. The electrochemical assay did not require any dilution. Table 1 shows the obtained results. The relative deviations were below 10% for concentrations below the cut-off value, which confirms the accuracy of the results. Although the use of the ELISA kit allows the determination of very low concentrations of the biomarker with an elevated precision, a serial dilution is required

since direct analysis leads to values outside the range of concentrations in real cases. Furthermore, the ELISA has a very narrow linear range (Fig. S1) and much longer assay (4 h 45 min) and hands-on times (1 h 20 min) than the assay described in this work (1 h 30 min and 20 min, respectively). The results demonstrate that the performance of the immunomagnetic assay can be compared to that of the ELISA, and it provides an important diagnostic tool for cancer biomarker analysis. Because of the huge importance of screening and early diagnosis, the new analytical methodology can be adequate for patient follow-up.

In addition, the stability of the MBs was also studied. The biomodified MBs were stored at 4 °C in PBS-T, and the signal was monitored during several weeks, using 0 and 50 ng·mL⁻¹ HER2-ECD solutions. No significant differences in the analytical signals were observed for at least 60 days; the signal was 99.5% of the initial signal (Fig. 3b).

Table 1 Recovery values (%), relative standard deviations (RSD, %) and relative deviations (%) for the electrochemical and ELISA analysis of HER2-ECD in human serum: 1.0, 2.5, 10, 20 and 50 ng·mL⁻¹.

Technique	Added (ng·mL ⁻¹)	Found (ng·mL ⁻¹)	Recovery (%)	RSD (%)	Relative deviation (%)	Label	Platform	Assay time	Hands-on time
Electrochemistry	1.0	1.01	101.4	0.49	*	QDs	Single-use SPCE	1 h 30 min	20 min
	2.5	2.70	108.0	0.46	0.75				
	10	10.52	105.2	0.95	-8.36				
	20	20.0	99.8	0.67	-18.57				
	50	50.9	101.8	2.44	*				
ELISA	2.5	2.68	107.2	0.01		TMB	96-well plate	4 h 45 min	1 h 20 min
	10	11.48	114.8	0.01					
	20	24.5	122.5	0.02					

*Human HER2 ELISA Kit absorbance values for 1 ng·mL⁻¹ and 50 ng·mL⁻¹ concentrations are outside of the calibration range

Analysis of live breast cancer cells

The electrochemical magnetic immunoassay was also used to detect live breast cancer cell-lines: the HER2-positive SK-BR-3, the HER2-negative MDA-MB-231 and the low HER2-expression MCF-7 cell lines. The selectivity of the assay towards the SK-BR-3 cell line was assessed by comparing the signals obtained with the ones obtained for the MDA-MB-231 and MCF-7 cell lines. In Fig. 4a can be observed that SK-BR-3 provided a concentration-dependent signal that was 12.5× higher than the signal obtained for HER2-negative cells MDA-MB-231 and 4× higher than the signal obtained for the MCF-7 cells, confirming the selectivity of the assay for HER2-positive cells. So, the SK-BR-3 cells that overexpress HER2 can easily be captured by the Ab-C. This explains the higher analytical signal because of the higher amount of cells that were captured. The calibration straight for SK-BR-3 cells was established in the range between 1×10^2 – 5×10^3 cells·mL⁻¹ ($i_p = 0.15 \pm 0.02 \log[\text{SK-BR-3}] - 0.20 \pm 0.06$, $r = 0.983$) (Fig. 4b), obtaining a limit of detection of 2 cells·mL⁻¹. Additional figures of merit of the magnetic immunoassay for the analysis of SK-BR-3 are indicated in Table S2.

The magnetic immunoassay was compared with other electrochemical bioassays for the determination of HER-positive cancer cells [30–35] (Table 2). Although an electrochemical nanobiosensor for the detection of SK-BR-3 cell line in a 30-min test has been described in the literature [31], the time required for both the preparation of the transducer and for the modification with the biorecognition element is high (>

16 h), and the use of costly materials leads to an expensive analysis. Comparatively, the present work reports a simplified experimental procedure with a total time for both the sensing surface preparation and the assay of less than 3 h.

One of the limitations of the assay is the use of a heavy metal for detection purposes. Therefore, we minimized the used quantities: 70 μL of a 5.0-nM solution, so only 0.35 pmol of QDs are used in each assay. The generated waste can selectively be collected and sent to a certified entity operating in accordance with European standards regarding waste management. A way of replacing the present strategy by a non-polluting material is by using, for example, enzymes. However, enzymes can lose their bioactivity and the method includes an additional step (the addition of the enzymatic substrate). This leads to a longer assay time. The assay can be optimized further by using a detection antibody that is directly labelled with the QD. Like this one of the steps of the assay can be eliminated, reducing the total assay- and hands-on times.

Conclusion

Determination of HER2-ECD and cancer cells in biological samples is critical for an efficient diagnosis and follow-up of (eventually) HER2-positive breast cancer. With an assay time of 90 min, a sensitive immunomagnetic assay was developed using MBs and SPCE as transducer surface and core/shell CdSe@ZnS QDs as electroactive labels. The Cd²⁺ ions, released through acid dissolution of the QDs, were analysed by DPASV. Human serum samples were used to test the sensor's

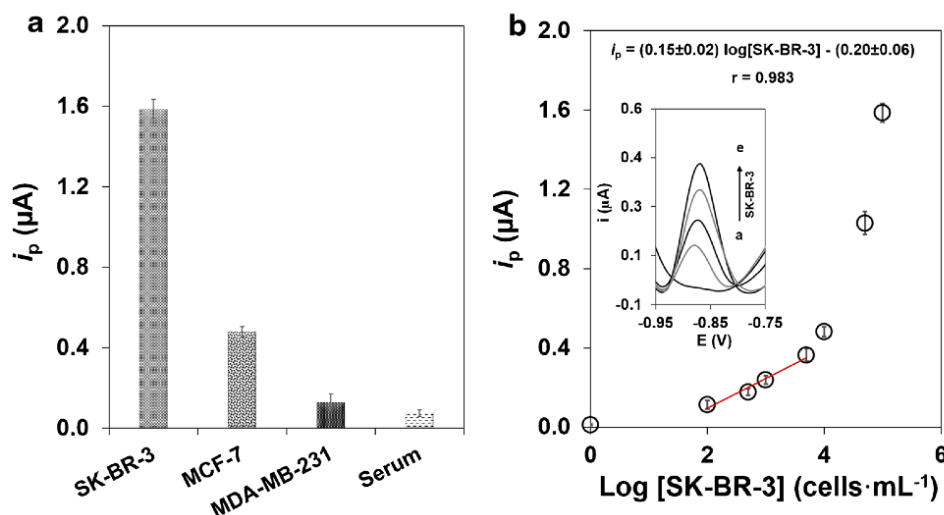


Fig. 4 Results obtained for cancer cell analysis. **a** Selectivity study of the magnetic immunoassay in the presence of 1×10^5 cells·mL⁻¹ for SK-BR-3, MDA-MB-231 and MCF-7 cells. **b** Results obtained for distinct concentrations of HER2-positive cancer cells SK-BR-3 in human serum. Inset: Differential pulse anodic stripping voltammograms of [SK-BR-3]

(a–e) 0, 1×10^2 , 5×10^2 , 1×10^3 and 5×10^3 cells·mL⁻¹. DPASV parameters: preconcentration +1.00 V for 60 s and –1.10 V for 300 s, potential scan –1.00 V to –0.70 V, pulse amplitude 0.05 V, step potential 0.01 V, modulation time 0.01 s, interval time 0.1 s

Table 2 Summary of experimental parameters of electrochemical bioassay-based procedures for HER2-expressing breast cancer cell lines

HER2 ⁺ Cell type	Sensing surface		Sample		Detection strategy		LOD (cells/ mL)	Selectivity	Ref			
	Transducer	Transducer preparation time*	Modification with the biorecognition element*	Long-term stability	Label	Technique				Detection	Assay time	
SK-BR-3	SPCE/MBs	15 min	1 h	60 days	Human serum	CdSe@ ZnS QDs	DPV	Cadmium	1 h 30 min	2	MDA-MB-231, MCF-7	This
work												
SK-BR-3	SPCE/MBs	15 min	1 h	60 days	Human serum	AP	LSV	Silver	1 h 50 min	3	MDA-MB-231	[30]
SK-BR-3	FTO/NFG/AgNP/PANI	> 4 h	12 h	45 days	Whole blood	n.a.	DPV	[Fe(CN) ₆] ^{3-/4-}	30 min	2	ZR-75-1, MDA-MB-231, SW-742, MCF-10A	[31]
SK-BR-3	GCE/poly-DPB-(AuNP)	> 4 h	12 h	n.d.	Human serum	Hydrazin	SWSV	Silver	1 h 10 min	26	MCF10, MCF7, HeLa	[32]
SK-BR-3	NEEs	n.a.	2 h	n.d.	Buffer	HRP	CV	MB	6 h	n.d.	MCF-7	[33]
BT-474	SPCE/E	n.a.	20 min	n.d.	Human serum	n.a.	DPV	[Fe(CN) ₆] ^{3-/4-}	2 h	n.d.	MDA-MB-231	[34]
**MCF-7	AuE/MnFePBA@Au	5 h	2 h	15 days	Human serum	n.a.	EIS	[Fe(CN) ₆] ^{3-/4-}	1 h	36	L929	[35]

*Overnight incubations were considered as a 12-h period for comparison purposes

**SK-BR-3 and BT-474 naturally overexpresses HER2; however, MCF-7 is considered a low expressor

AgNP – silver nanoparticles; AP – alkaline phosphatase; AuNP – gold nanoparticles; CV – cyclic voltammetry; DPB – 2,5-bis(2-thienyl)-1H-pyrrole-1-(p-benzoic acid); DPV – differential pulse voltammetry; EIS – electrochemical impedance spectroscopy; FTO – fluorine doped tin oxide electrode; GCE – glassy carbon electrode; HRP – horseradish peroxidase; LSV – linear sweep voltammetry; MB – methylene blue; MnFePBA – MnFe Prussian blue analogue; n.a. – not applicable; n.d. – no data; NFG – nitrogen-doped graphene; NEEs – nanoelectrode ensembles; PANI – polyaniline; QDs – quantum dots; SPCE – screen-printed carbon electrode; SPCE-E – Extraavidin-modified screen-printed carbon electrodes; SWSV – square wave stripping voltammetry

applicability, and the selectivity was confirmed through the analysis of other cancer biomarkers and possible serum interferents. The immunomagnetic assay was further successfully applied to the determination of the HER2-positive SK-BR-3 breast cancer cell line and of HER2-negative (MDA-MB-231) and low-expression HER2 (MCF-7) breast cancer cell lines. The SK-BR-3 cell line provided a concentration-dependent signal that was more than 12.5× higher than the signal obtained for the other cells. The bioassay proved to be a fast, reliable and specific analytical tool for measuring tumour markers in cancer patients' serum.

Acknowledgements The authors are also thankful to Rui Rocha and CEMUP “Centro de Materiais da Universidade do Porto” for the SEM work.

Funding information The authors are grateful for the financial support from the Fundação para a Ciência e a Tecnologia (FCT) / the Ministério da Ciência, Tecnologia e Ensino Superior (MCTES) through national funds (Portugal) (LAQV - UID/QUI/50006/2019 and CINTESIS, R&D -Unit - UID/IC/4255/2019). Maria Freitas and Virgínia Cruz Fernandes are financially supported by FCT through a PhD grant (SFRH/BD/111942/2015) and a postdoc grant (SFRH/BPD/109153/2015), respectively.

Compliance with ethical standards

Conflict of interest The authors declare that they have no conflict of interest.

References

- Basu P, Ponti A, Anttila A, Ronco G, Senore C, Vale DB, Segnan N, Tomatis M, Soerjomataram I, Primic Žakelj M, Dillner J, Elfström KM, Lönnberg S, Sankaranarayanan R (2018) Status of implementation and organization of cancer screening in the European Union member states—summary results from the second European screening report. *Int J Cancer* 142:44–56. <https://doi.org/10.1002/ijc.31043>
- Mittal S, Kaur H, Gautam N, Mantha AK (2017) Biosensors for breast cancer diagnosis: a review of bioreceptors, biotransducers and signal amplification strategies. *Biosens Bioelectron* 88:217–231. <https://doi.org/10.1016/j.bios.2016.08.028>
- Sareyeldin RM, Gupta I, Al-Hashimi I et al (2019) Gene expression and miRNAs profiling: function and regulation in human epidermal growth factor receptor 2 (HER2)-positive breast cancer. *Cancers* 11: 646. <https://doi.org/10.3390/cancers11050646>
- Wolff AC, Hammond MEH, Allison KH, Harvey BE, Mangu PB, Bartlett JMS, Bilous M, Ellis IO, Fitzgibbons P, Hanna W, Jenkins RB, Press MF, Spears PA, Vance GH, Viale G, McShane L, Dowsett M (2018) Human epidermal growth factor receptor 2 testing in breast Cancer: American Society of Clinical Oncology/ College of American Pathologists Clinical Practice Guideline Focused Update. *J Clin Oncol* 36:2105–2122. <https://doi.org/10.1200/JCO.2018.77.8738>
- Perrier A, Gligorov J, Lefèvre G, Boissan M (2018) The extracellular domain of Her2 in serum as a biomarker of breast cancer. *Lab Invest* 98:696–707. <https://doi.org/10.1038/labinvest.2012.91>
- Mamdouhi T, Twomey JD, McSweeney KM, Zhang B (2019) Fugitives on the run: circulating tumor cells (CTCs) in metastatic diseases. *Cancer Metastasis Rev* 38:297–305. <https://doi.org/10.1038/s41374-018-0033-8>
- Freitas M, Nouws HPA, Delerue-Matos C (2018) Electrochemical biosensing in Cancer diagnostics and follow-up. *Electroanalysis* 30: 1576–1595. <https://doi.org/10.1002/elan.201800193>
- Sharma S, Zapatero-Rodríguez J, Saxena R, O'Kennedy R, Srivastava S (2018) Ultrasensitive direct impedimetric immunosensor for detection of serum HER2. *Biosens Bioelectron* 106:78–85. <https://doi.org/10.1016/j.bios.2018.01.056>
- Pacheco JG, Rebelo P, Freitas M et al (2018) Breast cancer biomarker (HER2-ECD) detection using a molecularly imprinted electrochemical sensor. *Sens Actuator B-Chem* 273:1008–1014. <https://doi.org/10.1016/j.snb.2018.06.113>
- Arkan E, Saber R, Karimi Z, Shamsipur M (2015) A novel antibody-antigen based impedimetric immunosensor for low level detection of HER2 in serum samples of breast cancer patients via modification of a gold nanoparticles decorated multiwall carbon nanotube-ionic liquid electrode. *Anal Chim Acta* 874:66–74. <https://doi.org/10.1016/j.aca.2015.03.022>
- Emami M, Shamsipur M, Saber R, Irajirad R (2014) An electrochemical immunosensor for detection of a breast cancer biomarker based on antiHER2-iron oxide nanoparticle bioconjugates. *Analyst* 139:2858–2866. <https://doi.org/10.1039/c4an00183d>
- Rostamabadi PF, Heydari-Bafrooei E (2019) Impedimetric aptasensing of the breast cancer biomarker HER2 using a glassy carbon electrode modified with gold nanoparticles in a composite consisting of electrochemically reduced graphene oxide and single-walled carbon nanotubes. *Microchim Acta* 186:495. <https://doi.org/10.1007/s00604-019-3619-y>
- Freitas M, Nouws HPA, Delerue-Matos C (2019) Electrochemical sensing platforms for HER2-ECD breast Cancer biomarker detection. *Electroanalysis* 31:121–128. <https://doi.org/10.1002/elan.201800537>
- Chocholova E, Bertok T, Lorencova L et al (2018) Advanced anti-fouling zwitterionic layer based impedimetric HER2 biosensing in human serum: Glycoprofiling as a novel approach for breast cancer diagnostics. *Sens Actuator B-Chem* 272:626–633. <https://doi.org/10.1016/j.snb.2018.07.029>
- Shamsipur M, Emami M, Farzin L, Saber R (2018) A sandwich-type electrochemical immunosensor based on in situ silver deposition for determination of serum level of HER2 in breast cancer patients. *Biosens Bioelectron* 103:54–61. <https://doi.org/10.1016/j.bios.2017.12.022>
- Marques RCB, Viswanathan S, Nouws HPA, Delerue-Matos C, González-García MB (2014) Electrochemical immunosensor for the analysis of the breast cancer biomarker HER2 ECD. *Talanta* 129:594–599. <https://doi.org/10.1016/j.talanta.2014.06.035>
- Al-Khafaji QAM, Harris M, Tombelli S et al (2012) An electrochemical immunoassay for HER2 detection. *Electroanalysis* 24: 735–742. <https://doi.org/10.1002/elan.201100501>
- Tallapragada SD, Layek K, Mukherjee R, Mistry KK, Ghosh M (2017) Development of screen-printed electrode based immunosensor for the detection of HER2 antigen in human serum samples. *Bioelectrochemistry* 118:25–30. <https://doi.org/10.1016/j.bioelechem.2017.06.009>
- Shen C, Liu S, Li X, Zhao D, Yang M (2018) Immunochemical detection of the human epidermal growth factor receptor 2 (HER2) via gold nanoparticle-based rolling circle amplification. *Microchim Acta* 185:547–548. <https://doi.org/10.1007/s00604-018-3086-x>
- Chai Y, Li X, Yang M (2019) Aptamer based determination of the cancer biomarker HER2 by using phosphate-functionalized MnO₂ nanosheets as the electrochemical probe. *Microchim Acta* 186:316–316. <https://doi.org/10.1007/s00604-019-3412-y>

21. Pastucha M, Farka Z, Lacina K, Mikušová Z, Skládal P (2019) Magnetic nanoparticles for smart electrochemical immunoassays: a review on recent developments. *Microchim Acta* 186:312–326. <https://doi.org/10.1007/s00604-019-3410-0>
22. Wu X, Xiao T, Luo Z, He R, Cao Y, Guo Z, Zhang W, Chen Y (2018) A micro-/nano-chip and quantum dots-based 3D cytosensor for quantitative analysis of circulating tumor cells. *J Nanobiotechnol* 16:65. <https://doi.org/10.1186/s12951-018-0390-x>
23. Boriachek K, Islam MN, Gopalan V et al (2017) Quantum dot-based sensitive detection of disease specific exosome in serum. *Analyst* 142:2211–2219. <https://doi.org/10.1039/c7an00672a>
24. Fernández-Delgado N, Herrera M, Tavabi AH et al (2018) Structural and chemical characterization of CdSe-ZnS core-shell quantum dots. *Appl Surf Sci* 457:93–97. <https://doi.org/10.1016/j.apsusc.2018.06.149>
25. Martín-Yerga D (2019) Electrochemical detection and characterization of nanoparticles with printed devices. *Biosens* 9:49. <https://doi.org/10.3390/bios9020047>
26. Freitas M, Neves MMPS, Nouws HPA, Delerue-Matos C (2020) Quantum dots as nanolabels for breast cancer biomarker HER2-ECD analysis in human serum. *Talanta* 208:120430. <https://doi.org/10.1016/j.talanta.2019.120430>
27. Economou A (2005) Bismuth-film electrodes: recent developments and potentialities for electroanalysis. *TrAC - Trends Anal Chem* 24: 334–340. <https://doi.org/10.1016/j.trac.2004.11.006>
28. Campuzano S, Yáñez-Sedeño P, Pingarrón JM (2018) Current trends and challenges in bioelectrochemistry for non-invasive and early diagnosis. *Curr Opin Electrochem* 12:81–91. <https://doi.org/10.1016/j.coelec.2018.04.015>
29. Martín-Yerga D, González-García MB, Costa-García A (2013) Biosensor array based on the in situ detection of quantum dots as electrochemical label. *Sens Actuator B-Chem* 182:184–189. <https://doi.org/10.1016/j.snb.2013.03.004>
30. Freitas M, Nouws HPA, Keating E, Delerue-Matos C (2020) High-performance electrochemical immunomagnetic assay for breast cancer analysis. *Sens Actuator B-Chem* 308:127667. <https://doi.org/10.1016/j.snb.2020.127667>
31. Salahandish R, Ghaffarnejad A, Naghib SM et al (2018) Nanobiosensor for highly sensitive detection of HER2 positive breast cancer. *Biosens Bioelectron* 117:104–111. <https://doi.org/10.1016/j.bios.2018.05.043>
32. Zhu Y, Chandra P, Shim YB (2013) Ultrasensitive and selective electrochemical diagnosis of breast cancer based on a hydrazine-gold nanoparticle-aptamer bioconjugate. *Anal Chem* 85:1058–1064. <https://doi.org/10.1021/ac302923k>
33. Mucelli SP, Zamuner M, Tormen M, Stanta G, Ugo P (2008) Nanoelectrode ensembles as recognition platform for electrochemical immunosensors. *Biosens Bioelectron* 23:1900–1903. <https://doi.org/10.1016/j.bios.2008.02.027>
34. Yadav S, Boriachek K, Islam MN et al (2017) An electrochemical method for the detection of disease-specific Exosomes. *ChemElectroChem* 4:967–971. <https://doi.org/10.1002/celec.201600391>
35. Zhou N, Su F, Li Z, Yan X, Zhang C, Hu B, He L, Wang M, Zhang Z (2019) Gold nanoparticles conjugated to bimetallic manganese(II) and iron(II) Prussian blue analogues for aptamer-based impedimetric determination of the human epidermal growth factor receptor-2 and living MCF-7 cells. *Microchim Acta* 186:75. <https://doi.org/10.1007/s00604-018-3184-9>

Publisher's note Springer Nature remains neutral with regard to jurisdictional claims in published maps and institutional affiliations.

Electronic Supporting Material
on the *Microchimica Acta* publication entitled

**Immunomagnetic bead-based bioassay for the
voltammetric analysis of the breast cancer biomarker
HER2-ECD and tumour cells using quantum dots as
detection labels**

**Maria Freitas¹, Henri P.A. Nouws^{1*}, Elisa Keating^{2,3}, Virginia Cruz
Fernandes¹, Cristina Delerue-Matos¹**

¹ REQUIMTE/LAQV, Instituto Superior de Engenharia do Porto, Politécnico do Porto, Porto, Portugal, R. Dr. António Bernardino de Almeida 431, 4200-072 Porto

² Department of Biomedicine – Unit of Biochemistry, Faculty of Medicine, University of Porto, Al. Prof. Hernâni Monteiro, 4200-319 Porto, Portugal

³ CINTESIS – Center for Health Technology and Services Research, Rua Dr. Plácido da Costa, 4200-450 Porto, Portugal

S1. Experimental section

S1.1 Reagents

The antibodies (Rabbit IgG monoclonal anti-human-HER2-ECD antibody, mouse IgG2a monoclonal biotinylated anti-human-HER2-ECD antibody) and the antigen (a recombinant human HER2/ErBb2 protein) were obtained from Sino Biological Inc. (China, www.sinobiological.com). Breast cancer cell lines MDA-MB-231 and MCF-7 were obtained from ATCC®. The SK-BR-3 cell line was kindly provided by the Department of Biomedicine – Unit of Biochemistry of the Faculty of Medicine of University of Porto. Qdot® 655 streptavidin conjugate (QD-Strep), Dynabeads™ MyOne™ (Carboxylic Acid functionalized magnetic beads; COOH-MB, 10 mg.mL⁻¹) and a Human ErbB2 (HER2) enzyme-linked immunosorbent assay (ELISA) kit were purchased from ThermoFisher Scientific (USA, www.thermofisher.com). Bismuth ICP standard was acquired from Merck (Germany, www.merck.com). PEG gold-coated magnetic nanoparticles (HOOC-Fe₃O₄@AuNP) were obtained from Nanoimmunotech (Spain, www.nanoimmunotech.eu). Human serum (from male AB clotted whole blood), albumin from bovine serum (BSA), carboxylic acid functionalized multiwalled carbon nanotubes (COOH-MWCNT), 2-Aminoethan-1-ol (EA), 1-(3-Dimethylaminopropyl)-3-ethylcarbodiimide hydrochloride (EDC), 1-Hydroxy-2,5-pyrrolidinedione (NHS), 2-Morpholinoethanesulfonic acid (MES) monohydrate, Tween® 20 (T), phosphate buffered saline (PBS) and 2-Amino-2-(hydroxymethyl)propane-1,3-diol (Tris) were obtained from Sigma-Aldrich (USA, www.sigmaaldrich.com). Male human serum was stored at -20 °C and used as received. Serum samples were spiked with HER2-ECD or CTCs at different concentrations and analysed without further treatments.

S1.2 ELISA kit for the determination of HER2-ECD

The evaluation of the accuracy of the assay's results was performed using a commercially available ELISA kit for the detection of HER2 in serum (Human ErbB2 (HER2) ELISA kit, ThermoFisher Scientific (USA, www.thermofisher.com)). The experimental procedure for this kit can be retrieved from www.thermofisher.com/elisa. A multi-mode microplate reader (BioTek Instruments, USA, www.biotek.com) was used and the data were treated with Gen5 Version 2.0 data analysis Software (BioTek Instruments). The obtained calibration straight ($\lambda = 450 \text{ nm}$) is indicated in Fig. S1.

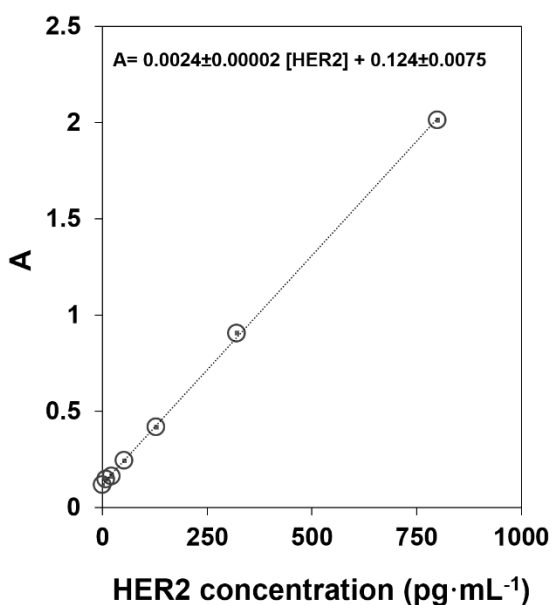


Fig. S1 Calibration straight (A vs. HER2-ECD concentration) for the analysis of HER2-ECD in human serum using the ELISA kit.

S2. Electrochemical behaviour of the QDs

The electrochemical response of the QDs was verified by adding HCl and Bi(III) in four different strategies: Format i - the biomodified-MBs were placed on the WE, which was totally dried before the addition of HCl and Bi(III); Format ii – HCl and Bi(III) were added to the microtube and its content was placed on the WE; Format iii and iv – HCl was added to the microtube (Fig. S2). In Format iii, the content of the microtube was placed on the WE and Bi(III) was added and in Format iv the MBs were retained in the microtube and only the solution was placed on the WE followed by addition of Bi(III). As can be observed in Fig. S2, and considering both the analytical and blank signals, only formats i and iii presented interesting results, however a relatively high blank signal was obtained for Format iii. Therefore, Format i was chosen to proceed the studies.

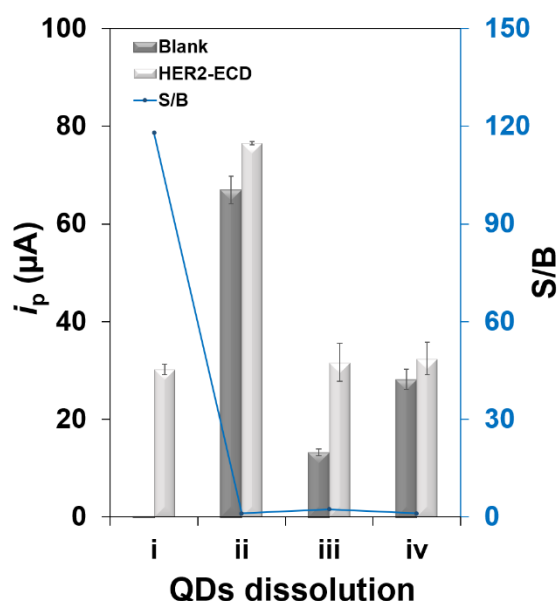


Fig. S2 Electrochemical determination of the QDs through the addition of HCl and Bi(III) in distinct formats.

S3. Optimization of the assay

The goal of the first study was to minimize the assay steps and to reduce the assay time. So, distinct assay formats were tested and compared to an assay (Format A) in which the immunoreagents were added in separate steps. Two distinct strategies were evaluated: in Format B a previously prepared mixture of the antigen and Ab-D was used and in Format C a previously prepared mixture of Ab-D and QDs was tested. The results are presented in Fig. S3a. Format B was selected to proceed the optimization studies since the signal-to-blank (S/B) ratio was similar to the one obtained with Format A and, more importantly, a 1-h reduction of the assay time was achieved. Format C shows high blank signals which can be due to the steric hindrance between the Ab-D and QDs when they are previously mixed.

Then, to select the optimum QD concentration the following concentrations were tested: 2.5, 5.0 and 10 nM. The highest S/B ratio was obtained for a 5.0-nM QD concentration (Fig. S3b). BSA 0.5% (m/V) was then added to this solution to minimize nonspecific adsorption. As can be seen in Fig. S3b, like this the blank signal was reduced without affecting the analytical signal.

Subsequently the amount of MBs (7.5, 15, 30 and 45 μg) was studied, obtaining the highest analytical signal and S/B ratio for 7.5 μg with almost a negligible blank signal (Fig. S3c).

Then, and using 7.5 μg of MBs and a 5.0-nM QD solution (containing 0.5% BSA), the concentration of both antibody solutions was optimized: Ab-C (10, 25 and 50 $\mu\text{g}\cdot\text{mL}^{-1}$) and Ab-D (1.0 and 2.0 $\mu\text{g}\cdot\text{mL}^{-1}$) (Fig. S3d). There was an increase in the analytical signal with increasing Ab-C concentration when Ab-D 1 $\mu\text{g}\cdot\text{mL}^{-1}$ was used; however, for twice the Ab-D concentration (2.0 $\mu\text{g}\cdot\text{mL}^{-1}$) the best result was observed for an intermediate concentration of Ab-C (25 $\mu\text{g}\cdot\text{mL}^{-1}$).

The combination of Ab-C $50 \mu\text{g}\cdot\text{mL}^{-1}$ and Ab-D $2.0 \mu\text{g}\cdot\text{mL}^{-1}$ led to a lower analytical signal when compared to the combination of Ab-C $25 \mu\text{g}\cdot\text{mL}^{-1}$ and Ab-D $2.0 \mu\text{g}\cdot\text{mL}^{-1}$, which may be due to an excess of Ab-C blocking the paratope and subsequently the ability to bind the antigen. Table S1 presents the experimental variables/parameters and the selected parameter/value.

Table S1 Optimization of the experimental parameters of the immunomagnetic assay.

Experimental variable	Tested parameter/range	Selected parameter/value
Assay format	A, B, C	B
[QDs] (nM)	2.5 – 10.0	5.0
MBs amount (μg)	7.5 – 45.0	7.5
[Ab-C] ($\mu\text{g}\cdot\text{mL}^{-1}$)	10.0 – 50.0	25.0
[Ab-D] ($\mu\text{g}\cdot\text{mL}^{-1}$)	1.0 – 2.0	2.0

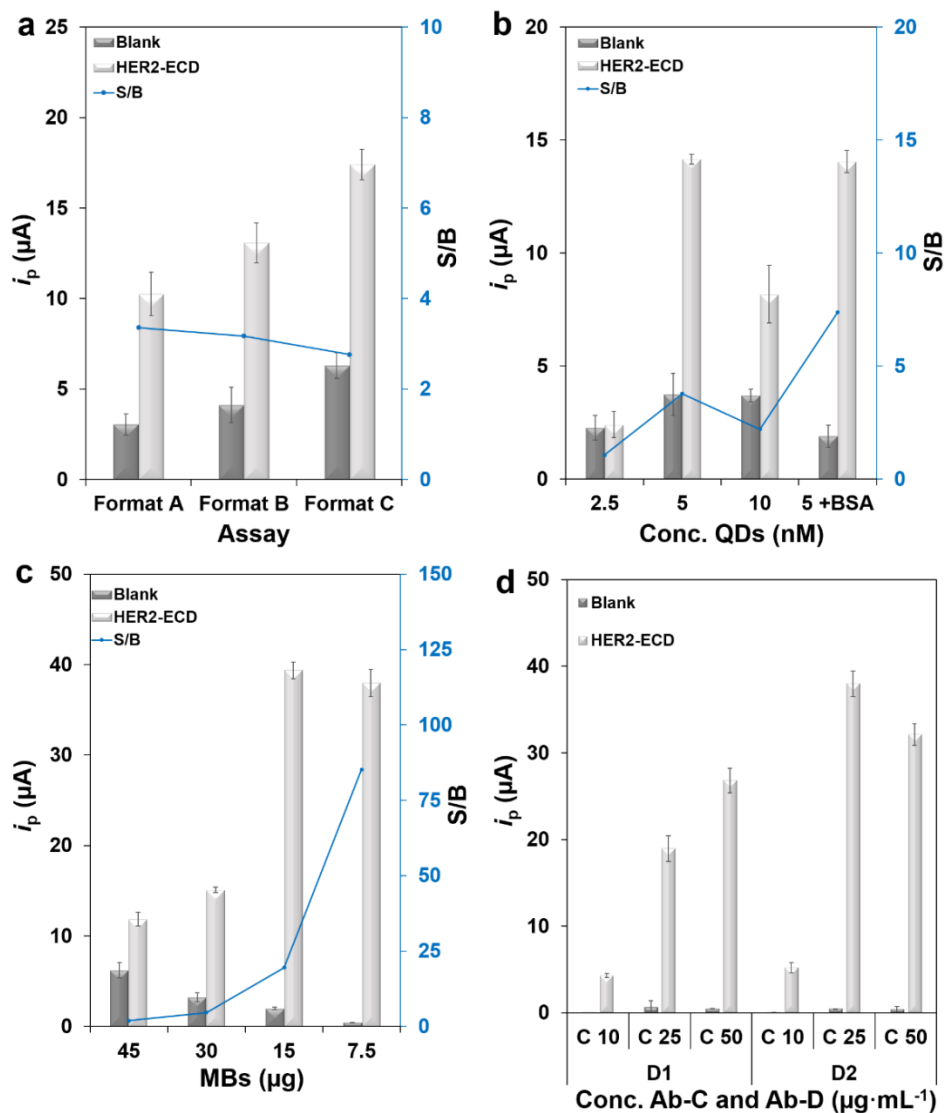


Fig. S3 Results of the optimizations. (a) Format assays (Format A: step-by-step assay, Format B: previously mixture step of antigen and Ab-detection, Format C: previously mixture step of Ab-detection and QDs), (b) QDs concentration (1.5, 5.0, 10 nM and 5.0 nM + BSA 0.5% (m/V)), (c) MBs amount (45, 30, 15 and 7.5 μg for each WE) and (d) concentration of Ab-C (10, 25 and 50 $\mu\text{g}\cdot\text{mL}^{-1}$) and Ab-D (1.0 and 2.0 $\mu\text{g}\cdot\text{mL}^{-1}$). (HER2-ECD (0 (blank) and 50 $\text{ng}\cdot\text{mL}^{-1}$)).

S4. Figures of merit of the assay for the analysis of HER2-ECD and cancer cell line SK-BR-3

Table S2 Figures of merit of the developed magnetic immunoassay for the analysis of HER2-ECD and the HER-positive breast cancer cell line SK-BR-3.

Figure of merit	HER2-ECD	SK-BR-3
Concentration interval (ng·mL ⁻¹) or (cells·mL ⁻¹)	0.50 - 50	1×10 ² - 5×10 ³
Correlation coefficient (r)	0.997	0.983
Slope (m) (μA·mL·ng ⁻¹)	0.75	0.15
Standard deviation of the slope (S _m) (μA·mL·ng ⁻¹)	0.03	0.02
Intercept (b) (μA)	4.99	-0.2
Standard deviation of the intercept (S _a) (μA)	0.58	0.06
Standard deviation of the linear regression (S _{y/x})	1.19	0.02
Standard deviation of the method (S _{x0})	0.17	0.01
Coefficient of variation of the method (V _{x0}) (%)	1.27	0.21
Limit of detection (LOD) (ng·mL ⁻¹) or (cells·mL ⁻¹)	0.29	2
Limit of quantification (LOQ) (ng·mL ⁻¹) or (cells·mL ⁻¹)	0.96	5

CHAPTER 5

GENERAL CONCLUSIONS AND FUTURE PERSPECTIVES

Conclusions

Improving diagnostic methodologies for breast cancer detection is a great challenge. The work presented in this thesis is a step towards the use of electrochemical immunosensors and magnetic immunoassays for breast cancer tumour marker analysis because early detection and follow-up can be performed noninvasively. This can be an effective approach to reduce mortality rates.

The diversity of biosensor publications for cancer biomarker analysis has increased exponentially. To highlight the progression, this thesis comprised a review article that covers the state of the art of the six most commonly diagnosed cancer types and related biomarkers used for the development of electrochemical bioassays. This was crucial to identify the research gaps, not only in breast cancer biosensor construction/development, but also for a broad overview of the subject. Poor access to urban centers of decentralized populations or high costs of analysis are some of the difficulties for efficient screening, diagnosis or follow-up. Accordingly, the use of biosensors can be an added advantage.

The main objectives of this thesis were attained and involved the development of electrochemical immunosensors and magnetic immunoassays for the determination of the breast cancer biomarker HER2-ECD. Quantification of HER2 overexpressing breast cancer cell lines and HER2-negative cancer cell lines was also achieved.

The developed analytical approaches contemplated important aspects: the use of low reagent and sample volumes, enhancing environmental sustainability, the use of miniaturized and low cost transducer platforms (screen-printed electrodes) to allow “in situ” analyses, avoiding additional steps such as sample processing and preservation, transport to the hospital or laboratory and subsequent analysis at a later time. The samples used throughout the work (serum and cancer cell lines) pretended to be close to real situations.

Transducer surface modifications with nanomaterials and/or magnetic beads were used due to their exceptional properties, providing not only the immobilization of a larger amount of recognition elements (antibodies) but also a better assay performance.

Two distinct detection approaches were employed: (i) the use of metalloenzymatic detection, where silver was determined and (ii) the use of electroactive quantum dots, where cadmium was analysed. Although the first strategy allowed a better sensitivity, it also implies the use of an enzymatic substrate. This requires additional steps in the assay that aren't needed when quantum dots are used. Therefore, the latter detection approach is faster and easier to perform for any user. An immunosensor and a magnetic immunoassay were developed using each detection strategy.

Recovery assays and the comparison of the results obtained for the analysis of HER2 in human serum with those obtained with an ELISA kit was performed. These studies confirmed that the developed assays provide accurate results. The analysis of the target biomarker in human serum and/or in the presence of interferents was tested (CA 15-3; AFP; Cystatin C; HSA), demonstrating an excellent selectivity of the assays. The long-term stability of the immunosensor and magnetic beads was also studied. For the immunosensor, the signal was stable for 7 days and for the magnetic immunoassays the analytical signal maintained stable for at least 60 days. The good stability allows multiple platforms to be prepared simultaneously, thus reducing laboratory waste and hands-on time for transducer preparation.

A huge problem faced throughout the work was the impossibility to obtain real patients' samples from the local oncology hospital. An additional study regarding the application of the magnetic assays to the analysis of live breast cancer cells was included (HER2-positive: SK-BR-3 and HER2-negative: MCF-7 and MDA-MB-231). It was possible to distinguish the different HER2 expression levels, showing high selectivity for HER2-positive cells.

Future perspectives

There has been a great investment in the development of biosensors and bioassays as alternative analytical tools. Rapid detection of prognostic biomarkers for accurate screening is important; however, the use of biosensors by medical staff is still limited. Among the alternatives reported in the literature, there is a need for large-scale commercialization, enabling their inclusion in routine practice.

Among the most interesting transducer, the ones that are based on paper undoubtedly surpass the highest demands and expectations. Since the purpose is the analysis of patient samples, incineration for their elimination is highly appealing, as it avoids contamination and/or any type of disease transmission or dissemination.

Furthermore, after the development of individual assays, their combination to form multiplexed detection systems is possible. Therefore, they can provide fast recording of biomarker tumour profiles, which can play an important role in early diagnosis and personalized medicine. Multiple analyte detection can be performed in several ways: using a single-WE SPCE but with distinct detection events, or by using the same construction and detection format on multiple-WE SPEs or screen-printed electrochemical arrays.

Finally, it should be mentioned that the main objective of these works is the development of appropriate methodologies to assist medical and clinical staff in cancer detection. Easy-to-use, low-cost, miniaturizable and user-adjustable sensors with rapid responses are features that should be considered when the main purpose is helping those who need it the most.

